KINETICS FOR OXIDATION OF PENICILLANIC ACID DERIVATIVES BY PER-IODATOCUPERATE (III) COMPLEXES IN THE PRESENCE OF COBALT (III) CATALYST IN ALKALINE MEDIUM

A THESIS SUBMITTED TO THE

CENTRAL DEPARTMENT OF CHEMISTRY

INSTITUTE OF SCIENCE AND TECHNOLOGY

TRIBHUVAN UNIVERSITY

NEPAL

FOR THE AWARD OF

DOCTOR OF PHILOSOPHY

IN CHEMISTRY

BY

YUV RAJ SAHU

JUNE 2024

KINETICS FOR OXIDATION OF PENICILLANIC ACID DERIVATIVES BY PER-IODATOCUPERATE (III) COMPLEXES IN THE PRESENCE OF COBALT (III) CATALYST IN ALKALINE MEDIUM

A THESIS SUBMITTED TO THE

CENTRAL DEPARTMENT OF CHEMISTRY

INSTITUTE OF SCIENCE AND TECHNOLOGY

TRIBHUVAN UNIVERSITY, NEPAL

FOR THE AWARD OF

DOCTOR OF PHILOSOPHY

IN CHEMISTRY

BY

YUV RAJ SAHU

JUNE 2024

TRIBHUVAN UNIVERSITY

Institute of Science and Technology

DEAN'S OFFICE

Kirtipur, Kathmandu, Nepal

Reference No.:

Institute of Science & Technology
Dean's Office
Kirtipur 2045

EXAMINERS

The Title of Ph.D. Thesis: " Kinetics for Oxidation of Penicillanic Acid Derivatives by Per-Iodatocuperate (III) Complexes in the Presence of Cobalt (III) Catalyst in Alkaline Medium "

Name of Candidate: Yuv Raj Sahu

Internal Examiner:

Dr. Surya Kant Kalauni
Central Department of Chemistry
Tribhuvan University, NEPAL

External Examiners:

(1) Prof. Dr. Hem Raj Pant
Far-Western University
Mahendranagar, NEPAL

(2) Prof. Dr. Ramesh L. Gardas
Indian Institute of Technology
Madras, INDIA

(3) Prof. Dr. Mehmet Akkurt
Erciyes University
Keyseri, TURKEY

11 December, 2024

(Dr. Surendra Kumar Gautam)
Asst. Dean

Telephone: 977-1-4330844, 4331755 (Administration), 4330120 (Exam)
Website: www.iost.tu.edu.np, E-mail: info@iost.tu.edu.np, exam@iost.tu.edu.np

DECLARATION

Thesis entitled **"KINETICS FOR OXIDATION OF PENICILLANIC ACID DERIVATIVES BY PER-IODATOCUPERATE (III) COMPLEXES IN THE PRESENCE OF COBALT (III) CATALYST IN ALKALINE MEDIUM"**, which is being submitted to Central Department of Chemistry, Institute of Science and Technology (IOST), Tribhuvan University, Nepal for the award of the degree of Doctor of Philosophy (Ph. D.), is a research work carried out by me under the supervision of Prof. Dr. Ajaya Bhattarai and co-supervised by Asst. Prof. Dr. Narendra Kumar Chaudhary, Chemistry Research Laboratory, Department of Chemistry, Mahendra Morang Adarsh Multiple Campus, Tribhuvan University, Biratnagar, Morang, Province number-1, Nepal.

This research work is purely original and has not been submitted earlier partially or fully in this or any other form to any other university or Institute, here or elsewhere, for the award of any degree.

YUV RAJ SAHU

RECOMMENDATION

This is to recommend that Mr. Yuv Raj Sahu has carried out the research work entitled **"KINETICS FOR OXIDATION OF PENICILLANIC ACID DERIVATIVES BY PER-IODATOCUPERATE (III) COMPLEXES IN THE PRESENCE OF COBALT (III) CATALYST IN ALKALINE MEDIUM"** for the award of **Doctor of Philosophy** (Ph.D.) in Chemistry under my supervision. As I know, this work has not been submitted completely or partially for any other degree anywhere.

He has fulfilled all the requirements laid down by the Institute of Science and Technology (IOST), Tribhuvan University, Kirtipur, Nepal for the submission of the thesis for the award of Ph. D. degree.

Ajaya Bhattarai

Prof. Dr. Ajaya Bhattarai

Supervisor

Professor, Department of Chemistry,

Mahendra Morang Adarsha Multiple Campus, Biratnagar, Tribhuvan University, Nepal.

.....

Dr. Narendra Kumar Chaudhary

Co-supervisor

Assistant Professor, Department of Chemistry,

Mahendra Morang Adarsha Multiple Campus, Biratnagar, Tribhuvan University, Nepal.

त्रिभुवन विश्वविद्यालय
TRIBHUVAN UNIVERSITY
विज्ञान तथा प्रविधि अध्ययन संस्थान
Institute of Science and Technology
रसायन शास्त्र केन्द्रीय विभाग
CENTRAL DEPARTMENT OF CHEMISTRY
कीर्तिपुर, काठमाडौं, नेपाल
Kirtipur, Kathmandu, NEPAL

पत्र संख्या:
Ref. No.:

Central Department of Chemistry T.U., Kirtipur

LETTER OF APPROVAL

Date: 11 December, 2024

On the recommendation of Prof. Dr. Ajaya Bhattarai (supervisor), and Dr. Narendra Kumar Chaudhary (co-supervisor), this Ph.D. thesis submitted by Yuv Raj Sahu, entitled **"Kinetics For Oxidation Of Penicillanic Acid Derivatives by Per-Iodatocuperate (III) Complexes in the Presents of Cobalt (III Catalyst in Alkaline Medium"** is forwarded by Central Department Research Committee (CDRC) to the Dean, IoST, T.U.

.....

Prof. Dr. Jagadeesh Bhattarai
Professor
Head
Central Department of Chemistry
Tribhuvan University
Kirtipur, Kathmandu, Nepal

Tel.: 977-1-4332034, Fax No.: +977-1-4330537, http://www.cdctu.edu.np e-mail: head@cdc.tu.edu.np

ACKNOWLEDGEMENTS

God's blessings go for beyond anything we could ever dream. I praise God, the almighty and merciful, for always being there for me and all as well as whose abundant blessings have made me who I am today.

First and foremost, I wish to express my profound sense of gratitude to my honorable supervisor and member of Tribhuvan University Service Commission (at present), Prof. Dr. Ajaya Bhattarai, Mahendra Morang Adarsh Multiple Campus (MMAMC), Department of Chemistry, Biratnagar, Morang, Tribhuvan University, Nepal for allowing me to work under his skilled guidance. It was a great privilege and honour to work under his wisdom, knowledge and committed guidance. I am extremely grateful for what he offered me. I am deeply indebted to him for his keen interest, inspirative guidance, stimulating discussions, and everlasting encouragement throughout the research carrier. I am extremely grateful to my co-supervisor, assistant Prof. Dr. Narendra Kumar Chaudhary, for his stimulating manure, fruitful discussions, all kinds of co-operation during research design, and proper guidance.

I would like to express my obligation to Assoc. Prof. Dr. Ram Avtar Sharan (Campus Chief of MMAMC, Biratnagar), and Assoc. Prof. Ashok Kumar Das (Head of Department, Chemistry) of MMAMC, Biratnagar, Nepal for their co-operation.

I would like to express my sincere gratitude to Prof. Dr. Jagadeesh Bhattarai, Head, Central Department of Chemistry (CDC), Kirtipur, Prof. Dr. Kedar Nath Ghimire, Prof. Dr. Megh Raj Pokhrel (former Head), Prof. Dr. Parash Nath Yadav, Prof. Dr. Amar Prasad Yadav, and Prof. Dr. Vinay Kumar Jha, Assoc. Prof. Dr Surya Kant Kalony, Assoc. Prof. Dr. Achyut Adhikari of CDC, Kirtipur, Kathmandu, Nepal.

I am thankful to Purwanchal Campus, Dharan, Sunsari, Institute of Engineering, Tribhuvan University, where I had been employed as a Faculty and for providing me study leave and financial support. I am thankful to Er. Om Prakash Dhakal (ex-campus chief), Er. Kaji Ram Karki (Campus Chief) for their valuable inspiration and co-operation. I am also thankful to my research-mates (Ph. D. scholars, TU) Dr. Rohit

Kumar Dev, Dr. Janak Adhikari, and Dr. Neelam Shahi for their kind cooperation during my research period.

I am extremely grateful to Diamond Jubilee and Lifetime Prof. Dr. Sharnappa T. Nandibewoor and Prof. Dr. Shivamurti A. Chimatadar, P.G. Department of Studies, Karnatak University, Dharwad, Karnataka, India for their fruitful discussion and guidance. It was my immemorial period that I spent there and understood the basic ethics of my research work.

My research period at MMAMC, Biratnagar was immemorial, comfortable, rejoiceful, and fruitful in large part due to the entangled discussions leading to unwinding debate, untiring support leading to undefined pleasure that made it unforgettable journey in my life. I wish to extend my thanks to all those friends, colleagues, and well-wishers who helped me knowingly or unknowingly in my research period. A note of thanks to every person who was directly or indirectly involved in this research work. 'Thanks a lot to everyone....for making me reach up to this landmark of my life'. I acknowledge all technical staff of the Surface Chemistry laboratory, MMAMC, Biratnagar, STIC Cochin, Kerala, SAIF, CDRI-CSIR, Lucknow, SAIF-IIT, Bombay, National Research Foundation, Birgunj for providing spectral evidence.

Words cannot express my deep sense of heartfelt gratitude to my beloved Dad (Pitaji) Late Shree Jay Chandra Sah and Mom Late Mrs. Fuleshwary Devi Sah, father-in law Late Shree Dip Narayan Sah (Former Assistant Professor of Thakur Ram Multiple Campus, Bigunj, Tribhuvan University), mother-in law Mrs. Prem Devi, Bhabhi Late Mrs. Mira Devi Sah, elder siblings Mr. Dhan Raj Sah, Mr. Shiv Raj Sah, elder sisters Gauri Devi and Janaki Devi for their blessings, passionate mental effort, eternal love and enlightened me as a source of inspiration. Finally, but by no means least nor last, I am grateful to my wife Sangita, son Yash Raj Shah, daughters Priyancka, Shruticka, nieces Mr. Dhruba Raj Shah, Er. Dharti Raj Shah, brother-in-law Er. Amar Shah for their endless co-operation. They all are life to me; I dedicate this thesis to them.

YUV RAJ SAHU

ABSTRACT

Ampicillin, amoxicillin, dicloxacillin carbenicillin, and oxacillin are penicillanic acid derivatives (PADs) or β-lactam antibiotics. After consumption of these PADs or antibiotics for a selected purpose, non-degraded forms of these species are accumulated in the environment from waste-water, hospitals, and sewage or land-fill sites. The oxidation process is a kind of degrading method of these antibiotics from environmental aqueous medium. The kinetics and mechanism of oxidation of Penicillanic acid derivatives by diperiodatocuprate [DPC (III)] and Co (III) Chloride catalyst in the aqueous alkaline medium were studied UV/Visible spectrophotometrically at 298 K and ionic strength of 0.10 mol dm^{-3}. After checking their melting points and re-crystallization of these penicillanic acids, from Sigma Aldrich trade, solutions were prepared and stored after confirmation of concentration iodometrically. The reagent DPC (III) was synthesized by Jaiswal and Yadava method. The formation of DPC (III) reagent was confirmed by the appearance of a peak by UV/Visible spectrophotometer and showed maximum absorbance peak at 415 nm. The reaction between DPC (III) and ampicillin in aqueous alkaline medium showed (AMP: DPC-III) 1:4 stoichiometry. The reaction between DPC (III) and amoxicillin showed (AMX: DPC-III) 1:2 stoichiometry. Similarly, one mole of dicloxacillin consumes 4 moles of DPC (III) and one mole of carbenicillin consumed 4 moles of DPC (III) in aqueous alkaline medium while stoichiometry of oxacillin and DPC (III) was declared to be 1:4. The reaction products, in each re-dox reaction, were identified by spot test, CHNS, FT-IR, and LC-MS spectral studies. The reactions were of pseudo-first-order with respect to DPC (III) concentration and fractional order with respect to AMP / AMX / DCLX / CRBC/OXC as well as alkali concentration.

The addition of periodate showed a retarding effect on the rate of oxidation and was of negative fractional order. Monoperiodatocuprate (MPC-III) was found to be the main active species in the alkaline medium in the form of $[Cu\ (H_2IO_6)(H_2O)_2]$ or $[Cu\ (H_3IO_6)(H_2O)_2]^+$.

Absorbance collected from UV/Visible spectrophotometer was converted into uncatalyzed ($\mathbf{k_U}$) , catalyzed ($\mathbf{k_c}$), and thence total rate constant ($\mathbf{k_T}$), and these data were used to verify the Beer-Lambert's law, and many more plots like order plots, verification plots, etc.

Catalytic constant ($\mathbf{K_C}$) was also calculated. Stoichiometry of different reactions for the complex formation was determined from Job's method. Depending on stoichiometry and other evidence like FT-IR, LC-MS, and CHNS, a probable reaction mechanism was also proposed for each redox reaction. Different equilibrium constants (K_1, K_2, and K_3) were calculated. Slopes and intercepts obtained from these verification plots were utilized to calculate variable activation as well as thermodynamic parameters and thence computed.

Keywords: - Kinetics, Mechanism, Monoperiodatocuperate (III), Activation, Rate constants

शोधसार

एम्पिसिलिन, एमोक्सिससिलिन, डिक्लोक्सासिलिन, कार्बेनिसिलिन र ओक्सासिलिन पेनिसिलिक एसिड डेरिभेटिभ्स (PADs) वा बिटा-ल्याक्टम एन्टिबायोटिक हुन्। यी PADs वा एन्टिबायोटिकहरू चयन गरिएको उद्देश्यका लागि उपभोग गरेपछि, यी प्रजातिहरूको गैर-अपघटित रूपहरू फोहोर-पानी, अस्पतालहरू, र ढल वा ल्यान्ड-फिल साइटहरूबाट वातावरणमा जम्मा हुन्छन्। ओक्सीकरण प्रक्रिया यी एन्टिबायोटिकहरूको एक प्रकारको क्षरण वा खण्डीकरण विधि हो। जलीय क्षारीय माध्यममा diperiodatocuprate [DPC (III)] र Co (III) क्लोराइड उत्प्रेरक द्वारा पेनिसिलिक एसिड डेरिभेटिभहरूको अक्सीकरणको गतिविज्ञान र संयन्त्रलाई 298 K र 0.10dmol को आयनिक शक्तिमा UV/दृश्यमान स्पेक्ट्रोफोटोमेट्रिक रूपमा अध्ययन गरियो। सिग्मा एल्ड्रिच ट्रेडका यी पेनिसिलिक एसिडहरूको पग्लने बिन्दुहरू र पुन: क्रिस्टलाइजेसन जाँच गरेपछि, आयोडोमेट्रिक विधिबाट Concentration पुष्टि भएपछि स्तरयुक्त घोलहरु तयार गरी भण्डार गरिएको थियो। अभिकर्मक अथवा अक्सिडेन्ट DPC (III) जैसवाल र यादव विधिबाट संश्लेषित गरिएको थियो। DPC (III) अभिकर्मक को गठन UV/दृश्य स्पेक्ट्रोफोटोमिटरबाट शिखर को उपस्थितिले पुष्टि गरिएको थियो र 415 nm मा अधिकतम अवशोषण शिखर देखायो। जलीय क्षारीय माध्यममा DPC (III) र एम्पिसिलिन बीचको प्रतिक्रिया (AMP: DPC-III) 1:4 stoichiometry देखायो। त्यस्तै, DPC (III) र amoxicillin बीचको प्रतिक्रिया (AMX: DPC-III) 1:2 stoichiometry देखायो। त्यसैगरी, DPC (III) र कार्बेनिसिलिनको बीचको प्रतिक्रिया (CRBC: DPC-III) 1:4 stoichiometry, DPC (III) र डाइक्लोक्सासिलिनको बीचको प्रतिक्रिया (DCLX: DPC-III) 1:4 stoichiometry र DPC (III) र oxacillin बीचको प्रतिक्रिया (OXC: DPC-III) 1:4 stoichiometry देखायो।

प्रत्येक अक्सीकरण (रिडक्सन–अक्सीडेसन) प्रतिक्रियाका उत्पादनहरू स्पट टेस्ट, CHNS, FT-IR, र LC-MS स्पेक्ट्रल अध्ययनहरूका सहयोगले पहिचान गरिएको थियो। प्रतिक्रियाहरू DPC (III) र AMP / AMX / DCLX / CRBC/ OXC साथै क्षार एकाग्रताको सन्दर्भमा आंशिक क्रमको सम्बन्धमा छद्म-पहिलो-क्रमका थिए। Periodate को थपले अक्सीकरण दरमा रिटार्डिङ प्रभाव देखायो र नकारात्मक अंशात्मक क्रमको पाइयो। मोनोपेरियोडाटोक्युप्रेट (MPC-III) क्षारीय माध्यममा [Cu $(H_2IO_6)(H_2O)_2$] वा [Cu $(H_3IO_6)(H_2O)_2]^+$ को रूपमा मुख्य सक्रिय रहेको पाइयो। UV/Visible spectrophotometer बाट सङ्कलन गरिएको absorbance लाई uncatalyzed (k_U) दर स्थिर, उत्प्रेरित (k_c) दर स्थिराँक र त्यसपछि कुल दर स्थिराँक (k_T), उत्प्रेरक स्थिराँक (K_C) र स्लो स्टेप दर (k) स्थिराँकमा रूपान्तरण गरिएको थियो । यी डाटाहरू बियर-

लाम्बर्टको नियम प्रमाणित गर्न प्रयोग गरियो र अर्डर रेखाचित्र, प्रमाणीकरण रेखाचित्रहरू आदि बनाइयो। कम्पलेक्स संरचनाको लागि विभिन्न अक्सीकरण प्रतिक्रियाहरूको स्टोइचियोमेट्री चाहि Job's विधिबाट निर्धारण गरिएको थियो। stoichiometry र FT-IR, LC-MS र CHNS जस्ता अन्य प्रमाणहरूमा निर्भर गर्दै, प्रत्येक अक्सीकरण प्रतिक्रियाको लागि एक सम्भावित प्रतिक्रिया संयन्त्र पनि प्रस्ताव गरिएको थियो। विभिन्न सन्तुलन स्थिरांक (K_1, K_2, र K_3) गणना गरियो। यी रेखाचित्रहरूबाट प्राप्त Slopes र Intercepts का सहयोगले Activational स्थिराँक चर सक्रियता र थर्मोडायनामिक प्यारामिटरहरू गणना गरियो।

LIST OF ACRONYMS AND ABBREVIATIONS

ABBREVIATIONS		FULL FORM
A_{cm}	:	Absorbance values of quencher at an emission wavelength
A_{cx}	:	Absorbance values of quencher at an excitation wavelength
AMP	:	Ampicillin
AMX	:	Amoxicillin
CRBC	:	Carbenicillin
DCLX	:	Dicloxacillin
OXC	:	Oxacillin
DMSO	:	Dimethylsulfoxide
DPC (III)	:	Diperiodatocuprate (III)
MPC (III)	:	Monoperiodatocuprate (III)
ESR	:	Electronic spin resonance
FT-IR	:	Fourier Transform Infrared Spectroscopy
IR	:	Infra Red
LC-MS	:	Liquid Chromatography Mass Spectroscopy
OXC	:	Oxacillin
PADs	:	Penicillanic Acid Derivatives
KOH	:	Potassium hydroxide
$H_2IO_6^{3-}$	:	Monoperiodatocuprate (triprotic)
$H_3IO_6^{2-}$	:	Monoperiodatocuprate (di-protic)
KIO_4	:	Potassium periodate
m/z	:	Mass by charge ratio

LIST OF SYMBOLS

SYMBOL		FULL FORM
€	:	Molar absorption coefficient
$\Delta G^{\neq}$	:	Free energy of activation
ΔG°	:	Standard free energy change
$\Delta H^{\neq}$	:	Enthalpy of activation
ΔH°	:	Standard enthalpy change
$\Delta\lambda$	:	Difference between excitation and emission wavelength
$\Delta S^{\neq}$	:	Standard entropy change of activation
ΔS°	:	Standard entropy change
A	:	Arrhenius Frequency factor / Collision frequency
C	:	Concentration
°C	:	Degree Centigrade/ Celsius
Co (III)	:	Cobalt metal with trivalent oxidation state (+3)
D	:	Dielectric constant
Ea	:	Energy of activation
H	:	Planck's constant
I	:	Ionic strength
k	:	Slow step rate constant
K	:	Kelvin
K_1	:	First equilibrium constant
K_2	:	Second equilibrium constant
K_3	:	Third equilibrium constant
k_C	:	Catalyzed rate constant
K_C	:	Catalytic constant
K_{eq}	:	Equilibrium constant
k_{obs}	:	Observed rate constant
k_T	:	Total rate constant
k_U	:	Uncatalyzed rate constant
λ_{max}	:	Maximum wavelength

R	:	Universal gas constant
R	:	Regression coefficient
S	:	Standard deviation
T	:	Temperature
[ ]	:	Concentration /Molarity

LIST OF TABLES

LIST OF FIGURES

LIST OF SCHEMES

APPENDIX

Title

Derivation of the rate constant from absorbance

Equations for calculation of activation parameters

Rate constant derivation for the oxidation of AMP

Rate constant derivation for the oxidation of AMX

Rate constant derivation for the oxidation of DCLX

Rate constant derivation for the oxidation of CRBC

Rate constant derivation for the oxidation of OXC

TABLE OF CONTENTS

CHAPTER 3

CHAPTER 4

CHAPTER 1

1. INTRODUCTION

1.1 General Perspective

Nature is widely concerned with numerous changes taking place every moment and chemistry is greatly related to the investigation of such changes occurring in nature. Every change is accompanied by the inter-conversion of one kind of chemical with well-defined properties into other chemicals with different properties suffering through simple or complex chemical reactions. In recent years, the study of chemical reactions, concerned with the formation of new substances from a given set of reacting species under suitable conditions, is always an interesting field of research for chemists. The steady-state approximation of Bodenstein and Lind, the Lindeman mechanism involving activated molecules for unimolecular dissociation, and the Michaelis-Menten plot or multi-step mechanism for enzyme kinetics are some milestones in the history of chemical kinetics that are connected with developing more realistic mechanisms.

The fundamental idea of chemical affinities, which emerged from the ancient and medieval alchemy and naturalism doctrine, is that chemical interaction is made simpler when there is similarity between them. At the end of the 17^{th} century, this intuitive principle becomes a theory, although quantitative, which justifies and classifies possible interactions between different chemicals. Hence, it becomes quite necessary to understand the reaction rate, mechanism, and influencing factors by which chemical reactions occur. The rate of reactions spans an enormous range, from which some complete within a fraction of a second like an explosion, precipitate formation, or complex formation, while some take thousands of years in the formation of diamond or other minerals in our earth's crust. H. Eyring and M. Polanyi developed a theory based on reactions in microscopic systems of individual molecules. When a molecule is provided a sufficiently high temperature, it reacts incredibly fast which led to introducing the concept of the energy barrier. A. Zewail performed a series of experiments that led to the

introduction of Femtochemistry, and involved the capturing of the existence of reacting species just at the transition state. Prof. R. A. Marcus (Nobel laureate in 1992) for "Electro Transfer Reactions", Prof. Ahmed Zewail (Nobel laureate in 1999) for the discovery of "Femtochemistry", Royji Noyori, K. B. Sharpless, and Prof. William Knowles (Nobel laureate in 2001) for their work on "Chirally Catalyzed Hydrogenation Reaction", Prof. Robert Grubbs, Richard Schrock and Yves Chauvin (Nobel laureate in 2005) for their work on "Metathesis Catalyst Technology" emphasized the importance of research field of reaction kinetics, and hence encouraged thereafter.

Researcher Henry Taube (Taube, 1967) performed research work in the redox system unequivocally and described the transport of electrons from the reducing agent to oxidizing agent. Outer sphere and outer sphere types (Eberson & Shaik, 1990) are the two general classes of transition stages occurring in reduction-oxidation reactions involving metal complexes. According to the Franck-Condon principle, an electron should have the same energy in both places prior to moving between two ions (Zuckerman, 1986). In the outer-sphere mechanism, reactants must get close together for tunneling to occur bond stretching and compressing by obeying Franck- Condon principle. The inner sphere mechanism must fulfill three steps as i) Substitution to form a bridge between reductant and oxidant ii) Reasonable electron transfer and iii) Separation of products (often with the transfer of the bridging ligand). An inner-sphere mechanism shares a ligand transitorily in their inner or primary coordination spheres forming a bridged intermediate-activated complex. Henry Taube, who discovered the inner sphere mechanism, received the 1983 Nobel Prize in chemistry for his groundbreaking research.

The summary of a very historic finding appears in the seminal publication: Taube's classical 1953 experiment (Taube *et al*., 1953).

$$[Co\ (NH_3)_5Cl]^{++} + [Cr\ (H_2O)_6]^{++} + 5H_2O \rightarrow [Co\ (H_2O)_6]^{++} + [Cr\ (H_2O)_5Cl]^{++} + 5\ NH_3$$

Electron transfer across a bridging group is**:-**

$[Co\ (NH_3)_5Cl]^{++} + \quad [Cr\ (H_2O)_6]^{++} \quad \rightarrow \quad [Co\ (NH_3)_5(H_2O)]^{++} + [Cr\ (H_2O)_5Cl]^{++}$

The chemical dissociation of a neutral molecule into two free radicals known as homolytic fission occurs when the bonding electrons are distributed symmetrically to each partner. Electrons may be removed singly from organic molecules forming free radicals leading to a chain reaction, dimerization, or disproportionations. Reactions in heterolytic fission can be explained by a series of basic mechanistic categories. The nucleophilic substitution (S_{N1} and S_{N2}), addition-elimination (E_1, and E_2) reactions are the basic mechanistic subtypes that are well-explained in introductory organic chemistry. With arrow pushing, each of these mechanistic subtypes can be illustrated. In heterolytic fission, oxidants attack the exposed electron pairs or loosely held pie electrons to yield molecular or ionic products in one or more subsequent steps, and chain reactions hardly ever result from them. Such reactions may involve electron transfers as required by the active site of the oxidant and reductant in one or several steps.

1.2 An Overview of Chemical Kinetics

Chemical kinetics is a unifying branch of chemistry that deals with fundamental facts and theories relating to rates and mechanisms of chemical reactions from macroscopic as well as microscopic points of view (Upadhyay, 2006). Chemical kinetics does not deal with direction or the spontaneity of reactions; it is concerned with thermodynamics which deals nothing with rate. Chemical kinetics relates to many aspects of engineering, biology, geology, cosmology, psychology, and many other fields along with far-reaching implications. Chemical kinetics includes the analysis of experimental data to shape a systematic collection of information that summarizes all the quantitative as well as qualitative kinetic information about any desired reaction.

Important steps in any kinetic investigation (Wright, 2004) can be listed as:-

i) Collection of kinetic and spectral data
ii) Establishment of the relationship between rate and reaction mixture composition

iii) Study of structural effects

iv) Characterization of oxidation products and intermediate detection

v) Development of a plausible reaction mechanism through the collected data

Many scientists developed different theories related to kinetics and reaction rates. Arrhenius (Zewail, 2000) (Nobel laureate in chemistry, 1903), inspired by Van't Hoff (1st Nobel laureate in 1901) presented a simple formula for reaction rate as a function of temperature as, $k = Ae^{\frac{-Ea}{RT}}$, where 'Ea' is the energy of activation, 'R' is the universal gas constant, 'T' is the absolute temperature and 'A' is a pre-exponential factor or Arrhenius factor, referred to as collision frequency for macroscopic systems only. Most transition metals, including iron, copper, and cobalt, have stable oxidation states that differ by one electron and interact with one another in a single equivalent step. Some other metals like Arsenic, Antimony, etc. differ by two electrons. Hence, this pattern of reactivity classifies reactions into complementary and non-complementary reactions.

1.2.1 Complementary Reactions

In complementary reactions, the oxidizing and reducing agents both undergo two equivalent changes or one equivalent change, and the reactions follow a bimolecular rate order. Electron transfer occurs in one step or two steps of one electron each. For example, in thallium [(Tl (I) -Tl (III)] exchange reaction, electrons are transferred in a single step due to the formation of intermediates, and thallium (II) is not detected during the reaction. Oxidation of arsenic [As (III)] and antimony [Sb (III)] are exceptional reactions (Sharma and Gupta, 1972). As (IV) is hypothetically made in the same way as in reaction (i), and two further intermediates, As (II) and As (IV), interact with one another before diffusing out of a solvent cage in which they are produced.

i) One equivalent- one –equivalent reactions

$$\text{As (III)} + \text{Tl (III)} \rightleftarrows \text{Tl (II)} + \text{As (IV)}$$

$$\text{As (IV)} + \text{Tl (III)} \rightarrow \text{Tl (II)} + \text{As (V)}$$

$$Ce\ (III) + Co\ (III) \rightarrow Ce\ (IV) + Co\ (II)$$

ii) Two equivalent-two equivalent reactions (Chalk et.al., 1959)

$$U\ (IV) + Tl\ (III) \rightarrow U\ (VI) + Tl\ (I)$$
$$Sn\ (II) + Hg\ (II) \rightarrow Sn\ (IV) + Hg\ (0)$$

1.2.2 Non-complementary Reactions

Such reactions lead to the formation of unstable oxidation states as well as unequal equivalent changes in the oxidant and reductant. For example, one equivalent oxidant reacts with two equivalent reductants and vice versa. In non-complementary reactions involving the nature of both the oxidant and the reductant, electron transfer reactions are very likely to occur. One of the most frequently occurring kinetic schemes was mentioned by Gupta & Sharma (1973).

$$Cr\ (VI) + Fe\ (II) \rightleftarrows Cr\ (V) + Fe\ (III)$$

Chromium reacts with Iron [Fe (+2)] ion in the rate-determining step by one of the following schemes:-

(i) $Cr\ (V) + Fe\ (II) \rightarrow Cr\ (IV) + Fe\ (III)$ Slow reaction

$Cr\ (IV) + Fe\ (II) \rightarrow Cr\ (III) + Fe\ (III)$ Rapid reaction

(ii) $Cr\ (V) + Fe\ (II) \rightarrow Cr\ (III) + Fe\ (IV)$ Slow reaction

$Fe\ (IV) + Fe\ (II) \rightarrow 2Fe\ (III)$ Rapid reaction

1.2.3 Multi-equivalent Reactions

Several transition metals, including chromium (Cr) and manganese (Mn), undergo repeated shifts of +3 and +5 units in their oxidation states during reactions in acidic media because of their unstable oxidation states. According to Christensen *et al*. (1973),

reactions of Cr (VI) with transition metal complexes typically take place in sequential one-electron steps. Electron transfer reactions proceed by (i) Michaelis principle of compulsory univalent oxidation steps (Michaelis *et al*., 1981) and (ii) Shaffer's principle of equivalent changes (Halpern, 1959).

1.2.4 Unstable Oxidation States

Thallium (II) by Fe (II) (Falcinella *et al*., 1975) and Cr (VI) by Tl (I) (Gokavi & Raju, 1987) are two examples of extremely reactive intermediates that develop during a non-complementary process, and their development can only be described by the appearance of unstable Tl (II) species. Catalysis by other transition metals like silver (I) (Gemeay *et al*., 2007), copper (III) (Hiremath & Nandibewoor, 2006), silver (III) (Malode *et al*, 2010) also involve unstable oxidation states in red-ox reactions.

1.2.5 Effect of Ions on the Rate of Reaction

The amount of other ions in the solution has a significant impact on how quickly redox reactions proceed. During similar reactions if the reductant is complexed, it becomes more stable in the oxidized form and the rate increases. An anion facilitates the easy approach of two cations; in the transition state, it may be even more effective if an anion is present between the two cations. However, if the oxidant is first complexed, the anion may stabilize by slowing down its rate. By generating sulphate complexes, the rate of Ce (IV) oxidation is slowed down (Savanur *et al*., 2009). Sangal (2020) has provided an illustration of the relationship between ionic strength and reaction rate.

1.2.6 Active Species and Selection of DPC (III) as Oxidant

All species may not be regarded active for a given reaction when a specific species, such as an oxidant, a reductant, or a catalyst, can exist independently in an aqueous medium. Species, which participate in the slow step and support to determine the rate of the reaction, can have an impact on the reaction. The nature of the active species will be

determined by the reaction conditions (Hosahalli *et al*., 2010). DPN (IV) contains Ni which is more carcinogenic for humans than Cu of DPC (III). Since DPA (III) contains Ag, it becomes quite expensive. After completion of reaction, Ag^{+} ion is left as reduced species that may interact with oxides and other side products by which isolation of main products may be difficult. As Cu^{3+} is highly reactive due to inter-conversion into Cu^{2+} ion, DPC (III) is selected as oxidant. The stability of some trivalent copper complexes was discussed by Lister (1953).

1.2.7 Catalytic Activity

Moelwyn- Hughes (Moelwyn-Hughes, E. A., 1947) established a relationship between uncatalyzed and catalyzed rate constant as- $k_T = k_U + K_c \times [\text{Catalyst}]^x$, where x represents the order of the reaction for the catalyst and k_T stands for the pseudo-first-order rate constant, k_U for the uncatalyzed rate constant, and K_c for the catalytic constant. The rate of reaction speeds up as the temperature rises, supporting an increase in the rate constant and catalytic constant. In this study, 'x' has a value of unity, or x = 1. Hence, determination of the catalytic constant becomes possible by the relation:-

$$K_c = \frac{(k_T - k_U)}{[\text{Catalyst}]^x} = \frac{k_T - k_U}{[\text{Co(III)}]} = \frac{k_c}{[\text{Co (III)}]}$$ [Since (x) = 1 for pseudo-first-order reaction].

1.3 Penicillanic Acid under Investigation (β-lactam Antibiotics)

Penicillanic acid is a penam that consists of 3, 3-dimethyl-7-oxo-4-thial-1-azabicyclo [3.2.0] heptanes bearing a carboxyl group at position 2 and having (2S, 5R) configuration. Its molecular formula is $C_8H_{11}NO_3S$ and molecular mass is 201.25 amu. It is a building block of penicillin, devoid of significant antibacterial activity. The word antibiotic (Gould, 2016) came from the word *Antibiosis*, a term coined by Louis Pasteur's pupil Paul Vuillemin in 1889 A.D. According to Waksman (1942 AD), antibiotics are chemical compounds produced by a variety of microorganism species, including fungi and bacteria, that have the ability, in small concentrations, to eradicate, kill, or impede the growth of other microorganism species. Figures 1 & 2 represent the basic structures of penicillin and amino-penicillin respectively.

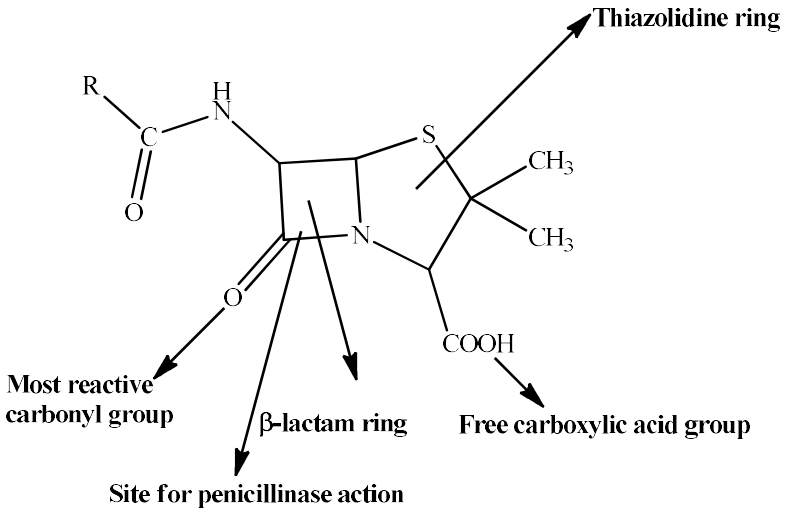

Figure 1: Structure of penicillin

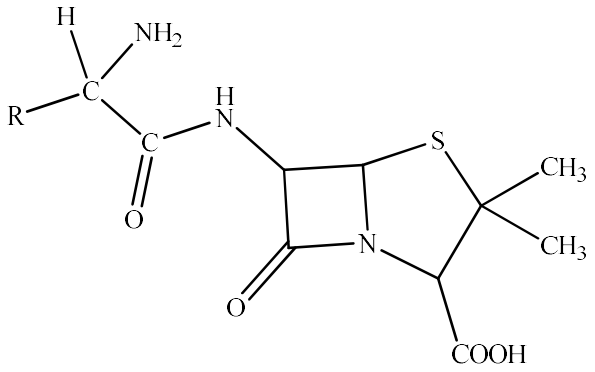

Figure 2: Structure of amino-penicillin

, where R = Ph for ampicillin & R = Ph-OH for amoxicillin

1.3.1 Penicillanic Acid Derivatives (PADs) or Semi-Synthetic Antibiotics

Ampicillin, amoxicillin, oxacillin, dicloxacillin, carbenicillin, methicillin, etc. are some examples of penicillanic acid derivatives (PADs) or semi-synthetic β-lactam antibiotics (Michael, 1984). Ampicillin and amoxicillin are amino penicillin while Carbenicillin and ticarcillin are carboxypenicillins (Raynor, 1997).

1.3.2 Broad and narrow-spectrum antibiotics or PADs

Both gram-positive and gram-negative bacteria that cause disease are susceptible to the effects of broad-spectrum antibiotics (Ory, 1963). Narrow-spectrum antibiotics are effective mainly against a single species of microorganisms either gram-positive or gram-negative bacteria like bacitracin, penicillin, nystatin, etc. Saleh & Alotaibi (2018) have mentioned the comparison of broad-spectrum and narrow-spectrum antibiotics to treat lower extremity cellulitis.

1.3.3 Characteristics of Penicillanic Acid Derivatives (PADs)

1. It should not produce adverse, and side effects that should be removed from the body.
2. It should have a wide spectrum of activity, and highly effective in low concentration.
3. It should be non-allergenic to the host, and capable to reach the infected site of the body easily.
4. It should be chemically stable, inexpensive, and easy to manufacture and active against many pathogenic organisms.

Hermann Staudinger created the first synthetic β-lactam in 1907 by cycloadditionally reacting aniline and benzaldehyde Schiff bases with diphenylketone. Up to 1970, most β-lactam research was focused on penicillin. Ampicillin is regarded as first-generation under cephalosporin (Abraham, 1987).

The penicillin nucleus consists of:-

i) Thiazolidine ring contains a sulphur atom with a carboxyl group.
ii) The side chain of the β-lactam ring is attached at position - 6 (NHCOR) through an amide linkage.

The basic structure of penicillanic acid is given in Figure 3.

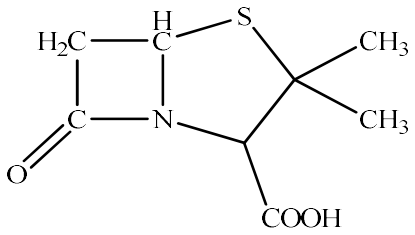

Figure 3: Structure of penicillanic acid

1.4 Some Penicillanic Acid Derivatives (PADs)

1.4.1 Ampicillin

It was discovered in 1958 and brought into use in 1961(Fischer *et al*., 2006). It acts as an antibacterial drug (Enrique, 2011). It can penetrate gram-positive and gram-negative bacteria (Delcour, 2009). Due to its moderate stability in acid and lower toxicity, it is also applied in chemotherapy (Alekseev & Samuilova, 2008). Its molecular formula and molar masses are $C_{16}H_{19}N_3O_4S$ and 349.4 g / mole respectively. Figure 4 represents the structure of ampicillin.

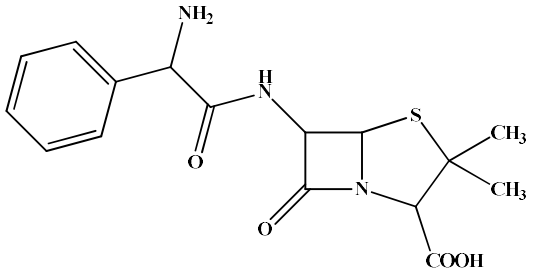

Figure 4: Structure of ampicillin

1.4.2 Amoxicillin

A broad-spectrum antibiotic, amoxicillin is active against a wide range of gram-positive and gram-negative bacteria. Aryee *et al*. (2022) have addressed the occurrence, detection and removal of amoxicillin in wastewater. Analogue-based drug discovery regarding amoxicillin has been explained (Fischer & Ganellin, 2006). Handsfield *et al*. (1973) have already addressed amoxicillin as a new penicillin antibiotic. Molecular formula and molar

masses of amoxicillin are $C_{16}H_{19}N_3O_5S$, and 365.4 g mol^{-1} respectively. Figure 5 represents the structure of amoxicillin.

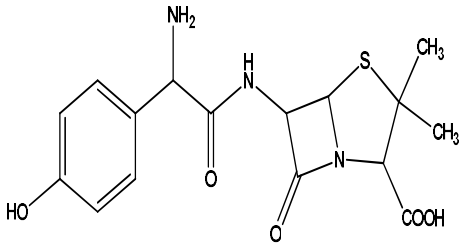

Figure 5: Structure of amoxicillin

1.4.3 Dicloxacillin

A narrow-spectrum chlorinated β-lactam antibiotic (Bush *et al*., 2019), dicloxacillin is quite effective against gram-positive bacteria and it produces *Staphylococcus aureus*. Molecular formula and molar mass of dicloxacillin are $C_{19}H_{17}Cl_2N_3O_5S$, and 470.327g mol^{-1} respectively. Figure 6 outlines its structure.

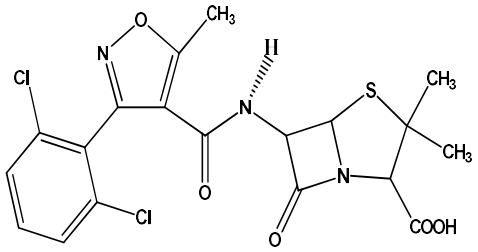

Figure 6: Structure of dicloxacillin

1.4.4 Carbenicillin

Carbenicillin (Basker *et al*., 1977) is a moderately synthetic bacteriolytic antibiotic which belongs to the carboxyl-penicillin sub-group, derived from the 6-aminopenieilIanic acid nucleus. Molecular formula and molar mass of carbenicillin are $C_{17}H_{18}N_2O_6S$, and 378.401 g mol^{-1}. Figure 7 illustrates its structure.

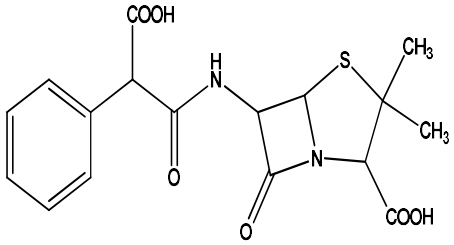

Figure 7: Structure of carbenicillin

1.4.5 Oxacillin

Oxacillin, one of the PADs, is a parenteral, 2nd generations' semi-synthetic penicillinase-resistant narrow spectrum penicillin in which the 6-aminopenicillanic acid nucleus consists of a five-membered thiazolidine ring attached to a four-membered β-lactam ring that responds to antibacterial activities. Oxacillin, a methicillin derivative, carries a 5-methyl-3-phenylisoxazole-4-carboxamide group at position 6 β-carbon, and it supports to counter infections caused by penicillin-resistant Staphylococcus aureus. It is soluble in water (88 mg/mL), ethanol, and dimethylsulfoxide (DMSO) (< 1 mg/mL) at 298 K. Its formula, molar mass, density, and boiling point are $C_{19}H_{19}N_3O_5S$, 401.44 g mol^{-1}, 1.49 g cm^{-3}, and 1177.75 K respectively. The structure of oxacillin is outlined in Figure 8.

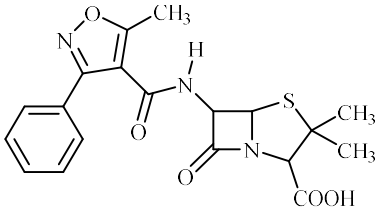

Figure 8: Structure of oxacillin.

1.5 Choice of Oxidizing Agents

1.5.1 Diperiodatonickelate (IV)

Also regarded as dihydroxydiperiodatonickelate (Hiremath *et al*., 2007) DPN (IV) contains nickel in + 4 oxidation states along with two periodate anions. Orange salt of Cobalt exists as $[Co\ (ethylenediamine)_3]_2[Ni\ (OH)_2(IO_5OH)_2]$ (Dengel *et al*., 1992). Hiremath *et al*. (2007) have explained the Ruthenium (III) catalyzed oxidation of Neurontin (gabapentin) by DPN (IV). Potassium Nickel periodates ($KNiIO_6.5H_2O$) and Sodium Nickel periodates ($NaNiIO_6.5H_2O$), which are both dark purple in color, underwent their first successful synthesis (Ray *et al*., 1946) by oxidizing nickel sulphate with sodium or potassium periodate, and potassium persulphate in boiling water. Alkali metal-nickel periodates ($MNiIO_6$) have been predicted to undergo structural, spectroscopic, and synthetic studies (Currie *et al*., 1994).

1.5.2 Diperiodatoargentate (III)

Patil *et al*. (2009) have mentioned regarding kinetics and mechanism of Diperiodatoargentate (III) or DPA (III) for Tyrosine oxidation. DPA (III) is a stable, and strong oxidizing oxygen donor complex (Hosmani *et al*., 2009). The mechanistic aspects of the Os (VIII)/Ru (III) catalyzed oxidation of L-phenylalanine by Ag(III) periodate complex in alkaline medium have been addressed by Lamani *et al.* (2009). Patil *et al*. (2009) have focused regarding Osmium (VIII) catalyzed oxidation of diclofenac sodium by DPA (III). Ray (1943) mentioned a new type of complex silver compounds with tervalent silver. Similarly, the kinetics of some amino acids' oxidative deamination was shown by Rao *et al.* (1985). Figure 9 illustrates the plausible structure of DPA (III).

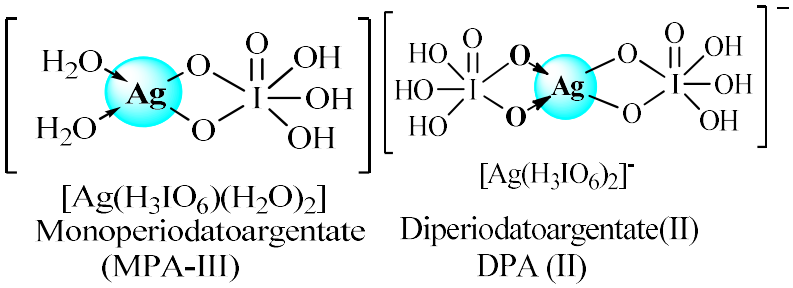

Figure 9: Structures of (mono and di) periodatoargentate (III)

1.5.3 Diperiodatocuprate (III)

Nadimpalli *et al*. (2010) identified the diperiodatocuprate (III) species in an aqueous alkaline medium by studying the oxidation of iodide ion in a kinetic and mechanistic manner. Similarly, periodates have been shown to affect the diperiodatocupratic (III) oxidation of sulphur-containing amino acids in aqueous alkaline media by Sharanabasamma *et al*. (2008). Likewise, diperiodatocuprate (III) has been reported to oxidize caffeine in an alkaline medium in the presence as well as absence of ruthenium (Thriveni *et al*., 2021; Abbar *et al*., 2010). Figure 10 lists DPC (III) and MPC (III) structures.

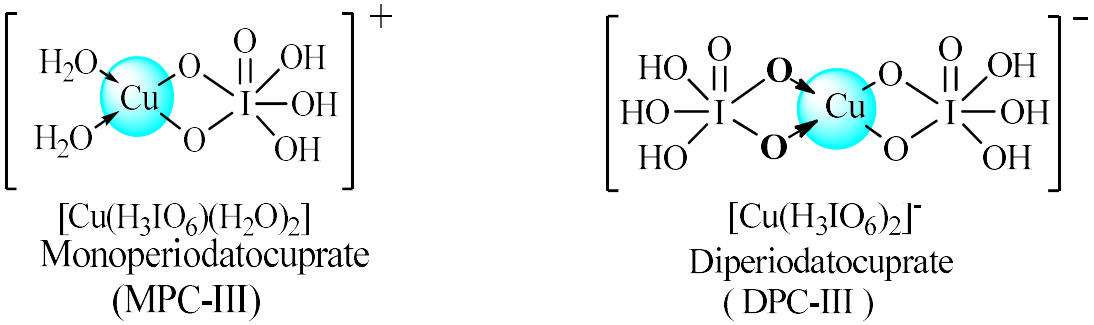

Figure 10: Structures of MPC (III) and DPC (III)

1.6 Choice of 3d Transition Metals under Investigation

1.6.1 Copper

Copper (Latin: Cuprum) is a transition metal with atomic number 29, and a molar mass of 63.5 g mol^{-1} and it belongs to Group-IB, period- IV, Block- d inside the periodic table. Red-orange colored, it is a face-centered cubic crystalline solid with a melting point of 1357.77K a boiling point of 2835.15K stable oxidation states +1 and +2. Copper (III) also exists in the form of potassium cuprate ($KCuO_2$) as a blue-black solid. Cu (III) and Copper (IV) fluorides are also detected in the form of K_3CuF_6 and Cs_2CuF_6 (McDonald *et al*., 1997). Complexes of copper (III) are identified in the reactions of organo-copper compounds (Lewis & Tolman, 2004). Levason and Spicer (1987) have studied the chemistry of Copper and Silver in their higher oxidation states.

1.6.2 Nickel

Nickel (Baldwin, W. H., 1931) is a chemical element having atomic number 28, molar mass of 58.69 g mol^{-1}, Group-VIII or 10, period –IV, d-block with a melting point of 2728.15K a boiling point of 3003.15K density 8.908 g cm^{-3} (when solid). The most common oxidation state of Nickel is + 2 but compounds of Ni^0, Ni^{+1}, and Ni^{+3} are also studied (Lascelles *et al*., 2005). Nickel is essential for Ni-enzyme like [Ni-Fe] hydrogenase. Robert–Austen (1898) utilized Mond's process to extract nickel from its ores. Frederick (1967), and Baucom *et al.* (1971) have mentioned dicarbollyl complexes of Nickel (III), and Nickel (IV) in their previous literature.

1.6.3 Cobalt

Cobalt belongs to the 3d-transition series with atomic number 27, molar mass 58.93 g mol^{-1}, Group- VIII, IV period; with a density, melting point, and boiling point are of 8.9 g cm^{-3}, 1768.15K and 3200.15K respectively. It is a hard lustrous bluish-grey metal with n electronic configuration of [Ar] $3d^7 4s^2$. Due to incomplete d-orbit, it readily undergoes

complex formation showing variable oxidation states of +1, +2, +3, +4 as well as +5 in the amphoteric oxide. It gives Co_3O_4 when heated in the air that loses oxygen at 900 °C to form CoO. Alfred Werner, the Nobel Prize winner in coordination chemistry, synthesized $[Co\ (NH_3)_6]^{3+}$ complex of cobalt as yellow gold needle-like crystals (Lewis *et al*., 2015). Photocatalytic activities, antibiofilm, and antibacterial effects of metals-substituted spinel cobalt ferrite nanoparticles have been reported (Maksoud *et al*., 2018).

1.7 Rationale of the Study & Research Gap

Rationale of study: - Various PADs and DPA (III), DPN (IV), HCF (III), and DPT (IV) as oxidants without any catalyst. The research work is continued further by selecting DPC (III) as an oxidizing agent and $CoCl_3$ (III) as a catalyzing agent to study the oxidation reaction as well as to predict plausible mechanisms of catalyzed oxidation. Similarly, PADs are crucial in antibiotic development, and their catalyzed oxidation can lead to a new derivative with improved efficacy or reduced resistance. Cobalt (III) catalyst may produce advantages over traditional methods like higher sensitivity and mild conditions which may be beneficial for preserving the integrity of sensitive compounds. The oxidation products might exhibit novel therapeutic characteristics.

Research Gap: - More detailed mechanistic studies are required to understand fully how cobalt (III) facilitates such oxidation reactions. Lack of comprehensive studies on how different parameters like pH, temperature, and solvent medium affect the oxidation process. Exploring a wider range of substrates could reveal the structure-activity relationship. Similarly, limited research on the environmental impact and safety processing the reagent like DPC (III), and catalyst cobalt (III) may bring about toxicity and environmental wastes. Such oxidation technique can also be applied for the degradation of several antibiotics/PADs in acidic medium by varying oxidants like hexacyanoferrate (III), diperiodatoargentate (III) as well as by varying catalysts like osmium (VIII), ruthenium (III) or even under different pH range. Active reactive intermediates, free radicals or products might disclose a novel mechanism if mixed with surfactants, drugs, poly-electrolytes, amino acids that might explore a new results.

1.8 Objectives

1.8.1 General Objectives

- Selection of PADs, synthesis of oxidant and complex, collection of absorbance data to study the kinetics of catalyzed oxidation of different PADs by DPC (III) within a fixed pH range

1.8.2 Specific Objectives

- To determine the proper stoichiometric ratio of PAD and DPC (III) to carry out further redox reaction.
- To collect absorbance data from UV/Visible spectrophotometer for each uncatalyzed and catalyzed reaction, and thence to determine various rate constants at different four temperatures.
- To identify the most active species of DPC (III), and to confirm stoichiometry for each PAD-DPC (III) reaction by Job's method
- To study the structural and spectral analysis of these complexes and stable products through LC-MS, FT-IR, melting point, and CHNS tests.
- To calculate different activation, and thermodynamic parameters along with equilibrium constants, catalytic constants, slow step rate constants, and catalyzed rate constants.
- To propose most suitable plausible mechanism for each PAD-DPC (III) oxidation reaction in an alkaline medium, and hence to represent a degradation process against PADs in solution form by using DPC (III) as reagent, and cobalt (III) chloride as catalyst.
- To validate of these spectral reports, elemental analysis, and melting points data with similar works carried out previously to arrive at targeted conclusion for the present research work.

1.9 Justification of Study

Penicillanic acid and its derivatives (PADs) are produced when reconstituted penicillins degrade in acidic solution under elevated temperature. Since the beginning of time, humans have been consuming PADs in medicine, animal husbandry, agriculture, cosmetics, nutraceutical products to treat bacterial infections by eradicating the activity and expansion of microbial communities for the betterment of our lives. As a result of the excretion or accumulation of such PADs into waste water, sewage plants, health care and industrial effluents, resistant mechanisms develop in these microbes. The majorities of PADs are excreted through our body in the form of urine (55-80%) and faeces (4.30%), and hence have a great potential to harm humans, flora, and fauna. Contemporary pathogenic organisms pose a terrible threat to established chemotherapeutic drugs, posing a worldwide challenge to medical science to discover and create novel antibiotics that are safe, effective, and efficient for the upcoming generation of chemists and drug designers. Several advanced oxidation processes (AOPs) have been applied for the degradation of these non-biodegradable PADs. Malatesta synthesized DPC (III) at first and Panigrahi, G. P. and A.C. Pathy followed the process. Nandibewoor, S. T. and his co-workers, as well as other researchers also gave continuity to this work by selecting different PADs and different oxidants without any catalyst. The present research work holds significant importance due to degradation technique by utilizing DPC (III), and Cobalt (III) chloride to disclose a novel application in the context of degrading non-biodegradable PADs in the aqueous alkaline medium through kinetic measurements to reduce pollution and illness by de-activating growing potentiality in future for the next generation.

The degradation of PADs or β-lactam antibiotics is generally more feasible in alkaline medium in comparison to acidic medium due to differences in chemical properties and stability factors of PADs under following conditions:-

1. Hydrolysis: - Many β-lactam antibiotics or PADs are highly susceptible to hydrolysis where PAD molecules get fractionated by addition of water leading to acceleration in alkaline medium due to facilitation by hydroxide ions.

2. Ionization: - PADs can exist in different ionized forms depending upon pH of the surrounding environment. In acidic medium, PAD molecules are more likely to undergo protonation making them more stable and resistant to degradation. Alkaline medium provides environment to exist in de-protonated form by which degradation process becomes easier.

3. Reactivity and specific degradation pathways: - Certain functional groups like amide, ester, and lactam are present within PAD molecules which are highly reactive in alkaline medium due the presence of hydroxide ions. Alkaline environment favors some of antibiotics in easy opening of their special rings like thiazolidine or lactam that supports in accelerating the rate of degradation

1.10 Limitations of the research work

The present research work owes quite importance in our daily life. However, depth studies for the anti-microbial test, and anti-oxidant test to confirm whether the oxidized products also carry anti-biotic properties or not need extra time. Similarly, the work could not be extended for the drug-protein interaction case. Lack of funding and proper testing instruments inside Nepal are the major limitations of my research work. Study of thermodynamic parameters is also possible through thermo-gravimetric analysis TGA) and differential thermal analysis (DTA) which could not be included in this research study. The research work could not be extended by including PAD with surfactant with and without polyelectrolyte. Similarly, kinetic study of PAD- amino acid in different media would be investigated experimentally with and without application of suitable catalyst.

While conducting research on the oxidation of penicillanic acid derivatives (PADs) by DPC (III) in the alkaline medium, several limitations were experienced that could affect the outcomes and interpretations of the study. Some key limitations can be pointed out as follows:-

a) pH sensitivity: - The reactions are highly sensitive to pH, which can affect the ionization state of PADs and the reactivity of DPC (III). Slight variations in pH could lead to inconsistent results.

b) Temperature control:-Temperature fluctuations can impact reaction rates and multiple equilibrium. Hence maintaining constant temperature becomes crucial for reproducibility.

c) Concentration effects: - The study could only be valid within specific concentration ranges for DPC (III) and PAD molecule. At higher or lower concentration ranges, substrate inhibition or aggregation might occur that may change reaction kinetics pattern leading to misleading conclusions.

d) Catalyst stability or deactivation of catalyst:-Cobalt (III) chloride may undergo deactivation over specified time period affecting its efficacy and reproducibility of results.

e) Accurate measurement of concentration by UV-Visible spectrophotometer may prove challenging in complex mixture due to overlapping spectra. Similarly, use of hazardous chemicals like DPC (III) in alkaline medium should be handled properly.

f) The potential environmental impact of using strong oxidants must be considered properly owing to toxic nature of by-products.

g) Proper usage of triple distilled water in washed and dried instruments is a must throughout the research work.

h) Presence of side reactions and un-expected by-products due elevated pH can complicate the reaction kinetics and mechanism.

CHAPTER 2

2. REVIEW OF LITERATURE

2.1 General Overview

A unique molecule known as penicillin has a strained β-lactam ring fused to a thiazolidine ring which is subject to cleavage by a variety of nucleophiles, acid-base reagents, metal ions, oxidizing agents, as well as suitable solvents or enzymes (Mukherjee & Singh, 1978).

As β-lactam is unstable in the aqueous solution, synthesis of new penicillanic acid derivatives and revolutionary development of existing penicillanic acids proved a major challenge before chemists and researchers. Lister and Sanderson had noticed the penicillin producing mould in 1911 by using fungal culture extract as claimed. Observation from the pioneering work by Ernest Boris Chain and Howard Walter Florey in 1940 (Chain *et al*., 1940; Gaynes, R., 2017) for the commercial production, and pronounced antibacterial activity of penicillin coupled with its low toxicity was the real beginning era of penicillin. The continuous research in chemistry and biology for penicillin led to extending the industrial and medicinal applications by a joint Anglo-British venture in 1941. Primitive penicillanic acid derivatives like streptomycin, chloramphenicol, neomycin, etc. proved the major successful outputs of that timework of metabolites isolated from soil samples that helped to develop newer penicillin-like 6-aminopenicillanic acids (Sheehan *et al*., 1957) which are devoid of biological activity but the key nucleus of all penicillanic acid derivatives. Amoxicillin, methicillin, oxacillin, dicloxacillin, carbenicillin, etc. belong to the penicillanic acid derivatives group while ampicillin belongs to the 1st generation cephalosporin group.

Penicillin can be classified as:

1. Natural penicillin-like penicillin- G & penicillin-V
2. Semi-synthetic penicillin-like methicillin, oxacillin, dicloxacillin
3. Extended-spectrum penicillin-like

3.1 Amino-penicillin like ampicillin, amoxicillin

3.2 Carboxy-penicillin like carbenicillin, ticarcillin

3.3 Ureido-penicillin like pipericillin, mezlocillin

3.4 Amidino-penicillin like mecillinam

Penicillin is a trading name that is given to six natural compounds with formula $C_9H_{11}N_2O_4SR$ differing from 'R' group as tabulated in Table 1.

Table 1: Classification of penicillin

R	Chemical Name	Other Name
- $CH_2CH=CHCH_2CH_3$	Pent-2-enylpenicillin	Penicillin I / F
-$CH_2C_6H_5$	Benzylpenicillin	Penicillin II / G
-$CH_2C_6H_4OH$ (p)	p-hydroxy benzylpenicillin	Penicillin III/ X
-$(CH_2)_6CH_3$	n-heptyl penicillin	Penicillin IV/K
-$(CH_2)_4CH_3$	n- amyl penicillin	Penicillin F
-$CH_2OC_6H_5$	Phenoxymethyl penicillin	Penicillin V

Antibiotics or drugs exert specific diverse physiological outcomes of therapeutic value that should be confined to a site in the body after administration to the host; this is the basis of Chemotherapy, contrived by Paul Ehrlich in 1990. Antibiotics are the most popular and extensively applicable class of drugs that play a vital role in the bacterial chemotherapy owing to their low mammalian toxicity, high potency and broad-spectrum activity due to desirable medicinal applications as chemotherapeutic agents, abundant rich chemistry and structural novelty (Fechtig *et al*., 1968).

Over the last few decades, researchers are attempting continuously to establish new pathways for prudent synthesis (Shivprasad, 2011). Since time immemorial, potent biochemical from plants are being utilized by converting them into marvelous assortments of multiple applications in various sectors like pharmacy, chemical research, dyes, pesticides, cosmetics, fragrances, nutraceutical products (Daughton & Ternes,

1999). Similarly, various pharmaceuticals and personal care products (PPCPs) are widely applied in our modern lives to improve the quality of personal health, and the growth of humans, and other organisms (Ellis, 2006), (Liu *et al*., 2023). Trace level antibiotics causing environmental pollution has been reported (Addis *et al*., 2024). Similarly, Fawzy & Alqarni (2020) have reported the oxidative degradation of some antibiotics by permanganate ion in alkaline medium. Ramotowska *et al*. (2020) have explained the comprehensive approach to antibiotic-metal complexes. Residues of such products may accumulate from pharmaceutical industries, hospital effluents (Lindberg *et al*., 2007), sewage treatment plants (Gulkowska *et al*., 2008), veterinary drugs, domestic waste, fertilizers, junk food-stuffs, heavy metal sediment (Kaizal *et al*. 2023), etc. Among them, antibiotics are extensively used to treat diseases and infections as well as in feed additives to promote the weight gain and growth of livestock (Larsson *et al*., 2007), (Kalli *et al*., 2023). Excretion of the metabolized and non-metabolized forms of antibiotics from animal bodies may enter into the water stream (Eckert *et al*., 2018), contamination in wastewater (Fatta-Kassinos *et al.*, 2011), groundwater and fish ponds (Avisar *et al*., 2009), drinking water, tap water, seawater, sediments, and soil might produce antibiotic-resistant bacteria as well as antibiotic-resistant genes by Guan *et al*. (2018), Wang *et al*. (2023), and damage internal organs of aquatic animals (Martinez, 2009). Gowda *et al.* (2015) have mentioned the spectroscopic and mechanistic investigations into the oxidation of aspartame by diperiodatocuprate (III) in aqueous alkaline medium. Cosmetic wastewater treatment using the Fenton, Photo-Fenton, and H_2O_2/UV processes has been documented (Marcinowski *et al*., 2014) & (Ikehata *et al.*, 2008). Ibrahim et al. (2022) have studied the novel synthesis of antibacterial pyrone derivatives like azithromycin. Consumption of such contaminated soil and water may result in food pollutants inside tissues and may trigger terrible allergic reactions inside the human body (Cabello *et al*., 2006). Antibiotic residues found in surface water, groundwater, and soil that have been overused and misused may increase the prevalence of antibiotic-resistant genes in the environment (Gao *et al*., 2018). Antibiotic-resistant genes are worse emerging contaminants because they pose a direct and serious threat to public health and food security because they can spread horizontally through the food production chain and water stream, as mentioned by Hughes *et al*. (2012), Guo *et al*. (2019), and Escher *et al*.

(2011). Several techniques are being applied to treat antibiotic contaminated water matrix like advanced oxidation process (AOPs) (Deng *et al*., 2015), degradation kinetics and mechanism of β-lactam antibiotics by the activation of H_2O_2 and $Na_2S_2O_8$ under UV-254 nm irradiation (He *et al*., 2014), prediction of hydrolysis pathways and kinetics for antibiotics under environmental conditions: a quantum chemical study on cephradine (Zhang *et al*., 2015), kinetics and thermodynamics studies of oxy-tetracycline mineralization using UV/H_2O_2 (Rahmah *et al*., 2012), waste water treatment (Herberer, T., 2002), (de Ilurdoz *et al*., 2022). Similar technologies for removing pharmaceuticals and personal care products (PPCPs) from aqueous solutions have been discussed by (Liu *et al*., 2023; Gajdos *et al*., 2023). Leone *et al*. (2019) have mentioned new antibiotics essential for treatment of serious infections in intensive care unit patients. Applications of veterinary antibiotics and their potential human health risks have been described (Mo *et al*., 2015), (Hassan *et al*., 2021).

2.2 Literature for ampicillin

The three soluble periodate complexes of copper are monoperiodatocuprate (MPC), diperiodatocuprate (DPC), and triperiodatocuprate (TPC), with DPC (III) as [Cu (H_2IO_6). The pair of copper (II) and copper (I) has been investigated (Kulkarni *et al*., 2006). Several media have reported on the optimization of the ampicillin oxidation process using hydrogen peroxide and potassium dichromate (Yahya, 2015). It has been reported that potassium hydrogenperoxomonosulphate can be used to determine the amounts of ampicillin and oxacillin quantitatively in the "Ampiox" preparation (Karpova, 2013). Chemiluminescence detection has been examined for the determination of amoxicillin, ampicillin, and penicillin G utilizing a flow injection analytical approach (Chivulescu *et al*., 2011). The effects of dissolved oxygen and pH have been described for Cu (II)-catalyzed breakdown of ampicillin (Guo *et al*., 2018). Shetti *et al*. (2009) have described the stopped flow technique, oxidation of the ampicillin antibiotic by copper (III) complex have been described.

According to Shokri *et al*. (2019), the enhanced oxidation process effectively removes ampicillin from aqueous solutions. Ampicillin oxidation as a special electron source by a denitrifying sludge was evaluated physiologically and kinetically by Yeny *et al*. (2022).

Electrocatalytic analysis of ampicillin using carbon-paste electrode modified with ferrocendicarboxylic acid was described by Khalilzadeh *et al*. (2009). The spectrophotometric determination of ampicillin with sulfanilic acid by oxidative coupling reaction has been described by Darweesh *et al*. (2020).

2.3 Literature for amoxicillin

Veena *et al*. (2015) looked into how chloramine-T oxidized amoxicillin in an acidic medium. Amoxicillin's oxidative degradation by thermally activated persulphate was explained by Zhao *et al*. (2019). The Fenton treatment of the antibiotics amoxicillin and cloxacillin was optimized according to Affam *et al*. (2013); Ay and Kargi (2010). Trovo *et al.* (2011) demonstrated how the photo-Fenton mechanism breaks down the antibiotic amoxicillin by chemical and toxicological analysis. Bian *et al*. (2019) addressed the electrode characterization, operating parameter optimization, and degradation process for the electrochemical removal of amoxicillin utilizing a Cu doped PbO_2 electrode. Petcu *et al*. (2020) discover hierarchical zeolite Y containing Ti and Fe oxides as photo-catalysts for amoxicillin degradation. Guerra *et al*. (2019) have discussed the oxidation mechanisms of amoxicillin and paracetamol in the photo-Fenton solar process. Herlina *et al*. (2018) investigated the use of Pt, Pt/Co, and $Pt/Co(OH)_2$ electrodes in the electrochemical oxidation of amoxicillin with Co (III) as the mediator in an acidic medium. The destiny, transformation, and mineralogical effects of amoxicillin's heterogeneous photo-catalysis under ambient settings and high-intensity light have been described by Ellepola *et al*. (2022). Li *et al*. (2012) have insighted the photo-degradation of amoxicillin by catalyzed Fe^{3+}/H_2O_2 process. The electrochemical oxidation of amoxicillin in its medicinal formulation at boron doped diamond (BDD) electrode has been studied by Quand-Meme *et al*. (2015). The activation of peroxymonosulphate into amoxicillin degradation has been addressed by Lashkaryani *et al*. (2019) by cobalt ferrite nanoparticles anchored on graphene ($CoFe_2O_4$@Gr). Barbooti (2020) has explained the removal of amoxicillin from water by adsorption method.

2.4 Literature for dicloxacillin

Mejia *et al*. (2022) reported on the investigation of a helicoidal flux photoreactor used to degrade dicloxacillin by UV-C/H_2O_2 and UV- A/photo-Fenton in addition to the impact of photon absorption. Bhinge and Malipatil (2016) provided details on the development and endorsement of a stability-indicating strategy for the simultaneous evaluation of cefixime and dicloxacillin using the RP-HPLC method. Dicloxacillin has been shown to facilitate CYP2C- and CYP3A-mediated drug metabolism both in vivo and in vitro by Stage *et al*. (2018). According to Acharya & Patel (2013), amoxicillin and dicloxacillin can be measured simultaneously using an RP-HPLC method in both bulk drugs and capsules. The impacts of water matrices during the sonochemical degradation of the antibiotic dicloxacillin were discussed by Villegas-Guzman *et al*. (2015). The kinetic and equilibrium investigations for the biosorption of dicloxacillin from pharmaceutical waste water using tannin from Indian almond leaf have been investigated by Sunsandee *et al*. (2020). Programmed humidifying studies by Xiao-Dong *et al*. (2005) were used to explain the stability of dicloxacillin sodium. Patil *et al*. (2014) have explained about development and validation of RP-HPLC method for simultaneous estimation of amoxicillin and dicloxacillin in bulk drug and capsules.

2.5 Literature for carbenicillin

Meti *et al*. (2016) reported on the electro-analytical uses of carbenicillin's voltammetric oxidation at the gold electrode. Davies *et al*. (1975) explained how carbenicillin and ticarcillin interact with gentamicin. Holt *et al*. (1976) addressed the relationship of carbenicillin with aminoglycoside antibiotics. Pharmaceutical aspects of the administration of carbenicillin were covered by Lynn (1973). The clinical experience with indanyl carbenicillin in treating urinary tract infections was documented by Giamareilou *et al*. (1976). The bacteriological, pharmacological, and clinical research of carbenicillin has been described by Meyers *et al*. (1970). Richardson *et al*. (1968) detailed their experiences with carbenicillin to treat meningitis and septicemia. The morphological and cytological effects of carbenicillin on Pseudomonas pseudomallei were reported by Dilworth *et al*. (1974). In a prospective, randomized, double-blind

research published in 1980, Stuart *et al*. compared the efficacy of carbenicillin-gentamicin versus carbenicillin-trimethoprim for the treatment of infections in granulocytopenic patients. The characteristics of pseudomonas aeruginosa's carbenicillin resistance were reported by Thomas and Broadbridge (1972). Hoffman and Bullock (1970) talked about treating gram-negative bacillary infections like pseudomonas with carbenicillin. The levels of carbenicillin in the biliary system were studied experimentally and clinically by Brogard *et al*. (1974). Effect of time and concentration between Gentamycin and carbenicillin or ticarcillin has been reported (Pickering & Gearhart, 1979).

2.6 Literature for oxacillin

Giraldo *et al*. (2015) have reported the degradation of oxacillin in water by anodic oxidation with Ti/IrO_2 anodes has been evaluated. Elimination of oxacillin, its toxicity and antibacterial activity by using ionizing radiation has been investigated by Takacs *et al*. (2022). Molecularly imprinted polyaniline, gold nanourchins, and graphene oxide were reported to a screen-printed electrode to enable the voltammetric detection of oxacillin by Moghadam *et al*. (2019). Staphylococcus aureus in Central Sydney, Australia, was detected to be resistant to methicillin and oxacillin by Merlino *et al*. (2002). Serna-Galvis *et al*. (2015) compared how pharmaceutical additives affect the removal of antibiotic activity during the photo-Fenton, TiO_2-photocatalysis, and electrochemical processes used to treat oxacillin in water. Mohammadi Tabar *et al*. (2022) reported that loading penicillin and oxacillin on PEGylated-graphene oxide increases the antibiotics' ability to combat methicillin-resistant staphylococcus aureus. Oxidative degradation of some antibiotics by permanganate ion in alkaline medium in terms of kinetic and mechanistic approach was addressed by Fawzy *et al*. (2020). Goh *et al*. (2015) mentioned that methicillin-resistant bacteria are sensitive to oxacillin methicillin-resistant Staphylococcus aureus antisense peptide nucleic acids against staphylococcus pseudintermedius in vitro. Coskun *et al*. (2017) have reported the electrochemical, spectroscopic and computational studies on complexation of oxacillin with Cu (II) and Co (II).

The consumption of antibiotics or penicillanic acid derivatives in different sectors of the ecosystem and common degradation ways can be represented in Figures 11 and 12.

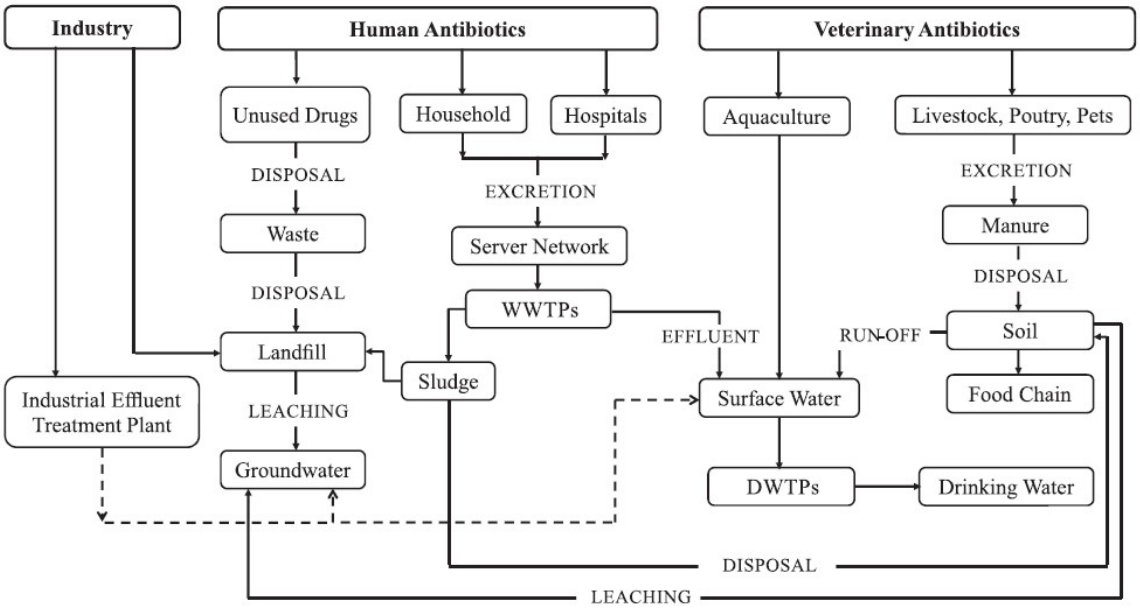

Figure 11: Flow-sheet diagram for the consumption of PADs/antibiotics
(Source: Homen & Santos, 2011)

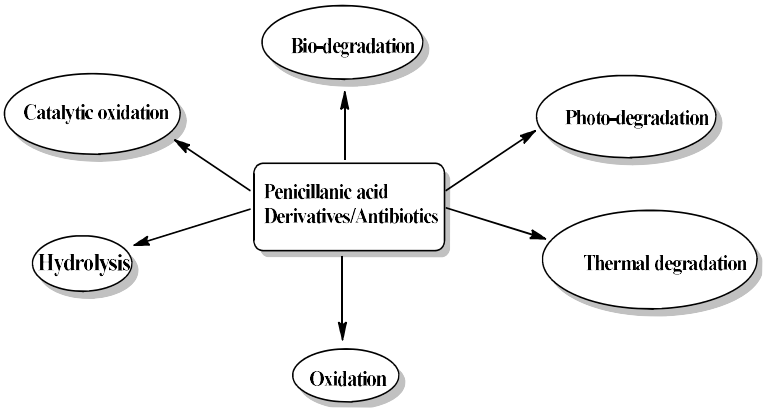

Figure 12: Flow-sheet diagram for the degradation ways of PADs/ antibiotics

2.7 Catalysis and Catalytic Applications

Berzelius coined the term catalysis in 1836 to explain different decomposition and transformation reactions. Transition metal ions are frequently different chemical reactions. Co (III) has been applied to catalyze for the oxidation of different penicillanic

acid derivatives in different media. Prof. Dr. Jens Hagen (2015) has reported some of practical approach for industrial catalysis.

i) Catalysis of amoxicillin

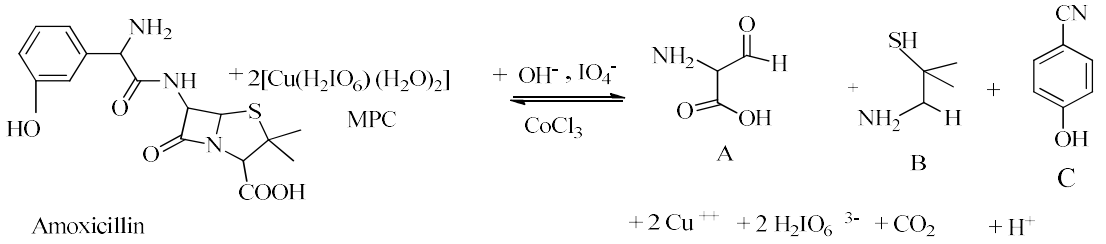

Amoxicillin

where A=2-amino-2-formylacetic acid, B = 1-amino-2-methylpropane-2- thiol, & and C= 4-hydroxybenzonitrile

ii) Catalysis of dicloxacillin

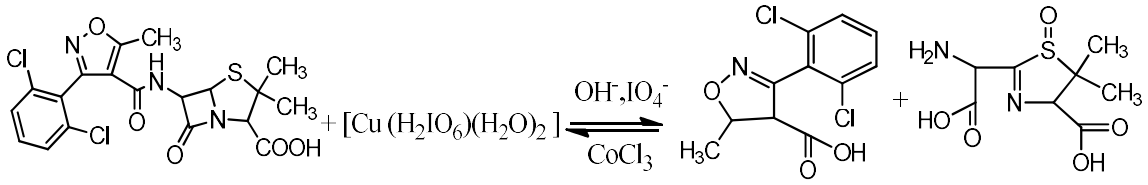

+4 Cu ++ + 4 $H_2IO_6^{3-}$ + 4 H^+ + 5 H_2O

'A' represents (2, 6)-dichlorophenyl-5 methyl-4-dihydroisoxazole-4-carboxylic acid 'B' means 3-(2-(amino (carboxyl) methyl-(5, 5)-dimethyl-(4, 5)-dihydrothiazole-4-carboxylic acid-1-oxide

iii) Catalysis of carbenicillin

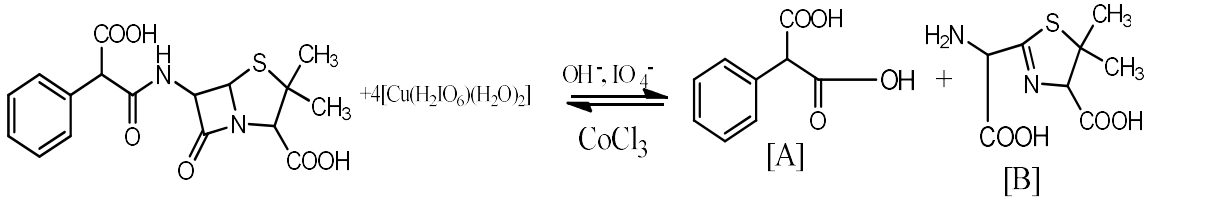

Carbenicillin

+ 4Cu + 4 $H_2IO_6^{3-}$ + 4 H^+ + H_2O

'A' represents 2-phenylmalonic acid, and 'B' means (2-(amino (carboxyl) methyl-(5, 5)-dimethyl-(4, 5)-dihydrothiazole-4-carboxylic acid-1-oxide.

iv) Catalysis of ampicillin

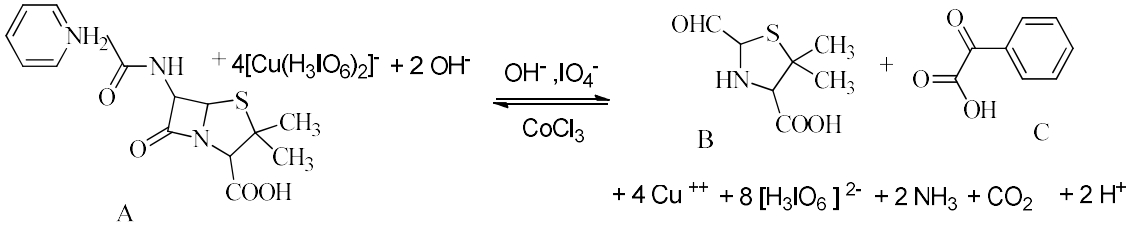

A represents Ampicillin, B represents 2-Formyl-5,5-dimethyl-thiazolidine-4 carboxylic acid, and C denotes oxo-phenyl acetic acid

v) Catalysis of oxacillin

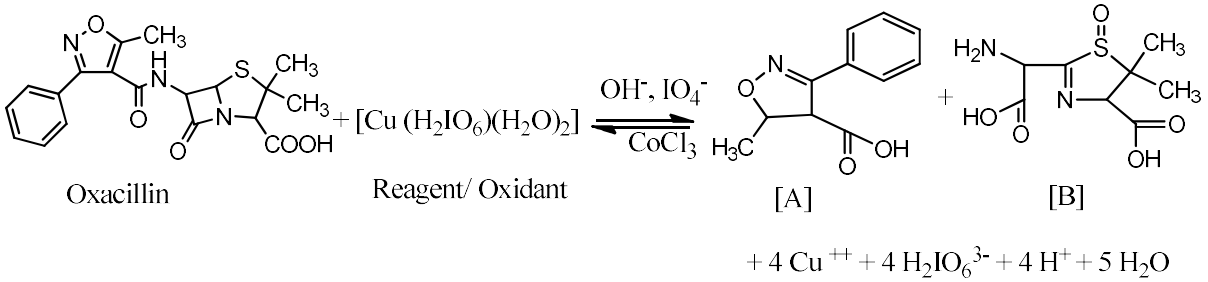

'A' represents 5-methyl-3-phenyl-4,5-dihydroisoxazole-4-carboxylic acid and 'B' represents 2-(amino (carboxy) methyl-(5, 5)-dimethyl-(4, 5)-dihydrothiazole-4-carboxylic acid-1-oxide

Some of the common catalytic applications can be listed:-

i) Iron in the Haber process

$$N_2 + 3H_2 \overset{Fe}{\rightleftharpoons} 2NH_3$$

ii) Nickel in the hydrogenation of C = C bonds

$$CH_2 = CH_2 + H_2 \overset{Ni}{\rightarrow} CH_3 - CH_3$$

iii) Vanadium Oxide in the contact process

$$2SO_2 + O_2 \overset{V_2O_5}{\rightleftharpoons} 2SO_3$$

iv) Iron ions in the reaction between persulphate ions and iodide ions

$$S_2O_8^{--} + 2I^- \overset{Fe}{\rightarrow} 2SO_4^{--} + I_2$$

2.8 Biological Applications

Schatzscneider (2010) has demonstrated the light-triggered release of CO from the coordination sphere of transition metal complexes (CORMs). Kretschmer *et al*. (2011) have provided detailing of light induced carbon monoxide releasing molecule based on iron CORM-S1. Slocik *et al*. (2001) have described the application of Ruthenium (III) by imidazole, Histidine, and iminodiacetate ligand for the complexation of caged NO complex by bio-cellular donors. Brown *et al*. (2004) have mentioned the present and future role of photodynamic therapy in the treatment of cancer disease. Magnetic drug delivery, radio-frequency hyperthermia, and magnetic resonance imaging all use cobalt ferrite. Similarly, Magnetic Resonance Imaging (MRI) has been applied to diagnose cancers, actual size and exact location of tumor. Cobalt is also used to manufacture rechargeable batteries, electronics, catalysts, alloys, and healthcare products. Cobalt imparts many vibrant colors and is found in the center of vitamin $\mathbf{B_{12}}$. Due to these qualities, cobalt is now used in many essential applications that are essential to a higher standard of living and a sustainable planet (Sah, S., 2013). Transition metals are also useful in organic systems as cofactors in enzymes for diagnostic and treatment purposes. A certain solution is fixed to attach an EDTA moiety to the terminal thiazole ring of BLM, radiolabeled to make the complex traceable. Activatable photosensitizes for imaging and therapy have been reported by Lovell *et al*. (2010).

2.9 Metals in Medicine.

Stephen (1994) has mentioned the possible applications of metals in medicine. Yang *et al.* (2012) prepared a similar complex from kaempferol and polyamines like ethylenediamine and diethylenetriammine to evaluate possible DNA interaction with CT DNA and mentioned the mode of interaction to be intercalation. Similar to this, Violet Dhayabaran *et al*. (2016) created complexes of Ni (II), Zn (II), and Co (II) using Schiff base and discussed the impact on the molecular docking system. Isatin-hydrazones-based Ni (II) complexes were synthesized by Rabia *et al*. (2013) to illustrate their physiochemical properties. Splith *et al.* (2010) have explained the protease-activatable

organometal-peptide bioconjugates with enhanced cytotoxicity on cancer cells. The role of transition metal complexes in photography, electro-photography, and ink-jet printing are well known. Cytotoxicitic studies support the ferromagnetic and mild anti-ferilative character against cancer cells cisplatin resistant ovarian cancer (A2780/CP70) and safe nature towards normal cells. Cisplatin, a platinum complex (cis-diamminedichloridoplatinum-II, CDDP), is used to treat testicular cancer, ovarian cancer, cervical cancer, breast cancer, lung cancer, brain tumors, esophageal cancer, etc as explained in Cisplatin Wikipedia, published by 'The American Society of Health-system Pharmacists, Dec 21, 2016', and side effects are explained by (Oun *et al.* (2018). Structures of Cisplatin, chlorophyll, and Hemoglobin are given in Figures 13 and 14 respectively.

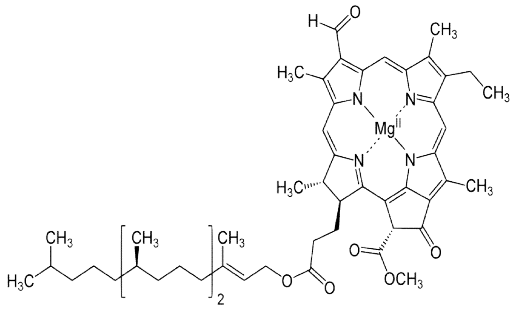

Figure 13: Structure of chlorophyll

(Source: Wikipedia)

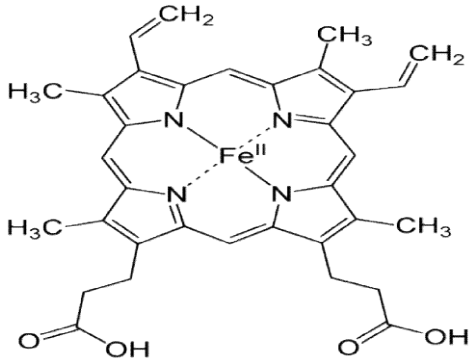

Figure 14: Structure of hemoglobin

(Source: Wikipedia)

CHAPTER 3

MATERIALS AND METHODS

3.1 Materials and reagents

Double-distilled water was utilized throughout the whole project, and all of the chemicals were of the analytical grade quality. To verify the purity of amoxicillin (Sigma Aldrich), a melting point of 469.15K (literature melting point 467.35K) was determined. The stock solution of amoxicillin was made by using 0.3654 g recrystallized amoxicillin with 100 mL water. Similarly, recrystallized samples of 0.4014 g oxacillin, 0.3494 g ampicillin, 0.3784 g carbenicillin, and 0.4703 g dicloxacillin were utilized to prepare 100 ml stock solutions of 0.01 mol dm^{-3} in triple distilled water respectively. A potassium periodate solution was made by dissolving 0.023 g of KIO_4 in 100 mL water; the iodometric method was applied to determine its' strength (Panigrahi & Misro, 1977).

3.2 Instrumentations

The pH of the mixture was determined using an ELICO LI 613 pH meter. On a Varian CARY 5000 UV-VIS spectrophotometer, the electronic absorption spectra were captured between 200 and 1000 nm. Thermo Nicolet's Avatar 370 FT-IR spectrometer, operating as KBr disc, was used to record the complexes' infrared spectra in the 4000-400 cm^{-1} wavelength region. On the UPLC-TQD Mass Spectrometer, LC-MS was captured in the positive mode between 0 and 1000 m/z. Melting points were recorded by the VEEGO ASD-10013 apparatus from NRF, Birgunj, Nepal.

3.3 Synthesis of Reagent: Diperiodatocuprate [DPC (III)]

Diperiodatocuperate [DPC (III)] was made in a 250 mL round-bottomed (RB) flask by combining 6.8 g of potassium periodate, 9.0 g of potassium hydroxide, 2.2 g of potassium persulphate, and 3.54 g of cupric sulphate (Jaiswal & Yadava, 1973) & (Jeffery *et al*., 1996). The entire mixture was roasted nearly 2.0 hours on a hot metal stirring plates, shaking it thoroughly each time. The liquid colored a bright crimson during this time, and

the flask was heated for a further 20 minutes to thoroughly decompose the potassium persulphate present in the mixture. After the reaction was finished, the filtrate was collected with the help of G-4 filter (sintered glass crucible). The dark reddish-brown solution was then diluted with double-distilled water to make 250 mL. By using the thiocyanate method to standardize the aqueous solution of DPC (III) using $Na_2S_2O_3$, starch, KI, and KH_2PO_4, the precise concentration was determined (Panigrahi & Misro, 1977). The presence and precise strength of DPC (III) was confirmed by a UV-visible spectrophotometer that showed an absorption band with a peak at 415 nm. Recent work (Chowdhury *et al*., 2018) has addressed the stability and redox behaviour of DPC (III) complex. Figure 15 lists potential DPC (III) and MPC (III) structures.

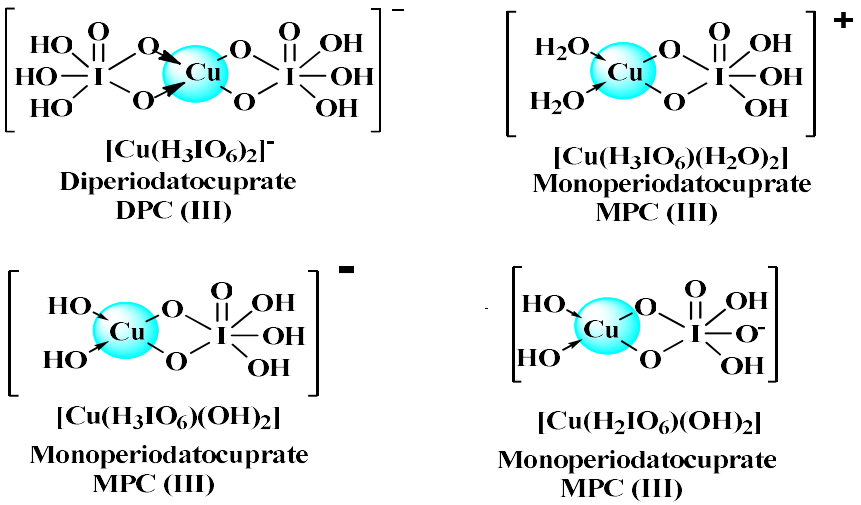

Figure 15: Structures of MPC (III) and DPC (III)

3.4 Synthesis of Complexes

3.4.1 Synthesis of Co (III) – AMX Complex

2 mL KOH solution was mixed with 1 mL of each KIO_4, KNO_3, and $CoCl_3$; then poured slowly into 10 mL of each amoxicillin and DPC (III) solutions followed by stirring, condensing and re-fluxing for 24 hours allowing to cooling for 72 hours; whatman no.1 was used to filter.

The probable Co (III)-AMX complex is shown in Figure 16 below.

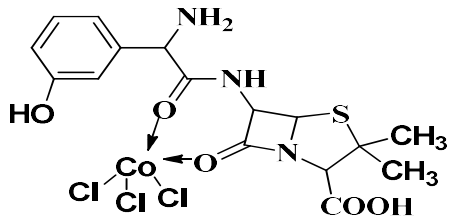

Figure 16: Proposed structure of Co (III) – AMX complex

3.4.2 Synthesis of Co (III) – AMP Complex

2 mL KOH solution was added into 1.0 mL of each KIO_4, KNO_3, $CoCl_3$ solutions which were transferred into a 100 mL RB flask containing 10 mL of each ampicillin and DPC (III) solution. The whole mixture was then heated on a metal stirrer for 24 hours along with re-fluxing with condensation. Following a three-day period of natural cooling, whatman No. 1 was used to filter the combination. Figure 17 represents the probable Co (III)-AMP complex.

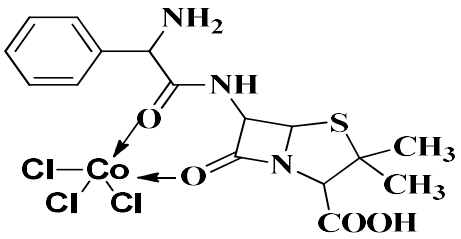

Figure 17: Proposed structure of Co (III) - AMP complex

3.4.3 Synthesis of Co (III) - Dicloxacillin Complex

2 mL KOH solution was relaxed with 1 mL of each KIO_4, KNO_3, and $CoCl_3$; then poured slowly into 10 mL of each dicloxacillin and DPC (III) solutions followed by stirring, condensing and re-fluxing for 24 hours allowing cooling for 72 hours; whatman no.1 was used to filter. Figure 18 represents the probable Co (III)-DCLX complex.

.

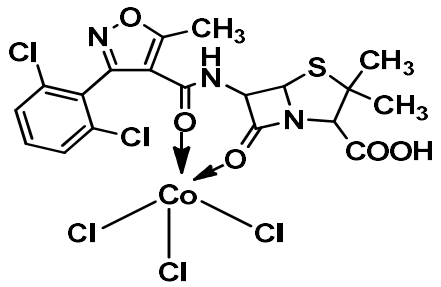

Figure 18: Proposed structure of Co (III) – DCLX complex

3.4.4 Synthesis of Co (III) - CRBC Complex

2 mL KOH solution was mixed with 1 mL of each KIO_4, KNO_3, $CoCl_3$ and poured slowly into 10 mL of each carbenicillin (0.132 mol dm^{-3}) and DPC (III) (0.528 mol dm^{-3}) solutions followed by stirring, condensing and re-fluxing for 24 hours allowing to cool for 72 hours; whatman no.1 was used to filter.

The probable Co (III) - CRBC complex is shown in figure 19 below.

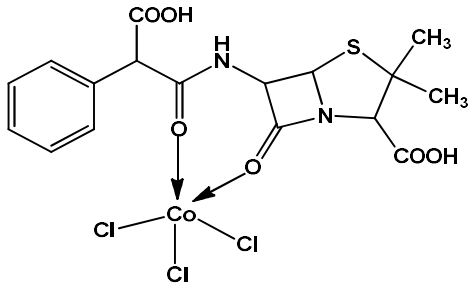

Figure 19: Proposed structure of Co (III) – CRBC complex

3.4.5 Synthesis of Co (III) - OXC Complex

2 mL KOH solution was added with 1 mL of each KIO_4, KNO_3, $CoCl_3$ and poured slowly into 10 mL of each oxacillin (0.132 mol dm^{-3}) and DPC (III) (0.528 mol dm^{-3}) solutions followed by stirring, condensing and re-fluxing for 24 hours allowing to cool for 72 hours; whatman no.1 was used to filter.

The probable Co (III) - Oxacillin complex is shown in figure 20 below.

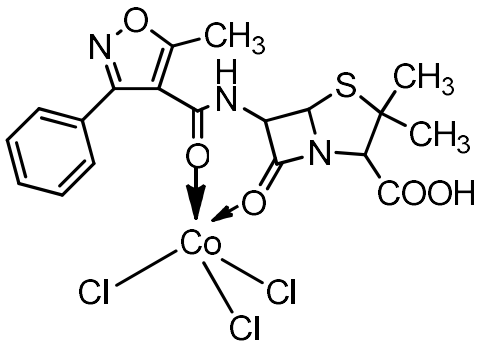

Figure 20: Proposed structure of Co (III) – OXC complex

3.5 Methods

The UV/Visible spectrophotometry is the basic methodology on which the entire research work has been carried out which is discussed in section **4.1** in detail. All of the complexes were synthesized after the determination of stoichiometry of DPC (III) and PADs by **Job's method**, also known as Job's plot or the method of continuous variation, which is widely used to determine the stoichiometry of a chelating agent in complex formation. Paul Job developed this method in 1928 AD when plotting the UV absorbance of Tl $(NO_3)/NH_3$ solutions against the mole fraction of Tl (NO_3). In solutions, prepared by dissolving species A and species B, either more than A may bind with a single B or less than A may bind with more of B. Stoichiometry can be determined by the amount of A binding to B with the help of Job's plot. Molar concentrations of two binding agents (eg. a transition metal and a ligand like DPC (III) and PADs in the present work) are kept constant throughout the experiment by varying their mole fractions frequently. An absorbance is plotted versus the mole fraction of two components. Let X_A be the mole fraction of components A and P be its physical property (also called UV absorbance). The maximum intersection or bisection point obtained in the plot corresponds to the stoichiometry of component A and B. Such a plot also supports understanding the equilibrium constant of that complex formation, which in turn, supports knowing the nature of the complex and the ratio of components present in that complex. The

primary condition for this experiment is to remain higher concentrations of both components, total concentrations of components, pH, and constant ionic strength of solutions but physical property being investigated must be variable (Parker *et al*., 2013; Renny *et al*., 2013). Stoichiometry and product analysis have been discussed in the **4.1.1** section in detail. Similarly, major products were characterized by melting point, elemental analysis, FT-IR, and LC-MS spectral analysis. Melting point determination is discussed in section **4.3.1**, elemental microanalysis in section **4.3.2** while details of FT-IR and LC-MS are well discussed in sections **4.3.3,** and **4.3.4** respectively. Order of reaction, the effect of influencing factors, and temperature are discussed in sections **4.2**, **4.3.5**, and **4.4** respectively.

CHAPTER 4

4. RESULTS AND DISCUSSION

4.1 Kinetic Measurements

Due to the rapid nature of the reaction between PADs and DPC (III), the reaction's development was tracked by measuring the absorbance of the mixture at 20°C, 25°C, 30°C, and 35°C ± 0.1°C along with lower strength of DPC (III) than AMX/AMP/DCLX/CRBC/OXC. A pH of (9.2-10) was maintained for the reaction mixture. At first, a set of all solutions were made ready in a quartz cuvette in which AMX/AMP/DCLX/CRBC/OXC solution was mixed separately and finally after keeping into a quartz cuvette. Transmittance and absorbance values were collected after fixing the UV-Visible spectrophotometer at and 415 nm wavelength and molar extinction coefficient (€) of **6144 ± 50** dm^3 $mol^{-1}cm^{-1}$ till 85% completion of the reaction. Finally, the reaction mixture loaded inside the quartz cuvette turned to colorless. Each kinetic run always contained fresh solutions only after washing the cuvette properly followed by drying it. Both uncatalyzed and catalyzed rate constants were calculated from each absorbance values separately for each concentration of AMX/AMP/DCLX/CRBC/OXC solution. Origin 9.6 (2017) software was applied to determine regression coefficient (r) and standard deviation (s) values. Straight lines were produced from the plots of log (abs) vs. time (in minute). Order of reactions were determined from the slopes obtained by plotting rate constants at Y-axis and concentration of each component like DPC (III), AMX/AMP/DCLX/CRBC/OXC, alkali, and periodate at x-axis respectively. Each rate constant value was within ± 5% error; taken as an average of at least three independent kinetic runs. Final concentration of KIO_4 was calculated by assuming the amount present in DPC (III) and mixed additionally. Kinetic tests were also carried out in the nitrogen atmosphere to examine the effects of periodates, ionic strength, dissolved oxygen, etc., but no appreciable alterations were seen there. The addition of carbonate, periodate, and dielectric constant had no impact. Figure 21 and Table 2 were utilized to ascertain the

application of Beer-Lambert's law (Figure 22) and revealed that very little interference with the reaction had been considered. DPC (III) was shown to have a maximum wavelength of 415 nm.

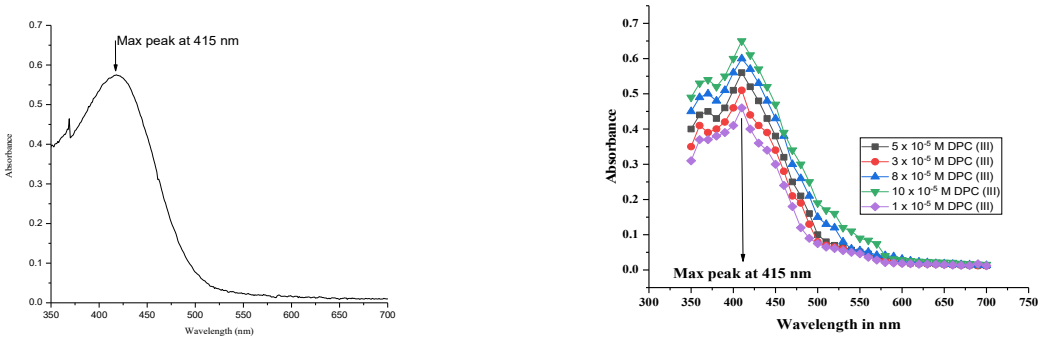

Figure 21: Plot of wavelength vs. Absorbance for DPC (III)

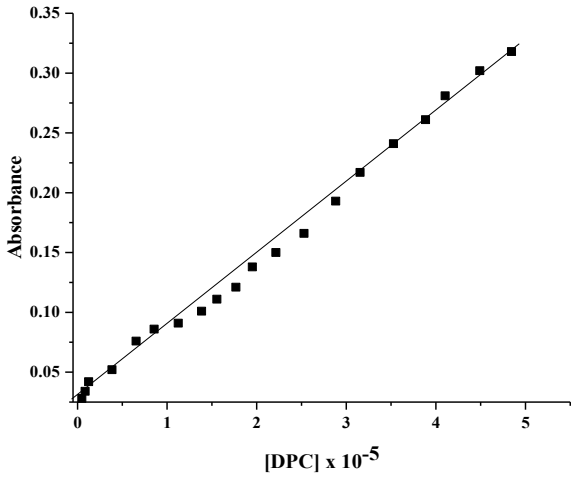

Figure 22: Plot of [DPC (III)] vs. Absorbance

Table 2: Data for the plot of [DPC (III)] vs. absorbance, where [DPC (III)] = 5.0 x 10^{-5} M, ionic strength (I) = 0.10 mol dm^{-3} and [PAD] = 5.0 x 10^{-4} M

Time in min	Absorbance at 415 nm	[DPC] x 10^{-5} M
0.0	0.318	4.845
0.2	0.302	4.491
0.4	0.281	4.104

0.6	0.261	3.885
0.8	0.241	3.527
1.0	0.217	3.154
1.2	0.193	2.883
1.4	0.166	2.528
1.6	0.15	2.215
1.8	0.138	1.952
2.0	0.121	1.768
2.2	0.111	1.556
2.4	0.101	1.385
2.6	0.091	1.125
2.8	0.086	0.856
3.0	0.076	0.654
3.2	0.052	0.385
3.4	0.042	0.125
3.6	0.034	0.085
3.8	0.028	0.0486

4.1.1 Stoichiometry and Product analysis

4.1.1.1 Stoichiometry and Product analysis for Co (III) - AMP complex

Stoichiometry of AMP: DPC (III) was confirmed to be 1:4. The first product was oxo-phenyl acetic acid ($C_8H_6O_3$), and the second product was confirmed as 2-formyl-5, 5-dimethyl-thiazolidine 4-carboxylic acid ($C_7H_{11}NO_3S$). These products were recrystallized with ethyl alcohol and column chromatography assisted to separate them over neutral aluminium oxide with benzene (80%) and chloroform (20%) in the form of eluent. Nitrogen gas was passed through the acidified solution to detect carbon dioxide gas as the side product. The similar procedure was repeated to isolate major products in each Co (III) catalyzed reaction conducted between PADs, and DPC (III). FT-IR, elemental analysis, and LC-MS results are included in the section of **3.5.**

4.1.1.2 Stoichiometry and Product analysis for Co (III) - AMX complex

Stoichiometry of AMX: DPC (III) was confirmed to be 1:2. The first product was 4-hydroxybenzonitrile, 2-amino-2-formylacetic acid, and the second product was confirmed as 1-amino-2-methylpropane-2-thiol. FT-IR, elemental analysis, and LC-MS results are included in the section **3.5.**

4.1.1.3 Stoichiometry and Product analysis for Co (III) – DCLX complex

Stoichiometry of DCLX: DPC (III) was known to be 1:4. The first and second products were 2, 6-dichlorophenyl-5-methyl-4, 5-dihydroisoxazole-4-carboxylic acid ($C_{11}H_9Cl_2NO_3$), and 3-(2-(amino (carboxy) methyl)-5, 5-dimethyl-4, 5-dihydrothiazole-4-carboxylic acid-1-oxide respectively. FT-IR, elemental analysis, and LC-MS results are included in the section of **3.5.**

4.1.1.4 Stoichiometry and Product analysis for Co (III) - CRBC complex

Stoichiometry of CRBC: DPC (III) was declared to be 1:4. The first and second products were 2-phenylmalonic acid ($C_9H_8O_4$), and 2-(amino (carboxy) methyl)-5, 5-dimethyl-4, 5-dihydrothiazole-4-carboxylic acid-1-oxide ($C_8H_{12}N_2O_4S$) respectively. FT-IR, elemental analysis, and LC-MS results are included in the section of **3.5.**

4.1.1.5 Stoichiometry and Product analysis for Co (III) - OXC complex

Stoichiometry of OXC: DPC (III) was confined to be 1:4. The first and second products were 2, 6-phenyl-5-methyl-4, 5-dihydroisoxazole-4-carboxylic acid ($C_{11}H_9NO_3$), and 3-(2-(amino (carboxy) methyl)-5, 5-dimethyl-4, 5-dihydrothiazole-4-carboxylic acid-1-oxide respectively. FT-IR, elemental analysis, and LC-MS results are included in the section of **3.5.**

4.2 Reaction Orders

Figure 37 and Table 8's log (absorbance) vs. time (in minutes) for various concentrations of DPC (III) show how orders of reaction were established by varying the concentrations of AMP, $CoCl_3$ (III), KIO_4, and KOH; other concentrations remained unchanged.

4.2.1 *Variations for concentrations of AMP, DPC (III), KOH, KIO_4, and $CoCl_3$ for the oxidation of AMP by DPC (III) at 298 K and ionic strength of 0.10 mol dm^{-3}

Table 3: Reaction Composition Table for AMP oxidation

[DPC] x10^5 M	[AMP] x10^4 M	[OH^-] x10^2 M	[IO_4^-] x10^5 M	[$CoCl_3$] x10^7 M	k_U x10^4 (s^{-1})	k_T x 10^3 (s^{-1})	k_C x 10^3 (s^{-1})
1.0	5.0	0.8	1.0	5.0	1.99	2.13	1.93
3.0	5.0	0.8	1.0	5.0	1.94	2.03	1.84
5.0	5.0	0.8	1.0	5.0	**1.86**	**1.97**	**1.78**
8.0	5.0	0.8	1.0	5.0	1.89	2.00	1.81
10.0	5.0	0.8	1.0	5.0	1.93	2.19	1.99
5.0	**1.0**	0.8	1.0	5.0	0.64	0.75	0.69
5.0	**3.0**	0.8	1.0	5.0	0.93	1.10	1.01
5.0	**5.0**	0.8	1.0	5.0	**1.86**	**1.97**	**1.78**
5.0	**8.0**	0.8	1.0	5.0	2.66	2.82	2.55
5.0	**10.0**	0.8	1.0	5.0	3.29	3.47	3.14
5.0	5.0	**0.2**	1.0	5.0	2.85	3.36	3.07
5.0	5.0	**0.4**	1.0	5.0	2.40	2.78	2.54
5.0	5.0	**0.6**	1.0	5.0	1.95	2.41	2.21
5.0	5.0	**0.8**	1.0	5.0	**1.86**	**1.97**	**1.78**
5.0	5.0	**1.0**	1.0	5.0	1.60	1.75	1.60
5.0	5.0	0.8	**1.0**	5.0	**1.86**	**1.97**	**1.78**
5.0	5.0	0.8	**3.0**	5.0	1.62	1.92	1.75
5.0	5.0	0.8	**5.0**	5.0	1.22	1.50	1.38
5.0	5.0	0.8	**8.0**	5.0	0.72	1.21	1.14
5.0	5.0	0.8	**10.0**	5.0	0.29	0.46	0.43
5.0	5.0	0.8	1.0	**1.0**	**1.86**	**0.49**	**0.31**
5.0	5.0	0.8	1.0	**3.0**	1.86	1.06	0.88
5.0	5.0	0.8	1.0	**5.0**	1.86	1.97	1.78
5.0	5.0	0.8	1.0	**8.0**	1.86	2.34	2.15
5.0	5.0	0.8	1.0	**10.0**	1.86	2.76	2.52

* Unit of concentration [ ]: mole dm^{-3}.

4.2.2 *Variations for concentrations of AMX, DPC (III), KOH, KIO_4, and $CoCl_3$ for the oxidation of AMX by DPC (III) at 25 °C and ionic strength of 0.10 mol dm^{-3}

Table 4: Reaction Composition Table for AMX oxidation

[DPC] x 10^5 M	[AMX] x 10^4 M	[OH^-] x10^2 M	[IO_4^-] x10^5 M	[$CoCl_3$] x10^7 M	$k_U x10^4$ (s^{-1})	k_T x 10^3 (s^{-1})	k_C x 10^3 (s^{-1})
1.0	5.0	0.8	1.0	5.0	3.95	4.14	3.75
3.0	5.0	0.8	1.0	5.0	3.99	4.39	3.99
5.0	**5.0**	**0.8**	**1.0**	**5.0**	**3.87**	**4.06**	**3.67**
8.0	5.0	0.8	1.0	5.0	3.82	4.07	3.69
10.0	5.0	0.8	1.0	5.0	3.84	4.03	3.65
5.0	**1.0**	0.8	1.0	5.0	1.5	1.35	1.20
5.0	**3.0**	0.8	1.0	5.0	2.12	2.67	2.48
5.0	**5.0**	**0.8**	**1.0**	**5.0**	**3.87**	**4.06**	**3.67**
5.0	**8.0**	0.8	1.0	5.0	5.43	5.75	5.21
5.0	**10.0**	0.8	1.0	5.0	7.56	6.99	6.23
5.0	5.0	**0.2**	1.0	5.0	1.87	2.02	1.83
5.0	5.0	**0.4**	1.0	5.0	2.66	2.90	2.63
5.0	5.0	**0.6**	1.0	5.0	2.99	3.38	3.08
5.0	**5.0**	**0.8**	**1.0**	**5.0**	**3.87**	**4.06**	**3.67**
5.0	5.0	**1.0**	1.0	5.0	4.52	4.42	3.97
5.0	**5.0**	**0.8**	**1.0**	**5.0**	**3.87**	**4.06**	**3.67**
5.0	5.0	0.8	**3.0**	5.0	2.99	3.02	2.72
5.0	5.0	0.8	**5.0**	5.0	1.98	2.45	2.25
5.0	5.0	0.8	**8.0**	5.0	1.00	1.87	1.77
5.0	5.0	0.8	**10.0**	5.0	0.69	1.69	1.63
5.0	5.0	0.8	1.0	**1.0**	3.87	1.44	1.05
5.0	5.0	0.8	1.0	**3.0**	3.87	2.79	2.40
5.0	5.0	0.8	1.0	**5.0**	3.87	4.14	3.75
5.0	5.0	0.8	1.0	**8.0**	3.87	4.39	3.99
5.0	**5.0**	**0.8**	**1.0**	**10.0**	**3.87**	**4.06**	**3.67**

* Unit of concentration []: mole dm^{-3}

4.2.3 *Variations for concentrations of DPC (III), DCLX, KOH, KIO_4, and $CoCl_3$ for the oxidation of DCLX by DPC (III) at 25 °C and ionic strength of 0.10 mol dm^{-3}

Table 5: Reaction composition table for DCLX oxidation

[DPC] x 10^5 M	[DCLX] x 10^4 M	[OH^-] x10^2 M	[IO_4^-] x10^5 M	[$CoCl_3$] x10^7 M	$k_U x10^4$ (s^{-1})	k_T x 10^3 (s^{-1})	k_C x 10^3 (s^{-1})
1.0	5.0	0.8	1.0	5.0	1.80	2.25	2.07
3.0	5.0	0.8	1.0	5.0	1.85	2.27	2.08
5.0	**5.0**	**0.8**	**1.0**	**5.0**	**1.86**	**2.32**	**2.13**
8.0	5.0	0.8	1.0	5.0	1.82	2.28	2.09
10.0	5.0	0.8	1.0	5.0	1.88	2.30	2.11
5.0	**1.0**	0.8	1.0	5.0	0.68	1.05	0.98
5.0	**3.0**	0.8	1.0	5.0	1.35	1.65	1.51
5.0	5.0	0.8	1.0	5.0	1.86	2.32	2.13
5.0	**8.0**	0.8	1.0	5.0	2.55	2.98	2.72
5.0	**10.0**	0.8	1.0	5.0	3.24	3.48	3.15
5.0	5.0	**0.2**	1.0	5.0	0.75	1.12	1.04
5.0	5.0	**0.4**	1.0	5.0	1.12	1.41	1.51
5.0	5.0	**0.6**	1.0	5.0	1.57	1.85	1.85
5.0	**5.0**	**0.8**	**1.0**	**5.0**	**1.86**	**2.32**	**2.13**
5.0	5.0	**1.0**	1.0	5.0	2.31	2.98	2.54
5.0	**5.0**	**0.8**	**1.0**	**5.0**	**1.86**	**2.32**	**2.13**
5.0	5.0	0.8	**3.0**	5.0	1.55	1.73	1.24
5.0	5.0	0.8	**5.0**	5.0	1.31	1.11	1.02
5.0	5.0	0.8	**8.0**	5.0	0.86	0.85	0.80
5.0	5.0	0.8	**10.0**	5.0	0.53	0.64	0.61
5.0	5.0	0.8	1.0	**1.0**	1.86	1.15	0.96
5.0	5.0	0.8	1.0	**3.0**	1.86	1.34	1.15
5.0	5.0	0.8	1.0	**5.0**	**1.86**	**2.32**	**2.13**
5.0	5.0	0.8	1.0	**8.0**	1.86	2.95	2.76
5.0	5.0	0.8	1.0	**10.0**	1.86	4.67	4.48

* Unit of concentration [ ]: mole dm^{-3}

4.2.4 *Variations for concentrations of DPC (III), CRBC, KOH, KIO_4, and $CoCl_3$ for the oxidation of CRBC by DPC (III) at 25 °C and ionic strength of 0.10 mol dm^{-3}

Table 6: Reaction composition table for CRBC oxidation

[DPC] x 10^5 M	[CRBC] x 10^4 M	[OH^-] x10^2 M	[IO_4^-] x10^5 M	[$CoCl_3$] x10^7 M	$k_U x10^4$ (s^{-1})	k_T x 10^3 (s^{-1})	k_C x 10^3 (s^{-1})
1.0	5.0	0.8	1.0	5.0	1.21	1.47	1.35
3.0	5.0	0.8	1.0	5.0	1.26	1.49	1.36
5.0	5.0	0.8	1.0	5.0	**1.25**	**1.49**	**1.37**
8.0	5.0	0.8	1.0	5.0	1.31	1.48	1.35
10.0	5.0	0.8	1.0	5.0	1.21	1.45	1.35
5.0	**1.0**	0.8	1.0	5.0	0.41	0.50	0.46
5.0	**3.0**	0.8	1.0	5.0	0.81	1.03	0.95
5.0	**5.0**	0.8	1.0	5.0	**1.25**	**1.49**	**1.37**
5.0	**8.0**	0.8	1.0	5.0	1.80	2.01	1.83
5.0	**10.0**	0.8	1.0	5.0	2.34	2.61	2.38
5.0	5.0	**0.2**	1.0	5.0	0.62	0.72	0.66
5.0	5.0	**0.4**	1.0	5.0	0.82	0.98	0.90
5.0	5.0	**0.6**	1.0	5.0	1.01	1.19	1.09
5.0	5.0	**0.8**	1.0	5.0	**1.25**	**1.49**	**1.37**
5.0	5.0	**1.0**	1.0	5.0	1.61	1.85	1.69
5.0	5.0	0.8	**1.0**	5.0	**1.25**	**1.49**	**1.37**
5.0	5.0	0.8	**3.0**	5.0	1.05	1.39	1.29
5.0	5.0	0.8	**5.0**	5.0	0.91	1.05	0.96
5.0	5.0	0.8	**8.0**	5.0	0.72	0.82	0.75
5.0	5.0	0.8	**10.0**	5.0	0.65	0.71	0.65
5.0	5.0	0.8	1.0	**1.0**	1.25	0.46	0.34
5.0	5.0	0.8	1.0	**3.0**	1.25	1.03	0.91
5.0	5.0	0.8	1.0	**5.0**	**1.25**	**1.49**	**1.37**
5.0	5.0	0.8	1.0	**8.0**	1.25	2.07	1.95
5.0	5.0	0.8	1.0	**10.0**	1.25	2.61	2.49

* Unit of concentration [ ]: mole dm^{-3}

4.2.5 *Variations for concentrations of DPC (III), OXC, KOH, KIO_4, and $CoCl_3$ for the oxidation of OXC by DPC (III) at 25 °C and ionic strength of 0.10 mol dm^{-3}

Table 7: Reaction composition table for OXC oxidation

[DPC]x 10^5 M	[OXC]x 10^4 M	[OH^-] x10^2 M	[IO_4^-] x10^5 M	[$CoCl_3$] x10^7 M	$k_U x10^4$ (s^{-1})	k_T x 10^3 (s^{-1})	k_C x 10^3 (s^{-1})
1.0	5.0	0.8	1.0	5.0	2.41	2.58	2.34
3.0	5.0	0.8	1.0	5.0	2.41	2.53	2.29
5.0	5.0	0.8	1.0	5.0	**2.23**	**2.46**	**2.24**
8.0	5.0	0.8	1.0	5.0	2.21	2.32	2.10
10.0	5.0	0.8	1.0	5.0	2.35	2.48	2.25
5.0	**1.0**	0.8	1.0	5.0	0.81	0.96	0.88
5.0	**3.0**	0.8	1.0	5.0	1.14	1.63	1.70
5.0	**5.0**	0.8	1.0	5.0	**2.23**	**2.46**	**2.24**
5.0	**8.0**	0.8	1.0	5.0	3.48	3.62	3.27
5.0	**10.0**	0.8	1.0	5.0	4.15	4.97	3.89
5.0	5.0	**0.2**	1.0	5.0	1.02	1.16	1.06
5.0	5.0	**0.4**	1.0	5.0	1.35	1.67	1.53
5.0	5.0	**0.6**	1.0	5.0	2.01	2.02	1.82
5.0	5.0	**0.8**	1.0	5.0	**2.23**	**2.46**	**2.24**
5.0	5.0	**1.0**	1.0	5.0	2.35	2.69	2.46
5.0	5.0	0.8	**1.0**	5.0	**2.23**	**2.46**	**2.24**
5.0	5.0	0.8	**3.0**	5.0	1.84	1.98	1.80
5.0	5.0	0.8	**5.0**	5.0	1.58	1.77	1.61
5.0	5.0	0.8	**8.0**	5.0	1.42	1.71	1.57
5.0	5.0	0.8	**10.0**	5.0	1.29	1.45	1.32
5.0	5.0	0.8	1.0	**1.0**	2.23	0.73	0.51
5.0	5.0	0.8	1.0	**3.0**	2.23	1.63	1.41
5.0	5.0	0.8	1.0	**5.0**	**2.23**	**2.46**	**2.24**
5.0	5.0	0.8	1.0	**8.0**	2.23	4.03	3.80
5.0	5.0	0.8	1.0	**10.0**	2.23	5.01	4.79

* Unit of concentration [ ]: mole dm^{-3}

4.3 Characterization

4.3.1 Melting Point Determination

Melting points of AMX-DPC (III) products were found to be 393.93K (395.4K), and 371.28K (368.5K) for 2-amino-2-formylacetic acid and 4-hydroxybenzonitrile, (C_7H_5NO) respectively. Melting points of OXC- DPC (III) products were found to be 518.3K (517.9K) and 710.01K (711.5K) the first product ($C_{11}H_{11}NO_3$) and the second product ($C_8H_{12}N_2O_5S$). Similarly, melting points of AMP- DPC (III) products were found to be 585.0K (587.3K) and 416.0K (413.5K) for oxo-phenyl acetic acid ($C_8H_6O_3$) and 2-formyl-5, 5-dimethyl-thiazolidine 4-carboxylic acid ($C_7H_{11}NO_3S$) respectively. The CRBC- DPC (III) products showed melting points of 523.31K (525.3K) and 767.71K (770.0K) for 2-phenylmalonic acid ($C_9H_8O_4$) and 2-(amino (carboxy) methyl)-5, 5-dimethyl-4, 5-didydrothiazole-4-carboxylic acid-1-oxide ($C_8H_{12}N_2O_4S$) respectively. Similarly, the first product ($C_{11}H_9Cl_2NO_3$) and the second product ($C_8H_{12}N_2O_5S$) of DCLX- DPC (III) showed melting points of 603.18K (601.5K) and 710.01K (708.2K) respectively.

4.3.2 Elemental Microanalysis (CHNS)

DCLX-DPC (III) complex and products {calculated **%**/ found **%**}

$C_{11}H_9Cl_2NO_3$, the first product, displayed C-48.20(48.35), H-3.31(3.25), Cl-(25.72), N-5.11(5.04) while the second product, $C_8H_{12}N_2O_5S$, also displayed C- 41.37(41.43), H-5.21(5.34) N-12.06(11.83) and S –13.81(13.95) in addition to oxygen.

Co (III) - AMX complex and products {calculated / (found)}

The first product 2-amino-2- formylacetic acid displayed C- 34.96(34.75), H- 4.89(4.95) besides oxygen. The second product 1-amino-2-methylpropane-2-thiol ($C_4H_{11}NS$), showed C- 45.67 (45.53), H-10.54(10.63) N-13.31(13.07) and S –30.48(30.11) besides oxygen. The third product 4-hydroxybenzonitrile, (C_7H_5NO) showed C-70.58 (70.26), H-4.23 (4.31), and N-11.76 (12.05) besides oxygen.

Co (III) - CRBC complex and products {calculated **%** / found**%** }

2-phenylmalonic acid displayed C- 60.00 (60.11) and H- 4.48 (4.55). The second product, ($C_8H_{12}N_2O_4S$) displayed C- 41.37(41.53), H-5.21 (5.37) N-12.06 (12.16) and S –13.81(13.88) in addition to oxygen.

Co (III) - AMP complex and products {calculated **%** / found **%**}

The first product oxo-phenyl acetic acid ($C_8H_6O_3$), showed C- 64.00 (64.11), H- 4.03 (3.95) while the second product $C_7H_{11}NO_3S$ showed C- 44.43 (44.53), H-5.86(5.97) N-7.4 (7.52) and S –16.94 (16.83) in addition to oxygen.

Co (III) - OXC complex and products {calculated **%**/ found **%**}

$C_{11}H_{11}NO_3$, the first product, displayed C-64.38(63.95), H-5.40(5.25), N-6.83(6.54) while the second product, $C_8H_{12}N_2O_5S$, also displayed C- 38.70(37.93), H-4.87(4.34) N-11.28(11.83) and S-12.92(12.65) in addition to oxygen.

4.3.3 FT-IR Spectra

4.3.3.1 FT-IR for Co (III) - AMX products

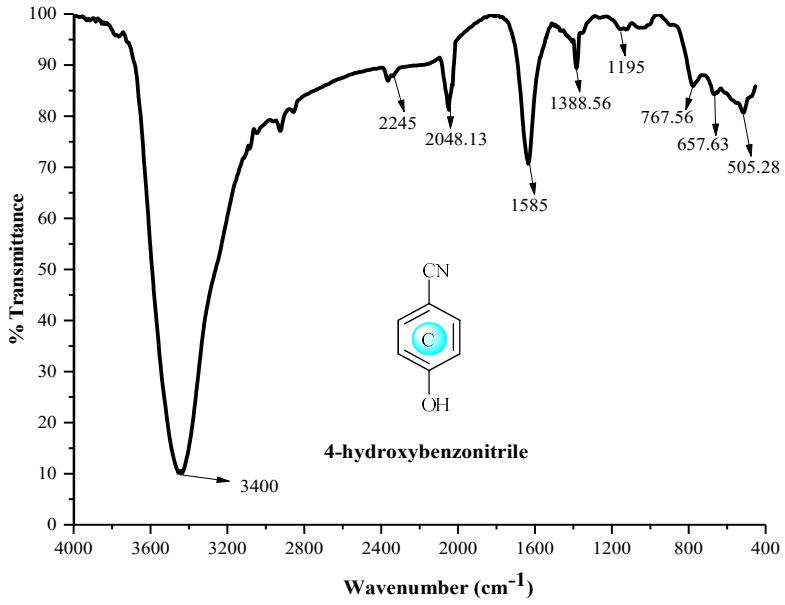

Figure 23: FT-IR Spectrum for product of Co (III)-AMX complex

One of the products, 4-hydroxybenzonitrile displayed nitrile group (CN) stretching vibration) around 2245 cm^{-1}, (O-H) stretch around 3400 cm^{-1}, (C=C) stretch around 1585 cm^{-1}, (C-O) stretch around 1195 cm^{-1}, and (C-H) out of plane bending at around 757.63 cm^{-1} due to aromatic ring.

4.3.3.2 FT-IR for Co (III) - AMP products

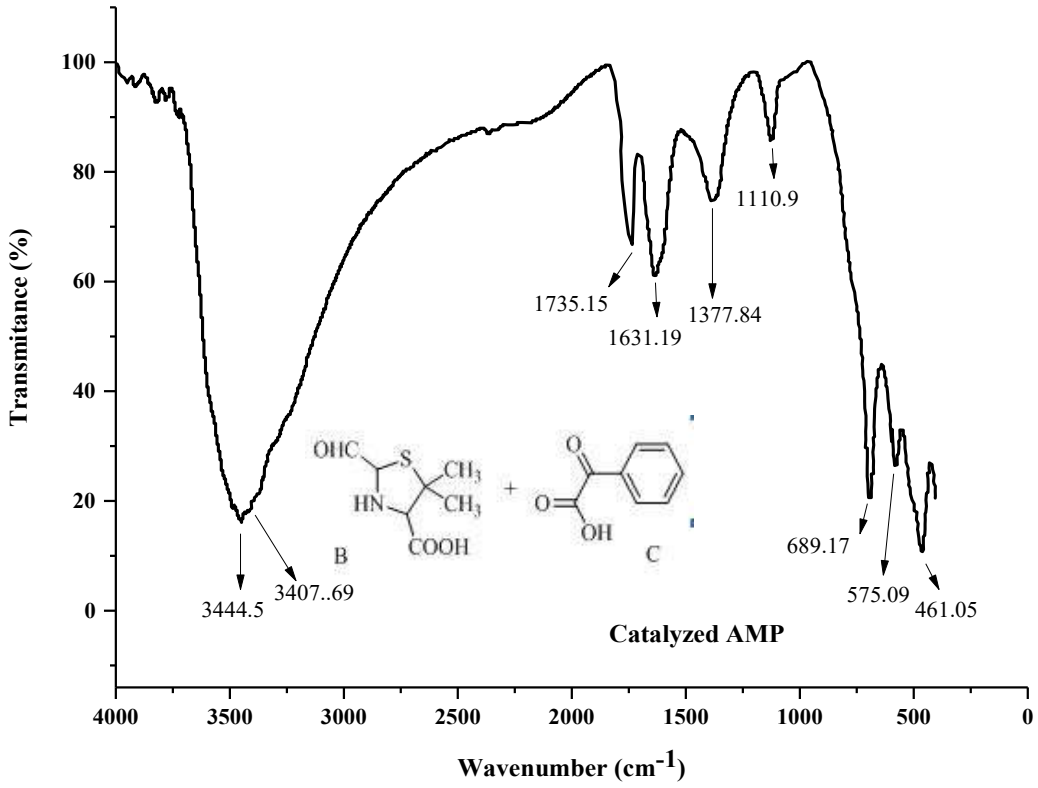

Figure 24: FT-IR Spectrum for products of Co (III) - AMP complex

The first product, oxo-phenyl acetic acid ($C_8H_6O_3$), displayed three distinct absorption peaks: a narrow peak at 3407.69 cm^{-1} (due to the carboxylic OH group), a sharp peak at 1735.15 cm^{-1} (due to the ketonic C=O stretch), and a broad peak at 1377.84 cm^{-1} (due to the carboxylic C=O stretch). The second product, 2-formyl-(5,5)-dimethyl-thiazolidine-4-carboxylic acid ($C_7H_{11}NO_3S$), displayed four distinct absorption bands: a narrow peak at 3444.5 cm^{-1} (due to N-H stretching), two sharp peaks at 1735.15cm^{-1} (due to aldehyde C=O stretch), and 1631.19 cm^{-1} (due to carboxylic C=O stretch) as well as a broad peak at 1377.84 cm^{-1} (due to CH_3 stretch), as seen in Figure 24.

4.3.3.3 FT-IR for Co (III) - DCLX products

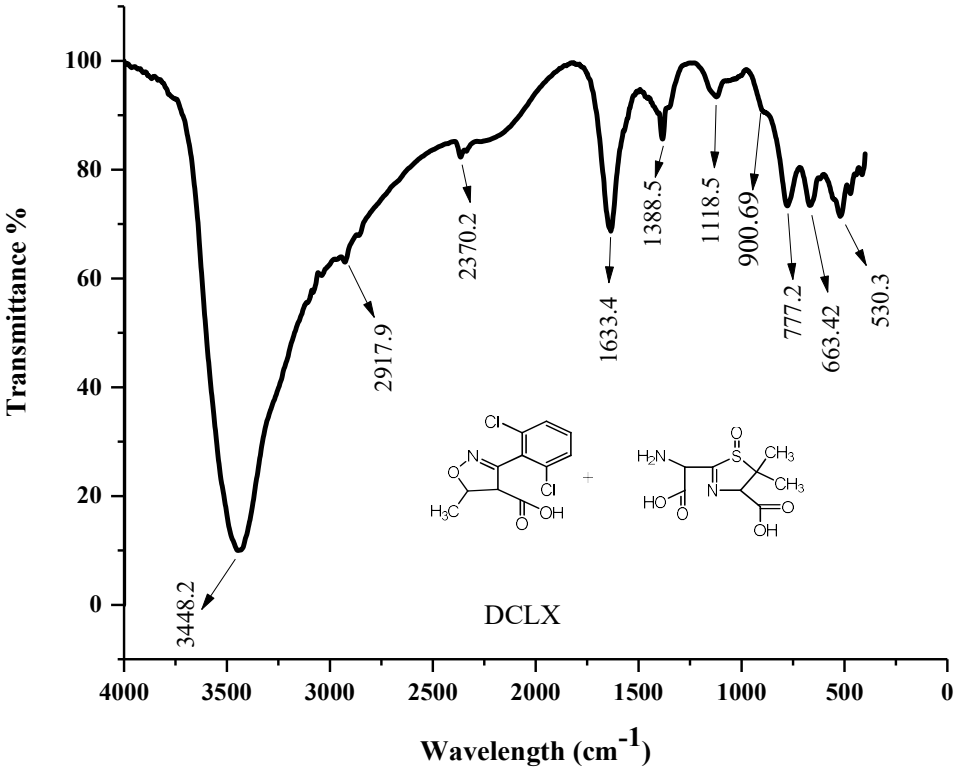

Figure 25: FT-IR spectrum for products of Co (III) - DCLX complex

Several peaks were seen, including a broad peak at 2917.9 cm^{-1} (caused by the carboxylic OH group), peaks at 1388.5 & 1118.5 cm^{-1} (caused by the stretching of the CH_3 atom), 3448.2 cm^{-1} (caused by the stretching of the N-H atom), and a sharp peak at 1633.4 cm^{-1}, as shown in Figure 25.

4.3.3.4 FT-IR for Co (III) - CRBC products

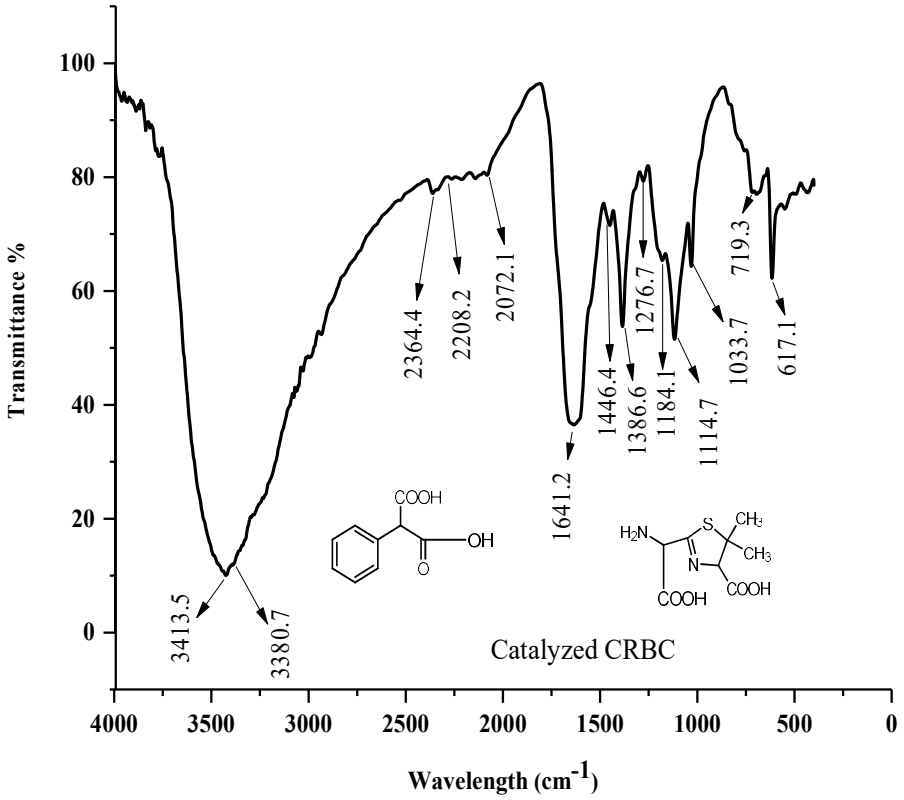

Figure 26: FT-IR spectrum for products of Co (III) - CRBC complex

Different peaks were noticed including two broad peaks at 3413.5 cm^{-1} (due to carboxylic OH group), and at 3380.7 cm^{-1} (due to N-H stretching), four sharp absorption peaks at 1641.2 cm^{-1} (due to ketonic/carboxylic C=O stretch), 1464.4 & 1386.6 cm^{-1} (due to CH_3 stretch), and 1276.7 cm^{-1} (due to carboxylic C=O stretch) were noticed, as seen in Figure 26.

4.3.3.5 FT-IR for Co (III) - OXC products

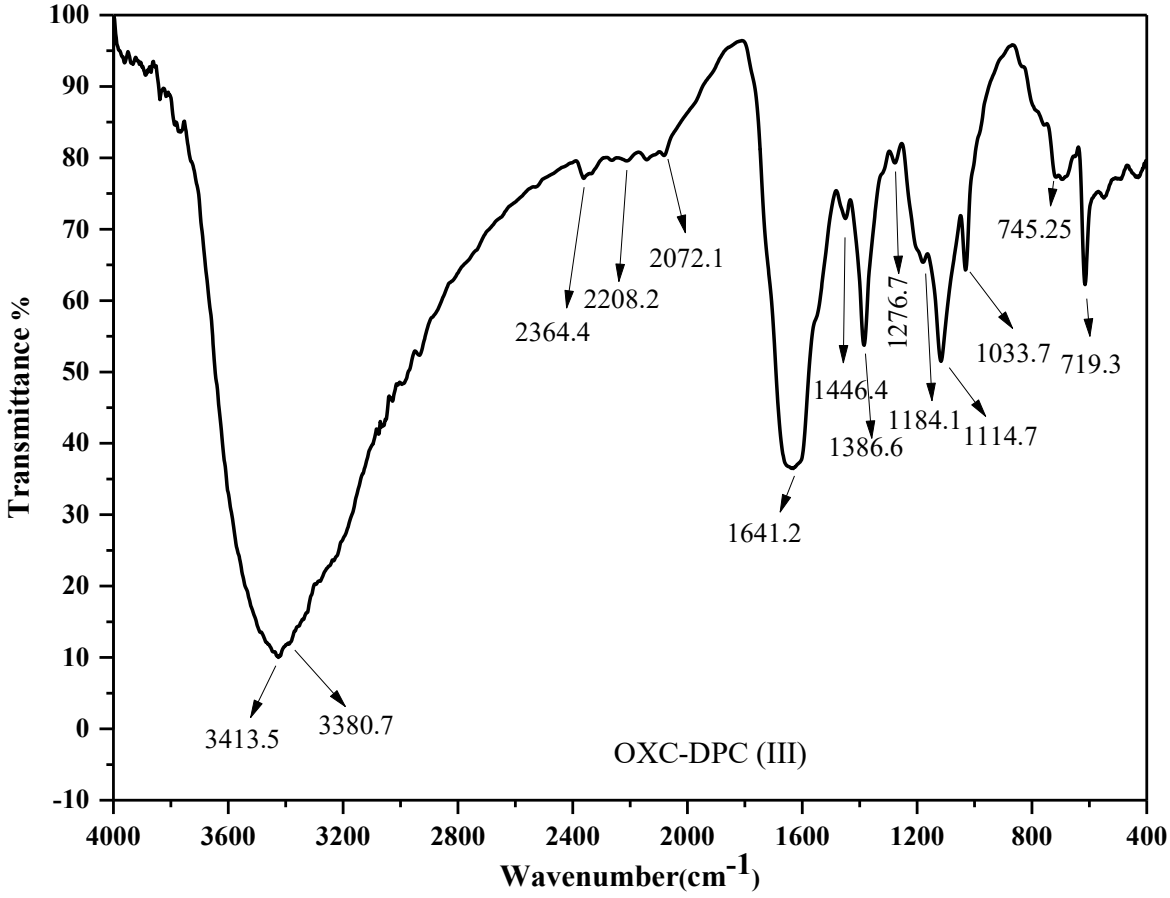

Figure 27: FT-IR spectrum for products of Co (III) - OXC complex

A broad absorption peak at 3413.5 cm^{-1} (due to carboxylic OH group), 1276.70 cm^{-1} (due to carboxylic C=O group) as well as a peak at 3380.70 cm^{-1} appeared due to N-H stretching. Similarly, two separate peaks at 1464.4 cm^{-1} and 1386.6 cm^{-1} were noticed due to geminal CH_3 as well as (C-N) stretching vibration group. Likewise, a peak at 1641.2 cm^{-1} was noticed due to carboxylic/ketonic (C=O) group.

4.3.4 LC-MS Spectra

4.3.4.1 LC-MS for Co (III) - AMX complex and products

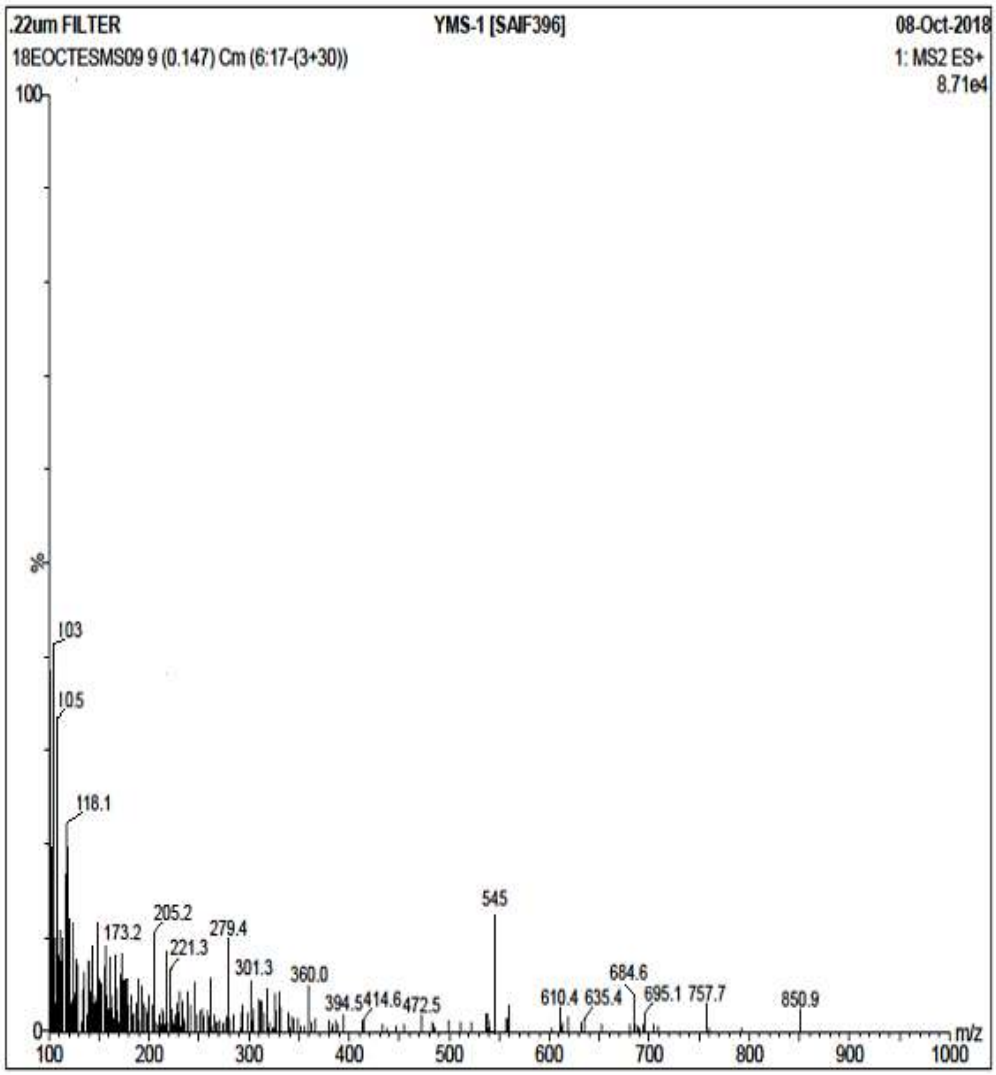

Figure 28: LC-MS Spectrum for the catalyzed oxidation of AMX by DPC (III)

A peak at 545 m/z value was observed for the complex ($C_{17}H_{22}Cl_3CoN_3O_5S$) whiles the second product, 1-amino-2-methylpropane-2-thiol ($C_4H_{11}NS$), displayed a peak at 105 m/z and the third product, 4-hydroxybenzonitrile (C_7H_5NO) at 118.1 m/z. The first product, 2-amino-2-formylacetic acid ($C_3H_5O_3$), showed a peak at 103 m/z value, Figure 28 represents the LC-MS spectrum of AMX by DPC (III). Figure 26 addresses such information.

4.3.4.2 LC-MS for Co (III) - AMP complex and products

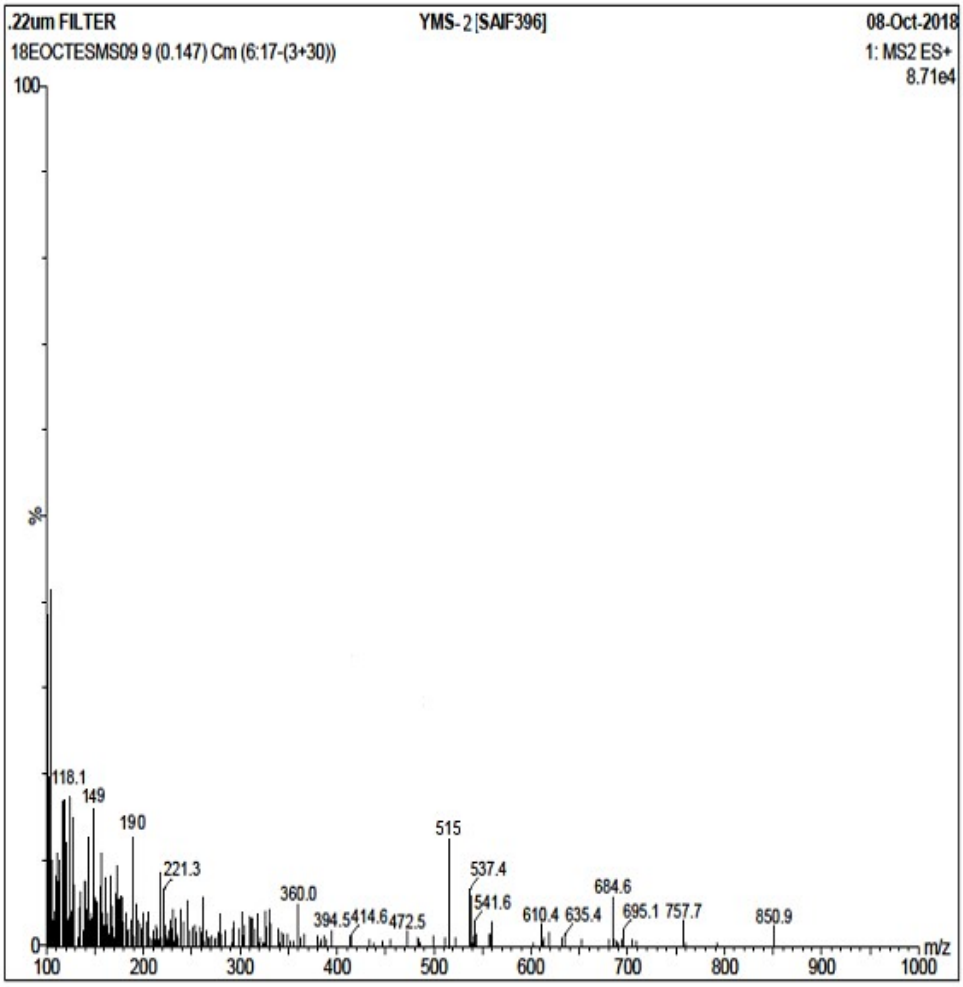

Figure 29: LC-MS Spectrum for the catalyzed oxidation of AMP by DPC (III)

The complex ($C_{16}H_{19}Cl_3CoN_3O_4S$) showed a peak at 515 m/z and the first product oxo-phenyl acetic acid ($C_8H_6O_3$) showed m/z at 149. The second product 2-formyl-5, 5-dimethyl-thiazolidine 4-carboxylic acid ($C_7H_{11}NO_3S$) gave m/z at 190.

4.3.4.3 LC-MS for Co (III) - DCLX complex and products

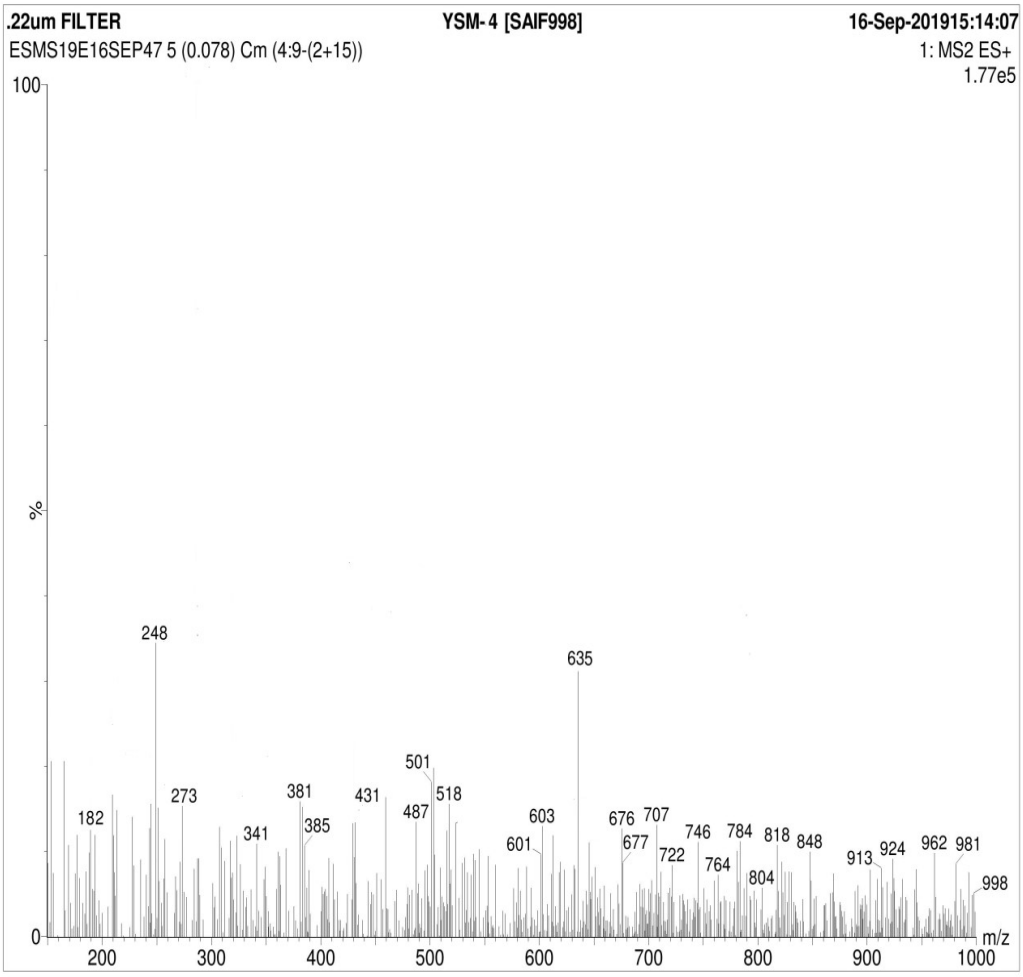

Figure 30: LC-MS Spectrum for the catalyzed oxidation of DCLX by DPC (III)

A peak at 635 m/z was observed for the complex ($C_{19}H_{17}Cl_5CoN_3O_5S$). The first product ($C_{11}H_9Cl_2NO_3$) gave m/z at 273 ($m^+$ 1) while the second product ($C_8H_{12}N_2O_5S$) showed m/z at 248.

4.3.4.4 LCMS for Co (III) - CRBC complex and products

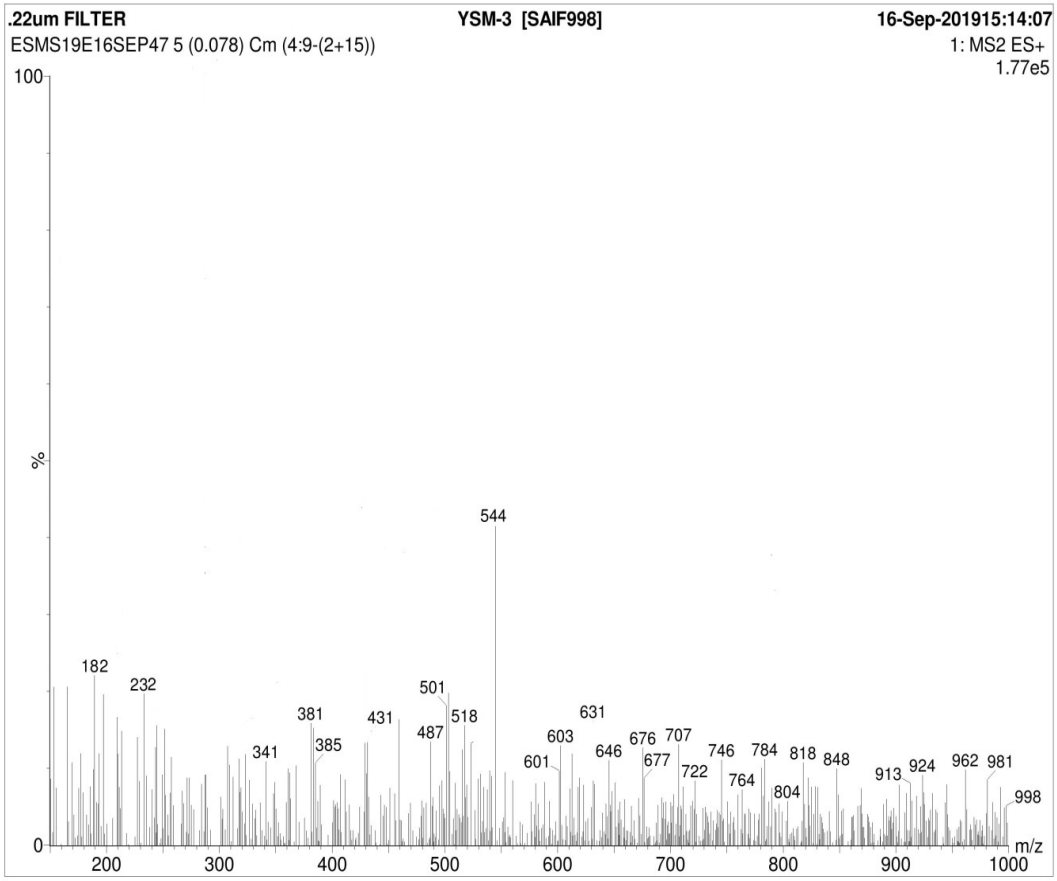

Figure 31: LC-MS Spectrum for the catalyzed oxidation of CRBC by DPC (III)

The complex ($C_{17}H_{18}Cl_3CoN_2O_6S$) showed m/z at 544, while 2-phenylmalonic acid ($C_9H_8O_4$) gave m/z at 182 (m^+2), while the second product ($C_8H_{12}N_2O_4S$) gave m/z at 232 (m^+1).

4.3.4.5 LCMS for Co (III) - OXC complex and products

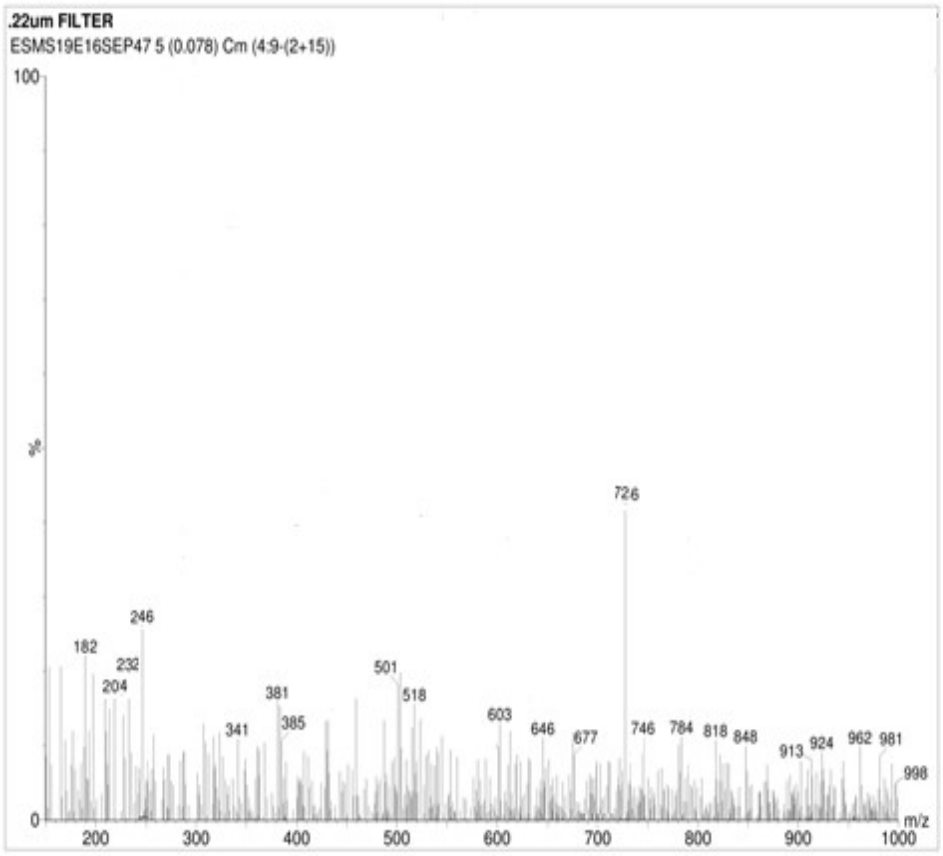

Figure 32: The LC-MS spectrum of the OXC-MPC (III) complex and its products

The complex showed m/z at 726, while the first product ($C_{11}H_{11}NO_3$) gave m/z at 204 (m^+1), while the second product ($C_8H_{12}N_2O_5S$) gave m/z at 246 (m^+2).

4.3.5 Effect of influencing factors

4.3.5.1 Effect of [DPC (III)]/Oxidant

The concentration of DPC (III) varied from 1.0 x 10^{-5} to 1.0 x 10^{-4} mol dm^{-3}. When other concentrations were kept constant and the log (absorbance) vs. time plots were linear and nearly parallel up to 85% reaction completion, it was clear that DPC (III) had a uniform reaction order. The pseudo-first-order response for DPC (III) is supported by Table 8 and figure 33. The verification of Beer-Lambert's law is shown in figure 34. As concentration

of DPC (III) decreased and the solution turned into colorless, absorbance also decreased correspondingly.

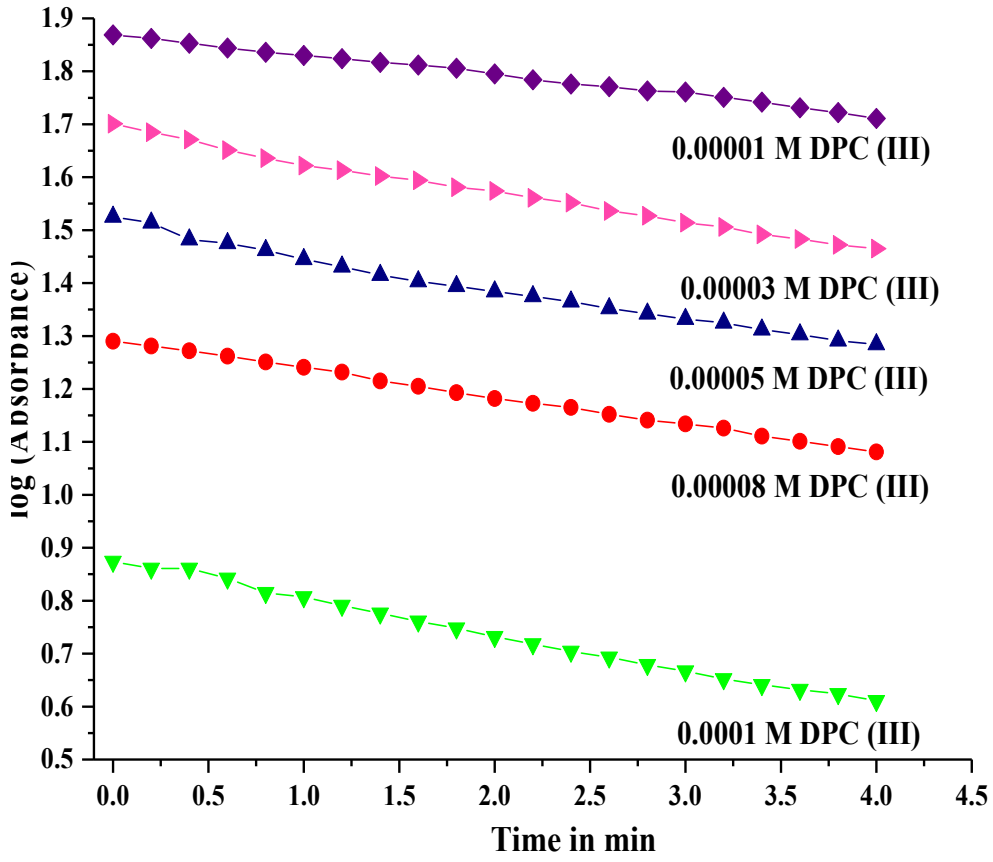

Figure 33: Order Plot of log (abs) vs. time for the oxidation of PADs by DPC (III)

Table 8: Data of order plot for oxidation of PADs by DPC (III), where [DPC (III)] = (1.0-10.0) x 10^{-5} M, I = 0.1 mol dm^{-3} at 25 °C

Time in min	Abs at 1 x 10^{-5} M DPC (III)	Abs at 3 x10^{-5} M DPC (III)	Abs at 5 x 10^{-5} M DPC (III)	Abs at 8 x 10^{-5} M DPC (III)	Abs at 10x 10^{-5} M DPC (III)
0	0.874	1.29	1.525	1.701	1.869
0.2	0.861	1.281	1.514	1.685	1.862
0.4	0.861	1.272	1.482	1.671	1.853
0.6	0.842	1.262	1.475	1.651	1.844
0.8	0.815	1.251	1.462	1.636	1.836
1	0.807	1.241	1.445	1.622	1.83

1.2	0.791	1.232	1.431	1.613	1.824
1.4	0.776	1.215	1.415	1.602	1.817
1.6	0.761	1.205	1.403	1.594	1.812
1.8	0.748	1.193	1.394	1.581	1.806
2	0.732	1.182	1.384	1.574	1.795
2.2	0.718	1.173	1.375	1.561	1.784
2.4	0.704	1.165	1.365	1.552	1.776
2.6	0.693	1.152	1.352	1.536	1.771
2.8	0.679	1.141	1.342	1.527	1.763
3	0.667	1.134	1.332	1.514	1.761
3.2	0.652	1.126	1.325	1.506	1.751
3.4	0.641	1.111	1.312	1.492	1.742
3.6	0.632	1.101	1.303	1.483	1.731
3.8	0.624	1.091	1.291	1.472	1.722
4	0.611	1.081	1.284	1.465	1.711

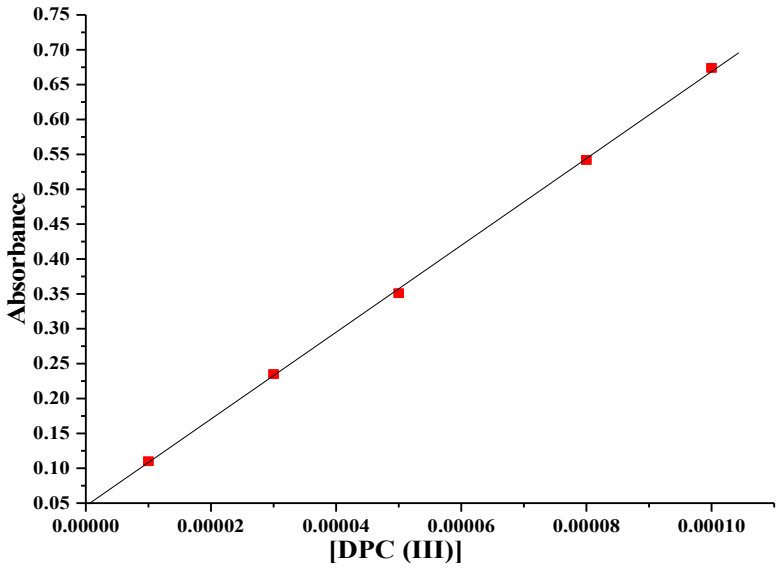

Figure 34: Plot of concentration of DPC (III) vs. Absorbance

4.3.5.2 Effect of activity of PADs/ Substrate

According to law of mass action, reaction rate always remains directly proportional to the active mass of substrate or PADs. Concentration of PADs is maximum before attainment of transition state or complex formation, order of oxidation reaction appeared positive and less than unity or fractional order with respect to PADs like ampicillin, amoxicillin, dicloxacillin, carbenicillin and oxacillin. Fractional order means the rate is proportional to the reactant concentration raised up to a fractional power. It also declares that whole of PADs (100%) is not converted into products within the reaction period. Fractional order indicates complex reaction mechanism with catalyst resulting reactive intermediates due to involvement of multiple steps in parallel pathways where the rate determining step does not bear a simple relationship to the reactant concentration. It occurs in a heterogeneous reaction involving a catalyst. The impact of AMX concentration was investigated between ranges of 1 x 10^{-4} to 1 x 10^{-3} mol dm^{-3}.

Effect of AMX concentration: Rate constants (k_c) elevated up as active mass of ampicillin increased, and the amoxicillin order was found to be 0.71 (r 0.9894, s 0.0071), shown by Figure 35 and Table 9.

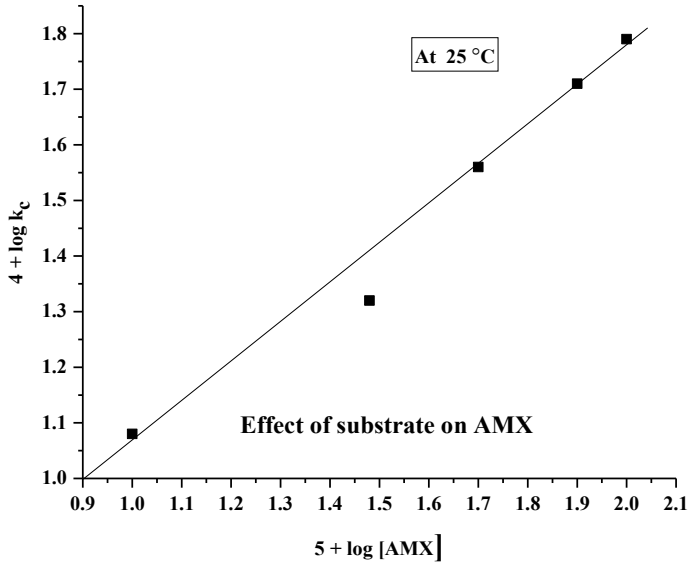

Figure 35: Plot of (4 + log k_c) vs. 5 + log [AMX]

Table 9: Data for plot of 5 + log [AMX] vs. 4 + log k_c

S. N.	5 + log [AMX]	k_C x 10^{-3}	4 + log k_C
1	1	1.2	1.08
2	0.477	2.08	1.32
3	0.698	3.67	1.56
4	0.903	5.21	1.716
5	2	6.23	1.79

Effect of AMP concentration:. Rate constants (k_c) enhanced up as concentration of AMP increased, and its order was noticed to be 0.67 ($r \geq 0.9894$, $s \leq 0.0051$), supported by Table 10 and Figure 36.

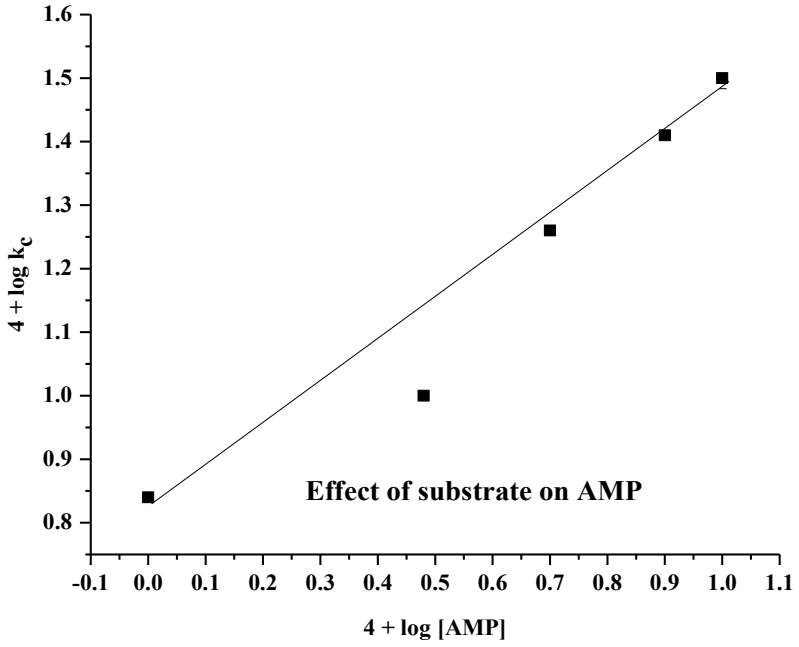

Figure 36: Plot of (4 + log k_c) vs. 4 + log [AMP]

Table 10: Data for plot of 4 + log [AMP] vs. 4 + log k_c

S. N.	4 + log [AMP]	k_C x 10^{-3}	4 + log k_C
1	0	0.69	0.84
2	0.48	1.01	1.0
3	0.7	1.78	1.25
4	0.9	2.57	1.41
5	1	3.14	1.50

Effect of DCLX concentration: Rate constants (k_c) increased as active mass of DCLX rose up and its order was noticed to be 0.62 ($r \geq 0.9968$, $s \leq 0.0016$), represented by Table 11 and Figure 37.

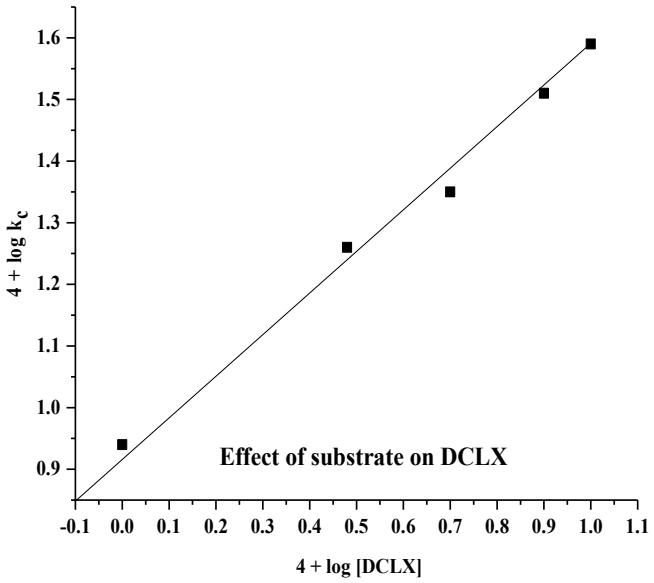

Figure 37: Plot of (4 + log k_c) vs. 4 + log [DCLX]

Table 11: Data for plot of 4 + log [DCLX] vs. 4 + log k_c

S. N.	4 + log [DCLX]	k_c x 10^{-3}	4 + log kc
1	0	0.87	0.94
2	0.48	1.82	1.26
3	0.7	2.13	1.35
4	0.9	3.23	1.51
5	1	3.89	1.59

Effect of CRBC concentration: Rate constants (k_c) were increased with raise in active mass of CRBC and its order was confirmed to be 0.593 ($r \geq 0.9977$, $s \leq 0.00103$), as shown in Table 12 and Figure 38.

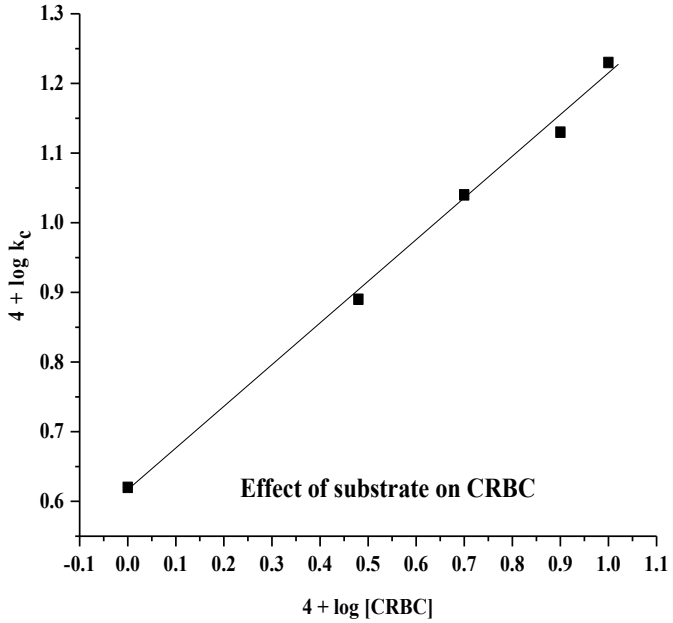

Figure 38: Plot of (4 + log k_c) vs. 4 + log [CRBC]

Table 12: Data for plot of 4 + log [CRBC] vs. 4 + log k_c

S.N.	4 + log [CRBC]	4 + log k_c
1	0	0.62
2	0.48	0.89
3	0.7	1.04
4	0.9	1.13
5	1.0	1.23

Effect of OXC concentration: Rate constants (k_c) were elevated with raise in molarity of OXC and its order was confirmed to be 0.656 ($r \geq 0.9975$, $s \leq 0.00105$), as displayed in Table 13 and Figure 39.

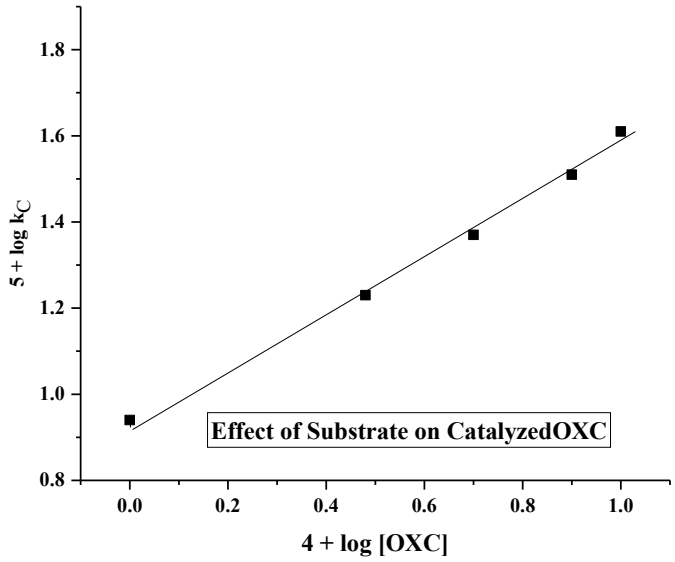

Figure 39: Plot of (5 + log k_c) vs. 4 + log [OXC]

Table 13: Data for plot of 4 + log [OXC] vs. 5 + log k_c

S.N.	4 + log [OXC]	5 + log k_c
1	0	0.94
2	0.48	1.23
3	0.7	1.37
4	0.9	1.51
5	1.0	1.61

4.3.5.3 Effect of Alkali Concentration

Alkali behaves as a substrate as well as catalyzing agent that produces de-protonated form of fresh DPC (III) when old DPC (III) interacts with hydroxide ions. Free periodate anion gets produced after hydrolysis of fresh DPC (III). In all cases, rate gets enhanced producing a positive fractional order reaction owing to complex reaction along with involvement of Cobalt (III) catalyst and formation of reactive intermediates. However, ampicillin shows a negative fraction order reaction due to suppression of periodate ion concentration by large excess concentration of hydroxide ions as the degradation reaction maintains an alkaline environment. The impact of KOH was investigated between 0.04 to 0.2 mol dm^{-3} ranges. Data presented herewith are in agreement with this fact.

Effect of alkali concentration for AMX: The rate constant (k_c) enhanced as active mass of KOH rose up. Its order of reaction was declared to be 0.484 ($r \geq 0.998$, $s \leq 0.002$), Table 14 and Figure 40 represent it.

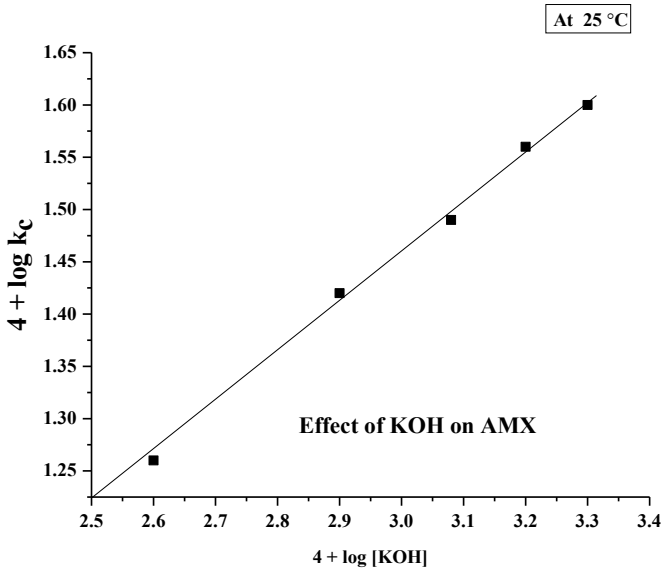

Figure 40: Plot of (4 + log k_c) vs. 4 + log [KOH]

Table 14: Data for plot of 4 + log [KOH] vs. 4 + log k_c

S. N.	4+ log [KOH]	k_C x 10^{-3}	4 + log k_c
1	2.6	1.83	1.26
2	2.9	2.63	1.42
3	3.1	3.08	1.49
4	3.2	3.67	1.56
5	3.3	3.97	1.60

Effect of alkali concentration for AMP: The rate constant (k_c) fell down as active mass of KOH rose up and order of reaction was declared to be - 0.419 ($r \geq 0.9918$, $s \leq 0.0008$), represented in Table 15 and Figure 41.

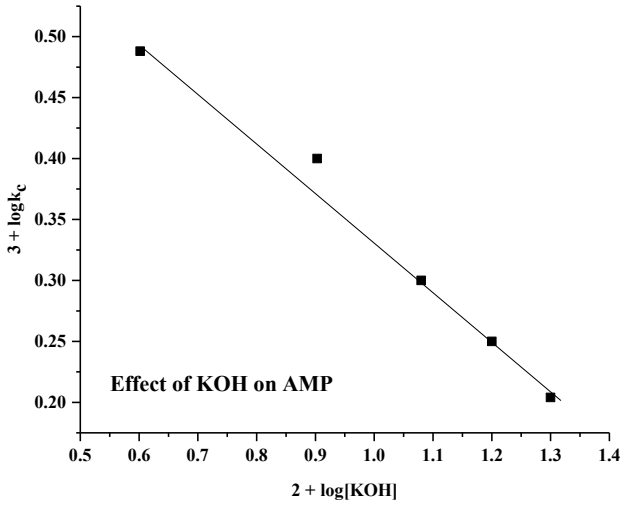

Figure 41: Plot of (4 + log k_c) vs. 2 + log [KOH]

Table 15: Data for plot of 2 + log [KOH] vs. 4 + log k_c

S. N.	2 + log [KOH]	k_C x 10^{-3}	3 + log k_c
1	0.602	3.07	0.488
2	0.903	2.54	0.40
3	1.08	2.21	0.30
4	1.20	1.78	0.25
5	1.30	1.60	0.20

Effect of alkali concentration for DCLX: Elevation in rate constants (k_c) was observed as active mass of KOH rose up. The order of DCLX reaction was found to be 0.50 ($r \geq 0.997$, $s \leq 0.00447$) as shown in Table 16 and Figure 42.

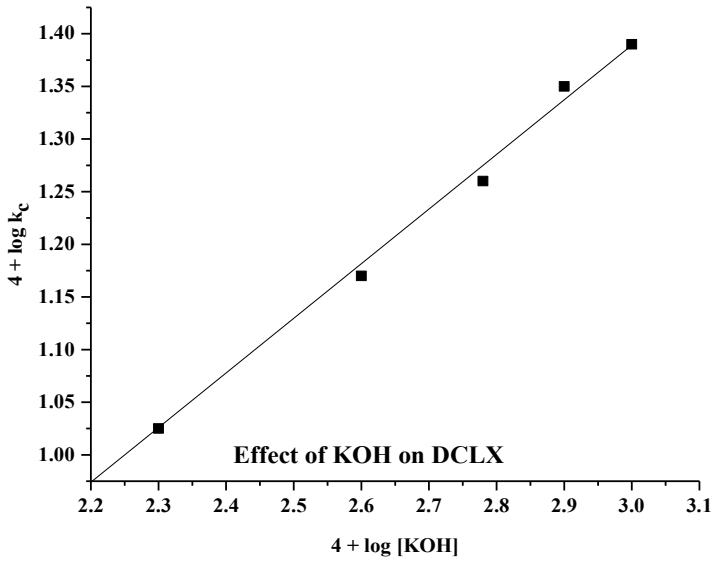

Figure 42: Plot of (4 + log k_c) vs. 4 + log [KOH]

Table 16: Data for plot of 4 + log [KOH] vs. 4 + log k_c

S. N.	4 + log [KOH]	k_c x 10^{-3}	4 + log k_c
1	2.3	1.06	1.025
2	2.6	1.48	1.17
3	2.78	1.82	1.26
4	2.9	2.24	1.35
5	3	2.45	1.39

Effect of alkali concentration for CRBC: Rate constants (k_c) for CRBC were elevated up with rise in concentration of KOH and its reaction order was determined to be 0.593 ($r \geq 0.9816$, $s \leq 0.0011$) as shown by Table 17 and Figure 43.

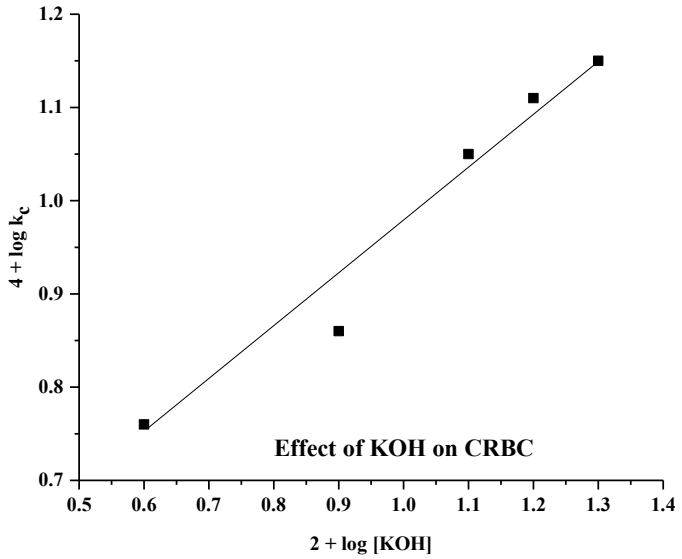

Figure 43: Plot of (4 + log k_c) vs. 2 + log [KOH]

Table 17: Data for plot of 2 + log [KOH] vs. 4 + log k_c

S. N.	2 + log [KOH]	4 + log k_c
1	0.6	0.76
2	0.9	0.86
3	1.1	1.05
4	1.2	1.11
5	1.3	1.15

Effect of alkali concentration for OXC: Rate constants (k_c) for OXC were raised up with rise in concentration of KOH. Reaction order was 0.524 ($r \geq 0.9977$, $s \leq 0.00133$) as represented by Table 18 and Figure 44.

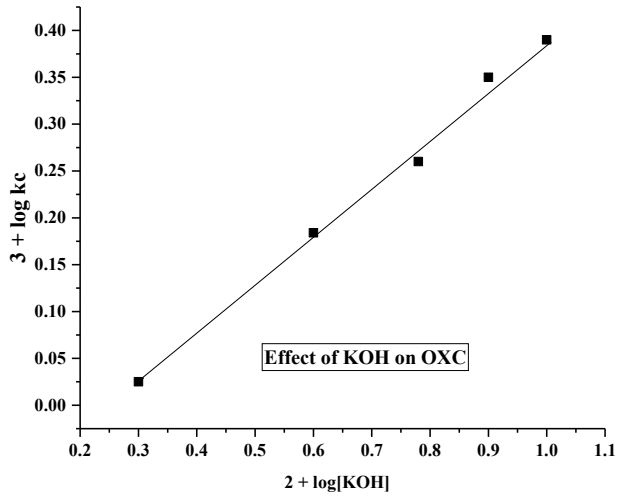

Figure 44: Plot of (3 + log k_c) vs. 2 + log [KOH]

Table 18: Data for plot of 2 + log [KOH] vs. 3 + log k_c

S. N.	2 + log [KOH]	3 + log k_c
1	0.3	0.025
2	0.6	0.184
3	0.78	0.26
4	0.9	0.35
5	1	0.39

4.3.5.4 Effect of Periodate Concentration

Order of oxidation of PADs with respect to periodate has been determined as negative fractional integer in case of all of PADs. Addition of periodate in the alkaline medium can be attributed to the complex reaction mechanism. Periodate ions can cat as oxidizing agent competing with alkali and PAD in the reaction system. There are two resources of periodate ions. DPC (III) provides free periodate as $H_2IO_6^{-1}$ or $H_3IO_6^{-3}$ as well as IO_4^{-1} from KIO_4 and there is a large accumulation of periodate ions in the reaction. When whole of periodate ion is not used up and begin to act as common ion, rate gets retarded causing negative fractional order. A negative fractional order suggests a complex reaction

mechanism indicating the presence of inhibition in which the reaction mechanism involves multiple steps and an initial reaction product or intermediate has a retarding effect on the rate of overall process. The presence of other species like common periodate ion or DPC (III) may compete with PAD for the active site on the catalyst leading to the decreased effectiveness of the catalyst. The impact of active mass of KIO_4 was observed within (1.0×10^{-5} to 1.0×10^{-4}) mol dm^{-3} ranges.

Effect of periodate concentration for AMX: Rate constants fell down with rise in active mass of KIO_4. The order of degradation of amoxicillin with respect to periodate was found to be - 0.343 ($r \geq 0.99$, $s \leq 0.00149$), as shown by Figure 45 and Table 19.

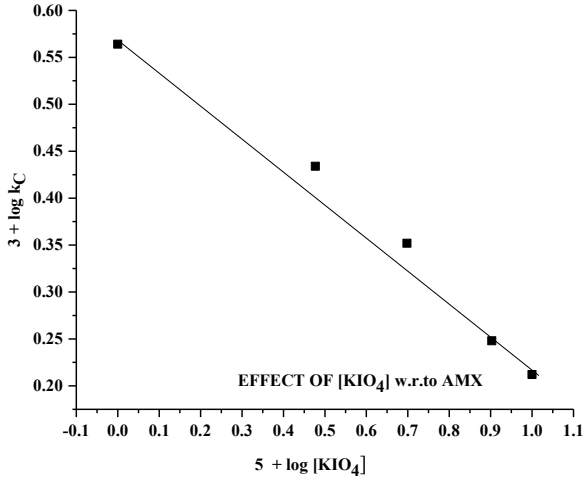

Figure 45: Plot of (3 + log k_c) vs. 5 + log [KIO_4]

Table 19: Data for plot of 5 + log [KIO_4] vs. 3 + log k_c

S. N.	5 + log [KIO_4]	$k_C \times 10^{-3}$	3 + log k_c
1	0	3.67	0.564
2	0.477	2.72	0.434
3	0.698	2.25	0.352
4	0.903	1.77	0.248
5	1.0	1.63	0.212

Effect of periodate concentration for AMP: Rate constants decreased with rise in concentration of KIO_4. The degradation order of ampicillin with respect to active mass of periodate was found to be -0.642 ($r \geq 0.998$, $s \leq 0.001$), represented by Table 20 and Figure 46.

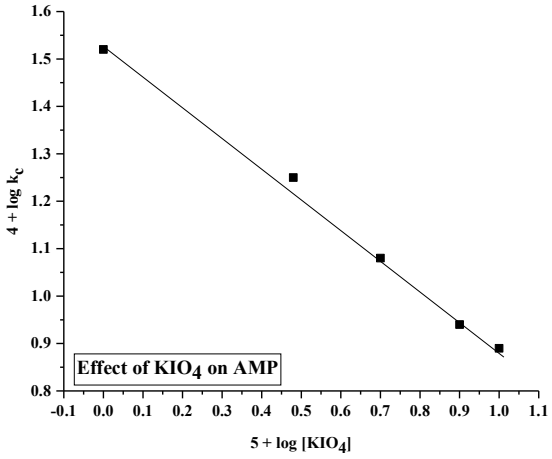

Figure 46: Plot of ($4 + \log k_c$) vs. $5 + \log [KIO_4]$

Table 20: Data for plot of $5 + \log [KIO_4]$ vs. $4 + \log k_c$

S. N.	$5 + \log [KIO_4]$	$k_C \times 10^{-3}$	$3 + \log k_c$
1	0	3.89	1.52
2	0.48	3.34	1.25
3	0.7	2.66	1.08
4	0.9	1.63	0.94
5	1	0.86	0.89

Effect of periodate concentration for DCLX: Rate constants (k_c) of DCLX depressed with a rise in active mass of KIO_4 and the degradation order of dicloxacillin with respect to active mass of periodate was found to be - 0.484 ($r \geq 0.996$, $s \leq 0.001$) as shown by Table 21 and Figure 47.

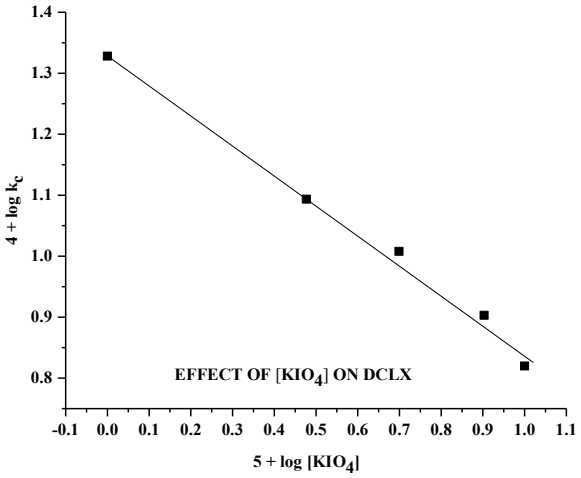

Figure 47: Plot of (4 + log k_c) vs. 5 + log [KIO_4]

Table 21: Data for plot of 5 + log [KIO_4] vs. 4 + log k_c

S. N.	5 + log [KIO_4]	k_c x 10^{-3}	4 + log k_c
1	0	2.13	1.328
2	0.48	1.26	1.1
3	0.7	1.0	1
4	0.9	0.79	0.9
5	1	0.63	0.8

Effect of periodate concentration for CRBC: - Catalyzed rate constants (k_c) of CRBC depressed with a rise in concentration of KIO_4. The degradation order of carbenicillin with respect to active mass of periodate was found to be - 0.488 ($r \geq 0.997$, $s \leq 0.00063$), as shown by Table 21 and Figure 47.

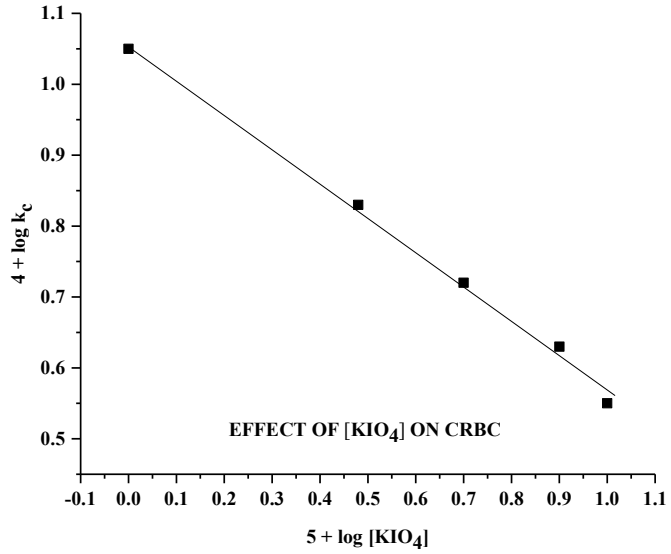

Figure 48: Plot of (4 + log k_c) vs. 5 + log [KIO_4]

Table 22: Data for plot of 5 + log [KIO_4] vs. 4 + log k_c

S. N.	5 + log [KIO_4]	4 + log k_c
1	0	1.05
2	0.48	0.83
3	0.70	0.72
4	0.90	0.63
5	1.00	0.55

Effect of periodate concentration for OXC: Rate constants (k_c) of OXC were noticed in the decreasing order with a rise in active mass of KIO_4. The degradation order of oxacillin with respect to active mass of periodate was found to be -0.230 ($r \geq 0.9987$, $s \leq 0.00073$), as shown by Table 21 and Figure 47.

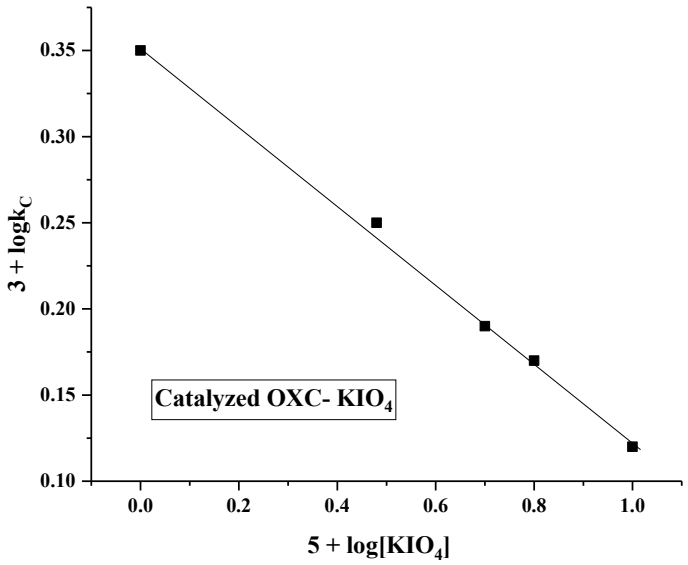

Figure 49: Plot of (3 + log k_c) vs. 5 + log [KIO_4]

Table 23: Data for plot of 5 + log [KIO_4] vs. 3 + log k_c

S. N.	5 + log [KIO_4]	3 + log k_c
1	0	0.35
2	0.48	0.25
3	0.7	0.19
4	0.8	0.17
5	1.0	0.12

4.3.6 Effect of Ionic Strength (I) and Dielectric Constant (D): By varying the concentration of KNO_3 between (0.1 - 0.2) M while maintaining the same concentration of other species, ionic strength was studied; an increase in ionic strength had no any discernible impact. Using the equation $D = D_1V_1 + D_2V_2$, where D_1 and D_2 are the dielectric constants of water and t-butyl alcohol, respectively; one can study the dielectric constant of the medium (D). However, no any discernible effect of the dielectric constant was found.

4.3.7 Effect of Initially Added Products: The initial addition of $CuSO_4$ (II) had no any discernible impact on the catalyzed reaction.

4.3.8 Polymerization Study: A fixed quantity of acrylonitrile monomer was first added to the reaction mixture, which was then left in the inert environment for 3.0 hours. No precipitate formed after the mixture was diluted with methanol, proving there were no free radicals present.

4.4 Effect of Temperature

The effect of temperature on reaction rate was investigated at four different temperatures (20°C, 25°C, 30°C, and 35°C) while maintaining constant concentrations of AMP/AMX/DCLX/CRBC/OXC, $CoCl_3$ (III), KOH, and DPC (III). It was discovered that the rate constants elevated up as the temperature rose. In order to calculate the activation parameter and energy of activation, slopes from a plot of the catalyzed rate constant (Kc), catalytic constant (Kc), and slow step rate constant (k) vs. 1/T were used. Equilibrium constants (K_1, K_2, and K_3) were calculated using the slopes and intercepts from the plot of [Co/k_c] data obtained from (AMX/AMP/DCLX/CRBC/OXC) vs. (1/T). Finally, slopes and intercepts obtained from Van't Hoff plots of **log (K_1/K_2 / K_3)** versus 1/T helped to calculate thermodynamic parameters. The least squares method, also known as linear regression analysis, was applied in each case. The generalized notation was **Y = a X + b** where a represents slope and b represents intercept. The most traceable type of linear regression analysis is one that only considers the values of the dependent variable Y to be affected by experimental error, while assuming that all values of independent variables X are accurately determined. Since observations can be measured with greater accuracy than chemical or physical quantities related to reactant active masses, the majority of sets of kinetic data approximate this situation. The common linear regression analysis's straight line is the one that minimizes the sum of the squares of Y's deviations from the straight line. Numerous mathematically equivalent but visually dissimilar experiments can be used to calculate the slope (a) and intercept (b) parameters for the aforementioned equation. The most familiar equations are:

$$\text{Slope: a} = \frac{n\sum xy - \sum x \sum y}{n\sum x^2 - (\sum x)^2} \qquad \text{and intercept: b} = \frac{\sum y \sum x^2 - \sum x \sum xy}{n\sum x^2 - (\sum x)^2}$$

The summations are for all the data points in the experimental sets, and 'n' is the number of data points. These data were replicated using the least squares method of analysis.

4.4.1 Activation and Thermodynamic Parameters for AMX

Activation parameters refer to the thermodynamic quantities associated with transition state or complex formation state of a chemical reaction. The key activation parameters can be listed as follows:-

1. Activation energy (Ea)- It represents the minimum amount of energy required by a reacting molecule for a successful collision between reacting molecules in order to break bonds to yield product by crossing the energy barrier. It can be given mathematically as-

$k = A\ e^{-Ea/RT}$, where 'k' is rate constant, 'A' is pre-exponential factor, 'Ea' is activation energy, 'R' and 'T' denote universal gas constant and absolute temperature. Lower activation energy indicates fast reaction.

2. Enthalpy of activation ($\Delta H^{\#}$):- Catalysts can stabilize the transition state of complex formation state by reducing the enthalpy change between reacting species and complex or transition state. It lowers the energy required to reach the transition state by accelerating the reaction rate.

3. Entropy of activation ($\Delta S^{\#}$):-Entropy represents the measurement of degree of disorder or randomness present in the system. Application of a catalyst can facilitate the proper organization of the transition state by increasing the entropy change between reacting species and the complex. Higher entropy change suggests the more ordered complex than reactants by increasing the reaction rate and makes complex reaction more favorable in predicting spontaneously.

4. Gibbs free energy of activation ($\Delta G^{\#}$):- Free energy corresponds to the minimum available energy in the system that can easily be converted into any useful work. Negative free energy indicates the spontaneity of a process. Lower free energy corresponds to a more favorable transition state by accelerating the rate of degradation.

Gibb's free energy change (ΔG°) helps to determine the spontaneity of reaction. A negative magnitude confirms spontaneous process under the set of conditions provided and informs whether the reaction is thermodynamically feasible or not. Similarly, signs and magnitudes of enthalpy change (ΔH°) and entropy change (ΔS°) provide insights into the nature of reaction. A highly exothermic reaction (-ve ΔH°) with a significant increase in entropy (+ve ΔS°) indicate a favorable and spontaneous process. Similarly, catalytic constants measure the effectiveness of catalyst in promoting the oxidation of PADs. Different rate constants quantify how quickly the PAD is oxidized under specific conditions. Faster rate constants indicate effective degradation of PAD in shorter time. Order of reaction indicates how the rate of degradation depends on the variable concentrations of PAD and other co-reactants.

i) The catalyzed rate constant (k_C) for activation parameters of AMX

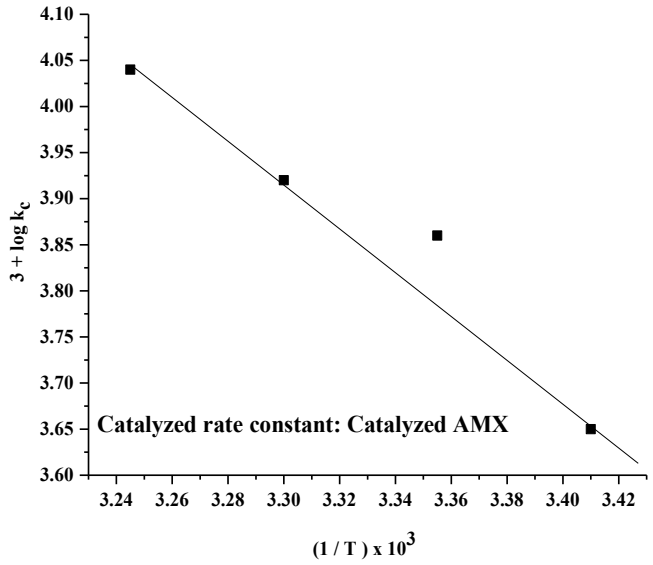

Figure 50: Plot of (3 + log k_c) vs. (1 / T) x 10^3 for AMX

Table 24: Data for plot of (1 / T) x 10^3 vs. 3 + log k_c

S. N.	1 / T x 10^3	k_C x 10^{-3}	3 + log k_C
1	3.412	2.23	0.35
2	3.355	3.67	0.56
3	3.003	4.19	0.62
4	3.246	5.52	0.74

Table 25: Activation parameters from catalyzed rate constant of AMX

Activation Parameters	Values
Ea	40 ± 1 (k $Jmol^{-1}$)
$\Delta H^{\neq}$	39 ±1 (k $Jmol^{-1}$)
$\Delta S^{\neq}$	-151 ± 2 ($JK^{-1}mol^{-1}$)
$\Delta G^{\neq}$	55 ± 4 (k J mol^{-1})
Log A	5 ± 0.3

ii) Catalytic constant **(K_C)** and activation parameters

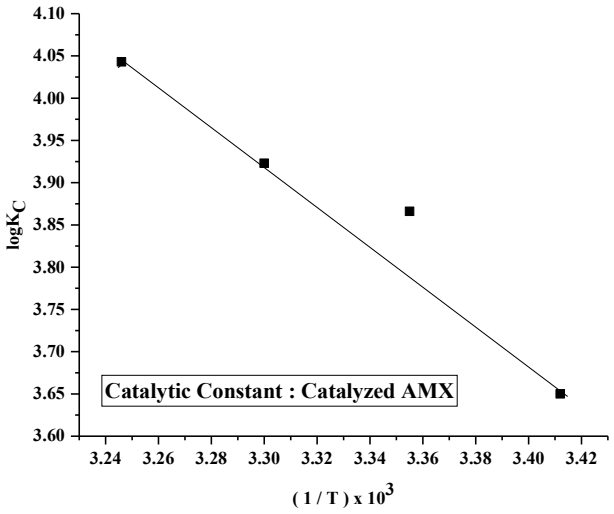

Figure 51: Plot of log Kc vs. (1 / T x 10^3) for AMX

Table 26: Data for the plot of Catalytic constant for AMX

S. N.	k_T x 10^{-3}	k_U x 10^{-4}	[Co] x 10^{-7}	K_C
1	2.42	1.86	5.0	4468
2	4.06	3.87	5.0	7346
3	4.6	4.1	5.0	8380
4	6.1	5.76	5.0	11048

Table 27: Data for the plot of {(1 / T) x 10^3 vs. log k_c}

S. N.	1 / T x 10^3	log K_C
1	3.412	3.65011
2	3.355	3.866
3	3.3	3.923
4	3.246	4.043

Table 28: Activation parameters from catalytic constant of AMX

Activation Parameters	Values
Ea	43 ± 1 (k $Jmol^{-1}$)
$\Delta H^{\neq}$	40 ± 0.6 (k $Jmol^{-1}$)
$\Delta S^{\neq}$	-36 ± 2 ($JK^{-1}mol^{-1}$)
$\Delta G^{\neq}$	51 ± 4 (k J mol^{-1})
Log A	11 ± 0.3

iii) Slow step rate constant (k) of AMX

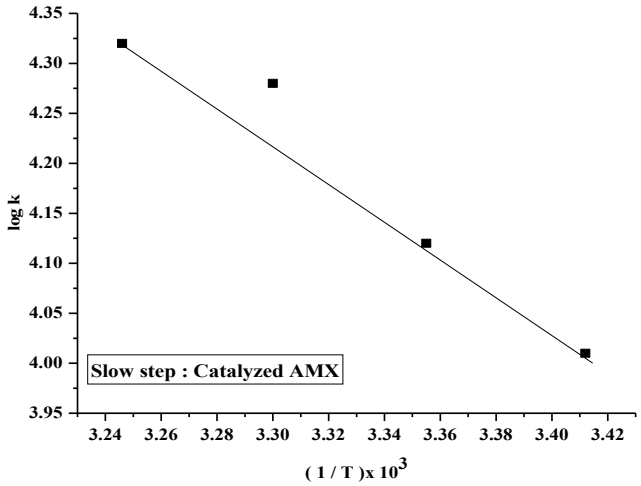

Figure 52: Plot of log k vs. (1 / T x 10^3) for AMX

Table 29: Data for slow step rate constant of AMX

S. N.	1 / T x 10^3	k (slow step)	log k
1	3.412	6466	3.81
2	3.355	10224.94	4.0
3	3.003	16162.4	4.21
4	3.246	20533.9	4.3

Table 30: Activation parameters from slow step rate constant of AMX

Activation Parameters	Values
Ea	59.5 (k $Jmol^{-1}$)
$\Delta H^{\neq}$	56.92 (k $Jmol^{-1}$)
$\Delta S^{\neq}$	25 ($JK^{-1}mol^{-1}$)
$\Delta G^{\neq}$	49.2 (k J mol^{-1})
Log A	14.3

iv) Plots of equilibrium Constants (K_1, K_2 & K_3) of AMX

In redox reactions, multiple equilibrium constants can have important significances in understanding the reaction dynamics and energetic. For a complex reaction, substrate or oxidant may exhibit multiple degree of ionization depending upon temperature, pH or solvent condition. There are three equilibrium constants.

1. First ionization constant (K_1):- Also known as primary ionization constant, it represents the main redox reaction that is occurring. It describes the ratio of concentration or activities of the oxidized and reduced species at equilibrium. It is an important constant that defines the overall feasibility, kinetics, and thermodynamics of the redox reactions.

2. Second and third ionization constant (K_2, K_3):- Also known as secondary equilibrium constants, they represent additional equilibrium that may be involved in the overall redox process. They can affect the overall redox behavior, shift the primary equilibrium, and can alter the observed redox potentials and reaction kinetics. They could include the following factors:-

i) It may involve proton transfer reactions like in acid-base equilibrium alongside the parallel redox reaction.
ii) Formation of complexes between the redox species and other ions or ligands present in the system. They may involve dimerization or self association process.

Significances of multiple equilibrium constants (K_1, K_2, and K3) are as follows:-

1) They provide a more complete thermodynamic description of the degradation process.
2) They allow modeling of pH dependent redox behavior and specification of redox species.
3) They provide basic concept of multiple equilibrium constant for accurate interpretation of electrochemical data to predict outcomes of degradation outcomes of PADs.

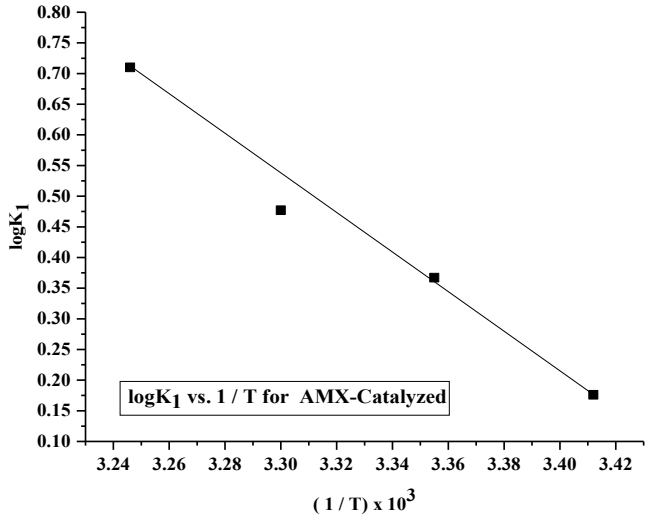

Figure 53: Plot of log K_1 vs. (1 / T) x 10^3 for AMX

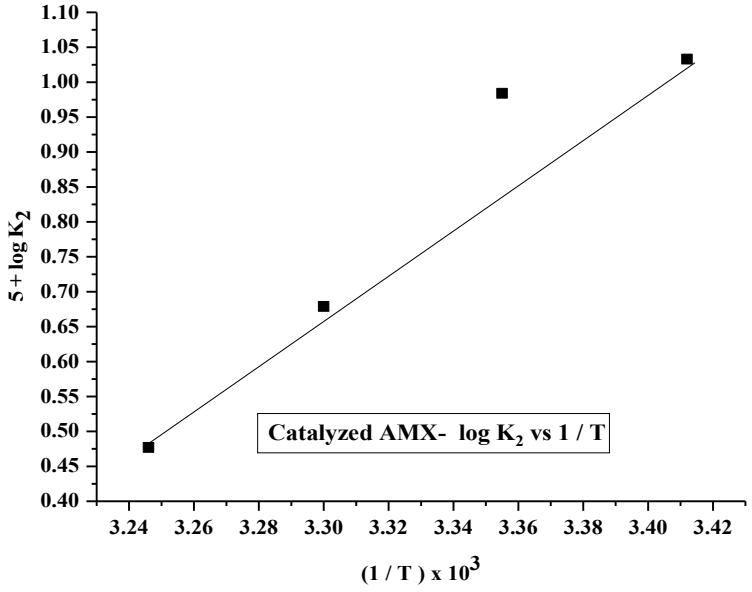

Figure 54: Plot of (5 + log K_2) vs. (1 / T) x 10^3 for AMX

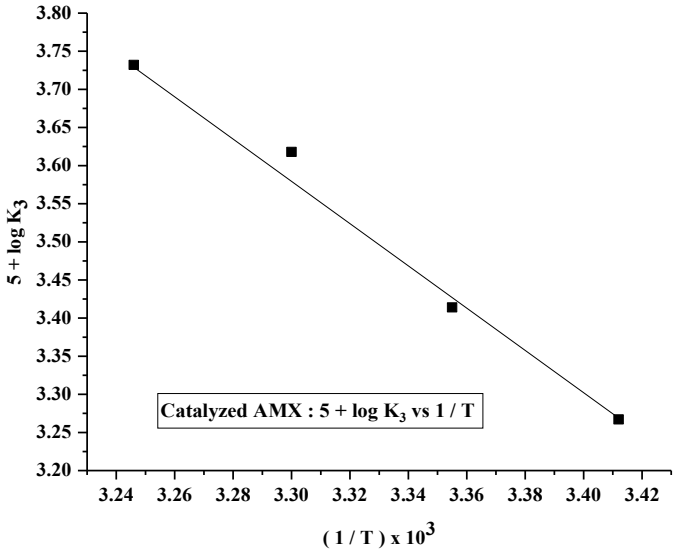

Figure 55: Plot of (5 + log K_3) vs. (1 / T) x 10^3 for AMX

iv) Plot of equilibrium constants of AMX

Table 31: Data for the plot of [1 / T) x 10^3] vs. log K_1

S. N.	Temperature	[1 / T) x 10^3]	K_1	logK_1
1	20 ℃	3.412	1.5	0.176
2	25 ℃	3.355	2.33	0.367
3	30 ℃	3.3	3	0.477
4	35 ℃	3.246	5.13	0.71

Table 32: Data for the plot of [1 /T x 10^3] vs.3 + log K_2

S. N.	Temperature	[1 / T x 10^3]	K_2 x10^{-4}	5 + logK_2
1	20 ℃	3.412	1.08	1.033
2	25 ℃	3.355	0.965	0.984
3	30 ℃	3.3	0.602	0.779
4	35 ℃	3.246	0.3	0.477

Table 33: Data for the plot of [1 /T) x 10^3] vs. 3 + logK_3

S. N.	Temperature	[1 / T x 10^3]	K_3 x 10^3	5 + logK_3
1	20 ℃	3.412	1.85	3.267
2	25 ℃	3.355	2.6	3.414
3	30 ℃	3.3	4.15	3.618
4	35 ℃	3.246	5.4	3.732

Verification plots of [Co/k_c] for AMX

Verification plots play a crucial role in the cobalt (III) catalyzed oxidation of PADs by DPC (III) in alkaline medium. This support in understanding the reaction kinetics by providing validation for visual representation of data and confine the reaction rates as well as reaction orders. Any variation in slopes and intercepts indicate different reaction pathways and forecast any anomalies or inconsistencies in the experimental results promoting further investigation like thermodynamic parameters calculation. These plots help in comparing the effects of different variables like pH, temperature on the oxidation process and facilitate a better understanding of the reaction conditions being favoured or hindered. These plots permit for the quantification of reactant and product active mass over time for calculation of proper yields and efficiency of products.

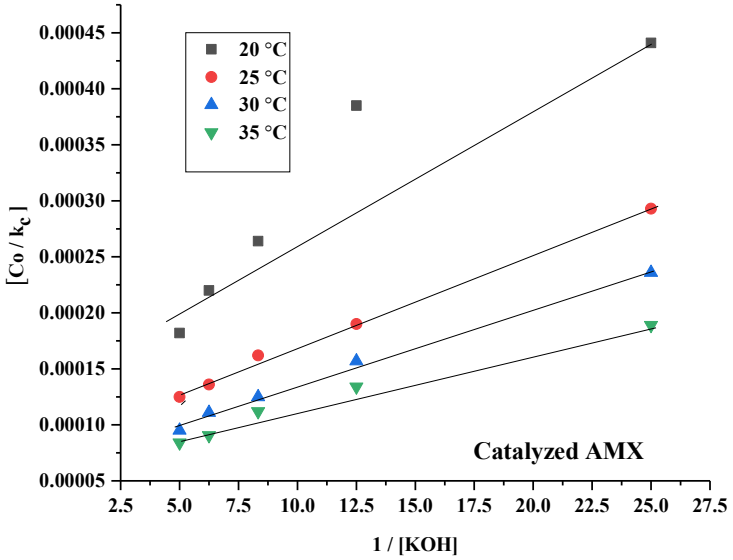

Figure 56: Plot of [Co/k_c] vs. 1/[KOH] for AMX

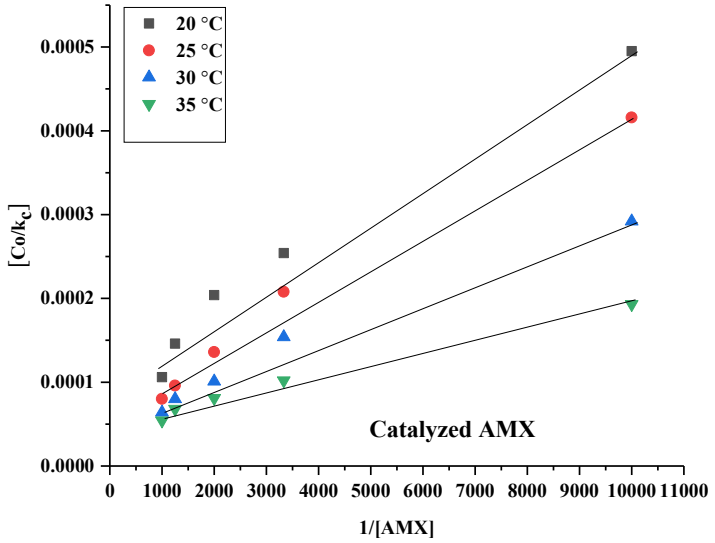

Figure 57: Plot of 1/[AMX] vs. [Co/k_c] for AMX

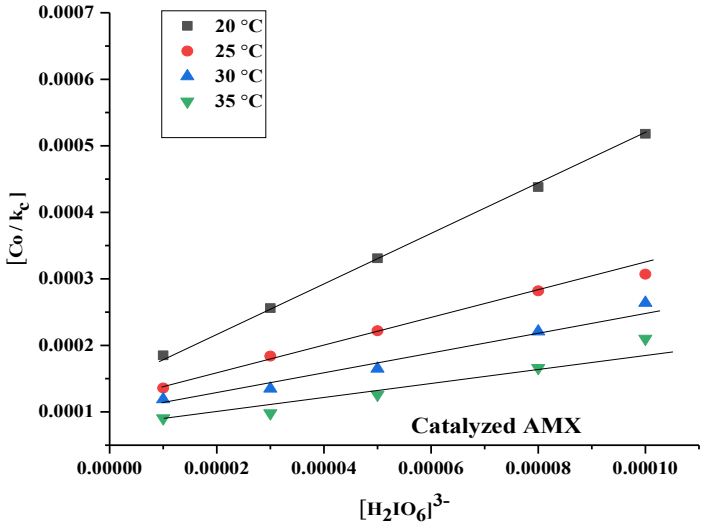

Figure 58: Plot of $[H_2IO_6]^{3-}$ vs. $[Co/k_c]$ for AMX

Four temperature data for verification plots

Table 34: Data for plot of $[Co/k_C]$ vs. 1/[AMX]

	TEMPERATURE			
	20°C	**25°C**	**30°C**	**35°C**
$[Co / k_C]$ x 10^{-4}	4.95	4.16	2.92	1.93
	2.54	2.08	1.54	1.02
	2.04	1.36	1.01	8.1
	1.46	9.6	8	6.8
	1.06	8.02	6.4	5.41

Table 35: Data for plot of $[Co/k_C]$ vs. 1/[KOH]

	TEMPERATURE			
	20°C	**25°C**	**30°C**	**35°C**
$[Co / k_C]$ x 10^{-4}	4.41	2.93	2.36	1.89
	3.85	1.9	1.57	1.34
	2.64	1.62	1.25	1.12
	2.2	1.36	1.11	9.05
	1.82	1.25	9.51	8.41

Table 36: Data for plot of $[Co/k_C]$ vs. $[H_2IO_6]^{3-}$

	TEMPERATURE			
	20°C	**25°C**	**30°C**	**35°C**
$[Co / k_C]$ x 10^{-4}	1.85	1.36	1.19	9.05
	2.56	1.84	1.35	9.8
	3.31	2.22	1.65	1.26
	4.38	2.82	2.21	1.66
	5.18	3.07	2.64	2.1

Table 37: k, K_1, K_2 and K_3 values for Catalyzed AMX

Equilibrium Constants ↓	**Absolute Temperatures**			
Temperature →	**20 °C**	**25 °C**	**30°C**	**35 °C**
k (Slow step rate constant)	1.03×10^4	1.32×10^4	1.9×10^4	2.08×10^4
K_1	1.5	2.33	3	5.13
K_2	1.08×10^{-4}	9.65×10^{-4}	6.02×10^{-5}	3×10^{-5}
K_3	1.85×10^3	2.6×10^3	4.15×10^3	5.4×10^3

The first and the third equilibrium constants (K_1, & K_3) are increasing, but the second equilibrium constant (K_2) is in the decreasing order. This suggests that the amoxicillin and DPC (III) react more easily in the favorable condition or the forward reaction rate is

increasing relative to the backward one; K_1 values increase certainly. Decrease in the second equilibrium constant (K_2) indicates the hindered formation of intermediate species or its inter-conversion to the next product or accumulation of intermediate species may be difficult or hindered; may shift the primary equilibrium away from the forward reaction causing a net diversion of reaction pathway leading a decreasing order for K_2. Finally, increasing order of third equilibrium constant (K_3) indicates the favorable condition for the final step in which the catalyst, Co (III), is facilitating the efficient conversion of intermediates into the final degradation products. Hence, a decrement in K_2 reports a bottleneck or unfavorable intermediate step that may need further optimization to increase the degradation reaction of amoxicillin in the alkaline medium.

Table 38: Thermodynamic parameters from equilibrium constants for AMX

Thermodynamic Parameters	**Values from K_1**	**Values from K_2**	**Values from K_3**
ΔH°_{298} (in k J mol^{-1})	59.44	-68.39	55.58
ΔS°_{298} (in J K^{-1} mol^{-1})	206.00	-212.37	252.41
ΔG°_{298} (in k J mol^{-1})	-1.94	-5.10	-19.63

Catalytic degradation of amoxicillin in alkaline medium is finally associated with negative free energy changes like (-1.94, -5.10, & and -19.63) kJ $mole^{-1}$ which ultimately predicts the feasibility for spontaneity of the ampicillin degradation in the alkaline medium. Entropy values from K_1 and K_3 in positive order indicating spontaneous feasibility of the degradation process. However, negative entropy indicates that pure ampicillin may have relatively low entropy in the initial state in comparison to that in the final state or in the degraded products. The catalyst, Co (III), reduces the activation energy to accelerate the degradation process and the system reaches the high entropy state more efficiently.

Gibb's free energy change (ΔG°) helps to determine the spontaneity of reaction. A negative magnitude confirms spontaneous process under the set of conditions provided and informs whether the reaction is thermodynamically feasible or not. Similarly, signs and magnitudes of enthalpy change (ΔH°) and entropy change (ΔS°) provide insights into the nature of reaction. A highly exothermic reaction (-ve ΔH°) with a significant increase in entropy (+ve ΔS°) indicate a favorable and spontaneous process. Similarly, catalytic constants measure the effectiveness of catalyst in promoting the oxidation of PADs. Different rate constants quantify how quickly the PAD is oxidized under specific conditions. Faster rate constants indicate effective degradation of PAD in shorter time. Order of reaction indicates how the rate of degradation depends on the variable concentrations of PAD and other co-reactants.

4.4.2 Activation and Thermodynamic Parameters for AMP

i) The catalyzed rate constant (k_c) of AMP

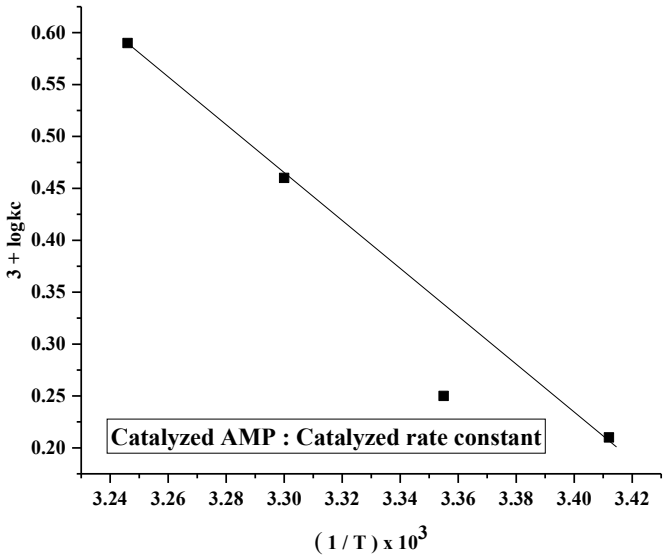

Figure 59: Plot of (3 + log k_c) vs. (1/T) x 10^3 for AMP

Table 39: Data for plot (3 + log k_c) vs. [1/T x 10^3]

S. N.	[1 / T x 10^3]	k_C x 10^{-3}	3 + log k_C
1	3.412	1.62	0.21
2	3.355	1.78	0.25
3	3.003	3.28	0.51
4	3.246	3.89	0.59

Table 40: Activation Parameters from catalyzed rate constant for AMP

Activation Parameters	Values
Ea	46.8 (k $Jmol^{-1}$)
$\Delta H^{\neq}$	44.3 ± 1.0 (k $Jmol^{-1}$)
$\Delta S^{\neq}$	-145 ± 3 ($JK^{-1}mol^{-1}$)
$\Delta G^{\neq}$	88 ± 2 (k J mol^{-1})
Log A	5.5 ± 0.2

ii) Catalytic constant ($\mathbf{K_C}$) of AMP

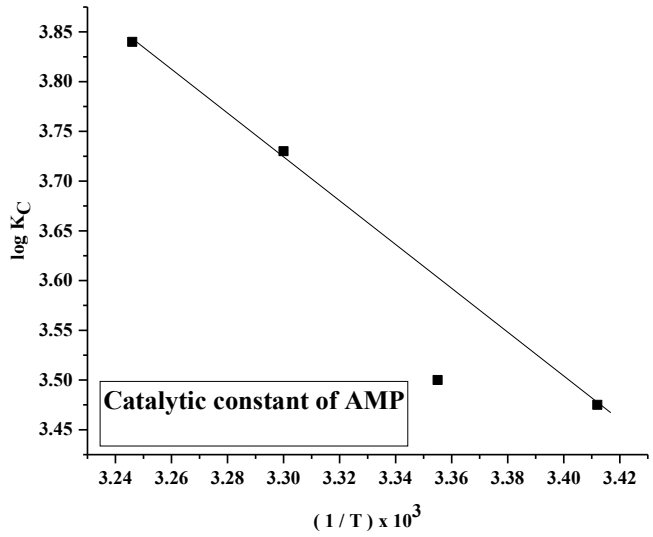

Figure 60: Plot of [1/T x 10^3] vs. log K_c of AMP

Table 41: Data for catalytic Constant (Kc) for AMP

S. N.	k_T x 10^{-3}	k_U x 10^{-4}	[Co] x 10^{-7}	K_C
1	2.42	1.86	5.0	2990
2	4.06	3.87	5.0	3188
3	4.6	4.1	5.0	6076
4	6.1	5.76	5.0	7006

Table 42: Data for plot of catalytic constant (Kc) vs. 1/T for AMP

S. N.	[1 / T x 10^3]	log K_C
1	3.412	3.47
2	3.355	3.5
3	3.3	3.78
4	3.246	3.84

Table 43: Activation parameters from catalytic constant (K_c) for AMP

Activation Parameters	Values
Ea	45.94 (k $Jmol^{-1}$)
$\Delta H^{\neq}$	43 ± 1.0 (k $Jmol^{-1}$)
$\Delta S^{\neq}$	-31 ± 1.5 ($JK^{-1}mol^{-1}$)
$\Delta G^{\neq}$	52 ± 2.0 (k J mol^{-1})
Log A	11.6 ± 0.2

iii) Slow step rate constant (k) for AMP

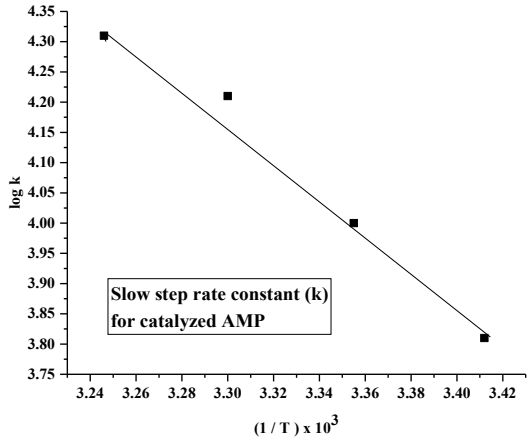

Figure 61: Plot of log k vs. (1/T x 10^3) of AMP

Table 44: Data for slow step rate constant (k) for AMP

S. N.	[1 / T x 10^3]	k (slow step)	log k
1	3.412	6466	3.81
2	3.355	10224.94	4
3	3.003	16162.4	4.21
4	3.246	20533.9	4.3

Table 45: Activation parameters from slow step rate constant (k) for AMP

Activation Parameters	Values
Ea	59.5 (k $Jmol^{-1}$)
$\Delta H^{\neq}$	56.92 (k $Jmol^{-1}$)
$\Delta S^{\neq}$	25 ($JK^{-1}mol^{-1}$)
$\Delta G^{\neq}$	49.2 (k J mol^{-1})
Log A	14.3

Verification plots of [Co/k_c] and data for AMP

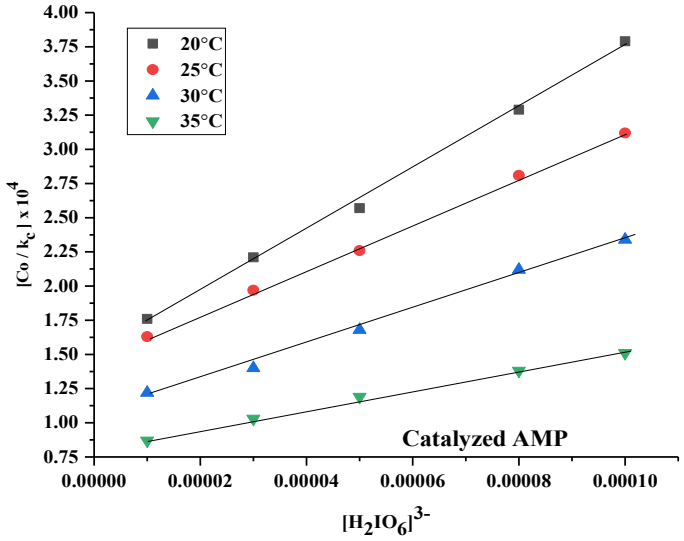

Figure 62: Plot of [Co/k_c] x 10^4 vs. $[H_2IO_6]^{2-}$ for AMP

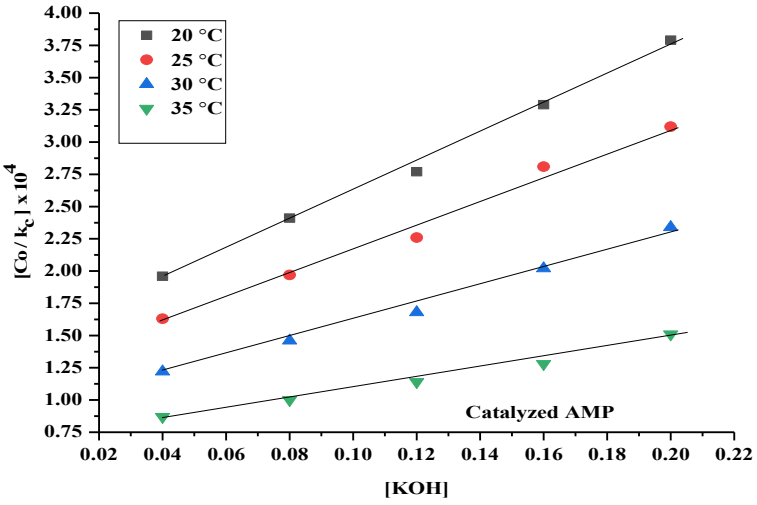

Figure 63: Plot of [Co/k_c] x 10^4 vs. [KOH] for AMP

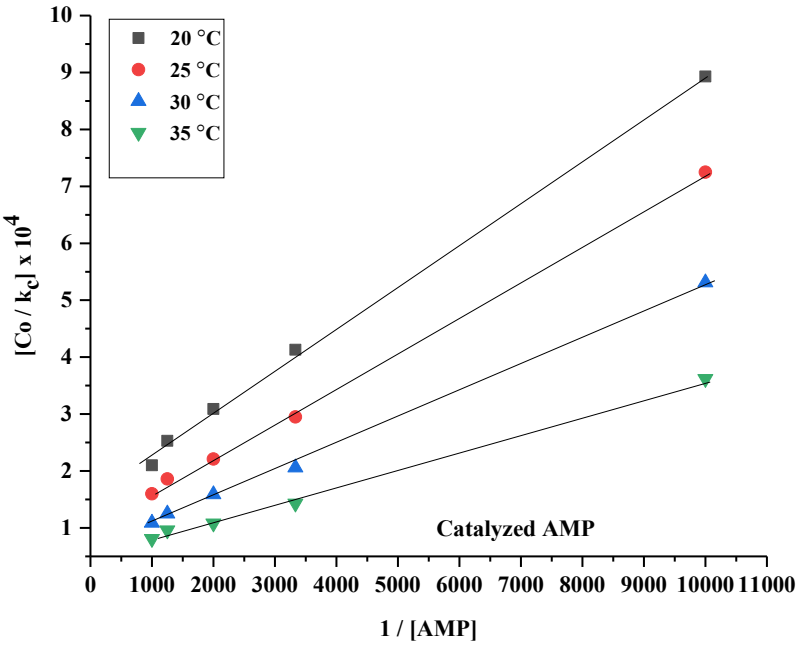

Figure 64: Plot of $[Co/k_c] \times 10^4$ vs. 1 / [AMP]

Four temperature data for verification plots

Table 46: Data for the plot of $[Co/k_C]$ vs. 1/[AMP]

	TEMPERATURE			
	20°C	**25°C**	**30°C**	**35°C**
$[Co / k_C] \times 10^{-4}$	8.93	7.25	5.31	3.62
	4.13	2.95	2.06	1.43
	3.09	2.21	1.59	1.08
	2.53	1.86	1.25	0.96
	2.1	1.6	1.09	0.81

Table 47: Data for the plot of [Co/k_C] vs. [KOH]

	TEMPERATURE			
	20°C	**25°C**	**30°C**	**35°C**
	1.96	1.63	1.22	0.87
[Co / k_C] x 10^{-4}	2.41	1.97	1.46	1.0
	2.77	2.26	1.68	1.14
	3.29	2.81	2.02	1.28
	3.79	3.12	2.34	1.51

Table 48: Data for the plot of [Co/k_C] vs. $[H_3IO_6]^{2-}$

	TEMPERATURE			
	20°C	**25°C**	**30°C**	**35°C**
	1.76	1.63	1.22	0.87
[Co / k_C] x 10^{-4}	2.21	1.97	1.4	1.03
	2.57	2.26	1.68	1.19
	3.29	2.81	2.12	1.38
	3.79	3.12	2.34	1.51

iv) Plots of equilibrium constants of AMP

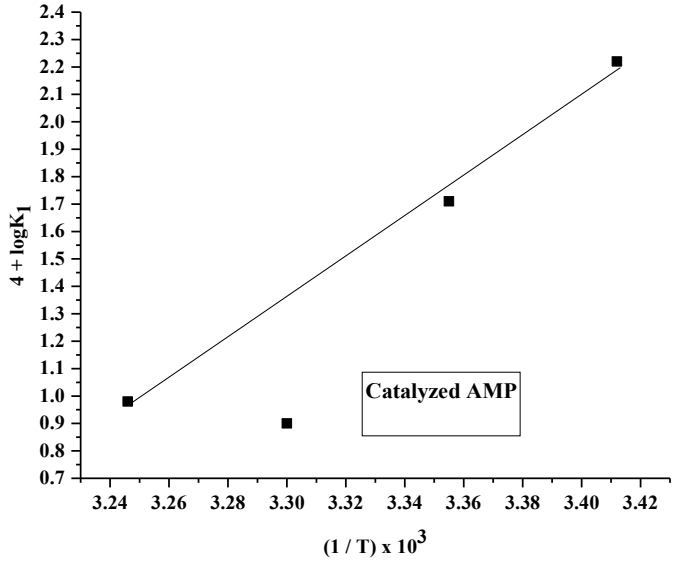

Figure 65: Plot of (4 +log K_1) vs. (1/T) x 10^3 for AMP

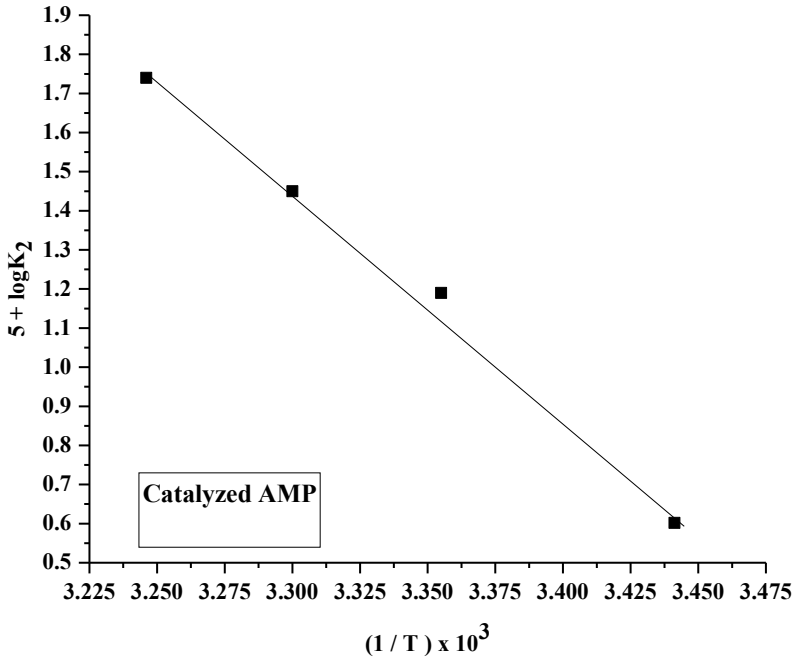

Figure 66: Plot of (5 + log K_2) vs. (1/T) x 10^3 for AMP

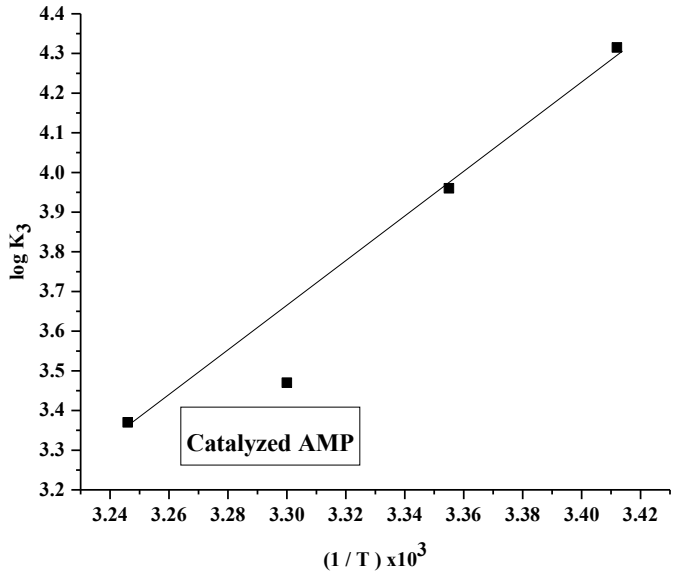

Figure 67: Plot of (log K_3) vs. (1/T) x 10^3 for AMP

Table 49: k, K_1, K_2 and K_3 values for catalyzed AMP

Equilibrium Constants ↓	**Absolute Temperatures**			
Temperature →	**20 °C**	**25 °C**	**30°C**	**35 °C**
k (Slow step rate constant)	6466	10224.94	16162.4	20533.9
K_1	0.01648	0.0016137	0.000794	0.0009633
K_2	4 x10^{-5}	1.56 x 10^{-4}	2.81 x 10^{-4}	5.46 x 10^{-4}
K_3	20666.66	4067.98	2936.15	2374.04

With increase in temperature, slow step rate constants go on increasing due to mechanism and kinetics of the redox reaction indicating the easier feasibility or spontaneity of the process. It also means that the rate determining step is becoming more favorable with increasing temperatures. The activation energy barrior for the slow step is already overcome more easily as it requires lower activation energy.

For the degradation of ampicillin by DPC (III) in alkaline medium, the second equilibrium constant is increasing while the first and the third equilibrium constants are found to be in the decreasing orders; it is related to the complex reaction mechanism and the specific chemical transformations taking place internally. Ampicillin reacts with DPC (III) in the alkaline medium with which the first equilibrium constant is related. With progress of reaction, intermediate products are formed that be less interactive with DPC (III), and decrease in the reactivity of initial species may cause a decreasing order. Second equilibrium constant is related to the stability and formation of intermediate species which become more favorable with progress of reaction, and hence the second equilibrium constant goes on increasing with raise it temperatures. The third equilibrium constant also goes on decreasing as the constant reports the final steps of the degradation of ampicillin which may become less favorable due to depletion of ampicillin or accumulation of side products. Decreasing order of the third constant reports the lower tendency for the formation of final degradation products of ampicillin.

Table 50: Thermodynamic parameters from equilibrium constants for AMP

Thermodynamic Parameters	**Values from K_1**	**Values from K_2**	**Values from K_3**
ΔH°_{298} (in k J mol^{-1})	-157.89	111.319	115.7
ΔS°_{298} (in JK^{-1} mol^{-1})	- 497.6	395.26	-312.51
ΔG°_{298} (in kJ mol^{-1})	- 9.62	- 6.47	- 22.57

Catalytic degradation of ampicillin by a powerful oxidant, DPC (III), is finally associated with negative free energy change like (-9.62, -6.47, and -22.57) $kJmole^{-1}$ which ultimately predicts the feasibility for spontaneity of the ampicillin degradation in the alkaline medium. However, negative entropy indicates that pure ampicillin may have relatively low entropy in the initial state in comparison to that in the final state or in the degraded products. The catalyst, Co (III) reduces the activation energy to accelerate the degradation process and the system reaches the high entropy state more efficiently.

4.4.3 Activation and Thermodynamic Parameters for DCLX

In alkaline environment, the higher pH can influence these activation parameters and impact degradation pathways for kinetics of PADs. The combined effects of lowered activation energy and more favorable enthalpy change as well as positive entropy change can result in a significant decrease in the Gibbs free energy of activation. Quantitative measurement of these parameters in alkaline medium leads to a faster degradation of PADs in comparison to the uncatalyzed reaction, even in alkaline medium. The specific change in activation parameters may depend on the nature of the catalyst, reaction mechanism, and specific PAD selected for the degradation process.

For the present research work, activation parameters of each PAD were determined with the help of catalyzed rate constant (k_c), catalytic constant (K_c) and slow step rate constant (k) by plotting the concerned values of these constants against reciprocal of temperature. Values of pre-exponential factor (A), related to the collision frequency between PAD and oxidant in the alkaline condition support the proper orientation of reacting species, and were also determined thereby. A higher value of 'A' signifies a favorable collision frequency or a faster reaction. These parameters provide an insight into the stable thermodynamic and kinetic studies. These data are in good agreement with the degradation of PADs in the alkaline medium.

Catalytic constant (Kc) refers to the measurement of the catalytic efficiency of a suitable catalyst. It represents the number of substrate molecules converted into product per unit time per active site of the catalyst. It is an important parameter for evaluating the performance and potency of a catalyst in the reaction. In complex reactions involving multiple equilibrium steps, the rate determining step often limits the overall reaction rate and hence it represents the rate of limiting step in the degradation reaction mechanism. Identification of the slow step rate constant, it becomes easier to understand the overall kinetics, order of reaction, and hence to optimize reaction conditions.

Similarly, catalyst cobalt (III) chloride supports in forming stable co-ordination complexes with PAD molecule that, in turn, enhances in stabilizing transition states of reaction by reducing activation energy required for the spontaneous feasibility of the

reaction. It also participates in catalytic re-cycling to facilitate in the re-generation of reactive intermediates or free radicals. It can lead towards a more favorable orientation of PAD for oxidation by stabilizing the transition state and makes the reaction pathways more efficient. The geometrical arrangement of cobalt (III) also helps in orienting reacting molecules properly to reduce steric hindrance.

i) The catalyzed rate constant (k_c) and activation parameters of DCLX

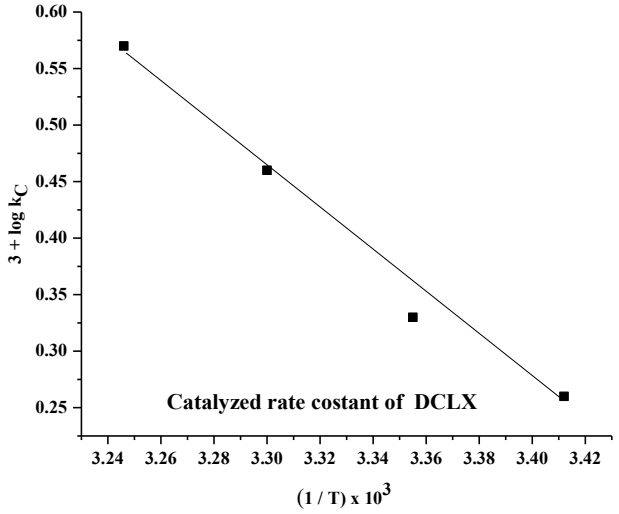

Figure 68: Plot of (1/T) x 10^3 vs. (3 + log k_c) for DCLX

Table 51: Data for plot of [1/T x 10^3] vs. (3 + log k_c) for DCLX

S. N.	[1 / T x 10^3]	k_c x 10^{-3}	3 + log k_c
1	3.412	1.82	0.26
2	3.355	2.13	0.33
3	3.303	2.88	0.46
4	3.246	3.715	0.57

Table 52: Activation parameters from slow step rate constant (k) for DCLX

Activation Parameters	Values
Ea	36.12 (k $Jmol^{-1}$)
$\Delta H^{\neq}$	33 ± 2 (k $Jmol^{-1}$)
$\Delta S^{\neq}$	-184 ± 2 ($JK^{-1}mol^{-1}$)
$\Delta G^{\neq}$	91 ± 2 (k J mol^{-1})
Log A	3.5 ± 0.2

ii) Catalytic constant (K_C) of DCLX and its activation parameters

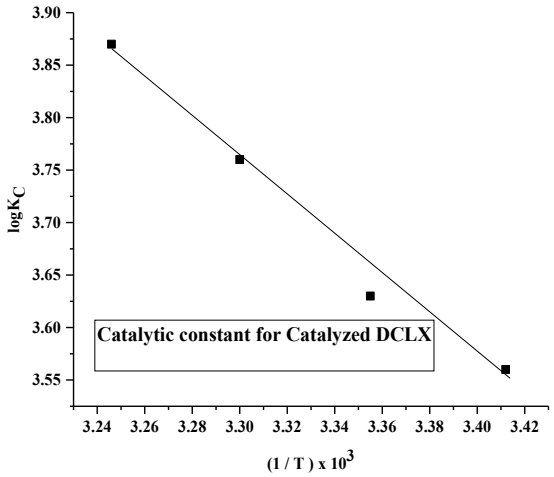

Figure 69: Plot of log K_C vs. (1 / T) x 10^3 for DCLX

Table 53: Data for plot of the catalytic constant of DCLX

S. N.	K_c x 10^{-3}	[Co] x 10^{-7}	K_C
1	1.82	5.0	3640
2	2.13	5.0	4260
3	2.88	5.0	5760
4	3.71	5.0	7420

Table 54: Data for the plot of log K_C vs. [1 / T x 10^3] for DCLX

S. N.	[1 / T x 10^3]	log K_C
1	3.412	3.47
2	3.355	3.5
3	3.3	3.78
4	3.246	3.84

Table 55: Activation parameters from catalytic constant for DCLX

Activation parameters	Values
Ea	36.79 (k $Jmol^{-1}$)
$\Delta H^{\neq}$	34 ± 1 (k $Jmol^{-1}$)
$\Delta S^{\neq}$	-181 ± 0.6 ($JK^{-1}mol^{-1}$)
$\Delta G^{\neq}$	89 ± 3 (k J mol^{-1})
Log A	3.79 ± 0.2

iii) Slow step rate constant (k) of DCLX and its activation parameters

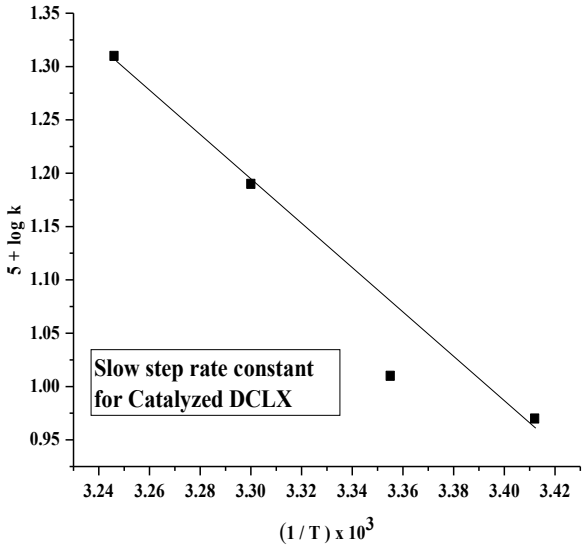

Figure 70: Plot of (1/T) x 10^3 vs. (5 + log k) for DCLX

Table 56: Data for the plot of [1/T x 10^3] vs. (5 + log k) for DCLX

Temp (K)	[1/T x 10^3]	k x 10^{-4}	5 + log k
293	3.411	0.93	0.97
298	3.355	1.02	1.01
303	3.3	1.57	1.2
308	3.245	2.06	1.31

Table 57: Activation parameters from slow step rate constant (k) for DCLX

Activation Parameters	Values
Ea	41.61 (k Jmol^{-1})
$\Delta H^{\neq}$	39 ± 2 (k Jmol^{-1})
$\Delta S^{\neq}$	-191 ± 2 (JK^{-1}mol^{-1})
$\Delta G^{\neq}$	96 ± 2 (k J mol^{-1})
Log A	3.2 ± 0.4

Verification plots of [Co/kc] for DCLX

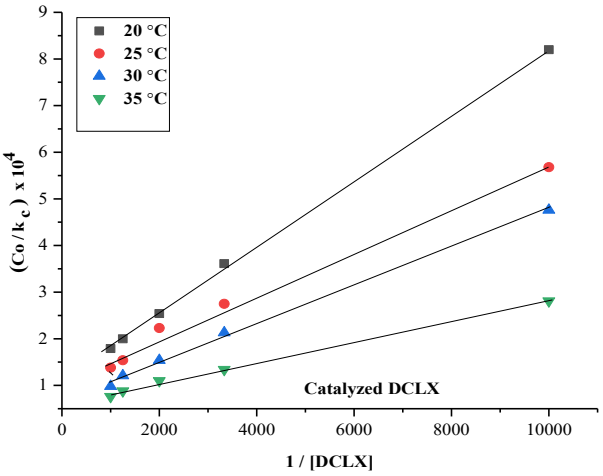

Figure 71: Plot of [Co/k_c] vs. (1/[DCLX] for DCLX

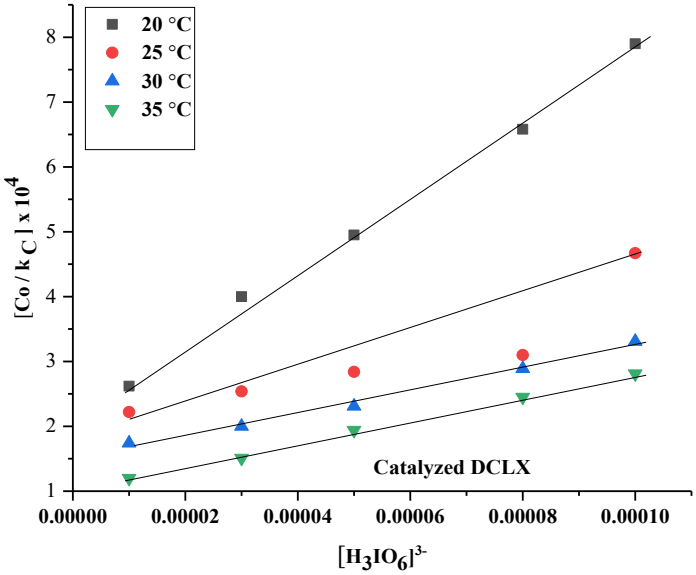

Figure 72: Plot of $[Co/k_c]$ vs. $[H_3IO_6]^{3-}$ for DCLX

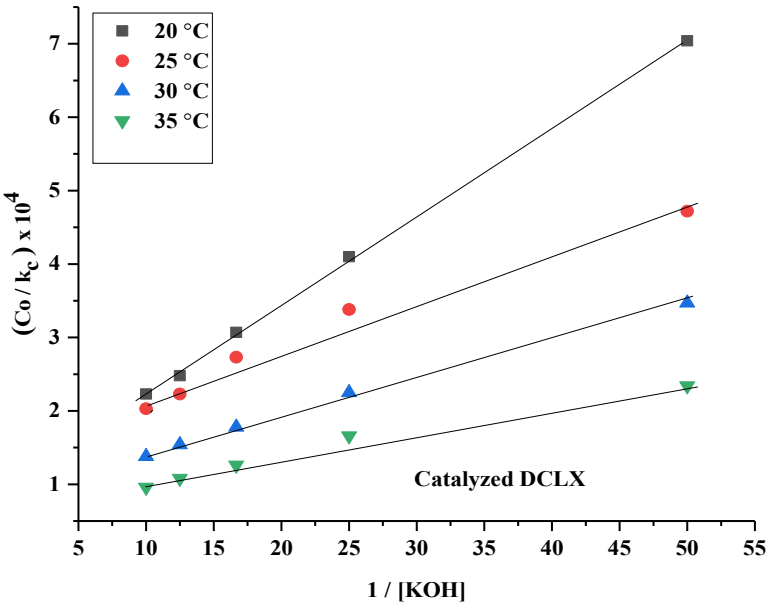

Figure 73: Plot of $[Co/k_c]$ vs. (1/[KOH] for DCLX

Four temperature data for verification plots

Table 58: Data for plot [Co/k_C] vs. 1/[DCLX]

	TEMPERATURE			
	20°C	**25°C**	**30°C**	**35°C**
[Co / k_C] x 10^{-4}	8.2	5.68	4.76	2.81
	4.0	2.75	2.43	1.64
	2.22	2.23	1.74	1.2
	2.0	1.54	1.25	0.98
	1.95	1.28	0.98	0.81

Table 59: Data for plot [Co/k_C] vs. 1/[KOH]

	TEMPERATURE			
	20°C	**25°C**	**30°C**	**35°C**
[Co / k_C] x 10^{-4}	7.04	4.72	3.47	2.34
	5.1	3.38	2.35	1.86
	3.97	2.73	1.92	1.56
	2.22	2.23	1.74	1.2
	2.13	2.03	1.38	0.96

Table 60: Data for plot [Co/k_C] vs. $[H_2IO_6]^{3-}$

	TEMPERATURE			
	20°C	**25°C**	**30°C**	**35°C**
[Co / k_C] x 10^{-4}	2.22	2.23	1.74	1.20
	4.0	2.54	2.0	1.51
	4.95	2.84	2.31	2.04
	6.58	3.0	2.59	2.55
	11.9	4.67	3.31	2.91

iv) Plots of equilibrium constants of DCLX

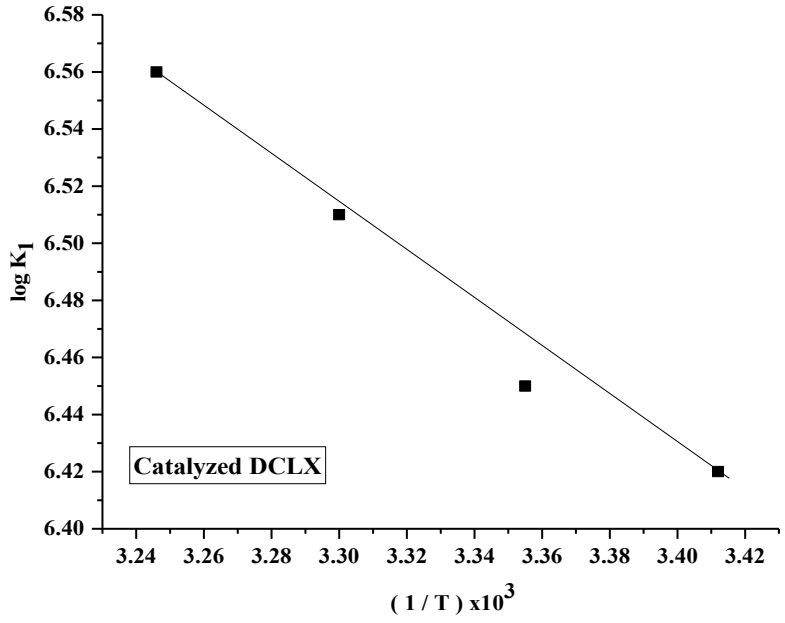

Figure 74: Plot of log K_1 vs. (1/T) x 10^3 for DCLX

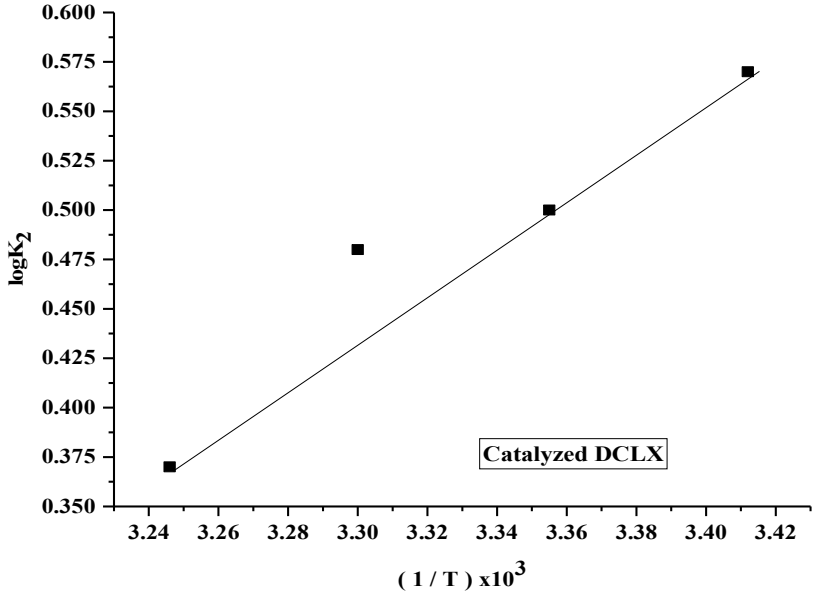

Figure 75: Plot of log K_2 vs. (1/T) x 10^3 for DCLX

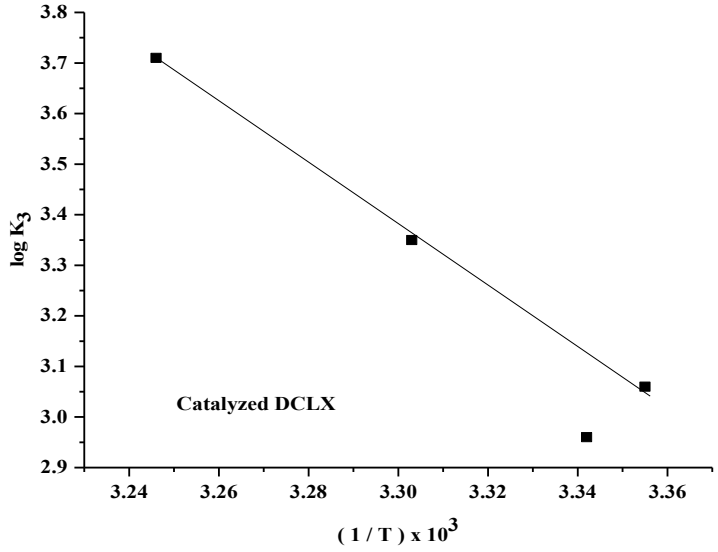

Figure 76: Plot of log K_3 vs. (1/T) x 10^3 for DCLX

(K_1, K_2 & K_3 vs. 1/T) DATA FOR DCLX

Table 61: Data for (1 / T) x 10^3 vs. log K_1 plot for DCLX

S. N.	Temperature	[1 / T x 10^3]	K_1 x10^6	logK_1
1	20 ℃	3.412	2.63	6.42
2	25 ℃	3.355	2.81	6.45
3	30 ℃	3.3	3.23	6.51
4	35 ℃	3.246	3.63	6.56

Table 62: Data for (1 / T) x 10^3 vs. log K_2 plot for DCLX

S. N.	Temperature	[1 / T x 10^3]	K_2	logK_2
1	20 ℃	3.412	3.715	0.57
2	25 ℃	3.355	3.17	0.50
3	30 ℃	3.3	3.019	0.48
4	35 ℃	3.246	2.344	0.37

Table 63: Data for (1 / T) x 10^3 vs. log K_3 plot for DCLX

S. N.	Temperature	[1 / T x 10^3]	K_3	logK_3
1	20 ℃	3.412	1318.25	3.12
2	25 ℃	3.355	1548.81	3.19
3	30 ℃	3.3	1659.59	3.22
4	35 ℃	3.246	2137.96	3.33

Table 64: (k, K_1, K_2 and K_3) values for DCLX

Equilibrium Constants ↓	**Absolute Temperatures**			
Temperature →	**20 ℃**	**25 ℃**	**30℃**	**35 ℃**
k (Slow step rate constant)	0.93 x 10^{-4}	1.02 x 10^{-4}	1.57 x 10^{-4}	2.06 x 10^{-4}
K_1	2.63 x 10^6	2.81 x 10^6	3.23 x 10^6	3.63 x 10^6
K_2	3.715	3.17	3.019	2.344
K_3	1318.25	1548.81	1659.59	2137.96

Only the second equilibrium constant (K_2) is reported in the decreasing order, while the first and third equilibrium constants (K_1, K_3) are found in the increasing order. This implies that either the forward reaction rate is increasing relative to the reverse one or dicloxacillin reacts quite easily with DPC (III) in the favorable conditions. Formation of intermediate species or their inter-conversion into next products or their accumulation might be hindered that may lower the K_2 values. Shifting the primary equilibrium constant away from the forward reaction may cause a deviation from forward reaction pathway and hence K_2 values are decreased. Rapid inter-conversion of intermediates into the final products might be enabled by the catalyst, Co (III), by which K_3 values are increasing.

Table 65: Thermodynamic parameters from equilibrium constants for DCLX

Thermodynamic Parameters	Values from K_1	Values from K_2	Values from K_3
ΔH°_{298} (in k J mol^{-1})	16.4 ± 2	21.45 ± 1	22.77 ± 1
ΔS°_{298} (in J K^{-1} mol^{-1})	176.35 ± 4	82.75 ± 2	138.5 ± 3
ΔG°_{298} (in k J mol^{-1})	-36.941 ± 0.6	-2.87 ± 0.4	-18.27 ± 0.5

Catalytic degradation of dicloxacillin by DPC (III) in alkaline medium is well supported by thermodynamic parameters where both positive entropy change and overall negative free energy change are in the strong support for feasibility of spontaneous degradation.

4.4.4 Activation and Thermodynamic Properties for CRBC

Followings key factors are responsible in influencing the rate of degradation of PADs:-

1. Chemical structure of PADs- Presence of specific functional groups, stereo-chemistry, and overall molecular structure of antibiotic or PADs can significantly impact the catalytic efficiency of degradation process.

2. PADs having more relative functional groups like amide, lactam always try to have higher catalytic constant values as these groups are more susceptible to alkaline mediated degradation.

3. Accessibility of relative ions-The ease of access for hydroxide ion to relative sites with antibiotic molecules can influence the catalytic efficiency.

4. Solvent effects- Properties of solvents like ionic strength, pH, and dielectric constant can influence this constant.

i) Catalyzed rate constant (k_c) and its activation parameters for CRBC

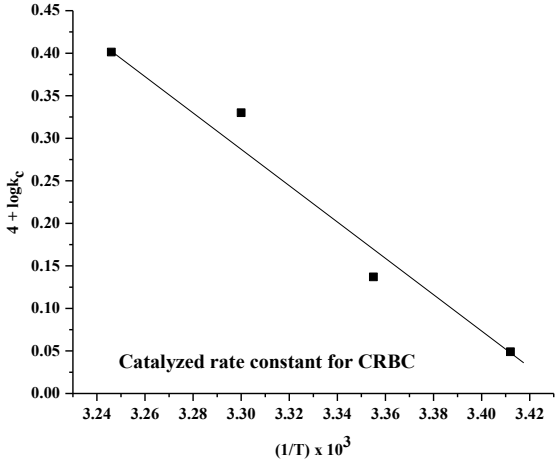

Figure 77: Plot of (4 + log k_c) vs. 1/T x 10^3 for CRBC

Table 66: Data for plot of the catalyzed rate constant (k_c) for CRBC

S. N.	[1/T]x 10^3	k_C x 10^{-3}	4 + log k_C
1	3.412	1.12	0.049
2	3.355	1.37	0.137
3	3.300	2.13	0.330
4	3.246	2.52	0.4014

Table 67: Activation parameters from catalyzed rate constant for CRBC

Activation Parameters	Values
Ea	40.84 (k $Jmol^{-1}$)
$\Delta H^{\neq}$	38 ± 1 (k $Jmol^{-1}$)
$\Delta S^{\neq}$	-169 ± 3 ($JK^{-1}mol^{-1}$)
$\Delta G^{\neq}$	87 ± 2 (k J mol^{-1})
Log A	4.3 ± 0.3

ii) Catalytic constant ($\mathbf{K_c}$) of CRBC

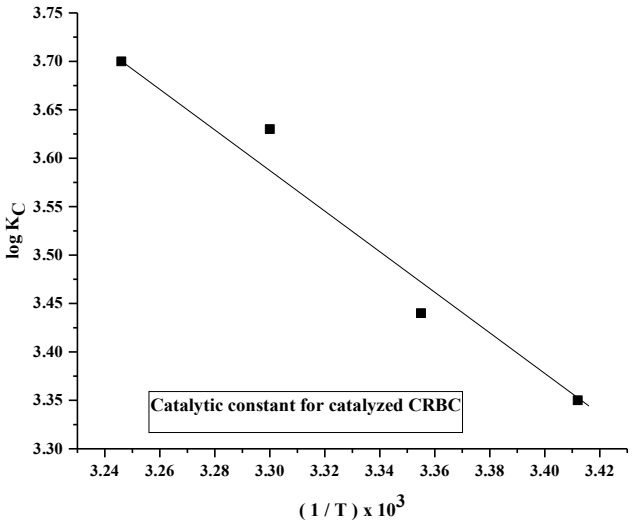

Figure 78: Plot of log K_C vs. (1/T) x 10^3 for CRBC

Table 68: Data for catalytic constant (K_C) of CRBC

S. N.	K_C x 10^{-3}	[Co] x 10^{-7}	K_C
1	1.12	5.0	2240
2	1.37	5.0	2740
3	2.13	5.0	4260
4	2.52	5.0	5040

Table 69: Data for plot of (1 /T) x 10^3 vs. log K_C for CRBC

S. N.	[(1/T) x 10^3]	log K_C
1	3.412	3.35
2	3.355	3.44
3	3.3	3.63
4	3.246	3.7

Table 70: Activation parameters from catalytic constant of CRBC

Activation Parameters	Values
Ea	43.095 (k $Jmol^{-1}$)
$\Delta H^{\neq}$	40 ± 1 (k $Jmol^{-1}$)
$\Delta S^{\neq}$	-163 ± 1 ($JK^{-1}mol^{-1}$)
$\Delta G^{\neq}$	89 ± 2 (k J mol^{-1})
Log A	10.6 ± 0.2

iii) Parameters of activation from CRBC slow step rate constant (k)

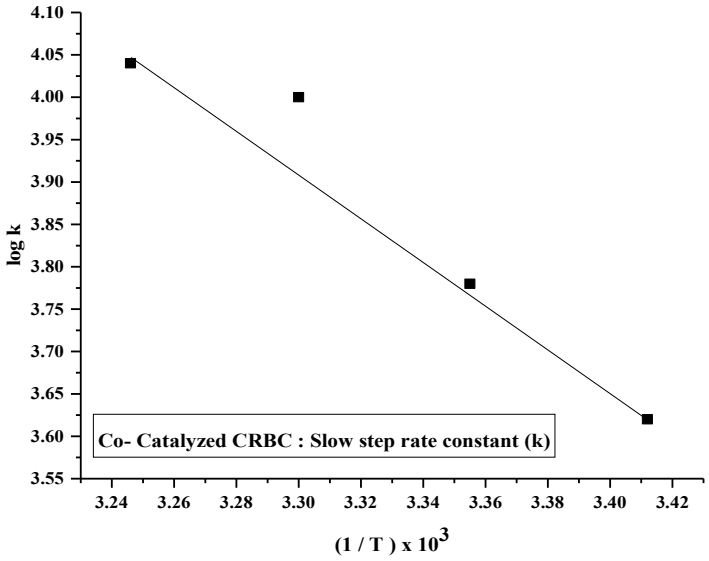

Figure 79: Plot of log k vs. (1/T) x 10^3 for CRBC

Table 71: Data for slow step rate constant of CRBC

S. N.	1/T x 10^3	k x 10^4	log k (slow step)
1	3.412	4.19	3.62
2	3.355	6.13	3.78
3	3.003	10.21	4
4	3.246	11.03	4.04

Table 72: Activation parameters from slow step rate constant for CRBC

Activation Parameters	Values
Ea	51.53 (k $Jmol^{-1}$)
$\Delta H^{\neq}$	49 ± 2 (k $Jmol^{-1}$)
$\Delta S^{\neq}$	-8.6 ± 0.8 ($JK^{-1}mol^{-1}$)
$\Delta G^{\neq}$	49 ± 2 (k J mol^{-1})
Log A	12.4 ± 0.4

Verification plots of [Co/k_c] for CRBC

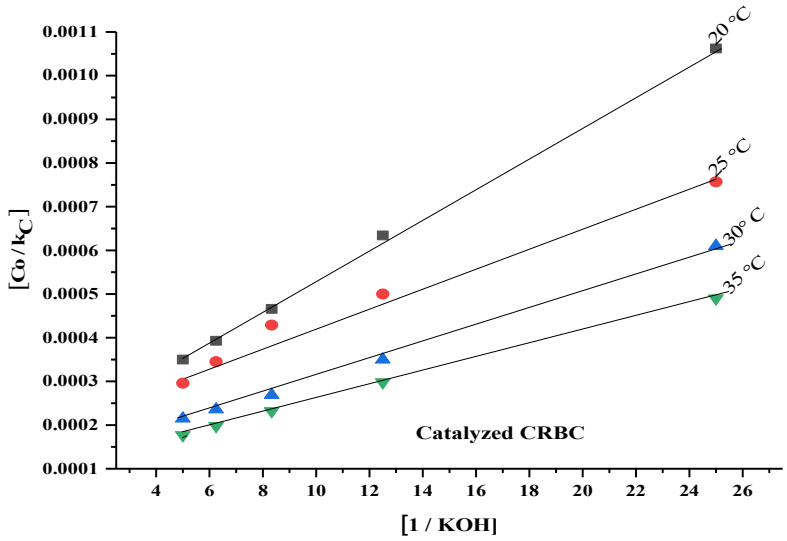

Figure 80: Plot of [Co/k_c] vs. 1/[KOH] for CRBC

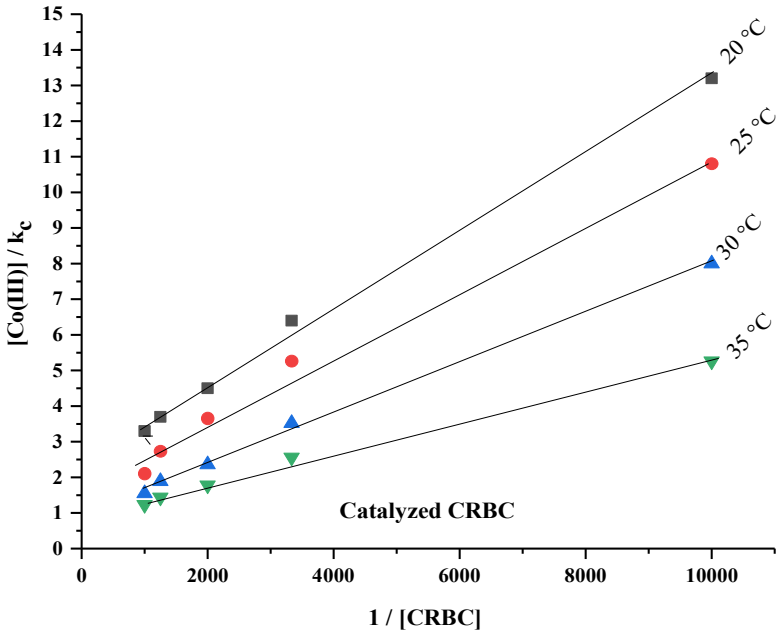

Figure 81: Plot of [Co/k_c] vs. 1/[CRBC] for CRBC

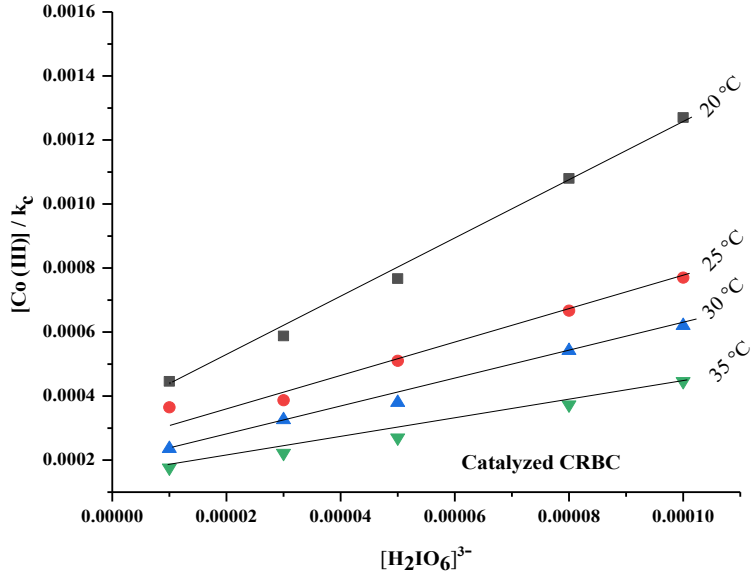

Figure 82: Plot of [H_2IO_6]$^{3-}$] vs. [Co/k_c] for CRBC

Four temperature data for verification plots

Table 73: Data for [Co/k_C] vs. 1/[CRBC] plot

	TEMPERATURE			
	20°C	**25°C**	**30°C**	**35°C**
[Co (III) / k_C] x 10^{-4}	13.2	10.8	8.0	5.26
	6.4	5.26	3.52	2.56
	4.5	3.65	2.36	1.78
	3.7	2.73	1.89	1.44
	3.3	2.1	1.55	1.23

Table 74: Data for [Co/k_C] vs. 1/[KOH] plot

	TEMPERATURE			
	20°C	**25°C**	**30°C**	**35°C**
[Co(III)/k_C] x 10^{-4}	10.6	7.57	6.1	4.9
	6.34	5.0	3.5	2.98
	4.66	4.29	2.69	2.32
	3.93	3.45	2.36	1.98
	3.5	2.96	2.15	1.77

Table 75: Data for [Co/k_C] vs. $[H_2IO_6]^{3-}$ plot

	TEMPERATURE			
	20°C	**25°C**	**30°C**	**35°C**
[Co(III)/k_C] x 10^{-4}	4.46	3.65	2.36	1.76
	5.88	3.87	3.26	2.22
	7.67	5.1	3.8	2.7
	10.8	6.67	5.42	3.73
	12.7	7.7	6.2	4.46

iv) Plots of equilibrium constants of CRBC

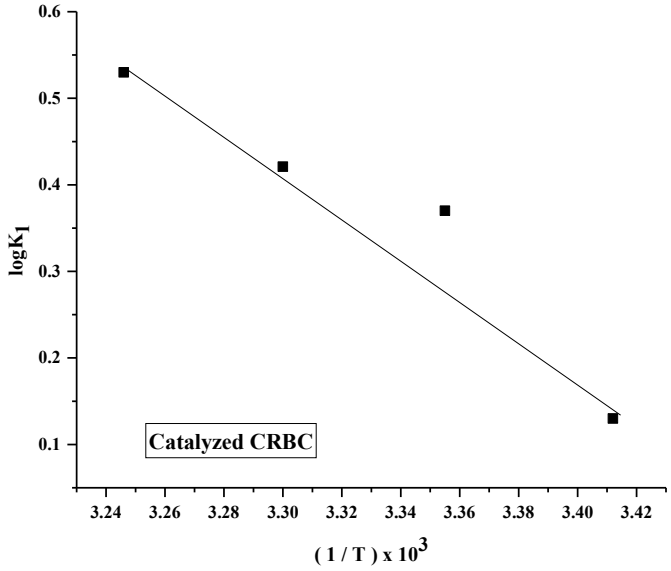

Figure 83: Plot of log K_1 vs. (1/T) x 10^3 for CRBC

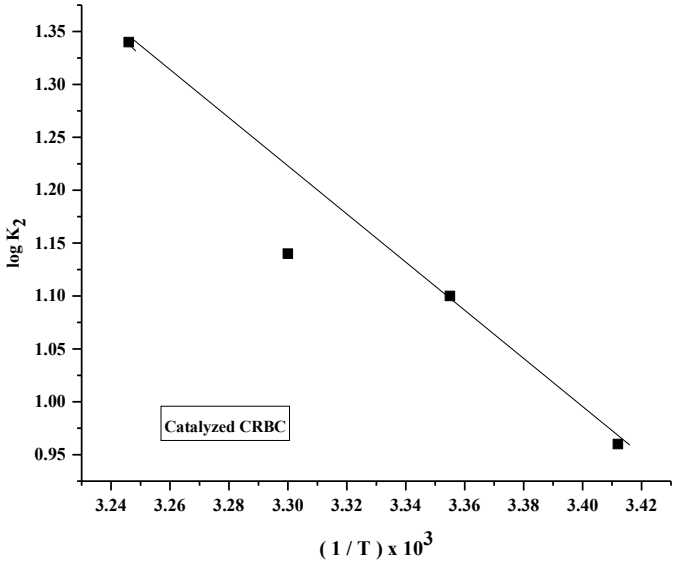

Figure 84: Plot of log K_2 vs. (1/T) x 10^3 for CRBC

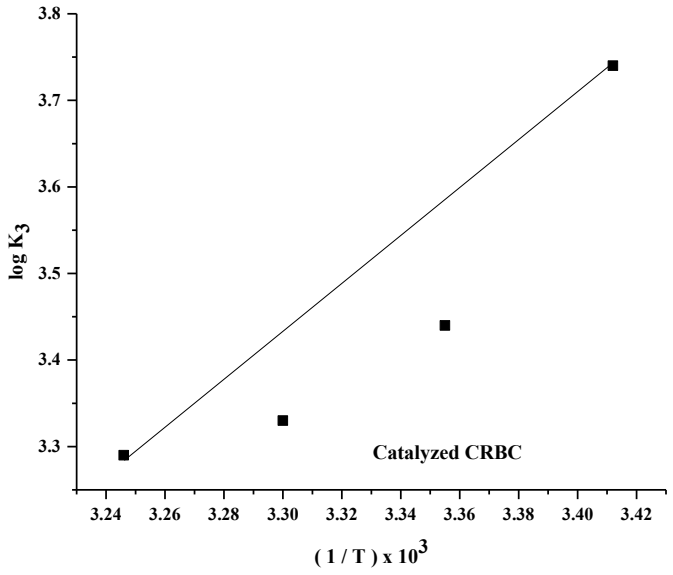

Figure 85: Plot of log K_3 vs. (1/T) x 10^3 for CRBC

Table 76: (k, K_1, K_2 and K_3) values for CRBC

Equilibrium Constant ↓	**Absolute Temperatures**			
Temperature →	**20 °C**	**25 °C**	**30°C**	**35 °C**
k (Slow step rate constant)	4192.87	6134.97	10214.5	11033.02
K_1	1.35	2.168	2.638	3.365
K_2 x10^{-4}	0.905	1.243	1.39	2.20
K_3	5470.18	2734	2160	1934.62

The rate determining step in often the slowest step in the complex reaction mechanism, and the rate constant related to it is the slow step rate constant (k). In the catalytic degradation of carbenicillin by DPC (III) in the alkaline medium, values of 'k' are in the increasing order. Degree of ionization of carbenicillin increases in the alkaline medium that results a higher concentration of the reactive anionic form that will enhance the relative reactivity and slow step rate constant. Higher the active mass of DPC (III), faster will be the rate of intermediate formation. Similarly, increment in temperature certainly favors the increasing order of slow step rate constant.

Meanwhile, K_1, and K_2 values are in the increasing order but K3 values are decreasing sharply. At first, rate if ionization of carbenicillin increases in the alkaline medium resulting higher concentration of reactive anionic that enhance K_1 values. Higher concentration of DPC (III) is also cause to shift the forward equilibrium, which in turn, supports to form intermediates rapidly and hence K_2 values also increase. Inter-conversion of intermediate into final product is reported as K_3 which gets suppressed due continuous decrement in the relative concentration of intermediates leading to a decreased value of K_3.

Table 77: Thermodynamic parameters from equilibrium constants for CRBC

Thermodynamic Parameters	**Values from K_1**	**Values from K_2**	**Values from K_3**
ΔH°_{298} (in k J mol^{-1})	44.41	41.9	-50.91
ΔS°_{298} (in J K^{-1} mol^{-1})	154.59	161.24	-103.17
ΔG°_{298} (in k J mol^{-1})	-1.66	-6.15	-20.16

Catalytic degradation of carbenicillin by DPC (III) and Co (III) catalyst in alkaline medium is finally associated with negative free energy change like (-1.66, -6.15, and -20.16) $kJmole^{-1}$ which ultimately predicts the feasibility for spontaneity of the ampicillin degradation in the alkaline medium. The decreasing values of K_3 might have reversed entropy change but entropy change from first and third equilibrium constant are found to be positive. However, negative entropy indicates that pure carbenicillin may have relatively low entropy in the initial state in comparison to that in the final state or in the degraded products. The catalyst, Co (III), reduces the activation energy to accelerate the degradation process and the system reaches the high entropy state more efficiently. Overall, the degradation process seems to be feasible.

(K_1, K_2 & K_3 vs. 1/T) data for CRBC

Table 78: Data for the plot of log K_1 vs. [1/T x10^3]

S. N.	Temperature	[1/T x 10^3]	K_1	logK_1
1	20 ℃	3.412	1.35	0.13
2	25 ℃	3.355	2.168	0.34
3	30 ℃	3.3	2.638	0.42
4	35 ℃	3.246	3.365	0.53

Table 79: Data for the plot of log K_2 vs. [1/T x10^3]

S. N.	Temperature	[1/T x 10^3]	K_2 x10^{-4}	5 + logK_2
1	20 ℃	3.412	0.905	0.96
2	25 ℃	3.355	1.243	1.09
3	30 ℃	3.3	1.39	1.14
4	35 ℃	3.246	2.2	1.34

Table 80: Data for the plot of log K_3 vs. [1/T x10^3]

S. N.	Temperature	[1/T x 10^3]	K_3	logK_3
1	20 ℃	3.412	5470.18	3.74
2	25 ℃	3.355	2734	3.44
3	30 ℃	3.300	2160	3.33
4	35 ℃	3.246	1934.62	3.29

4.4.5 Activation and Thermodynamic Parameters of Oxacillin (OXC)

i) Catalyzed rate constant (k_c) and activation parameters of OXC

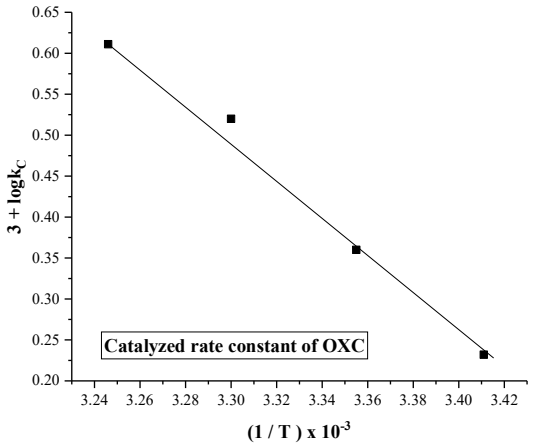

Figure 86: Plot of (3 + log k_c) vs. (1/T) x 10^3 for OXC

Table 81: Data for the plot of the catalyzed rate constant (k_c) for OXC

S. N.	[1 / T x 10^3]	k_C x 10^{-3}	3 + log k_C
1	3.412	1.70	0.232
2	3.355	2.29	0.360
3	3.003	3.31	0.520
4	3.246	4.08	0.611

Table 82: Parameters of activation from OXCs' catalyzed rate constant

Activation Parameters	Values
Ea	45.51 (kJmol^{-1})
$\Delta H^{\neq}$	43 ± 1 (k Jmol^{-1})
$\Delta S^{\neq}$	-150 ± 1.2 (JK^{-1}mol^{-1})
$\Delta G^{\neq}$	88 ± 2 (kJ mol^{-1})
Log A	5.34 ± 0.2

ii) Catalytic constant of OXC and its activation parameters

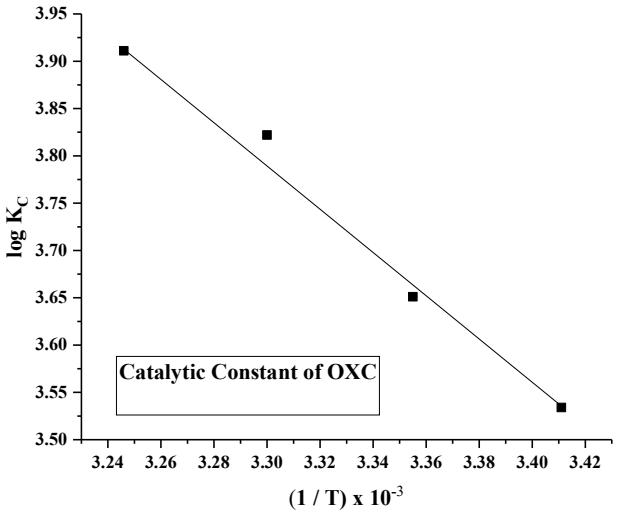

Figure 87: Plot of log K_C vs. (1/T) x 10^3 for OXC

Table 83: Data for catalytic constant (K_C) of OXC

S. N.	K_C x 10^{-3}	[Co] x 10^{-7}	K_C
1	1.71	5.0	3420
2	2.24	5.0	4480
3	3.32	5.0	6640
4	4.08	5.0	8160

Table 84: Data for the plot log K_C vs. [1/T x 10^3] for OXC

S. N.	[(1/T) x 10^3]	log K_C
1	3.412	3.534
2	3.355	3.651
3	3.3	3.822
4	3.246	3.911

Table 85: Parameters of activation from OXC catalytic constant

Activation Parameters	Values
Ea	45.339 ($kJmol^{-1}$)
$\Delta H^{\neq}$	42 ± 1.5 (k $Jmol^{-1}$)
$\Delta S^{\neq}$	-138 ± 1 ($JK^{-1}mol^{-1}$)
$\Delta G^{\neq}$	83 ± 2 (kJ mol^{-1})
Log A	5.3 ± 0.2

iii) Parameters of activation from OXC slow step rate constant (k)

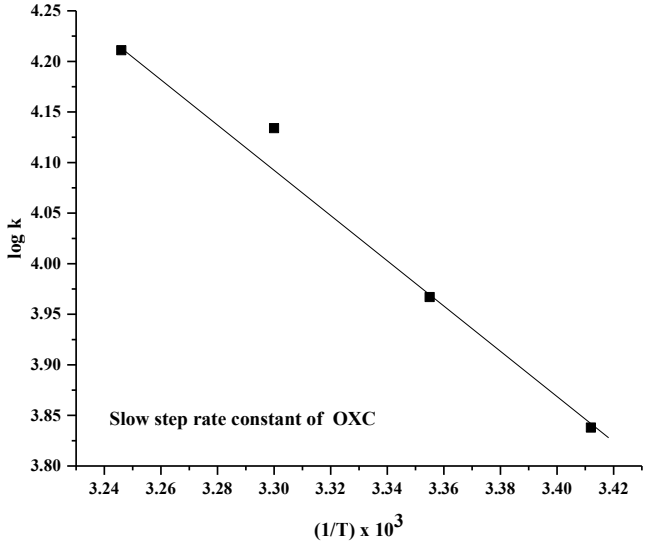

Figure 88: Plot of log k vs. (1/T) x 10^3 for OXC

Table 86: Data for the plot of OXC slow step rate constant

S. N.	1/T x 10^3	k x 10^4	log k (slow step)
1	3.412	6.89	3.838
2	3.355	9.29	3.968
3	3.003	13.62	4.134
4	3.246	16.28	4.211

Table 87: Parameters of activation from OXC slow step rate constant (k)

Activation Parameters	Values
Ea	44.46 ($kJmol^{-1}$)
$\Delta H^{\neq}$	42 ± 1 ($k\ Jmol^{-1}$)
$\Delta S^{\neq}$	-27.59 ± 0.8 ($JK^{-1}mol^{-1}$)
$\Delta G^{\neq}$	76 ± 1 ($kJ\ mol^{-1}$)
Log A	11.7 ± 0.2

Verification plots of [Co/k_c] and data for OXC

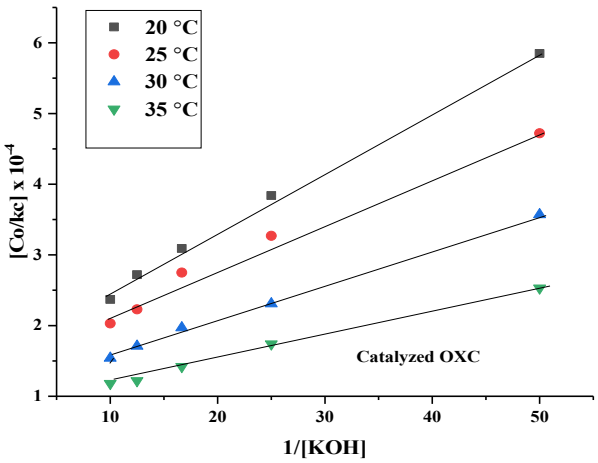

Figure 89: Plot of 1/[KOH] vs. [Co/k_c] x 10^{-4}

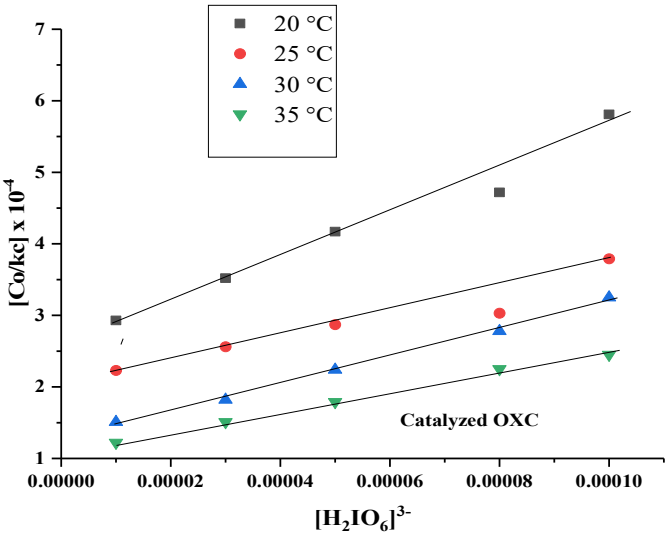

Figure 90: Plot of $[H_2IO_6]^{3-}$] vs. $[Co/k_c]$ for OXC

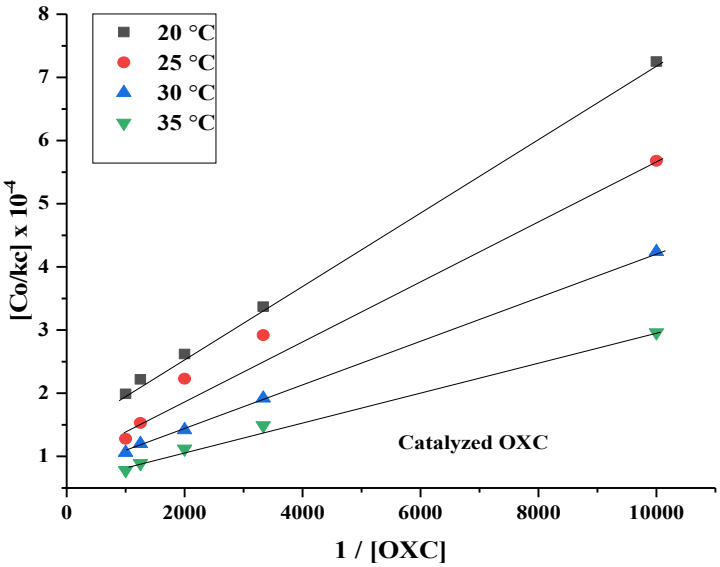

Figure 91: Plot of $[Co/k_c]$ vs. 1/[OXC] for OXC

Four temperature data for verification plots

Table 88: Data for $[Co/k_C]$ vs. 1/[OXC] plot

	TEMPERATURE			
	20°C	**25°C**	**30°C**	**35°C**
$[Co\ (III)/k_C]\ x\ 10^{-4}$	7.25	5.68	4.24	2.96
	3.37	2.92	1.92	1.49
	2.62	2.23	1.42	1.12
	2.22	1.53	1.20	0.89
	1.99	1.28	1.06	0.78

Table 89: Data for $[Co/k_C]$ vs. 1/[KOH] plot

	TEMPERATURE			
	20°C	**25°C**	**30°C**	**35°C**
$[Co(III)/k_C]\ x\ 10^{-4}$	5.85	4.72	3.57	2.53
	3.84	3.27	2.31	1.74
	3.09	2.75	1.97	1.42
	2.72	2.23	1.71	1.22
	2.37	2.03	1.54	1.18

Table 90: Data for $[Co/k_C]$ vs. $[H_2IO_6]^{3-}$ plot

	TEMPERATURE			
	20°C	**25°C**	**30°C**	**35°C**
$[Co(III)/k_C]\ x\ 10^{-4}$	2.93	2.23	1.51	1.22
	3.52	2.56	1.82	1.51
	4.17	2.87	2.24	1.79
	4.72	3.03	2.78	2.25
	5.81	3.79	3.25	2.45

iv) Plots of equilibrium constants vs. 1/T for OXC

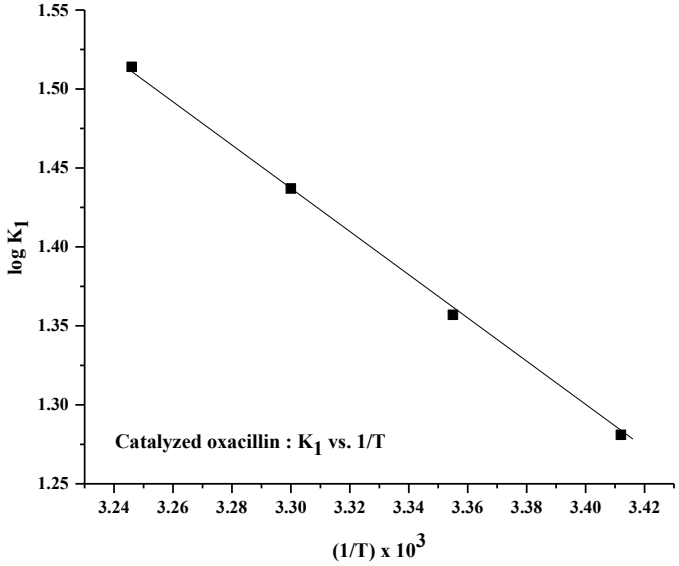

Figure 92: Plot of log K_1 vs. (1/T) x 10^3 for OXC

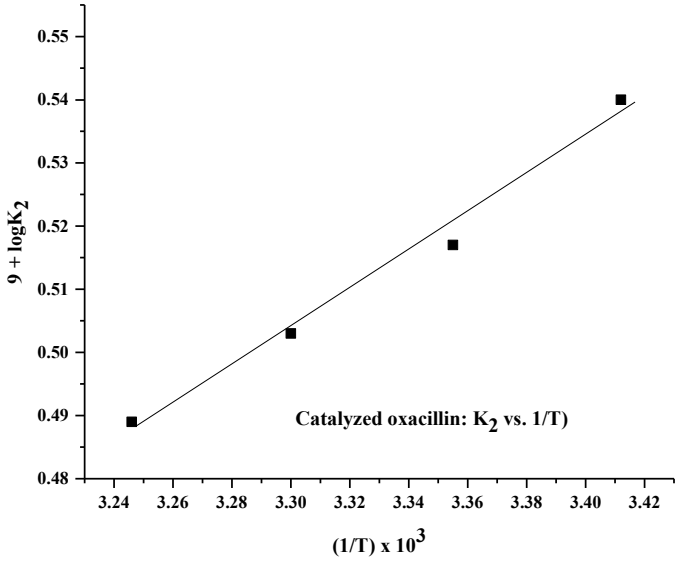

Figure 93: Plot of (9 + log K_2) vs. (1/T) x 10^3 for OXC

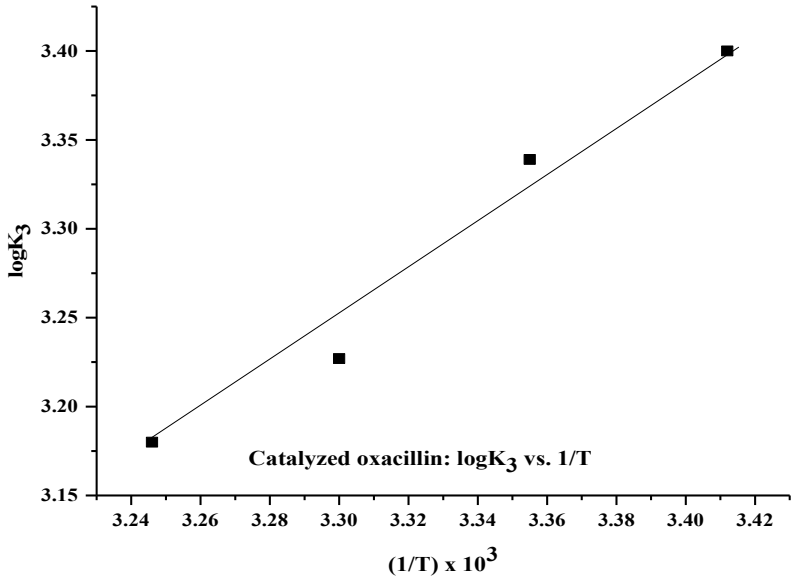

Figure 94: Plot of log K_3 vs. (1/T) x 10^3 for OXC

(K_1, K_2 & K_3 vs. 1/T) DATA FOR OXC

Table 91: Data for the plot of log K_1 vs. [1/T x10^3]

S. N.	Temperature	[1/T x 10^3]	K_1	logK_1
1	20 ℃	3.412	19.113	1.281
2	25 ℃	3.355	22.746	1.357
3	30 ℃	3.301	27.370	1.437
4	35 ℃	3.246	32.650	1.514

Table 92: Data for the plot of log K_2 vs. [1/T x10^3]

S. N.	Temperature	[1/T x 10^3]	K_2 x10^{-9}	9 + logK_2
1	20 ℃	3.412	3.548	0.549
2	25 ℃	3.355	3.291	0.517
3	30 ℃	3.300	3.190	0.503
4	35 ℃	3.246	3.084	0.489

Table 93: Data for the plot of log K_3 vs. [1/T x10^3]

S. N.	Temperature	[1/T x 10^3]	K_3	logK_3
1	20 ℃	3.412	2511.966	3.400
2	25 ℃	3.355	2184.039	3.339
3	30 ℃	3.3	1687.577	3.227
4	35 ℃	3.246	1516.001	3.180

Table 94: (**k, K_1, K_2 and K_3)** values for OXC

Equilibrium Constant ↓	**Absolute Temperatures**			
Temperature →	**20 ℃**	**25 ℃**	**30℃**	**35 ℃**
(Slow step rate constant) k x 10^4	6.890	9.293	13.698	16.286
K_1	19.133	22.746	27.370	32.650
K_2 x10^{-9}	3.548	3.291	3.190	3.084
K_3 x 10^4	2.511	2.184	1.687	1.516

The degradation of oxacillin by DPC (III) as oxidant and Co (III) as catalyst is followed by increasing order of both slow step rate constant (k) and the first equilibrium constant (K_1) while second and third equilibrium constant (K_2 & K_3) go on decreasing simultaneously. Enough active sites become available when active masses of DPC (III) and Co (III) increase which in turn enhance the frequency of successful collisions between oxacillin and the catalyst leading to an elevation in the slow step rate constant. The first equilibrium constant represents the initial complex formation which gets accelerated up due to increasing concentration of both oxacillin and Co (III) ions and hence values of K_1 also goes on increasingly. The second and third equilibrium constant (K_2 & K_3) represent subsequent steps in the overall reaction mechanism. Higher reaction rate through subsequent steps rapidly reduce active masses of the reacting species resulting a sharp decrease in their values. Hence, the increasing active mass of the catalyst, Co (III), the equilibrium shifts towards the formation of the initial reactant-

catalyst complex, intermediates and products in which the catalyst facilitates the various steps more effectively. The overall reaction rate may increase due to the combined effects of the changing equilibrium constants and lead to a faster degradation of oxacillin in the alkaline medium.

Table 95: Thermodynamic parameters from OXC equilibrium constant

Thermodynamic Parameters	**Values from K_1**	**Values from K_2**	**Values from K_3**
ΔH°_{298} (in k J mol^{-1})	26.965	-5.790	-26.730
ΔS°_{298} (in J K^{-1} mol^{-1})	116.499	-9.463	-26.041
ΔG°_{298} (in k J mol^{-1})	-7.751	-2.970	-18.970

The standard free energy change is determined to be negative (-7.751, -2.970, & -18.970) $kJmole^{-1}$ at 298 K temperature from all three equilibrium constants (K_1, K_2, & K_3) indicating a successful degradation of oxacillin by DPC (III) and Co (III) catalyst in the alkaline medium. Slight negative standard entropy change might be due to decreasing values of second and third equilibrium constants. The degradation process proceeds easily and spontaneously leading to product formation.

4.5 Probable Mechanism

4.5.1 A probable mechanism for Co (III) – AMX oxidation (**Scheme 1**)

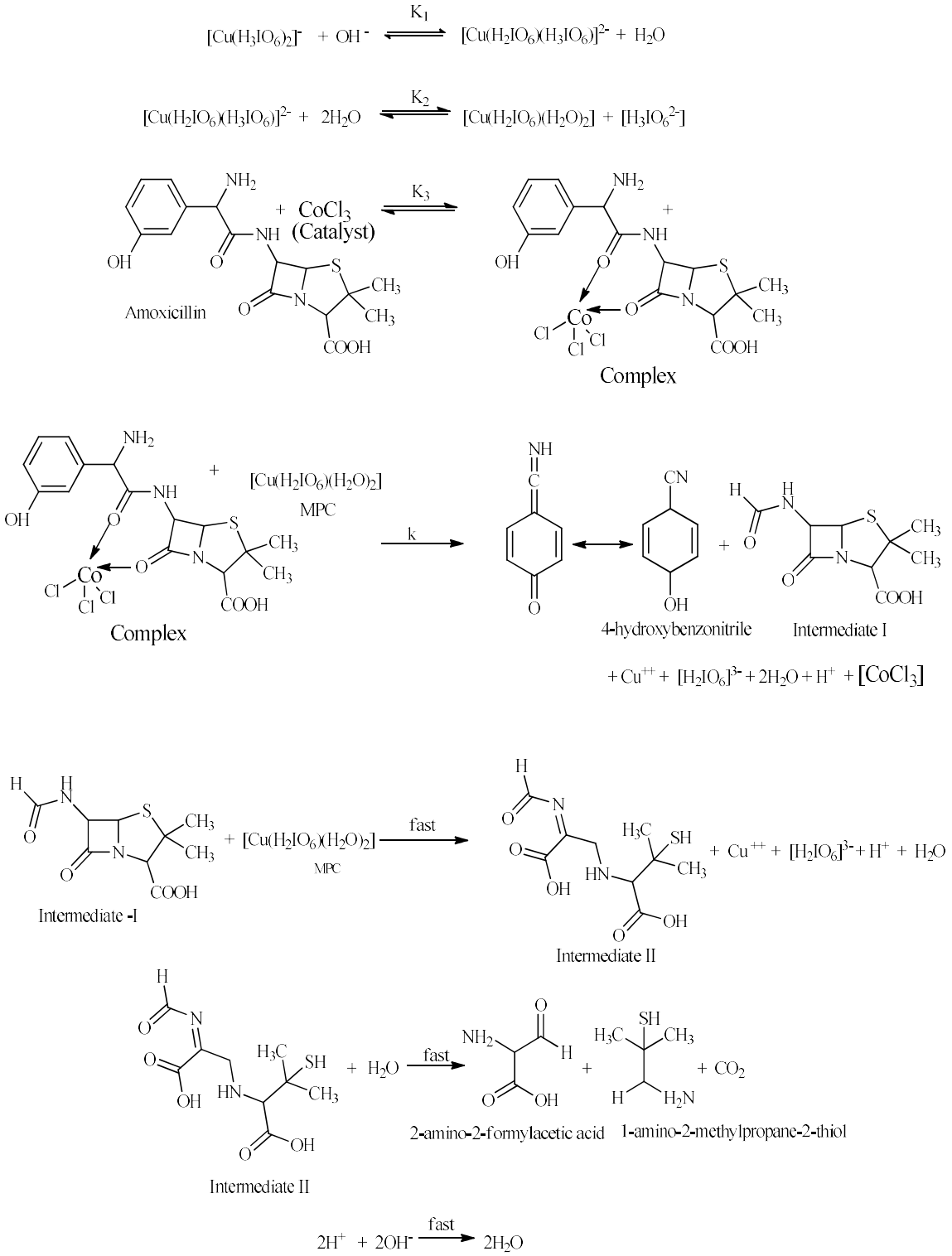

Scheme 1: This experimental data, spectral findings, and elemental analyses have all been used to support a viable mechanism and the proper participation of all species. The de-protonated form of DPC (III), in the first step, reacts with the hydroxide ion in the presence of water to create MPC (III) and free periodate. The development of the complex as a result of the interaction between AMX and the Co (III) catalyst is likely what causes the occurrence of fractional order with regard to AMX. After rearranging a molecule of fresh MPC (III), this complex reacts with it to produce an intermediate (I), 4-hydroxybenzonitrile, and regenerate the catalyst, Co (III). The active intermediate I react with a new one molecule of MPC (III) in the second step to create intermediate II, which is then hydrolyzed to produce the end products as 2-amino-2-formylacetic acid and 1-amino-2-methylpropane-2-2thiol, as represented according to **Scheme 1.**

4.5.2 A probable mechanism for Co (III) – AMP oxidation (**Scheme 2**)

Scheme 2: A suitable mechanism is suggested along with the appropriate involvement of all species in light of this experimental evidence. The formation of the complex between ampicillin and the Co (III) catalyst is thought to be the cause of the fractional order with respect to ampicillin. Co (III) and active intermediates (I and II) are released by the complex after it interacts with DPC (III). Following amide hydrolysis, one active intermediate reacts with freshly protonated DPC (III) to quickly produce oxo-phenyl acetic acid. In this instance, an abundance of alkali strengthens the nucleophilic attack on the β-lactam carbonyl carbon atom and aids in the opening of the unstable four-member β-lactam ring. A second free radical of ampicillin quickly forms 2-formyl-5, 5-dimethyl thiazolidine -4-carboxylic acid when it reacts with freshly protonated DPC (III) through decarboxylation and deamination, along with Cu^{++} and periodates species, as mentioned according to **Scheme 2.**

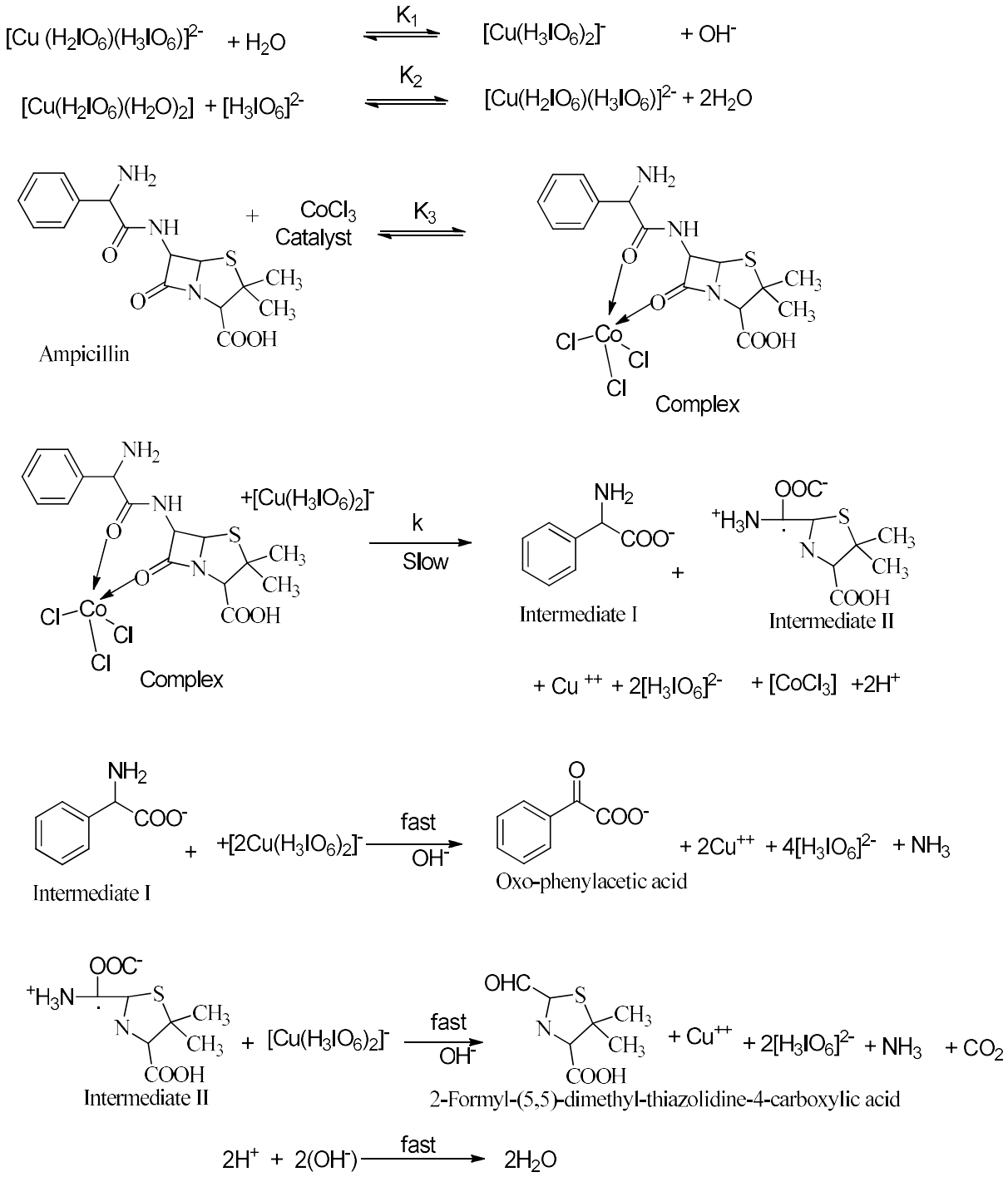
[Cu (H2IO6)(H3IO6)]2- + H2O
K1
[Cu(H3IO6)2]- + OH-
[Cu(H2IO6)(H2O)2] + [H3IO6]2-
K2
[Cu(H2IO6)(H3IO6)]2- + 2H2O
CoCl3
Catalyst
K3
Ampicillin
Complex
+[Cu(H3IO6)2]-
k
Slow
Intermediate I
Intermediate II
Complex
+ Cu ++ + 2[H3IO6]2- + [CoCl3] +2H+
+[2Cu(H3IO6)2]-
fast
OH-
Oxo-phenylacetic acid
+ 2Cu++ + 4[H3IO6]2- + NH3
Intermediate I
+ [Cu(H3IO6)2]-
fast
OH-
2-Formyl-(5,5)-dimethyl-thiazolidine-4-carboxylic acid
+ Cu++ + 2[H3IO6]2- + NH3 + CO2
Intermediate II
2H+ + 2(OH-)
fast
2H2O

(Scheme 2)

4.5.3 A probable mechanism for Co (III) – DCLX oxidation (**Scheme 3**)

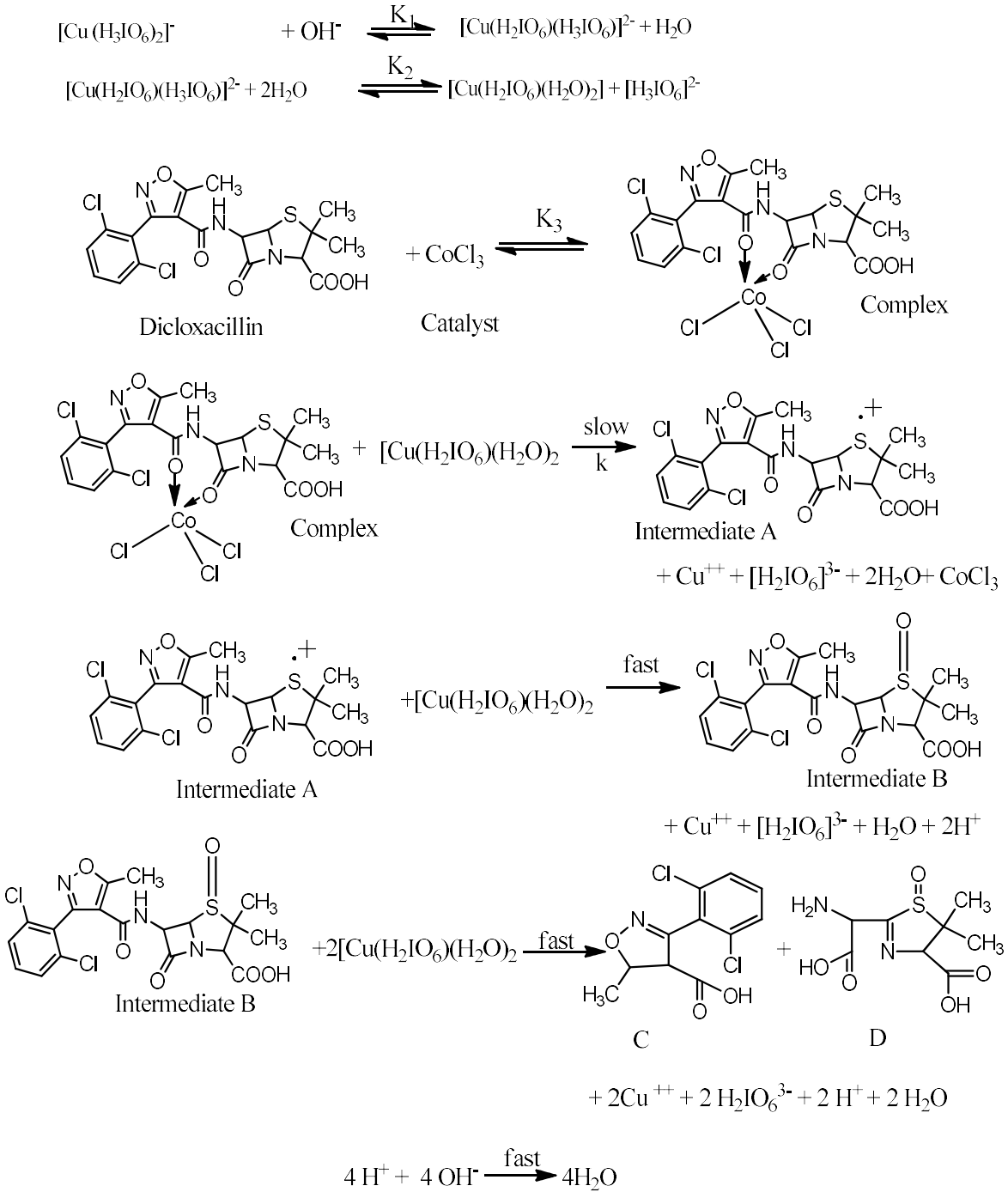

Scheme 3: In light of this experimental evidence, a pertinent mechanism is proposed, along with the proper involvement of all species. The deprotonated form of DPC (III) is created during the first stage of the reaction when DPC (III) interacts with the hydroxide ion. This form of DPC (III) is then combined with water to create MPC (III) and free periodate. The complex reacts with a new one molecule of MPC (III) to create an intermediate (A) and regenerate the catalyst, Co (III). The next step involves the participation of active intermediate (A) with a fresh molecule of MPC (III) to create another intermediate (B), which subsequently combines with new two molecules of MPC (III) to produce the final products as 2, 6-dichlorophenyl-5-methyl-4, 5-dihydroisoxazole-4-carboxylic acid and 3-(2-(amino (carboxy) methyl)-5, 5-dimethyl-4, 5-dihydrothiazole-4-carboxylic acid-1-oxide, as mentioned by **Scheme 3**.

4.5.4 A probable mechanism for Co (III) – CRBC oxidation (**Scheme 4**)

Scheme 4: The deprotonated form of DPC (III), which is created in the initial stage by the interaction of DPC (III) and the hydroxide ion, reacts with water to produce MPC (III) and free periodate. It is believed that the occurrence of fractional order with regard to AMX is caused by the complex that is created by the reaction between CRBC and the Co (III) catalyst. This complex interacts with a fresh one molecule of MPC (III) to produce an intermediate (A) and regenerate the catalyst, Co (III). The active intermediate (A) reacts with a brand-new molecule of MPC (III) in the second step to create another intermediate B, which reacts with two additional moles of MPC (III) to produce the final products, 2-phenylmalonic acid (C9H8O4) and the second product was 2-(amino (carboxy)methyl)-5,5-dimethyl-4,5-dihydrothiazole-4-carboxylic acid-1-oxide ($C_8H_{12}N_2O_4S$), as mentioned according to **Scheme 4**.

$$[Cu(H_3IO_6)_2]^- + OH^- \underset{}{\overset{K_1}{\rightleftharpoons}} [Cu(H_2IO_6)(H_3IO_6)]^{2-} + H_2O$$

$$[Cu(H_2IO_6)(H_3IO_6)]^{2-} + 2H_2O \overset{K_2}{\rightleftharpoons} [Cu(H_2IO_6)(H_2O)_2 + H_3IO_6^{2-}$$

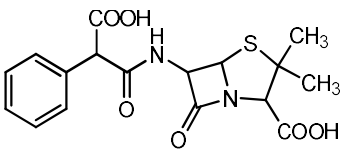

Carbenicillin

$+ CoCl_3$ Catalyst $\overset{K_3}{\rightleftharpoons}$

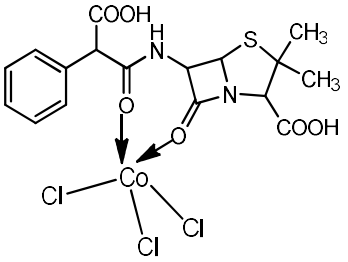

Complex

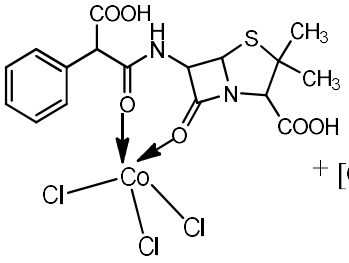

Complex

$+ [Cu(H_2IO_6)(H_2O)_2] \xrightarrow[k]{slow}$

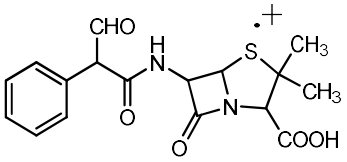

Intermediate A

$Cu^{++} + H_2IO_6^{3-} + 2\,H_2O + CoCl_3$

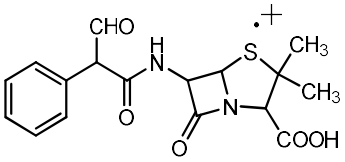

Intermediate A

$+ [Cu(H_2IO_6)(H_2O)_2] \xrightarrow{fast}$

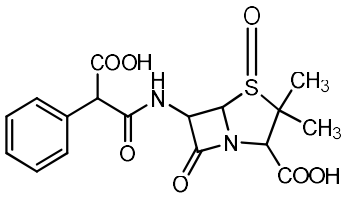

Intermediate B

$Cu^{++} + H_2IO_6^{3-} + H_2O + 2H^+$

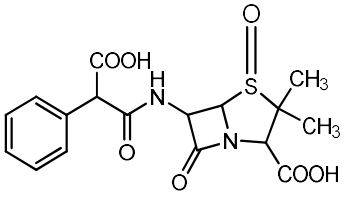

Intermediate B

$+2\,[Cu(H_2IO_6)(H_2O)_2] \xrightarrow{fast}$

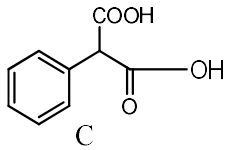

C

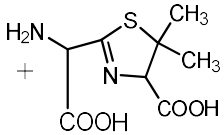

D

$+ 2Cu + 2\,H_2IO_6^{3-} + 2\,H^+ + 2\,H_2O$

$$4\,H^+ + 4\,OH^- \xrightarrow{fast} 4\,H_2O$$

4.5.5 A probable mechanism for Co (III) – OXC oxidation (**Scheme 5**)

Different β-lactam antibiotics have been subjected to oxidation in an alkaline medium because DPC (III) functions as both a chelating and an oxidizing agent. Higher alkali concentrations cause the equilibrium forms of periodic acid (H_5IO_6) to change into dimerizing $H_4IO_6^{-1}$, $H_3IO_6^{-2}$, and $H_2IO_6^{-3}$ periodate ions. An appropriate reaction mechanism is suggested along with the appropriate participation of all reacting species in light of this experimental evidence. When DPC (III) interacts with the hydroxide ion during the initial phase of the reaction, the deprotonated form of DPC (III) is produced. Then, MPC (III) and free periodate are produced by mixing this form of DPC (III) with water. A new one molecule of MPC (III) and the complex combine to form the intermediate (A). A new molecule of MPC (III) and an active intermediate (A) are combined in the following step to produce an intermediate (B), which combines with two more moles of MPC (III) to create phenyl-5-methyl-4,5-dihydroisoxazole-4-carboxylic acid and 3-(2-(amino(carboxy)methyl)-5,5-dimethyl-4,5-dihydrothiazole-4-carboxylic acid-1-oxide, respectively as mentioned by **Scheme 5**.

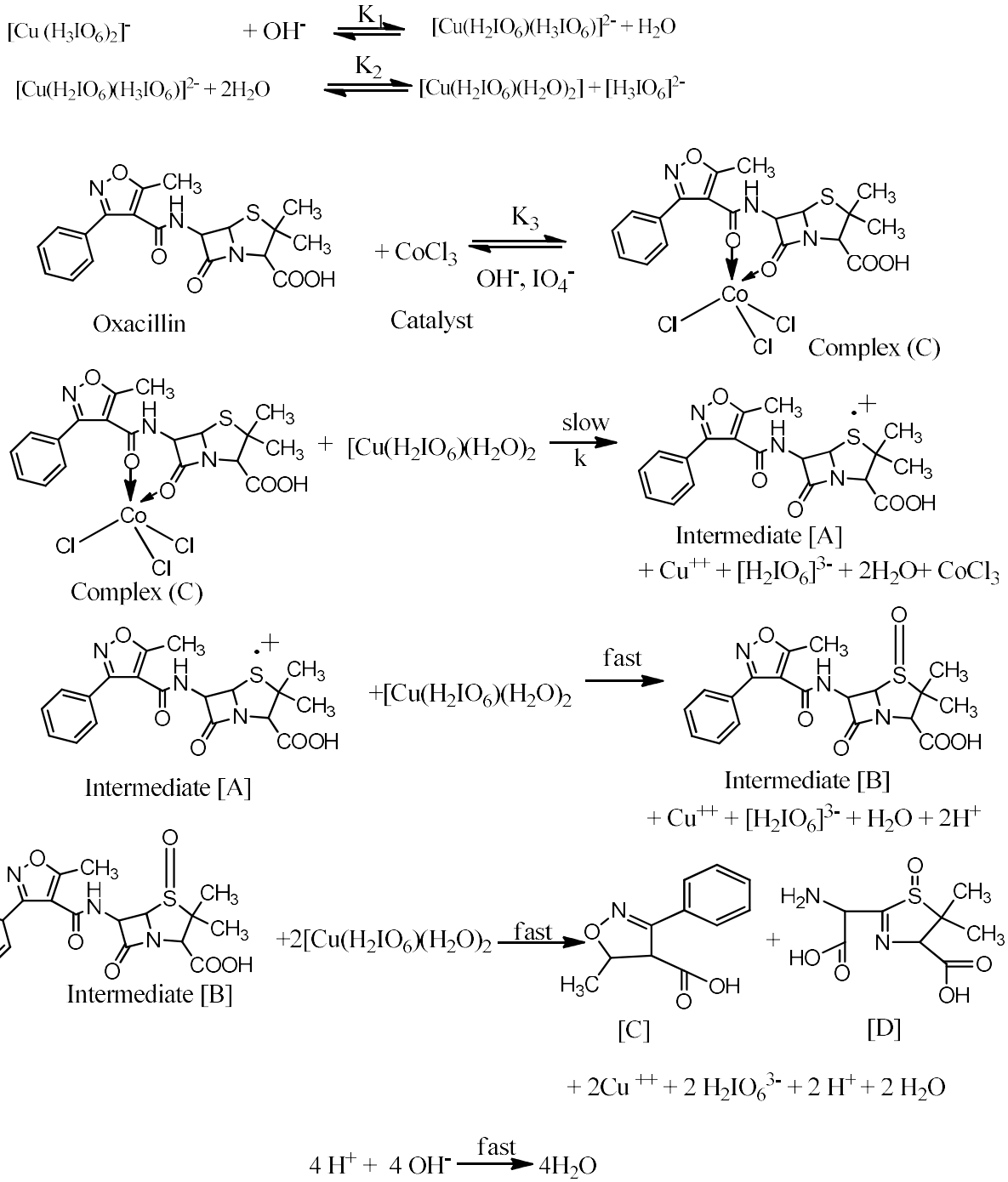
[Cu (H3IO6)2]- + OH- K1 [Cu(H2IO6)(H3IO6)]2- + H2O
[Cu(H2IO6)(H3IO6)]2- + 2H2O K2 [Cu(H2IO6)(H2O)2] + [H3IO6]2-
Oxacillin
+ CoCl3
K3
OH-, IO4-
Catalyst
Complex (C)
+ [Cu(H2IO6)(H2O)2
slow
k
Intermediate [A]
+ Cu++ + [H2IO6]3- + 2H2O+ CoCl3
Complex (C)
+[Cu(H2IO6)(H2O)2
fast
Intermediate [B]
+ Cu++ + [H2IO6]3- + H2O + 2H+
Intermediate [B]
+2[Cu(H2IO6)(H2O)2
fast
[C]
[D]
+ 2Cu ++ + 2 H2IO6 3- + 2 H+ + 2 H2O
4 H+ + 4 OH- fast 4H2O

CHAPTER 5

5. CONCLUSION AND RECOMMENDATION

Several β-lactam antibiotics or penicillanic acid derivatives (PADs) are broad-spectrum anti-bacterial with rising demand in homes, healthcare facilities, and veterinary uses. Antibiotics released into the aquatic environment have the potential to affect drinking water, which is a big concern for public health care. Contamination of PADs has been widely reported in a variety of aquatic environments around the world, including discharge or waste samples, surface water, and groundwater. Since the majority of comprised intermediates can be mineralized into CO_2, water, and mineral species during the oxidation-degradation process, interesting remedial strategies are desired for the degradation of PADs in aqueous solutions. The oxidation method is the most likely drug transformation pathway to be followed, and based on a kinetic and mechanistic analysis of the oxidation-reduction reactions between some of the most efficient PADs and non-toxic oxidants like diperiodatocuprate (III) and Cobalt (III) chloride as a catalyst. The proposed effort will reveal a novel application in the fields of kinetics and degradation of PADs in the alkaline medium.

5.1 Conclusion

Based on the observation within the experimental limits, a suitable mechanism is proposed for every reaction. In the reaction molecular bonds break and atoms rearrange according to the order of a reaction with respect to distinct reactive species, this is known as the reaction mechanism. The rate of reaction can explain various practical applications during the kinetic study. Although, kinetic studies exactly implement the fundamental facts of the reaction with analytical aspects. Regrettably, the order of a reaction concerning the reactants and thermodynamic specifications can’t explain all the chemical events in a chemical reaction mainly owing to the evidence that the reactions infrequently follow in a single step. Chemical kinetics has immense scope in which experimental

studies include the effect of the concentration, temperature, and hydrostatic pressure is discussed on numerous types of reactions. To interrogate these effects, various types of chemical reactions and a broad range of empirical approaches have been used.

The present research work evaluates the technique for the degradation of β-lactam antibiotics or derivatives of penicillanic acid. Administration or application of these drugs for human health or pharmacy or veterinary purpose help to cure the disease but are exposed in the environment in a non-biodegradable form that enhances the anti-bacterial resistance of most β-lactam antibiotics. Absorbance data, obtained from the UV/Visible spectrophotometer, has been converted into corresponding un-catalyzed, catalyzed and total rate constant. Plots of these data supported along with a concentration of PADs, alkali, periodate (free), DPC (III), and Co (III) catalyst provided slopes and intercepts, which in turn, helped to determine the energy of activation and essential activation as well as thermodynamic parameters. The catalytic constant, also regarded as the degree of catalytic efficiency, has been calculated. These values for particular PADs have been placed in the respective chapter.

The main conclusions can be pointed out as:-

- The Co (III) catalyzed oxidation between PADs-DPC (III) was of fractional order with respect to alkali and PADs, pseudo-first order with respect to periodate, and retarding fractional order with respect to DPC (III).
- Rate constants increased with a temperature rise. For every 10°C rise in temperature, rate constants become nearly double and can increase by 10 times in the presence of a catalyst.
- Negative free energy indicates the spontaneity of the process favored by positive entropy while negative entropy indicates the highly ordered intermediates than products.
- Mechanism and spectral evidence support the active participation of Monoperiodatocuprate (MPC-III) in the reaction.

- Overall, the present work develops an insight into the degradation of un-metabolized PADs (10-90%) that can disclose a way to modify old PADs into newer but potent PADs.

5.2 Recommendations

Researchers have been attempting to explore new oxidation techniques for non-biodegradable PADs accumulating rapidly in our environment, the research work is a continuation step towards that process along with the following objectives for future studies.

- To investigate the *in vitro* antibacterial study of the complex as well as products collected after isolation.
- To have a TGA/DTA test for comparison of thermodynamic parameters.
- To enhance or modify the efficiency of these PADs or β-lactam antibiotics.
- To compare the effectiveness of uncatalyzed and catalyzed reaction rate altered by variable temperature and thence to investigate variable activational and thermodynamic parameters.
- To develop degradation technique for amino acids, proteins, as well as for protein-PADs interaction technique.

Furthermore, some of specific recommendations are considered for the catalytic oxidation of PAD using DPC (III) as oxidant and cobalt (III) chloride as catalyst.

- The catalyst selected should be of higher analytical grade with higher purity percentage and pH during complex synthesis should be maintained between 9-11.
- DPC (III) should be synthesized at higher concentration and further dilution should be made. Whole reactions should be carried out between 293.15K–308.15K by avoiding possible any decomposition of sensitive substrates.
- Uniform distribution of substrate, oxidant and catalyst should be considered carefully along with proper magnetic stirring under controlled temperature.

CHAPTER 6

6. SUMMARY

The thesis entitled “Kinetics for Oxidation of Penicillanic Acid Derivatives by diperiodatocuprate (III) Complexes in the Presence of Cobalt (III) Catalyst in Alkaline Medium” has been documented in different six chapters. Each chapter has been summarized herein to represent all mandatory facts related to the present research work.

Chapter 1 represents a general and specific introduction to Penicillin and penicillanic acid derivatives (also regarded as β-lactam antibiotics) and their 3d-transition metallic complexes along with some potential oxidizing agents like diperiodatocuprate (III) in an alkaline medium. Proper structure and chemical information regarding these chemicals are paramount briefly. The presence of such antibiotics inside living organisms plays a vital role in regular metabolic processes. The chemistry of these organo-metallic compounds has been outlined along with objectives (future goal also) and scope in this chapter along with proper references.

Chapter 2 represents the overall literature regarding the present research work which authenticates the research. Present applications of penicillanic acid derivatives (β-lactam antibiotics) and bio-medical utilities of such drugs, in the modified form in the future, have been described briefly.

Chapter 3 represents the details of all materials and methods used entire the present research work. The physical parameters such as CHNS, melting point determination, spectral characterization techniques like FT-IR, LC-MS, and UV/Visible spectrophotometer are described in this chapter. The methodology applied to synthesize the targeted complex has been presented herein.

Chapter 4 represents the complete detailing of results and discussions of the present experimental research work. This part represents the application of absorbance and rate

constant for determination of catalyzed rate constant (k_c), slow step rate constant (k), and catalytic constant (K_C) to justify the pseudo-first-order reaction, various equilibrium constants (K_1, K_2, and K_3) involved in the reaction mechanism along with proper thermodynamic parameters. Various activation parameters with respect to the catalyzed rate constant, slow step rate constant, and catalytic constant have been presented herewith. All of the experimental evidence, including product formation, spectrum analysis, mechanisms, and kinetic studies, is consistent with the overall sequences described here in support of a pseudo-first-order reaction. The tables and figures representing the analyzed data have been arranged in the proper position in the text of this chapter. The reaction is of first order in terms of DPC (III), but fractional in terms of penicillanic acid derivatives, and alkali, while the retarding effect of periodate has been seen with a negative fractional order. Ionic strength and dielectric constant have essentially no impact.

Chapter 5 represents the overall conclusion of the present research work along with recommendations and prospects as a continuation of the present research work.

Chapter 6 represents the summary of overall chapters described in this thesis. This chapter is a summary of my research work in brief.

The present research is aimed to degradation technique for penicillanic acid derivatives in alkaline medium with support of diperiodatocuprate (III) as an oxidant and Cobalt (III) as a catalyst. Proper references and extra facts related to my research work are also included in the form of an appendix containing some essential mandatory academic participation that supported my research activity.

REFERENCES

Abbar, J. C., Malode, S. J., & Nandibewoor, S. T. (2010). Osmium (VIII) Catalyzed and Uncatalyzed Oxidation of a Hemorheologic Drug Pentoxifylline by Alkaline Copper (III) Periodate Complex: A Comparative Kinetic and Mechanistic Approach. *Polyhedron*, **29**(15): 2875-2883. https://doi.org/10.1016/j.poly.2010.07.009

Abraham, E. P. (1987). Drugs. *Cephalosporin,* **34**(Suppl 2): 1-14. ISSN: 1179-1950. https://doi.org/10.2165/00003495-198700342-00003.

Acharya, D. R., & Patel, D. B. (2013). Development and Validation of RP-HPLC Method for Simultaneous Estimation of Cefpodoxime Proxetil and Dicloxacillin Sodium in Tablets. *Indian Journal of Pharmaceutical Sciences*, **75**(1): 31-35. https://doi.org/10.4103/0250-474X.113538

Addis, T. Z., Adu, J. T., Kumarasamy, M., & Demile, M. (2024). Occurrence of Trace-Level Antibiotics in the Msunduzi River: An Investigation into South African Environmental Pollution. *Antibiotics*, **13**(2), 174. https://doi.org/10.3390/antibiotics13020174

Affam, A. C., & Chaudhuri, M. (2014). Optimization of Fenton Treatment of Amoxicillin and Cloxacillin Antibiotic Aqueous Solution. *Desalination and Water Treatment*, **52**(10-12):1878-1884. https://doi.org/ 10.1080/19443994.2013.794015

Alekseev, V. G., & Samuilova, I. S. (2008). Complex Formation in Systems Cobalt (II) - Glycine-B-Lactam Antibiotics. *Russian Journal of Inorganic Chemistry,*

53(2): 327-329, https://doi.org/10.1134/S0036023608020289

Almulhim, A. S. & Alotaibi, F. M. (2018). Comparison of Broad-Spectrum Antibiotics and Narrow-Spectrum Antibiotics in the Treatment of Lower Extremity Cellulitis. *Internationa Journal of Health Sciences*, **12**(6): 3-7. https://orcid.org/0000-0002-3727-7543

Amer, I. A. (2021). Kinetics and Mechanism of the Oxidation of 2-Methylindole by Alkaline Potassium Hexacyanoferrate (III). *Egyptian Journal of Chemistry,* **64**(3): 1441-1446. https://doi.org/10.21608/ejchem.2020.22459.2338

Amiri, S., & Shokrollahi, H. (2013). The Role of Cobalt Ferrite Magnetic Nanoparticles in Medical Science. *Material Science and Engineering: C*, **33**(1): 1-8. https://doi.org/:10.1016/j.msec.2012.09.003

Aryee, A. A., Han, R., & Qu, L. (2022). Occurrence, Detection and Removal of Amoxicillin in Wastewater: A Review. *Journal of Cleaner Production*, Volume **368**, 133140. https://doi.org/10.1016/j.clepro.2022.133140

Austen, W. C. R. (1899). The Extraction of Nickel from its Ores by the Mond's Process. (Including Plate at Back of Volume). *Minutes of the Proceedings of the Institution of Civil Engineers*, **135(**1899): 29-44. https://doi.org/10.1680/imotp.1899.19046

Avisar, D., Levin, G., & Gozlan, I. (2009). The Processes Affecting Oxytetracycline Contamination of Groundwater in Phreatic Aquifer Underlying Industrial Fish Ponds in Israel. *Environmental Earth Sciences*, **59**(4): 939-945. https://doi.org/10.1007/s12665-009- 0088-3

Ay, F., & Kargi, F. (2010). Advanced Oxidation of Amoxicillin by Fenton's Reagent Treatment. *Journal of Hazardous Materials*, **179**(1-3): 622-627. https://doi.org/10.1016/j.jhazmat.2010.03.048

Baldwin, W. H. (1931). The Story of Nickel (III) Ore, Matte, and Metal. *Journal of Chemical Education,* **8**(12):2325. https://doi.org/10.1021/ed008p2325

Barbooti, M. M. (2020). Removal of Amoxicillin from Water by Adsorption on Water Treatment Residues. *Baghdad Science Journal*, **17**(3): 1071-1079. http://dx.doi.org/10.21123/bsj.2020.17.3(Suppl.).1071

Basker, M. J., Comber, K. R., Sutherland, R., & Valler, G. H. (1977). Carfecillin: Aantibacterial Activity in Vitro and in Vivo. *Chemotherapy*, **23**(6): 424-435 https://doi.org/10.1159%2F000222012.

Baucom, E. I., & Drago, R. S. (1971). Nickel (II) and Nickel (IV) Complexes of 2, 6-Diacetylpyridine Dioxime. *Journal of the American Publication Society*, **93**(24): 6469-6475. https://doi.org/10.1021/ja00753a022

Bhinge, S., & Malipatil, S. (2015). Development and Validation of Stability Indicating Method for Simultaneous Estimation of Cefixime and Dicloxacillin Using RP-HPLC Method. *Journal of Taibah for Science*. https://doi.org/10.1016/j.jtusci.2015.10.011

Bian, X., Xia, Y., Zhan, T., Wang, L., Zhou, W., Dai, Q., & Chen, J. (2019). Electrochemical Removal of Amoxicillin Using a Cu Doped PbO_2 Electrode: Electrode Chacterization, Operational Parameters Optimization, and Degradation Mechanism *Chemosphere.* https://doi.org/10.1016/j.chemosphere.2019.05.226

Brogard, J. M., Haegele, P., Dorner, M., & Lavillaureix, J. (1974). Biliary Levels of Carbenicillin: Experimental and Clinical Study. *Journal of International Medical Research*, **2**(2): 142-148. https://doi.org/10.1177/030006057400200207

Brown, S. B., Brown, E. A., & Walker, I. (2004). The Present and Future Role of Photodynamic Therapy in Cancer Treatment. *The Lancet Oncology,* **5**(8): 497–508. doi.org/10.1016/s1470-2045 (04)01529-3 045(04)01529-3.

Bush, K., & Bradford, P. A. (2019). The Interplay Between B-Lactamases and New B-Lactamase Inhibitors. *Nature Reviews. Microbiology,* **17**(5): 295–306. https://doi.org/10.1038/s41579-019-0159-8

Cabello, F. C. (2006). Heavy Use Of Prophylactic Antibiotics In Aquaculture: A Growing Problem For Human And Animal Health and the Environment. *Environmental Microbiology,* **8**(7): 1137–1144. https://doi.org/10.1111/j.1462-2920.2006.01054.x

Chain, E., Florey, H. W., Gardner, A. D., Heatley, N. G., Jennings M. A., Orr-Ewing J., & Sanders, A. G. (1940). Penicillin as a Chemotherapeutic Agent. *The Lancet*, **236**(6104): 226-228. https://doi.org/ 10.1016/s0140-6736(01)08728-1

Chang, E. L, Simmers, C., & Knight, D. A. (2010). Cobalt Complexes as Antiviral and Antibacterial Agents. *Pharmaceuticals*, **3**: 1711-1728. https://doi.org/10.3390/ph3061711

Chivulescu, A. I., Doni, M. B., Cheregi, M. C., & Danet, A. F. (2011). Determination Of Amoxicillin, Ampicillin, and Penicillin G Using a Flow Injection Analysis Method with Chemiluminescence Detection. *Revue Roumaine de Chimie.,* **56**(3): 247-254

Chowdhury, B., Mondal, M. H., Barman, M. K., & Saha, B. (2018). A Study on the Synthesis of Alkaline Copper (III)-Periodate (DPC) Complex with an Overview of Its Redox Behavior in Aqueous Micellar Media. *Research on Chemical Intermediates (Springer)*. https://doi.org/10.1007/S11164-018-3643-2

Christensen, R. J., Espenson, J. H., & Butcher, A. B. (1973). Kinetics of the Reduction of Cobalt (III) and Chromium (III) Complexes by Ytterbium (II) Ions. *Inorganic Chemistry*, **12**(3): 564-569. https://doi.org/ 10.1021/ic50121a014

Coskun, E., Duman, E., Acar, N., & Bicer, E. (2017). Electrochemical, Spectroscopic and Computational Studies on Complexation of Oxacillin with Cu (II) and Co (II) Ions. Synthesis and Ligand Hydrolysis. *International Journal of Electrochemical Science*, **12**: 9364-9377. https://doi.org/10.20964/2017.10.43

Currie, D. B, Levason, W., Oldroyd, R. D., & Weller, M. T. (1994). Synthesis, Spectroscopic, and Structural Studies of Alkali Metal-Nickel Periodates [$MNiIO_6$] (M = Na, K, Rb, Cs, or NH_4^+). *Journal of Chemical Society, Dalton Transactions*, **9**: 1483-1487. https://doi.org/10.1039/DT9940001483

Darweesh, S. A., Yaseen, H. M., Mahmood, R. M., Al-Khalisy, S. R., & Khalaf, H. S. (2020). Spectrophotometric Determination of Ampicillin with Sulfanilic Acid by

Oxidative Coupling Reaction. *Indian Journal of Forensic Medicine & Toxicology*, **14**(4): 2016-2021. https://doi.org/10.37506/ijfmt.v14i4.11844

Daughton, C. G., & Ternes, T. A. (1999). Pharmaceuticals and Personal Care Products in the Environment: Agents of Subtle Change? *Environmental Health Perspectives*, **107**(suppl. 6): 907-938. https://doi.org/ 10.2307/3434573

Davies, M., Morgan, J. R., & Anand, C. (1975). Interactions of Carbenicillin and Ticarcillin with Gentamicin. *Antimicrob Agents Chemother*, **7**(4): 431-434. PMID: 1147579; PMCID: PMC429157. https://doi.org/ 10.1128/aac.7.4.431

de Ilurdoz, M. S., Sadhwani, J. J., & Vaswani, R. J. (2022). Antibiotic Removal Processes from Water & Wastewater for the Protection of the Aquatic Environment - A Review. *Journal of Water Process Engineering*, 45: 102474. https://doi.org/10.1016/j.jwpe.2021.102474

Delcour, A. H. (2009). Outer Membrane Permeability and Antibiotic Resistance. *Biochimica et Biophysica Acta (BBA)-Proteins and Proteomics,* **1974** (5): 808–816. https://doi:10.1016/j.bbapap.2008.11.005

Deng, Y., & Zhao, R. (2015). Advanced Oxidation Processes (AOPs) in Wastewater Treatment. *Current Pollution Reports,* **1**(3): 167–176. https://doi.org/10.1007/s40726-015-0015-z

Dengel, A. C., El-Hendawy, A. M., Griffith, W. P., Mostafa, S. I., & Williams, D. J. (1992). Transition Metal Periodato Complexes, Preparations and Properties as Catalytic Oxidants, and X-ray Crystal Structure of $Na_4K[Au\{IO_5(OH)\}_2].KOH.15H_2O$. *Journal of the Chemistry Society (Dalton Transactions)*, **24**: 3489-3495. https://doi.org/10.1039/DT9920003489

Dhayabaran, V. V., Prakash, T. D., Renganathan, R., Friehs, E., & Bahnemann, D. W. (2016). Novel Bioactive Co (II), Cu (II), Ni (II) and Zn (II) Complexes with Schiff Base Ligand Derived from Histidine and 1, 3-Indandione: Synthesis,

Structural Elucidation, Biological Investigation, and Docking Analysis. *Journal of Fluorescence*, **27**(1): 135–150. https://doi.org/ 10.1007/s10895-016-1941-x

Dilworth, C. R., Franklin, M., & Bance, G. N. (1974). Morphological and Cytological Effects of Carbenicillin on Pseudomonas Pseudomallei. *Canadian Journal of Microbiology*, **20**(9). https://doi.org/10.1139/m74-189

Eberson, L., & Shaik, S. S. (1990). Electron-Transfer Reactions of Radicals Anions: Do They Follow Outer- or Inner Sphere Mechanisms? *Journal of the American Chemical Society,* **112**(11): 4484-4489. https://doi.org/10.1021/ja00167a055

Eckert, E. M., Cesare, A. D., Coci, M., & Corno, G. (2018). Persistence of Antibiotic Resistance Genes in Large Subalpine Lakes: The Role of Anthropogenic Pollution and Ecological Interactions. *Hydrobiologia,* **824**: 93-108. https://doi.org/ 10.1007/s10750-017-3480-0

Ellepola, N., & Rubasinghege, G. (2022). Heterogeneous Photo-Catalysis of Amoxicillin Under Natural Conditions and High Intensity Light: Fate, Transformation, and Mineralogical Impacts. *Environments*, **9**, 77. https://doi.org/10.3390/envoronments9070077

Ellis, J. B. (2006). Pharmaceutical and Personal Care Products ((PCPs) in Urban Receiving Waters. *Environmental pollution*, **144**(1): 184-189. https://doi.org/10.1016/j.envpol.2005.12.018

Enrique, R. (2011). The Evolution of Drug Discovery: From Traditional Medicines to Modern Drugs. (*1st Ed.). Weinheim: Wiley-VCH.* p. 262. ISBN: 9783527326693

Escher, B. I., Baumgartner, R., Koller, M., Treyer, K., Lienert, J., & McArdell, C. S. (2011). Environmental toxicology and risk assessment of pharmaceuticals from hospital wastewater. *Water Research*, **45**(1): 75–92. https://doi.org/10.1016/j.watres.2010.08.019

Falcinella, B., Felgate, P. D., & Laurence, G. S. (1975). The Aqueous Chemistry of Thallium (II). Part II. Kinetics of Reaction of Thallium (II) with Manganese (II), Iron (II), and Cobalt (III) Ions. *Journal of the Chemical Society, Dalton Transactions*, **1**:

1- 9. https://doi.org/10.1039/DT9750000001

Fatta-Kassinos, D., Meric S., & Nikolaun A. (2011). Pharmaceutical Residues in Environment Waters and Wastewater: Current State of Knowledge and Future Research. *Analytical and Bioanalytical Chemistry,* **399**: 251-275. https://doi.org/ 10.1017/s00216-010-4300-9

Fawzy, A., Abdallah, M., & Alqarni, N. (2020). Oxidative Degradation of Some Antibiotics by Permanganate Ion in Alkaline Medium: A Kinetic and Mechanistic Approach. *Tropical Journal of Pharmaceutical Research*, **19**(9): 1999-2007. http://dx.doi.org/10.4314/tjpr.v19i9.28

Fechtig, B., Peter H., Bickel, H., & Vischer, E. (1968). Modifikationen Von Antibiotika.2. Mitteilung, Uber Die Darstellung Von 7- amino-cephalosporansaure. *Helvetica Chimica Acta*, **51**(5): 1108-1119. https://doi.org/ 10.1002/hlca.19680510513

Fischer, J., & Ganellin, C. R. (2010). Analogue-Based Drug Discovery. *Chemistry International—Newsmagazine for IUPAC*, **32**(4): 12-15. https://doi.org/10.1515/ci.2010.32.4.12

Frederick, H. M. (1967). (3)-1, 2-Dicarbollyl Complexes of Nickel (III) and Nickel (IV). *ACS Publications*, **89**(2): 470-471. https://doi.org/10.1021/ja00978a065

Gajdos, S., Zuzakova, J., Pacholska, T., Kuzel, V., Karpisek, I., Karmann, C., Sturmova, R., Bindzar, J., Smrckova, S., Sykorova, Z., Srb, M., SmejkalovaG, P., Kok, D., & Kouba, V. (2023). Synergistic Removal of Pharmaceuticals and Antibiotic Resistance from Ultra filtered WWTP Effluent: Free-Floating Args Exceptionally Susceptible to Degradation. *Journal of Environmental Management*, **340**: 117861. https://doi.org/10.1016/j.jenvman.2023.117861

Gao, Q., Li, Y., Qi, Z., Yue, Y., Min, M., Peng, S., Shi, Z., & Gao, Y. (2018). Diverse and Abundant Antibiotic Resistance Genes from Mariculture Sites of China's Coastline. *Science of the Total Environment,* **630**: 117–125. https://doi.org/10.1016/j.scitotenv.2018.02.122

Gaynes, R. (2017). The Discovery of Penicillin—New Insights after More than 75 Years of Clinical Use. *Emerging Infectious Diseases*, **23**(5): 849–853. https://doi.org/10.3201/eid2305.161556

Gemeay, A. H., Habib, A. F. M., & El-Din, M. A. B. (2007). Kinetics and Mechanism of the Uncatalyzed and Ag (I)-catalyzed Oxidative Decolorization of Sunset Yellow and Ponceau 4R with Peroxydisulphate. *Dyes and Pigments*, **74**(2): 458-463. https://doi.org/10.1016/j.dyepig.2006.03.006

Giamareilou, E., Papazachos, G., Piperakis, G., & Daikos, G. (1976). Clinical Experience with Indanyl Carbenicillin in Urinary Tract Infections. *Current Medical Research and Opinion*, **4**(2): 170-176 | 2008. https://doi.org/10.1185/03007997609109298

Giraldo, A. L., Erazo- Erazo, E. D., Florez-Acosta, O. A., Serna-Galvis, E. A., & Torres-Palma, R. A. (2015). Degradation of the Antibiotic Oxacillin in Water by Anodic Oxidation with Ti/Iro$_2$ Anodes: Evaluation of Degradation Routes, Organic By-Products and Effects of Water Matrix Components. *Chemical Engineering Journal*, **279**: 103-114. https://doi.org/10.1016/j.cej.2015.04.140

Gokavi, G. S., & Raju, J. R. (1987). Chromium (VI) Oxidation of Thallium (I). *Polyhedron*, **6**(9): 1721-1725. https:// doi.org/ 10.1016/S0277-5387 (00)86542-0

Gould K. (2016). Antibiotics: from Prehistory to the Present Day. *Journal of Antimicrobial Chemotherapy*, **71**(3): 572–575. https://doi.org/10.1093/jac/dkv484

Gowda, J. I., Nayak, S. S., Langote, S. R., Joshi, P. S., & Nandibewoor, S. T.(2015). Spectroscopic and Mechanistic Investigations into the Oxidation of Aspartame by Diperiodatocuprate (III) in Aqueous Alkaline Medium. *Cogent Chemistry.* **1**(1): 1015909. https://doi.org/10.1080/23312009.2015.1015909

Guan, Y., Jia. J., Wu, L., Xue, X., Zhang, G., & Wang, Z. (2018). Analysis of Bacterial Community Characteristics, Abundance of Antibiotics and Antibiotic Resistance Genes Along a Pollution Gradient of Ba River in Xi'an, China. *Frontiers in Microbiology*. **9**: 3191. https://doi.org/10.3389/fmicb.2018.03191

Guerra, M. M. H., Alberola, I. O., Rodriguez, S. M., Lopez, A. A., Merino, A. A., & Alonso, J. M. Q. (2019). Oxidation Mechanisms of Amoxicillin and Paracetamol in the Photo-Fenton Solar Process. *Water Research*, **156**: 232-240. https://doi.org/10.1016/j.watres.2019.02.055

Gulkowska, A., Leung, H. W., So, M. K., Taniyasu, S., Yamashita, N., Yeung, L. W. Y., Richardson, B. J., Lei, A. P., Giecy, G. P., & Lam, P. K. S. (2008). Removal of Antibiotics from Wastewater by Sewage Treatment Facilities in Hong Kong and Shenzhen, China. *Water Research,* **42**(1-2): 395–403. https://doi.org/10.1016/j.watres.2007.07.031

Guo, X., Feng, C., Gu, E., Tian, C., & Shen, Z. (2019). Spatial Distribution, Source Apportionment and Risk Assessment of Antibiotics in the Surface Water and Sediments of the Yangtze Estuary. *Science of the Total Environment*, **671**: 548–557. https://doi.org/10.1016/j.scitotenv.2019.03.393

Guo, Y., Tsang, D. C. W., Zhang, X., & Yang, X. (2017). Cu (II)-Catalyzed Degradation of Ampicillin: Effect of p^H and Dissolved Oxygen. *Environmental Science and Pollution Research,* **25**(5):4279–4288. https://doi.org/10.1007/s11356-017-0524-y

Gupta, Y. K., & Sharma, P. D. (1973). Determination of Hydrogen Peroxide by Thallium (III) in the Presence of Iron (II). *Talanta,* **20**(9): 903-905. https://doi.org/10.1016/0039-9140(73)80209-7

Hagen, Prof. Dr. Jens. (2015). Industrial Catalysis-a Practical Approach,3rd edition, *Wiley- VCH Verlag GmbH & Co. KGaA,Boschstr*, *Weinheim,Germany*,12,69469.

Halpern, J. (1959). Shaffer's Principle of Equivalent Changes for Homogeneous Catalytic Activation of Molecular Hydrogen by Metal Ions and Complexes. *J. Phys. Chem.,* **63**(3): 398-403. https://doi.org/ 10.1021/j150573a015

Handsfield, H. H., Clark, H., Wallace, J. F., Holmes, K. K., Turck, M. (1973). Amoxicillin, a New Penicillin Antibiotic. *Antimicrobial Agents and Chemotherapy*, **3**(2): 262-265. https://doi.org/10.1128/AAC.3.2.262

Hassan, M., Zhu, G., Lu, Y. Z., Al-Falahi, A. H., Lu, Y., Huang, S. & Wan, Z. (2021). Removal of Antibiotics from Wastewater and its Problematic Effects on Microbial Communities by Bioelectrochemical Technology: Current Knowledge and Future Perspectives. *Environmental Engineering Research*, **26**(1): 190405. https://doi.org/10.4491/eer.2019.405

He, X., Mezyk, S. P., Michael, I., Fatta-Kassinos, D., & Dionysiou, D. D. (2014). Degradation Kinetics and Mechanism of β-Lactam Antibiotics by the Activation of H_2O_2 and $Na_2S_2O_8$ under UV-254nm irradiation. *Journal of Hazardous Materials,* **279**:375-83. https://doi.org/10.1016/j.jhazmat.2014.07.008.

Herberer, T. (2002). Tracking Persistent Pharmaceutical Residues from Municipal Sewage to Drinking Water. *Journal of Hydrology, (Elsevier)*, **266**: 175-189. PII: S 0022- 1694(02)00 165-8

Herlina, H., Zulfikar, M. A., & Buchari, B. (2018). Cyclic Voltammetry in Electrochemical Oxidation of Amoxicillin with Co (III) as Mediator in Acidic Medium Using Pt, Pt/Co and Pt/$Co(OH)_2$ Electrodes. *MATEC Web of Conferences*, **197**, 05004. https://doi.org/10.1051/matecconf/201819705004

Hiremath, C. V., Hiremath D. C., & Nandibewoor, S. T. (2007). Ruthenium (III) Catalyzed Oxidation of Gabapentin (Neurontin) by Diperiodatonickelate (IV) in Aqueous Alkaline Medium: A Kinetic and Mechanistic Study. *Journal of Molecular Catalysis A: Chemical,* **269**(1-2): 246-253. https://doi.org/10.1016/j.molcata.2007.01.024

Hiremath, D. C., Kiran, T. S., & Nandibewoor, S.T. (2007). Oxidation of Vanillin by Diperiodatocuprate (III) in Aqueous Alkaline Medium: A Kinetic and Mechanistic Study by Stopped-Flow Technique. *International Journal of Chemical Kinetics*, **39**(4):236-244. https://doi.org/ 10.1002/kin.20233

Hiremath, M. I., & Nandibewoor, S. T. (2006). Kinetics and Mechanism of Ruthenium (III) Catalyzed Oxidation of L-Proline by Copper (III): A Free Radical Intervention and Decarboxylation. *Russ. J. Phys. Chem. B,* **80**: 1029–1033 https://doi.org/10.1134/S0036024406070053

Hoffman, T. A., & Bullock, W. E. (1970). Carbenicillin Therapy of Pseudomonas and Other Gram-Negative Bacillary Infections. *Annals of Internal Medicine,* **73**(2): 165-171. https://doi.org/10.7326/0003-4819-73-2-165

Holt, H. A., Broughall, J. M., McCarthy, M., & Reeves, D. S. (1976). Interactions Between Aminoglycoside Antibiotics and Carbenicillin or Ticarcillin. *Infection*, **4**(2): 107–109. https://doi.org/10.1007/bf01638726

Homem, V., & Santos, L. (2011). Degradation and Removal Methods of Antibiotics from Aqueous Matrices – A Review. *Journal of Environmental Management,* **92**(10): 2304–2347. https://doi.org/10.1016/j.jenvman.2011.05.023

Hosahalli, R. V., Savanur, A. P., Nandibewoor, S. T., & Chimatadar, S. A. (2009). Kinetics, and Mechanism of Uncatalyzed and Ruthenium (III) - Catalyzed Oxidation of D-Panthenol by Alkaline Permanganate. *Transition Metal Chemistry*, **35**(2): 237–246**.** https://doi.org/ 10.1007/s11243-009-9319-4

Hosmani, R. R., & Nandibewoor, S. T. (2009). Mechanistic Study of Ruthenium (III) Catalyzed Oxidation of L-Lysine by Diperiodatoargentate (III) in Aqueous Alkaline Medium. *Journal of Chemical Sciences*, **121**(3): 275-281. https://www.ias.ac.in/article/fulltext/jcsc/121/03/0275-0281.

Hosamani, R. R., Shetti, N. P., & Nandibewoor, S. T. (2008). Mechanistic Investigation on the Oxidation of Ampicillin Drug by Diperiodatoargentate (III) in Aqueous Alkaline Medium. *Journal of Physical Organic Chemistry*, **22**(3): 234-240. https://doi.org/10.1002/poc.1460

Hughes, S. R., Kay, P., & Brown, L. E. (2012). Global Synthesis and Critical Evaluation of Pharmaceutical Data Sets Collected from River Systems. *Environmental Science & Technology*, **47**(2): 661–677. https://doi.org/10.1021/es3030148

Ibrahim, S. M., Saad, N., Ahmed, M. M., & El-Aal, M. A. (2022). Novel Synthesis of Antibacterial Pyrone Derivatives Using Kinetics and Mechanism of Oxidation of Azithromycin by Alkaline Permanganate. *Bioinorganic Chemistry*, **119**: 105553. https://doi.org/10.1016/j.bioorg.2021.105553

Ikehata, K., El-Din, G. M., & Snyder, S. A. (2008). Ozonation and Advanced Oxidation Treatment of Emerging Organic Pollutants in Water and Wastewater. *Ozone: Science & Engineering,* **30**(1): 21–26. https://doi.org/10.1080/01919510701728970

Jaiswal, P. K., & Yadava, K. L. (1973). Determination of Sugars and Organic Acids with Periodato Complex of Cu (III). *Indian Journal of Chemistry*, **11**: 837-838

Jeffery, G. H., Basset, J., Mendham, J., R. C., & Denney, R. C. (1996). *Vogel's Textbook of Qualitative Chemical Analysis. 5th Edition, ELBS, Longman, Essex U.K,* 455

Kaizal, A. F., Salman, J. M., & Kot, P. (2023). Evaluation of Some Heavy Metals, Their Fate and Transportation in Water, Sediment, and Some Biota within AL-Musayyib River, Babylon Governorate, Iraq. *Baghdad Science Journal,* **20**(2): 600-615. http://dx.doi.org/10.21123/bsj.2022.7599

Kalli, M., Noutsopoulos, C., & Mamais, D. (2023). The Fate and Occurrence of Antibiotic-Resistant Bacteria and Antibiotic Resistance Genes during Advanced Wastewater Treatment and Disinfection: A Review. *Water*, **15**(11): 2084. https://doi.org/10.3390/w15112084

Kathari, C., Pol, P., & Nandibewoor, S. T. (2002). The Kinetics and Mechanism of Oxidation of Vanillin by Diperiodatonickelate (IV) in Aqueous Alkaline Medium. *Turkish Journal of Chemistry*, **26**(2): 229-236. https://journals.tubitak.gov.tr/chem/vol26/iss2/11

Karpova, S. (2013). Quantitative Determination of Ampicillin and Oxacillin in the "Ampiox" Preparation Using Potassium Hydrogenperoxomonosulphate. *Journal of Chemical and Pharmaceutical Research,* **5**(10): 57-64

Khalilzadeh, M. A., Khaleghi, F., Gholami, F. & Karimi-Maleh, H. (2009). Electrocatalytic Determination of Ampicillin Using Carbon-Paste Electrode Modified with Ferrocendicarboxylic Acid. *Analytical Letters*, **42**(3): 584-599. https://doi.org/ 10.1080/00032710802677126

Kretschmer, R., Gussner, G., Gorls, H., Heinemann, S. H., & Westerhausen, M. (2011). Dicarbonyl- bis (cysteamine) iron (II): A Light Induced Carbon Monoxide Releasing Molecule Based on Iron (CORM-S1). *Journal of Inorganic Biochemistry*, **105**(1): 6-9**.** https://doi.org/10.1016/j.jinorgbio.2010.10.006

Krupa, P., Bystron, J., Podkowik, M., Empel, J., Mroczkowska, A., & Bania, J. (2015). Population Structure and Oxacillin Resistance of Staphylococcus Aureus from Pigs and Pork Meat in South-West of Poland. *BioMed Research International*, **2015** (Article ID 141475): 9 Pages. https://dx.doi.org/10.1155/2015/141475

Kulkarni, S. D., & Nandibewoor, S. T. (2006). A Kinetic and Mechanistic Study on Oxidation of Isoniazid Drug By Alkaline Diperiodatocuprate (III) – A Free Radical Intervention. *Transition Metal Chemistry*, **31**(8): 1034-1039. https://doi.org/ 10.1007/s11243-006-0103-4

Lamani, S. D., Abbar, J. C., & Nandibewoor, S. T. (2009). Mechanistic Aspects of Os (VIII)/ Ru (III) Catalyzed Oxidation of L-Phenylalanine by Ag (III) Periodate Complex in Aqueous Alkaline Medium. *Catalysis Letters,* **133**(1-2): 142–155. https://doi.org/10.1007/s10562-009-0134-5

Larsson, D. G. J., Pedro .C. D., & Paxeus N. (2007). Effluent from Drug Manufactures Contains Extremely High Levels of Pharmaceuticals. *Journal of Hazardous Materials*, **148**(3): 751-755. https://doi.org/ 10.1016/j.jhazmat.2007.07.008

Lascelles, K., Morgan, L. G., Nicholls, D., & Beyersmann, D. (2005). Nickel Compounds. *Ullmann's Encyclopedia of Industrial Chemistry.* https://doi.org/10.1002/14356007.a17_235.pub2

Lashkaryani, E. B., Kakavandi, B., Kalantary, R. R., Jafari, A. J., & Gholami, M. (2019). Activation of Peroxymonosulfate into Amoxicillin Degradation Using Cobalt Ferrite Nanoparticles Anchored on Graphene ($CoFe_2O_4$@Gr). *Toxin Reviews*, 1-10. https://doi.org/10.1080/15569543_2019.1582066

Leone S., Cascella M., Pezone I., & Flore M. (2019). New Antibiotics for the Treatment of Serious Infections in Intensive Care Unit Patients. *Current Medical Research and Opinion*, **35**(8):1331-1334. https://doi.org/10.1080/03007995.2019.1583025

Levason, W., & Spicer, M. D. (1987). The Chemistry of Copper and Silver in Their Higher Oxidation States. *Coordination Chemistry Reviews*, **76**: 45-120.

https://doi.org/10.1016/0010-8545 (87)85002-6

Lewis, E. A., & Tolman, W. B. (2004). Reactivity of Di-oxygen-copper Systems. *Chemical Reviews*, **104**(2): 1047-1076**.** https://doi.org/ 10.1021/cr020633r

Lewis, K. G., Ghosh, S. K., Bhuvanesh, N., & Gladysz, J. A. (2015). Cobalt (III) Werner Complexes with 1, 2-Diphenylethylenediamine Ligands: Readily Available, Inexpensive, and Modular Chiral Hydrogen Bond Donor Catalysts for Enantioselective Organic Synthesis. *ACS Central Sci*ence, **1**(1): 50-56. https://doi.org/10.1021/acscentsci.5b00035

Li, X., Shen, T., Wang, D., Yue, X., Liu, X., Yang, Q., Cao, J., Zheng W., & Zeng, G. (2012). Photodegradation of Amoxicillin by Catalyzed Fe^{3+}/H_2O_2 Process. *Journal of Environmental Sciences*, **24**(2): 269-275. ISSN 1001-0742. https://doi.org/10.1016/S1001-0742 (11)60765-1

Lindberg, R. H., Bjorklund, K., Rendahl, P., Johansson, M. I., Tysklind, M., & Andersson, B. A. V. (2007). Environmental Risk Assessment of Antibiotics in the Swedish Environment with an Emphasis on Sewage Treatment Plants. *Water Research,* **41**(3): 613–619. https://doi.org/10.1016/j.watres.2006.11.014

Lister, M. W. (1953). The Stability of Some Complexes of Trivalent Copper, *Canadian Journal of Chemistry,* **31**(7): 638-652. https://doi.org/10.1139/v53-087

Liu, J. L., & Wong, M. H. (2013). Pharmaceuticals and Personal Care Products (PPCPs): a Review on Environmental Contamination in China. *Environment International*, **59**: 208-224. https://doi.org/10.1016/j.envint.2013.06.012

Liu, T., Aniagor, C. O., Ejimofor, M. I., Menkiti, M. C., Tang, K. H. D., Chin, B. L. F., Chan, Y. H., Yiin, C. L., Cheah, K. W., Chai, Y. H., Lock, S. S. M., Yap, K. L., & Wee, M. X. J. (2023). Technologies for Removing Pharmaceuticals and Personal Care Products (PPCPS) from Aqueous Solutions: Recent Advances, Performances, Challenges and Recommendations for Improvements. *Journal of Molecular Liquids*, Volume **374**, 121144. https://doi.org/10.1016/j.molliq.2022.121144

Lovell, J. F., Tracy W. B., Chen, L. J., & Zheng, G. (2010). Activatable Photosensitizes for Imaging and Therapy. *Chemical Reviews,* **110**(5):2839-2857 https://doi.org/10.1021/cr900236h

Lynn, B. (1973). Administration of Carbenicillin and Ticarcillin—Pharmaceutical Aspects. *European Journal of Cancer (1965*), **9**(6): 425–433**.** https://doi.org/10.1016/0014- 2964(73)90107-2

Maksoud, M. I. A. A., El-Sayyad, G. S., Ashour, A. H., El-Batal, A. I., Elsayed, M. A., Gobara, M., El-Khawaga, A., Abdel-Khalek, E. K., and El-Okr, M. M. (2018). Antibacterial, Antibiofilm, and Photocatalytic Activities of Metals-Substituted Spinel Cobalt Ferrite Nanoparticles. *Microbial Pathogenesis*. https://doi.org/10.1016/j.micpath.2018.11.045

Malode, S. J., Abbar, J. C., & Nandibewoor, S. T. (2010). Mechanistic Aspects of Uncatalyzed and Ruthenium (III) Catalyzed Oxidation of Dl-Ornithine Monohydrochloride sy Silver (III) Periodate Complex in Aqueous Alkaline Medium. *Inorganica Chimica Acta,* **363**(11): 2430–2442. https://doi.org/10.1016/j.ica.2010.03.081

Marcinowski, P. P., Bogacki, J. P., and Naumczyk, J. H. (2014). Cosmetic Wastewater Treatment Using the Fenton, Photo-Fenton, and H_2O_2/UV Processes. *Journal of Environmental Science and Health*, Part A, **49**(13): 1531–1541**.** https://doi.org/10.1080/10934529.2014.938530

Martinez, J. L. (2009). Environmental Pollution by Antibiotics and by Antibiotic Resistance Determinants. *Environmental Pollution,* **157**(11):2893–2902. PMID: 19560847. https://doi.org/10.1016/j.envpol.2009.05.051

Martinez, J. L., Coque, T. M., & Baquero, F. (2015). What Is a Resistance Gene? Ranking Risk in Resistomes. *Nature Reviews Microbiology*, **13**(2)**:**116-123. https://doi.org/10.1038/nrmicro3399

McDonald, M. R., Fredericks, F. C., & Margerum, D. W. (1997). Characterization of Copper (III)-Tetrapeptide Complexes with Histidine as the Third Residue. *Inorganic Chemistry*, **36**(14): 3119-3124. https://doi.10.1021/ic9608713

Mejia, G. H., Penuela, G. A., & Mueses, M. A. (2022). Evaluation of a Helicoidal Flux Photoreactor Applied in the Dicloxacillin Degradation by UV-C/H_2O_2 and UV-A/Photo-Fenton Including the Effect of Photon Absorption. *Results in Engineering,* 15,100519**.** https://doi.org/10.1016/j.rineng.2022.100519

Meti, M. D., Abbar, J. C., Nandibewoor, S. T., & Chimatadar, S. A. (2016). Voltammetric Oxidation of Carbenicillin and its Electroanalytical Applications at the Gold Electrode. *Cogent Chemistry*, **2** (1). https://doi.org/10.1080/23312009.2016.1235459

Meti, M. D., Nandibewoor, S. T., & Chimatadar, S. A. (2020). Oxidation of Procainamide by Diperiodatocuprate (III) Complex in Aqueous Alkaline Medium: A Comparative Kinetic Study. *Inorganic and Nano-Metal Chemistry*, **50**(4): 195-204. https://doi.org/10.1080/24701556.2019.1662041

Meyers, B. R., Sabbaj, J., & Weinstein, L. (1970). Bacteriological, Pharmacological, and Clinical Studies of Carbenicillin. *Archives of Internal Medicine,* **125**(2): 282–286. https://doi.org/10.1001/archinte.1970.00310020088009

Michaelis, L., Schubert, M. P., & Granick, S. (1981).The Free Radicals of the Type of Wurster's Salts. *Journal of the American Chemical Society*, **61**(8): 1981-1992. https://doi.org/10.1021/ja01877a013

Mo, W. Y., Chen, Z., Leung, H. M., & Leung, A. O. W. (2015). Application of Veterinary Antibiotics in China's Aquaculture Industry and Their Potential Human Health Risks. *Environmental Science and Pollution Research,* **24**(10): 8978– 8989. https://doi.org/10.1007/s11356-015-5607-z

Moelwyn-Hughes, E. A. (1947). Kinetics of Reactions in Solutions, *Oxford University Press,* London: 297.

Mukherjee, A. K., & Singh, A. K. (1978). B-Lactams: Retrospect and Prospect. *Tetrahedron*, **34**(12): 1731-1767. https://doi.org/ 10.1016/0040-4020(78)80209-9

Mohammadi, T. M., Khaleghi, M., Bidram, E., Zarepour, A., & Zarrabi, A. (2022). Penicillin and Oxacillin Loaded on PEGylated-Graphene Oxide to Enhance the Activity of the Antibiotics against Methicillin-Resistant Staphylococcus aureus. *Pharmaceutics,***14**(10):2049.https://doi.org/10.3390/pharmaceutics14102049

Rohani Moghadam, M., Salehi, L., Jafari, S., Nasirizadeh, N., & Ghasemi, J. (2019). Voltammetric sensing of oxacillin by using a screen-printed electrode modified with molecularly imprinted polyaniline, gold nanourchins and graphene oxide. *Microchimica Acta*, **186**:1-7. https://doi.org/10.1007/s00604-019-3981-9.

Nadimpalli, S., Padmvasthy, J., & Yusuff, K. K. M. (2001). Determination of the Nature of the Diperiodatocuprate (III) Species in the Aqueous Alkaline Medium Through A Kinetic and Mechanistic Study on the Oxidation of Iodide Ion. *Transition Metal Chemistry,* **26**(3): 315–321. https://doi.org/ 10.1023/A: 1007116932047

Ory, E. M. (1963). The Use and Abuse of the Broad Spectrum Antibiotics. *JAMA: The Journal of the American Medical Association*, **185** (4): 273. https://doi:10.1001/jama.1963.03060040057022.

Oun, R., Moussa, Y. E., & Wheate, N. J. (2018). The Side Effects of Platinum-Based Chemotherapy Drugs: a Review for Chemists. *Dalton Transactions*, **47**(19):6645–6653. https://doi:10.1039/c8dt00838h

Parker, K. M., Pignatello, J. J., & Mitch, W. A. (2013). Influence of Ionic Strength on Triplet-State Natural Organic Matter Loss by Energy Transfer and Electron Transfer Pathways. *Environmental Science and Technology (ACS Publications)*, **47**(19): 10987-10994. https://doi.org/10.1021/es401900j

Panigrahi, G. P., & Misro, P. K. (1977). Kinetics and Mechanism of Oxidation of Osmium (VIII) Catalyzed Oxidation of Unsaturated Acids by Sodium Periodates. *Indian Journal of Chemistry,* **15 A**: 1066 -1069

Patil, H., Naik, P., & Nandibewoor, S. T. (2009). Osmium (VIII) Catalyzed Oxidation of Diclofenac Sodium by Diperiodatoargentate (III) Complex in Aqueous Alkaline Medium. *The Open Catalysis Journal*, **2**(1): 140-149. https://doi.org/10.2174/1876214X00902010140

Patil, J. K., Patil, K. A., & Pawar, S. P. (2014). Development and Validation of RP-HPLC Method for Simultaneous Estimation of Amoxicillin and Dicloxacillin in Bulk Drug and Capsules. *Pharma Science Monitor, an International Journal of Pharmaceutical Sciences,* **5**(2): 39-47, sup-1.

Patil, R. K., Patil, R. H., Nandibewoor, S. T., & Chimatadar, S. A. (2009). Kinetics and Mechanism of the Oxidation of Tyrosine by Diperiodatoargentate (III) in Aqueous Alkaline Medium. *Synthesis and Reactivity in Inorganic, Metal-Organic, and Nano-Metal Chemistry*, **39**(10): 637-644. https://doi.org/10.1080/15533170903433097

Petcu, G., Anghel, E. M., Somacescu, S., Preda, S., Culita, D. C., Mocanu, S.,& Parvulescu, V. (2020). Hierarchical Zeolite Y Containing Ti, and Fe Oxides as Photocatalysts for Degradation of Amoxicillin. *Journal of Nanoscience and Nanotechnology,* **20** (2): 1158–1169. https://doi.org/10.1166/jnn.2020.16981

Pickering, L. K., & Gearhart, P. (1979). Effect of Time and Concentration Upon Interaction Between Gentamicin, Tobramycin, Netilmicin, or Amikacin and Carbenicillin or Ticarcillin. *Antimicrobial Agents and Chemotherapy,* **15**(4): 592–596**.** https://doi.org/10.1128/aac.15.4.592

Quand-Meme G. C., Auguste, A. F. T., Marie, H. L. E., Ibrahima, S., & Lassine, O. (2015). Electrochemical Oxidation of Amoxicillin in its Pharmaceutical Formulation at Boron Doped Diamond (BDD) Electrode. *Journal of Electrochemical Science and Engineering,* **5**(2): 129-143. https://doi.org/ 10.5599/jese186.

Rabia, M. K., Mohamad, A. D. M., Ismail, N. M., & Mahmoud, A. A. (2013). Synthesis and Physico-Chemical Properties of Some Ni (II) Complexes with Isatin-Hydrazones. *Russian Journal of General Chemistry*, **83**(12): 2502–2509. https://doi.org/10.1134/S1070363213120487

Rahbarimanesh, A., Mojtahedi, S. Y., Sadeghi, P., Ghodsi, M., Kianfar, S., Khedmat, L., Siyahkali, S. J. M., Yazdi, M. K., & Izadi, A. (2019). Antimicrobial Stewardship Program (ASP): an Effective Implementing Technique for the Therapy Efficiency of Meropenem and Vancomycin Antibiotics in Iranian Pediatric Patient. *Annals of Clinical Microbiology and Antimicrobials* , **18**(1): 6. https://doi.org/10.1186/s12941-019-0305-1

Rahmah, A. U., Harimurti, S., Omar, A. A., & Murugesan, T. (2014). Kinetics and Thermodynamic Studies of Oxytetracycline Mineralization Using UV/H_2O_2.

Clean – Soil, Air, Water, **43**(4): 496-503. https://doi,org/10.1002/clen.201200637

Ramotowska, S., Wysocka, M., Brzeski, J., & Chylewska, A. (2020). A Comprehensive Approach to the Analysis of Antibiotic-Metal Complexes. *TrAC Trends in Analytical Chemistry*, **123**: 115771. https://doi.org/10.1016/j.trac.2019.115771

Rao, J. P., Sethuram B., & Navaneeth, R. T. (1985). Kinetics of Oxidative Deamination of Some Amino Acids by Diperiodatoargentate (III) in Aqueous Alkaline Medium. *Reaction Kinetics and Catalysis Letters*, **29**: 289-296. https://doi.org/10.1007/BF02067981

Ray, P. (1943). A New Type of Complex Silver Compounds with Tervalent Silver. *Nature,* **151**(3840): 643-643. https://doi.org/10.1038/151643a0

Ray, P., & Sharma B. (1946). Tetra positive Nickel as AlkaliNickelPeriodates. *Nature*, **157**(3993):627-627. https://doi.org/ 0.1038%2F157627a0

Raynor, B. D. (1997). Penicillin and Ampicillin. *Primary Care Update for OB/GYNS*. **4**(4):147–152. https://doi:10.1016/s1068-607x(97)00012-7

Reberski, J. L., Terzic, J., Maurice, L. D., Lapworth, D. L. 2022. Emerging Organic Contaminants in Karst Groundwater: A Global Level Assessment. *Journal of Hydrology*, **604**: 127242. https://doi.org/10.1016/j.jhydrol.2021.127242

Renny, J. S., Tomasevich, L. L., Tallmadge, E. H., & Collum, D. B. (2013). Method of continuous variations: applications of job plots to the study of molecular associations in organometallic chemistry. *Angewandte Chemie International Edition*, **52**(46):11998-12013. https://doi.org/10.1002/anie.201304157

Richardson, A. E., James, K. W., Spittle, C. R., & Robinson, O. P. W. (1968). Experiences with Carbenicillin in the Treatment of Septicaemia and Meningitis. *Postgraduate Medical Journal*, **44**(517): 844-847. http://dx.doi.org/10.1136/pgmj.44.517.844

Sangal, V. (2020). Effects of Ionic Strength on the Reaction Rate Between Aromatic Aldehyde and Tertiary Butyl Hypochlorite. *Research Journal of Chemical Science*, **10**(3): 30-34. ISSN 2231-606X

Savanur, A. P., Nandibewoor, S. T., & Chimatadar, S. A. (2009). Manganese (II) Catalyzed Oxidation of Glycerol by Cerium (IV) in Aqueous Sulphuric Acid Medium: A Kinetic and Mechanistic Study. *Transition Metal Chemistry*, **34**(7): 711–718. https://doi.org/10.1007/s11243-009-9252-6

Schatzscneider, U. (2010). Photo CORMs: Light-Triggered Release of Carbon Monoxide from the Coordination Sphere of Transition Metal Complexes for Biological Applications. *Inorganica Chimica Acta*, **374**(1): 19-23. https://doi.org/10.1016/j.ica.2011.02.068

Serna-Galv.is, E. A., Silva-Agredo, J., Giraldo, A. L., Florez-Acosta, O. A, & Torres-Palma, R. A. (2016). Comparative Study of the Effect of Pharmaceutical

Additives on the Elimination of Antibiotic Activity During the Treatment of Oxacillin in Water by the Photo-Fenton, Tio_2-Photocatalysis and Electrochemical Processes. *Science of the Total Environment*, **541**: 1431-1438. https://doi.org/10.1016/j.scitotenv.2015.10.029

Sharma, P. D., & Gupta, Y. K. (1972). Kinetics and Mechanism of the Reduction of Thallium (III) by Arsenic (III) in Perchloric Acid Solution. *Journal of the Chemical Society, Dalton Transactions,* (**1**)1: 52-55. https://doi.org/10.1039/dt9720000052

Shan, J. H., Li, Y., Huo, S. Y., & Yin, C. H. (2013). The Oxidation of 2-(2-Methoxyethoxy) Ethanol and 2-(2-Ethoxyethoxy) Ethanol by Ditelluratocuprate (III): A Kinetic and Mechanistic Study. *Journal of Chemistry (Hindawi)*, **2013**: Article ID 627324 (5 pages). https://doi.org/10.1155/2013/627324

Shan, J., Liu, Y., & Zhang, J. 2011. Kinetics and Mechanism of Oxidation of 1-Methoxy-2-Propanol and 1-Ethoxy-2-Propanol by Ditelluratocuprate (III) in Alkaline Medium. *Chinese Journal of Chemistry*, **29**(4): 639-642. https://doi.org/10.1002/cjoc.201190134

Sharanabasamma, K., Salunke, M. S. & Tuwar, S. M. (2008). Periodate Influencing Diperiodatocuprate (III) Oxidation of Sulfur Containing Amino Acid in Aqueous Alkaline Medium. *Journal of Solution Chemistry,* **37**(9): 1217–1225. https://doi.org/10.1007/s10953-008-9307-x

Sheehan, J. C., Henery-Logan, & Kenneth. R. (1957). The Total Synthesis of Penicillin V. *Journal of the American Chemical Society*, **79** (5): 1262-1263. https://doi.org/10.1021/ja01562a063

Shetti, N. P., & Nandibewoor, S. T. (2009). Kinetic and Mechanistic Investigations on Oxidation of L-Tryptophan by Diperiodatocuprate (III) in Aqueous Alkaline Medium. *Zeitschrift fur Physikalische Chemie*, **223**(3): 299–317. https://doi.org/10.1524/zpch.2009.5432.

Shetti, N. P., Hegde, R. N., & Nandibewoor, S. T. (2009). Structure Reactivity and Thermodynamic Analysis on the Oxidation of Ampicillin Drug by Copper (III) Complex in Aqueous Alkaline Medium (Stopped-Flow Technique). *Journal of Molecular Structure*, **930**(1): 180-186.

https://doi.org/10.1016/j.molstruc.2009.05.013

Shivprasad, C. (2011). Sheehan′s syndrome: Newer Advances. *Indian Journal of Endocrinology and Metabolism,* **15**(7): 203. https://doi.org/10.4103/2230-8210.84869

Shokri, R., Yengejeh, R. J., Babaei, A. A., Derikvand, E., & Almasi, A. (2019). Advanced Oxidation Process Efficiently Removes Ampicillin from Aqueous Solutions. *Iranian Journal of Toxicology*, **14**(2): 123-132. http://doi. org/10.32598/ijt.14.2.483.3

Slocik, J. M., Ward, M. S., Somayajula, K. V., & Shepherd, R. E. (2001). Coordination of $RuCl_3$ (NO) $(H_2O)_2$ by Imidazole, Histidine and Iminodiacetate Ligands: A Study of Complexation of 'Caged NO' by Simple Bio-Cellular Donors. *Transition Metal Chemistry*, **26**(3): 351-364. https://doi.org/ 10.1023/A: 1007194314107

Splith, K., Hu, W., Schatzscneider, U., Gust, R., Ott, I., Onambele, L. A., Prokop, A., & Neundorf, I. (2010). Protease-Activatable Organometal-Peptide Bioconjugates with Enhanced Cytotoxicity on Cancer Cells. *Bioconjugate Chemistry,* **21**(7): 1288-1296. https://doi.org/ 10.1021/bc100089z

Spit, T., Van der Hoek, J. P., de Jong, C., Van Halem, D., de Kreuk, M., & Perez, B. B. (2022). Removal of Antibiotic Resistance from Municipal Secondary Effluents by Ozone-Activated Carbon Filtration. *Frontiers in Environmental Science*, **10**: 335. https://doi.org/10.3389/fenvs.2022.834577

Stage, T. B , Graff, M., Wong, S., Rasmussen, L. L., Nielsen, F., Pottegård, A., Brøsen K., Kroetz, D. L., Khojasteh, S. C., & Damkier, P. (2018). Dicloxacillin Induces

CYP2C19, CYP2C9, and CYP3A4 in Vivo and in Vitro. *British Journal of Clinical Pharmacology*, **84**(3): 510-519. https://doi.org/ 10.1111/bcp.13467

Stephen, L. (1994). Metals in Medicine. B*ioinorganic Chemistry, Mill City: University Science Books*, p. 505-583

Stuart, R. K., Braine, H. G., Lietman, P. S., Saral, R., & Fuller, D. J. (1980). Carbenicillin-Trimethoprim/Sulfamethoxazole Versus Carbenicillin-Gentamicin as Empiric Therapy of Infection in Granulocytopenic Patients: A Prospective, Randomized, Double-Blind Study. *The American Journal of Medicine*, **68**(6): 876-885. https://doi.org/10.1016/0002-9343 (80)90217-x.

Sunsandee, N., Ramakul, P., Phatanasri, S., & Pancharoen, U. (2020). Biosorption of Dicloxacillin From Pharmaceutical Waste Water Using Tannin from Indian Almond Leaf: Kinetic and Equilibrium Studies. *Biotechnology Reports*, 27, e00488, https://doi.org/10.1016/j.btre.2020.e00488

Takacs, E., Wang, J., Chu, L., Toth, T., Kovacs, K., Bezsenyi, A., Szabo, L., HomLok, R., & Wajnarovits, L. (2022). Elimination of Oxacillin, its Toxicity and Antibacterial Activity by Using Ionizing Radiation. *Chemosphere*, **286**(1): 131467. https://doi.org/10.1016/j.chemosphere.2021.131467

Taube, H. (1967). Intramoleculer electron transfer. *ScienceDirect, XVIth International Conference on Coordination Chemistry*, p. 25-42. https://doi.org/10.1016/B978-0-408-70726-8.50006-4

Taube, H., Myers, H., & Rich, R. L. (1953). Observations on the Mechanism of Electron Transfer in Solution 1. *Journal of the American Chemical Society*, **75**(16): 4118-4119. https://doi.org/ 10.1021/ja01112a546

Thomas, A. H., & Broadbridge, R. A. (1972). The Nature of Carbenicillin Resistance in Pseudomonas Aeruginosa. *Journal of General Microbiology*, **70**(2): 231-241 https://doi.org/10.1099/00221287-70-2-231

Thriveni, M.K., Mallikarjuna, I., Bellappa, S., & Shivalingaswamy, T. (2021). Oxidation of Caffeine by Diperiodatocuprate (III) with and without Ruthenium (III) in

Alkaline Medium. *Russian Journal of Physical Chemistry A* **95** (Suppl 1), S44–S55. https://doi.org/10.1134/S0036024421140235

Trovo, A. G., Pupo Nogueira, R. F., Agüera, A., Fernandez-Alba, A. R., & Malato, S. (2011). Degradation of the Antibiotic Amoxicillin by Photo-Fenton Process-Chemical and Toxicological Assessment. *Water Research*, **45**(3): 1394-1402. https://doi.org/10.1016/j.watres.2010.10.029

Upadhyay, S. K. (2006). Chemical Kinetics and Reaction Dynamics. *Springer*, **1**(256): 1-45. https://doi.org/ 10.1007/978-1-4020-4547-9

Velo-Gala, I., Farre, M. J., Radjenovic, J., & Gernjak, W. 2023. Influence of Water Matrix Components on the UV/Chlorine Process and its Reactions Mechanism. *Environmental Research*, **218**: 114945. https://doi.org/10.1016/j.envres.2022.114945

Veena, M. S., Prashanth, M. K., Yogesh Kumar, K., Muralidhara, H. B., & Arthoba Nayaka, Y. (2015). Kinetics and Mechanistic Study of Oxidation of Amoxicillin by Chloramine-T in Acid Medium. *Journal of the Chilean Chemical Society,* **60**(3): 3063–3068. https://doi.org/10.4067/s0717-97072015000300019

Villagas-Guzman P., Silva-Agredo, J., Gonzalez-Gomez, D., Giraldo-Aguirre, A. L. Florez-Ocesta, O., & Torres-Palma, R. A. (2015). Evaluation of Water Matrix Effects, Experimental Parameters, and the Degradation Pathway During the Tio_2 Photocatalytic Treatment of the Antibiotic Dicloxacillin. *Journal of environmental science and health- Part A, Toxic/hazardous substances & environmental engineering*, **50**(1): 40-48. https://doi.org/10.1080/10934529.2015.964606

Vorosmarty, C. J., Mclntyre, P. B., Gessner, M. O., Dudgeon, D., Prusevich, A., Green, P., Glidden, S., Bunn, S. E., Sullivan, C. A., Reidy Liermann, C., & Davies, P. M. (2010). Global Threats to Human Water Security and River Biodiversity. *Nature*, **467**:555–561. https://doi.org/10.1038/nature09440

Wang, J., Xu, S., Zhao, K., Song, G., Zhao, S., & Liu, R. (2023). Risk Control of Antibiotics, Antibiotic Resistance Genes (ARGs) and Antibiotic Resistance Bacteria (ARB) During Sewage Sludge Treatment and Disposal: A Review. *Science of the Total Environment*, **877**: 162772. https://doi.org/10.1016/j.scitotenv.2023.162772

Wright, M. R. (2004). An Introduction to Chemical Kinetics. *John Wiley & Sons Ltd*., ISBN: 0-470-09058-8(hbk) 0-470-09059-6(pbk)

Xiang, S., Wang, X., Ma, W., Liu, X., Zhang, B., Huang, F., Liu, F., & Guan, X. (2020). Response of Microbial Communities of Karst River Water to Antibiotics and Microbial Source Tracking for Antibiotics. *Science of The Total Environ*ment, **706**: 135730. https://doi.org/10.1016/j.scitotenv.2019.135730

Xiao-Dong, Y., Xian-Cheng, Z., Lin-Li, L., Cheng-Rong, L., Tao, L., Qiang, Z., & Ning, H. (2005). Studies on Stability of Dicloxacillin Sodium with Programmed Humidifying Experiments. *Acta Chimica Sinica*, **63**(6): 512-518

Xie, H. Y., Wang, Z. R., & Fu, Z. F. (2014). Highly Sensitive Trivalent Copper Chelate-Luminol Chemiluminescence System for Capillary Electrophoresis Chiral Separation and Determination of Ofloxacin Enantiomers in Urine Samples. *Journal of pharmaceutical analysis*, **4**(6): 412- 416. https://doi.org/10.1016/j.jpha.2014.05.004

Yahya, M.Q. (2015). Optimization of Ampicillin Oxidation Reaction with Hydrogen Peroxide, and Potassium Dichromate in Different Media. *International Journal of Chem Tech Research*, **8**(4): 1689-1694. ISSN: 0974-4290

Yang, X. B., Wanga, Q., Huangb, Y., Fu, P. H., Zhang, J. S., & Zeng, R. Q. (2012) Synthesis, DNA Interaction, and Antimicrobial Activities of Copper (II) Complexes with Schiff Base Ligands Derived from Kaempferol and Polyamines. *Inorganic Chemistry Communications,* **25**: 55-59. https://doi.org/10.1016/j.inoche.2012.08.010

Yeny, B., Anne-Claire, T., & Flor de Maria, C. L. (2022). Physiological and Kinetic Evaluation of Ampicillin Oxidation as Unique Electron Source by A Denitrifying Sludge. *Journal of Chemical Technology & Biotechnology*, **97**(6): 1457-1467. https://doi.org/10.1002/jctb.7014

Zewail, A. H. (2000). Femtochemistry: Atomic-Scale Dynamics of the Chemical Bond. *Journal of Physical Chemistry A*, **104**(24): 5660-5694.

https://doi.org/10.1021/jp001460h

Zhang, H., Xie, H., Chen J., & Zhang, S. (2015). Prediction of Hydrolysis Pathways and Kinetics for Antibiotics under Environmental pH Conditions: A Quantum Chemical Study on Cephradine. *Environmental Science and Technology*, **49**(3):

1552-1558. https://doi.org/10.1021/es505383b

Zhang, Y., Zhao, Y. G., Maqbool, F., & Hu, Y. (2022). Removal of Antibiotics Pollutants in Wastewater by UV-Based Advanced Oxidation Processes: Influence of Water Matrix Components, Processes Optimization and Application: A Review. *Journal of Water Process,* **45**: 102496. https://doi.org/10.1016/j.jwpe.2021.102496

Zhao, J., Sun, Y., Wu, F., Shi, M., & Liu, X. (2019). Oxidative Degradation of Amoxicillin in Aqueous Solution by Thermally Activated Persulfate. *Journal of Chemistry,* Article ID 2505823, 1-10.https://doi.org/10.1155/2019/2505823

Zhao, Y., Qi, M., Hao, R., Jiang, J., & Yuan, B. (2020). A Novel Catalytic Oxidation Process for Removing Elemental Mercury by Using Diperiodatoargentate (III) in The Catalysis of Trace Ruthenium (III). *Journal of Hazardous Materials*, **381**: 120964. https://doi.org/10.1016/j.jhazmat.2019.120964

Zhuang, M., Achmon, Y., Cao, Y., Liang, X., Chen, L., Wang, H., Siame, B. A. & Leung, K. Y. (2021). Distribution of Antibiotic Resistance Genes in the Environment. *Environmental Pollution*, **285**: 117402. https://doi.org/10.1016/j.envpol.2021.117402

Zuckerman, J. J. (1986). Inorganic Reactions and Methods: Electron- Transfer and Electrochemical Reactions; Photochemical and Other Energized Reactions. *VCH Publishing Group,* 15. https://doi.org/10:0895732653

APPENDIX

1) Derivation of the rate constant from absorbance

$$\ln(\mathrm{Abs})_t = -kt + \ln(\mathrm{Abs})_o$$

$$2.303\log(\mathrm{Abs})_t = -kt + 2.303\log(\mathrm{Abs})_o$$

$$k\,t = 2.303\log(\mathrm{Abs})_o - 2.303\log(\mathrm{Abs})_t$$

$$k = \frac{2.303}{t}\left[\log\frac{(\mathrm{Abs})_o}{(\mathrm{Abs})_t}\right] \ldots\ldots\ldots\ldots\ldots\ldots\ldots\ldots\ldots\ldots (1)$$

Here $(Abs)_o$ = Initial Absorbance at time 0 sec or just before mixing penicillanic acid derivative and $(Abs)_t$ stands for Absorbance at any time t sec.

2) Equations for calculation of activation parameters

$$E_a = -2.303\ R\ Slope$$

The Arrhenius factor 'A' was calculated by,

$$\log A = \log k_c + \frac{E_a}{2.303RT}$$

The entropy of activation was calculated by,

$$\frac{\Delta S^{\#}}{4.576} = \log k_c - 10.753 - \log T + \frac{E_a}{4.576T}$$

Where, k is in sec^{-1}, t is the temperature in Kelvin and E_a in calories.

The enthalpy of activation was calculated by,

$$\Delta H^{\#} = E_a - RT$$

The free energy of activation was calculated by,

$$\Delta G^{\#} = \Delta H^{\#} - T\Delta S^{\#}$$

$$\Delta G^{\#} = -2.303RT\log K_{eq}$$

3) Rate constant derivation for the oxidation of Ampicillin

$$\text{rate} = -\text{d}\frac{[\text{DPC}]}{\text{dt}} = \text{k(Complex)}[\text{Cu}(\text{H}_3\text{IO}_6)_2]^-$$

$$\text{K}_1 = \frac{[\text{Cu}[\text{H}_3\text{IO}_6)_2[\text{OH}]^{2-}}{[\text{Cu}[\text{H}_2\text{IO}_6][\text{H}_3\text{IO}_6]^{2-}}$$

$$\text{So,} \quad [\text{Cu}(\text{H}_3\text{IO}_6)_2]^- = \text{K}_1\frac{[\text{Cu}[\text{H}_2\text{IO}_6][\text{H}_3\text{IO}_6]^{2-}}{[\text{OH}^-]}$$

$$\text{Since,} \quad \text{rate} = \text{kK}_1[\text{C}]\frac{[\text{DPC}]}{[\text{OH}^-]}$$

$$\text{Or,} \quad \text{K}_2 = \frac{[\text{C}]}{[\text{AMP}][\text{Co(III)}]}$$

$$\text{Or,} \quad \text{C} = \text{K}_2[\text{AMP}][\text{Co(III)}]$$

$$\text{Rate} = \text{kK}_1\text{K}_2\frac{[\text{AMP}]_f[\text{Co(III)}]_f[\text{DPC}]_f}{[\text{OH}^-]} \text{..... (A-1)}$$

The total concentration of DPC (III) can be given as

$$[\text{DPC}]_T = [\text{DPC}]_f + +[\text{Cu}(\text{H}_3\text{IO}_6)_2]^{2-} \text{ ..... (A-2)}$$

$$= [\text{DPC}]_f + \text{K}_1\frac{[\text{DPC}]}{[\text{OH}^-]}$$

$$=[\text{DPC}]_f[1 + \frac{\text{K}_1}{[\text{OH}^-]}]$$

$$=[\text{DPC}]_f\left[\frac{[\text{OH}^-]+\text{K}_1}{[\text{OH}^-]}\right]$$

$$\text{Where } [\text{DPC}]_f = \frac{[\text{DPC}]_T[\text{OH}^-]}{[\text{OH}^-]+\text{K}_1} \text{..... (A-3)}$$

$$\text{Similarly, } [\text{AMP}]_T = [\text{AMP}]_f + \text{C}$$

$$[\text{AMP}]_T = [\text{AMP}]_f + \text{K}_2[\text{AMP}]_f[\text{Co(III)}]$$

$$[\text{AMP}]_T = [\text{AMP}]_f[1 + \text{K}_2[\text{Co(III)}]$$

$$\text{So,} \quad [\text{AMP}]_f = \frac{[\text{AMP}]_T}{1+\text{K}_2[\text{Co(III)}]}$$

Where 'T' and 'f' represent total and free concentration respectively.

In case of very low concentration of AMP and Co (III)

$$[\mathrm{AMP}]_\mathrm{T} = [\mathrm{AMP}]_\mathrm{f}\ , \quad \ldots\ldots\ldots \text{(A-4)}$$

$$\text{Similarly,} \quad [\mathrm{Co(III)}]_\mathrm{T} = [\mathrm{Co(III)}]_\mathrm{f} + \mathrm{C}$$

$$= [\mathrm{Co(III)}]_\mathrm{f} + \mathrm{K_2}[\mathrm{AMP}][\mathrm{Co(III)}]_\mathrm{f}$$

$$[\mathrm{Co(III)}]_\mathrm{f}] = [\frac{[\mathrm{Co(III)}]_\mathrm{T}]}{1 + \mathrm{K_2}[\mathrm{AMP}]}] \ldots\ldots\ldots\ldots\ldots \text{(A-5)}$$

Substituting values of eq^n (A-3), (A-4) and (A-5) in eq^n (A-1)

and omitting T and f subscripts,

$$\text{We get,} \quad \text{rate} = -\frac{\mathrm{d[DPC]}}{\mathrm{dt}}$$

$$\text{rate} = \frac{\mathrm{kK_1K_2[AMP][DPC]_T[Co(III)][OH^-]}}{\mathrm{[OH^-]([OH^-] + K_1)(1 + K_2\,[AMP]}}$$

$$= \frac{\mathrm{KK_1K_2[AMP][DPC][Co(III)]}}{\mathrm{[OH^-]+K_1+K_2[OH^-][AMP]+K_1K_2[AMP]}}$$

$$\frac{\text{rate}}{\mathrm{[DPC]}} = \mathrm{k_{obs}} = \frac{\mathrm{KK_1K_2[AMP][Co(III)]}}{\mathrm{[OH^-]+K_1+K_2[OH^-][AMP]+K_1K_2[AMP]}} \ldots\ldots\ldots \text{(A-6)}$$

After rearrangement, we get

$$\frac{\mathrm{[Co(III)}}{\mathrm{k_{obs}}} = \frac{\mathrm{[OH^-]}}{\mathrm{kK_1K_2[AMP]}} + \frac{1}{\mathrm{kK_2[AMP]}} + \frac{\mathrm{[OH^-]}}{\mathrm{kK_2}} + \frac{1}{\mathrm{k}} \ldots\ldots\ldots\ldots \text{(A-7)}$$

4) Rate constant derivation for the oxidation of amoxicillin

$$\text{rate} = -\mathrm{d}\frac{\mathrm{[AMX]}}{\mathrm{dt}} = \mathrm{k(Complex)}$$

$$= \mathrm{kK_1K_2K_3}\frac{\mathrm{[AMX][OH^-][Co(III)][DPC]}}{\mathrm{[H_3IO_6]^{2-}}} \ldots\ldots\ldots\ldots\ldots\ldots\ldots (1)$$

The total concentration of DPC (III) can be given as

$$[\mathrm{DPC}]_\mathrm{T} = [\mathrm{DPC}]_\mathrm{f} + [\mathrm{Cu(H_2IO_6)(H_3IO_6)}]^{2-} + [\mathrm{Cu(H_3IO_6)_2(H_2O)_2}]^{2-}$$

$$= [\mathrm{DPC}]_\mathrm{f}\,[\frac{\mathrm{K_1K_2[OH^-]+[H_3IO_6]^{2-}+K_1[OH^-]\,[H_3IO_6]^{2-}}}{\mathrm{[H_3IO_6]^{2-}}}]$$

$$[\mathrm{DPC}]_\mathrm{f} = [\frac{\mathrm{[DPC]_T[H_3IO_6]^{2-}}}{\mathrm{K_1K_2[OH]^-+[H_3IO_6]^{2-}+K_1[OH^-]\,[H_3IO_6]^{2-}}}] \ldots\ldots\ldots (2)$$

$$\text{Similarly,} \quad [\mathrm{AMX}]_\mathrm{T} = [\mathrm{AMX}]_\mathrm{f} + [\mathrm{C}]$$

$$= [\mathrm{AMX}]_\mathrm{f} + \mathrm{K_3}[\mathrm{AMX}]_\mathrm{f}\,[\mathrm{Co(III)}]$$

$$= [\mathrm{AMX}]_\mathrm{f}\,[1 + \mathrm{K_3}[\mathrm{Co(III)}]$$

Where (T and f) represent total and free concentration respectively.

In case of very low concentration of AMX and $CoCl_3$

$$[AMX]_T = [AMX]_f \ , \ [OH^-]_T = [OH^-]_f \quad \ldots\ldots\ldots (3)$$

$$\text{And } [H_3IO_6^{2-}]_T = [H_3IO_6^{2-}]_f \ldots\ldots\ldots\ldots\ldots\ldots (4)$$

$$[Co(III)_T] = [[Co(III)_f] + [C]$$

$$= [Co]_f + K_3[AMX][Co(III)_f]$$

$$[Co(III)]_f = [\frac{[Co(III)_T]}{1 + K_3[AMX]}] \ldots\ldots\ldots\ldots\ldots (5)$$

Substituting values of eq^n (2),(3),(4) and (5) in (1), we get

$$\text{rate} = -\frac{d[DPC]}{dt}$$

$$= \frac{kK_1K_2K_3\ [AMX][Co(III][DPC][OH]}{K_1K_2[OH]^- + [H_3IO_6]^{2-} + K_1[OH]^-\ [H_3IO_6]^{2-} + K_1K_2K_3[AMP][OH]^-} \quad \ldots\ldots\ldots (6)$$

After rearrangement, we get

$$\frac{1}{k_{obs}} = \frac{[H_3IO_6]^{2-}}{kK_1K_2K_3[OH]^-[AMX]} + \frac{[H_3IO_6]^{2-}}{kK_2K_3[AMX]} + \frac{1}{kK_3[AMX]} + \frac{1}{k} \ldots\ldots\ldots\ldots (7)$$

5) Rate constant derivation for the oxidation of Dicloxacillin

$$\text{rate} = -d\frac{[DCLX]}{dt} = k(\text{Complex})$$

$$= kK_1K_2K_3\frac{[DCLX][OH^-][Co(III)][DPC]}{[H_3IO_6]^{2-}} \ldots\ldots\ldots\ldots\ldots\ldots (1)$$

The total concentration of DPC (III) can be given as

$$[DPC]_T = [DPC]_f + [Cu(H_2IO_6)(H_3IO_6)]^{2-} + [Cu(H_3IO_6)_2(H_2O)_2]^{2-}$$

$$= [DPC]_f\ [\frac{K_1K_2[OH^-] + [H_3IO_6]^{2-} + K_1[OH^-]\ [H_3IO_6]^{2-}}{[H_3IO_6]^{2-}}]$$

$$[DPC]_f = [\frac{[DPC]_T[H_3IO_6]^{2-}}{K_1K_2[OH]^- + [H_3IO_6]^{2-} + K_1[OH^-]\ [H_3IO_6]^{2-}}] \ldots\ldots\ldots (2)$$

$$\text{Similarly, } [DCLX]_T = [DCLX]_f + [C]$$

$$= [DCLX]_f + K_3[DCLX]_f[Co(III)]$$

$$= [DCLX]_f[1 + K_3[Co(III)]$$

Where (T and f) represent total and free concentration respectively.

In case of very low concentration of AMP and $CoCl_3$

$$[DCLX]_T = [DCLX]_f \ , \ [OH^-]_T = [OH^-]_f \quad \ldots\ldots\ldots (3)$$

$$\text{And } [H_3IO_6^{2-}]_T = [H_3IO_6^{2-}]_f \ldots\ldots\ldots\ldots\ldots\ldots (4)$$

$$[Co(III)_T] = [[Co(III)_f] + [C]$$

$$= [Co]_f + K_3[DCLX][Co(III)_f]$$

$$[Co(III)]_f = [\frac{[Co(III)_T]}{1 + K_3[DCLX]}] \ldots\ldots\ldots\ldots\ldots\ldots\ldots\ldots (5)$$

Substituting values of eq^n (2), (3), (4) and (5) in eq^n (1), we get

$$\text{rate} = -\frac{d[DPC]}{dt}$$

$$= \frac{kK_1K_2K_3\ [DCLX][Co(III][DPC][OH]}{K_1K_2[OH]^- + [H_3IO_6]^{2-} + K_1[OH]^-[H_3IO_6]^{2-} + K_1K_2K_3[DCLX][OH]^-} \ldots\ldots.. (6)$$

After rearrangement, we get

$$\frac{1}{k_{obs}} = \frac{[H_3IO_6]^{2-}}{kK_1K_2K_3[OH]^-[DCLX]} + \frac{[H_3IO_6]^{2-}}{kK_2K_3[DCLX]} + \frac{1}{kK_3[DCLX]} + \frac{1}{k} \ldots\ldots\ldots\ldots (7)$$

6) Rate constant derivation for the oxidation of Carbenicillin

$$\text{rate} = -d\frac{[CRBC]}{dt} = k(\text{Complex})$$

$$= kK_1K_2K_3\frac{[CRBC][OH^-][Co(III)][DPC]}{[H_3IO_6]^{2-}} \ldots\ldots\ldots\ldots\ldots\ldots\ldots (1)$$

The total concentration of DPC (III) can be given as

$$[DPC]_T = [DPC]_f + [Cu(H_2IO_6)(H_3IO_6)]^{2-} + [Cu(H_3IO_6)_2(H_2O)_2]^{2-}$$

$$=[DPC]_f [\frac{K_1K_2[OH^-] + [H_3IO_6]^{2-} + K_1[OH^-][H_3IO_6]^{2-}}{[H_3IO_6]^{2-}}]$$

$$[DPC]_f = [\frac{[DPC]_T[H_3IO_6]^{2-}}{K_1K_2[OH]^- + [H_3IO_6]^{2-} + K_1[OH^-][H_3IO_6]^{2-}}] \ldots\ldots\ldots (2)$$

Similarly, $[CRBC]_T = [CRBC]_f + [C]$

$$= [CRBC]_f + K_3[CRBC]_f[Co(III)]$$

$$= [CRBC]_f[1 + K_3[Co(III)]$$

Where (T and f) represent total and free concentration respectively.

In case of very low concentration of AMP and $CoCl_3$

$$[CRBC]_T = [CRBC]_f\ ,\ [OH^-]_T = [OH^-]_f \quad \ldots\ldots.. (3)$$

And $[H_3IO_6{}^{2-}]_T = [H_3IO_6{}^{2-}]_f \ldots\ldots\ldots\ldots\ldots (4)$

$$[Co(III)_T = [[Co(III)_f] + [C]$$

$$= [Co]_f + K_3[CRBC][Co(III)_f]$$

$$[Co(III)]_f = [\frac{[Co(III)_T]}{1 + K_3[CRBC]}] \ldots\ldots\ldots\ldots\ldots (5)$$

Substituting values of eq^{n} (2),(3),(4) and (5) in (1), we get

$$\text{rate} = -\frac{d[DPC]}{dt}$$

$$= \frac{kK_1K_2K_3\ [CRBC][Co(III][DPC][OH]}{K_1K_2[OH]^- + [H_3IO_6]^{2-} + K_1[OH]^-\ [H_3IO_6]^{2-} + K_1K_2K_3[CRBC][OH]^-} \quad \ldots\ldots\ldots (6)$$

After rearrangement, we get

$$\frac{1}{k_{obs}} = \frac{[H_3IO_6]^{2-}}{kK_1K_2K_3[OH]^-[CRBC]} + \frac{[H_3IO_6]^{2-}}{kK_2K_3[CRBC]} + \frac{1}{kK_3[CRBC]} + \frac{1}{k} \ldots\ldots\ldots\ldots (7)$$

7. Rate constant derivation for the oxidation of Oxacillin

$$\text{Rate} = -\frac{d[DPC]}{dt} = k[\text{Complex}] = k[C] \qquad \textbf{[A-1]}$$

The third equilibrium constant can be calculated using the law of mass action and is given by

$$K_3 = \frac{[C]}{[Cu(H_2IO_6)(H_2O)_2[OXC]}$$

Upon rearrangement,

$$[C] = K_3[Cu(H_2IO_6)(H_2O)_2][OXC] \qquad \textbf{[A-2]}$$

Replacing the value of C from eq$^{n.}$ [**A-2**]

$$\text{Rate} = -\frac{d[DPC]}{dt} = K_1K_3[Cu(H_2IO_6)(H_2O)_2[OXC] \qquad \textbf{[A-3]}$$

In the above equation, OXC represents oxacillin.

Second equilibrium constant can be calculated by

$$K_2 = \frac{[Cu(H_2IO_6)(H_2O)_2[H_3IO_6{}^{2-}]}{[Cu(H_2IO_6)(H_3IO_6]^{2-}}$$

This can be rearranged into:-

$$[Cu(H_2IO_6)(H_2O)_2] = \frac{K_2\ [Cu(H_2IO_6)(H_3IO_6]^{2-}}{[H_3IO_6]^{2-}} \qquad \textbf{[A-4]}$$

The first equilibrium constant can be represented by

$$K_1 = \frac{[Cu(H_2IO_6)(H_3IO_6]^{2-}}{[Cu(H_3IO_6)_2]^-[OH^-]}$$

This can be rearranged into

$$[Cu(H_2IO_6)(H_3IO_6]^{2-} = K_1\ [Cu(H_3IO_6)_2]^-[OH^- \qquad \textbf{[A-5]}$$

Substituting eq$^{n.}$ [**A-4**] to [**A-5**] in eq$^{n.}$ [**A-3**], we get

$$\text{Rate} = -\frac{d[DPC]}{dt} = \frac{kK_1K_2K_3[OXC]_f[DPC]_f[OH^-]_f}{[H_3IO_6)_2]^-} \quad \textbf{[A-6]}$$

The total concentration of [DPC] can be given as

$$[DPC]_T = [DPC]_f + [Cu(H_2IO_6)(H_3IO_6]^{2-} + [Cu(H_2IO_6)(H_2O)_2] + [C] \quad \textbf{[A-7]}$$

Where T and f denote total and free concentrations

$$= [DPC]_f + K_1[Cu(H_2IO_6)_2]^-[OH^-] + \frac{K_1K_2[Cu(H_2IO_6)_2]^-[OH^-]}{[H_3IO_6{}^{2-}]} + \frac{K_1K_2K_3[Cu(H_3IO_6)_2]^-[OH^-][OXC]}{[H_3IO_6]^{2-}}$$

$$[DPC]_T = [DPC]_f + K_1[DPC]_f[OH^-] + \frac{K_1K_2[DPC]_f[OH^-]}{[H_3IO_6{}^{2-}]} + \frac{K_1K_2K_3[DPC]_f[OH^-][OXC]}{[H_3IO_6{}^{2-}]}$$

$$[DPC]_f = \frac{[DPC]_T[H_3IO_6{}^{2-}]}{[H_3IO_6{}^{2-}] + K_1[OH^-][H_3IO_6{}^{2-}] + K_1K_2[OH^-] + K_1K_2K_3[OH^-][OXC]} \quad \textbf{[A-8]}$$

The total concentration of [OH^-] can be given by

$$[OH^-]_T = [OH^-]_f + [Cu(H_2IO_6)(H_3IO_6]^{2-} + [Cu(H_2IO_6)(H_2O)_2] + [C]$$

$$[OH^-]_T = [OH^-]_f + K_1[DPC][OH^-]_f + \frac{K_1K_2[DPC][OH^-]_f}{[H_3IO_6]^{2-}} + \frac{K_1K_2K_3[DPC][OH^-]_f[OXC]}{[H_3IO_6]^{2-}}$$

$$[OH^-]_T = [OH^-]_f\{1 + K_1[DPC] + \frac{K_1K_2[DPC]}{[H_3IO_6]^{2-}} + \frac{K_1K_2K_3[DPC][OXC]}{[H_3IO_6]^{2-}}\}$$

Because DPC (III) and $H_3IO_6^{-2}$ were used in such small amounts, these terms can be neglected.

$$[OH^-]_T = [OH^-]_f \quad \textbf{[A-9]}$$

Similarly, in case of low concentrations of DPC (III) and $H_3IO_6^{2-}$ used

$$[OXC]_T = [OXC]_f \quad \textbf{[A-10]}$$

Substituting the value of $[DPC]_f$ from eq$^{n.}$ [**A-8**], $[OH^-]_f$ from eq$^{n.}$ [**A-9**] and $[OXC]_f$ from eq$^{n.}$ [**A-10**] in eq$^{n.}$ [**A-6**] after omitting subscripts T and f ,we get,

$$\text{Rate} = -\frac{d[DPC]}{dt} = \frac{kK_1K_2K_3[OXC][DPC][OH^-]}{[H_3IO_6{}^{2-}] + K_1[OH^-][H_3IO_6{}^{2-}] + K_1K_2[OH^-] + K_1K_2K_3[OH^-][OXC]}$$

$$\text{Or, } \frac{1}{k_{obs}} = \frac{[H_3IO_6{}^{2-}]}{kK_1K_2K_3[OXC][OH^-]} + \frac{[H_3IO_6{}^{2-}]}{k\,K_2K_3[OXC]} + \frac{1}{kK_3[OXC]} + \frac{1}{k} \quad \textbf{[A-11]}$$

List of Research Publications

1. **Sahu, Y. R.,** Chaudhary N. K., & Bhattarai, A. (2024). Kinetic Perspectives for Degradation of Oxacillin: A Penicillanic Acid Derivative. *Edelweiss Applied Science and Technology (The Learning Gate), 8(3):102-124. https://doi.org* /10.55214/25768484.v4i3

2. **Sahu, Y. R.,** Dev, R. K., Chaudhary N. K., & Bhattarai, A (2023). Kinetics of Catalytic Oxidation of Carbenicillin: A Degradation Approach for Penicillanic Acid Derivatives (PADs). *Journal of Nepal Chemical Society,* 43(2):159-170. https://doi.org/10.3126/jncsv43i2.53814

3. **Sahu, Y. R.**, & Mishra Parashuram (2020). Kinetics and mechanism of oxidation of Carbenicillin by Copper (III) Periodate Complex in Aqueous alkaline medium. *Hindawi- Journal of Chemistry,* Volume 2020, Article ID 4060984, 13 pages. https://doi.org/10.1155/2020/4060984

4. **Sahu, Y. R**., Mishra, P., & Chaudhary, N. K. (2020). Kinetics and Mechanism of

   Oxidation of Dicloxacillin by Copper (III) Diperiodate Complex in Aqueous Alkaline Medium. *Journal of Chemical Science and Engineering,* 3(2): 163-168, ISSN: 2642-0406

List of Conferences and Workshops Attended

Scientific Research Article: Oral Presentation

2024, September 2-7, 18th International Congress on *Thermal Analysis and Calorimetry (ICTAC 2024)* in "Kinetics and Mechanism for Catalyzed Oxidation of Oxacillin", Organized by Indian Institute of Technology (IIT), Madras, India.

2024, Baisakh 25-26, Regional Conference on *Science and Tech (RCST 2024)* in "Kinetics and mechanism for catalyzed oxidation of oxacillin: a penicillanic acid derivative", Organized by Central Campus of Technology (CCT), Dharan in association with Institute of Science and Technology (IoST), Kathmandu, Nepal.

2019, January 3rd, International Seminar on *Recent Trends in Chemistry (RTC_2019)* in "Kinetics and mechanism of oxidation of ampicillin by diperiodatocuprate and cobalt chloride (III) in the alkaline medium", Organized by Department of Chemistry, P. D. Women's College, Jalpaiguri, in association with Indian Chemical Society, Kolkata, India.

2019, February 20-23, 7th International Symposium on *Current Trends in Drug Discovery Research* in "Kinetics and mechanism of oxidation of amoxicillin by cobalt (III) chloride catalyst in the presence of diperiodatocuprate (III) in the aqueous alkaline medium", Organized by CSIR-CDRI, Lucknow, India.

2018, November 16-18, 23rd International Conference of International Academy of Physical Sciences (CONIPAS XXIII) on *Advances in Physical Sciences to Achieve Sustainable Development Goals* in " Kinetics and mechanism of oxidation of ampicillin by cobalt (III) chloride catalyst in the presence of diperiodatocuprate (III) in the aqueous alkaline medium", Organized by NAST, CONIPAS XXIII Kathmandu, Nepal.

Workshop /Training

2022, August 2, Carbon Dots (CDs): An amazing multi functional nano particle, organized by Department of Chemistry, Mahendra Morang Adarsh Multiple Campus, Biratnagar, TU and Nepal Chemical Society, Biratnagar, Koshi Province, Nepal

2019, March 29-30, **2 Days Workshop** on "Research Writing and Publishing", organized by Nepal Physical Society in association with MMAMC, Biratnagar and HISSAN Morang, Biratnagar, Nepal

2019, April 2-4, **3 Days Workshop** on "Tools and Techniques in Chemistry", organized by Nepal Chemical Society & Central Department of Chemistry, Kirtipur, Kathmandu, Nepal

2018, February 7-9, **3 Days Workshop** on "Diffraction Techniques: X-Ray and Electron Diffraction", organized by Sophisticated Test and Instrumentation Centre (STIC) and Kerala State Council for Science Technology and Environment (HSCSTE), Cochin University Campus, Kochi, Kerala, India

Scientific Research Article: Poster Presentation

2023, May 25-27, International Chemical Congress (*Chemistry for Sustainable Development*- ICC-2023), in "Kinetics of Catalytic Oxidation of **Carbenicillin**: A Degradation Approach for Penicillanic Acid Derivatives (PADs)", organized by Nepal Chemical Society In association with Central Department of Chemistry, TU, Nepal & School of Materials Science and Engineering, Liaocheng University, China.

2019, March 1-2, National Youth Council in Provincial Youth Symposium on Science and Technology, , in "Kinetics and mechanism of oxidation of **ampicillin** by cobalt (III) chloride catalyst in the presence of diperiodatocuprate (III)) in an

aqueous alkaline medium", Biratnagar, Morang, organized by National Youth Council, Sanothimi, Bhaktapur at Province No. 1, Biratnagar, Nepal.

2018, March 8-10, International Chemical Congress (*Chemistry for Sustainable Development)* in "Kinetics and mechanism of oxidation of **amoxicillin** by cobalt (III) chloride catalyst in the presence of diperiodatocuprate (III)) in an aqueous alkaline medium", organized by Nepal Chemical Society and Birendra Multiple Campus, Chitwan, Nepal.

Participation

2018, 27th August 2018, participated in International Seminar in "Frontiers in Chemistry, 2018", organized by Department of Chemistry, University of North Bengal and CSIR-North Bengal Local Chapter, Siliguri, India.

2013, March 4-6, participated in International Conference on Emerging Trends in Research and Development organized by Nepal Chemical Society, Biratnagar.

2012, December 28-29, participated in seminar on Modern Trends in Science and Technology organized by Nepal Chemical Society, Eastern Chapter, Biratnagar, Nepal.

2011, March 24-26, participated in International Conference on Research Design, organized by Nepal Chemical Society, Man Mohan Polytechnic, Budhiganga, Morang.

2010, May 14-15, participated in "Eastern Regional Chemical Symposium", organized by Nepal Physical Society, Biratnagar, Nepal.

2010, August 30-31, participated in "Regional Seminar", organized by Nepal Physical Society, Biratnagar, Nepal.

Edelweiss Applied Science and Technology
ISSN: 2576-8484
Vol. 8, No. 3, 102-124
2024
Publisher: Learning Gate
DOI: 10.55214/25768484.v8i3.1095

Kinetic perspectives for the degradation of oxacillin: A penicillanic acid derivative

Yuv Raj Sahu[1], Narendra Kumar Chaudhary[1], Ajaya Bhattarai[1*]
[1]Department of Chemistry, Mahendra Morang Adarsh Multiple Campus, Biratnagar, Tribhuvan University, Nepal; sahuyuvraj09@gmail.com (Y.R.S.), chem_narendra@yahoo.com (N.K.C.), ajaya.bhattarai@mmamc.tu.edu.np (A.B.).

Abstract: Oxidation of oxacillin, a penicillanic acid derivative, has been predicted by monoperiodatocuprate [MPC (III)] at 25°C with 0.10 mol dm^{-3} ionic strength, in an aqueous alkaline medium by UV/Visible spectrophotometric analysis, for which 1:4 stoichiometry of oxacillin: MPC (III) is visible. The appearance of a sharp peak by the spectrophotometer confirmed the formation of the complex. The reaction products have been recognized using spectral reports from the FT-IR, LC-MS, melting point, and other spot tests. A pseudo-first-order reaction has been confirmed for the oxidant, fractional order for the substrate, and alkali, even though periodate claimed a delaying effect due to the accumulation of periodate ions from both potassium periodate and monoperiodatocuprate as a common ion effect. The primary active species in the alkaline medium [Cu(H2IO6)(H2O)2] was discovered to be monoperiodatocuprate [MPC (III)]. To figure out the activation and thermodynamic parameters, it is helpful to know the uncatalyzed rate constants, the slow step rate constants, and the equilibrium constants. We have evaluated the dependence of reaction rates on different temperatures. We have calculated rate constants using absorbance data collected from the UV/visible spectrophotometer. We have thoroughly examined the potential rate constant derivation and a plausible mechanism that could explain the experimental findings.

Keywords: *Equilibrium constant, Kinetics, Mechanism, Monoperiodatocuprate (III), Oxacillin, Oxidation.*

1. Introduction

β-lactam antibiotics, which are penicillanic acid derivatives (PADs), have been used by humans since the beginning of time to treat bacterial infections. They are widely used in medicine, animal husbandry, nutraceutical products, agriculture, and cosmetics to stop the activity and growth of microbial communities to make our lives better and avoid risks [1]. As a result of these PADs being spread out, excreted, or building up in waste water, sewage plants, hospitals, and industrial effluents, microbes have been developing ways to fight them [2]. Critical evaluation of pharmaceuticals concludes that a majority of PADs are excreted in our urine (55–80%) and feces (4.30%), either alone or in combination with other chemicals that render them inactive [3]. The environmental microbiota of the riverine ecosystem carries out numerous crucial biogeochemical processes, including nutrient cycling and pollutant degradation [4, 5]. Emerging contaminants, or pollutants, are micro-biological pollutants that have the potential to harm humans, flora, and fauna [6]. These contaminants can be harmful to aquatic ecosystems, cause severe infections in people and livestock, and pose a terrible potential threat if misused, overused, transmitted, or dispersed into the environment. Globally deteriorating water quality has overtaken public concern, ecological biodiversity, and even social stability as critical environmental concerns [7]. Prolonged antibiotic exposure can also cause the transfer, proliferation, and diffusion of microbial antibiotic resistance genes (ARGs), as well as the development of "super-resistant bacteria" in the environment or the human body [8]. There are several advanced oxidation processes (AOPs) available, including photo-

History: Received: 3 January 2024; Revised: 8 March 2024; Accepted: 15 March 2024; Published: 19 March 2024
* Correspondence: ajaya.bhattarai@mmamc.tu.edu.np

Fenton, stopped-flow, voltammetric oxidation, UV/H2O2, ozonation, and UV/visible spectrophotometry. Researchers continue to investigate the degradation of these PADs in wastewater, organic pollutants, and pharmaceutical waste treatment [9]. On a global scale, organic contaminants are emerging in karst groundwater [10, 11]. Environmental pollution evaluates the occurrence of trace-level antibiotics and personal care products (PPCPs) in Chinese rivers [12, 13]. Similarly, researchers report on the distribution of antibiotic resistance genes in the environment [14] and the processes for removing antibiotics from water and wastewater to safeguard the aquatic environment [15]. We discuss in detail the removal of antibiotics from wastewater and its effects on microbial communities [16]. Water matrix elements, process enhancements, and application influence the removal of antibiotic pollution from wastewater using cutting-edge UV oxidation techniques [17]. Wastewater treatment plant effluent removes pharmaceuticals and antibiotic resistance genes (ARGs), degrades particularly vulnerable free-floating ARGs [18], and facilitates the evolution of antibiotic-resistant bacteria and genes during advanced wastewater treatment and disinfection [19]. Ozone-activated carbon filtering eliminates antibiotic resistance from municipal secondary effluents [19]. Researchers have already examined the impact of water matrix components on the UV/Chlorine process and its response mechanism [20]

Reconstituted penicillins break down in an acidic solution at an elevated temperature to produce penicillanic acid and its derivatives (PADs). Oxacillin, one of the PADs, is a parenteral, 2nd generation semi-synthetic penicillinase-resistant narrow-spectrum penicillin in which the 6-aminopenicillanic acid nucleus consists of a five-membered thiazolidine ring attached to a four-membered beta-lactam ring that responds to antibacterial activities. Oxacillin is a methicillin derivative that has a 5-methyl-3-phenylisoxazole-4-carboxamide group at position 6 β-carbon. It helps fight infections caused by Staphylococcus aureus, which is resistant to penicillin [22]. It is soluble in water (88 mg/ml), ethanol, and dimethylsulfoxide DMSO (< 1 mg/ml) at 298 K. Its formula, molar mass, density, and boiling point are $C_{19}H_{19}N_3O_5S$, 401.44 g mol^{-1}, 1.49 g cm^{-3}, and 1177.75 K, respectively. Figure 1 outlines the structure of oxacillin.

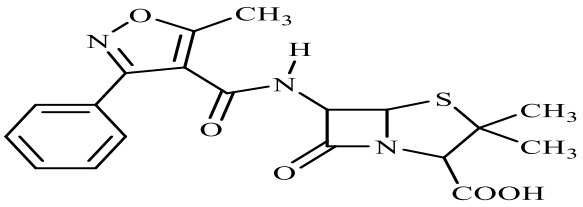

Figure 1.
Displays the structure of oxacillin.

Several polydentate ligands, like ditelluratocuprate-III [23, 24] and hexacyanoferrate-III [25], diperiodatocuprate-III [26, 27], diperiodatonickelate-IV [28], and diperiodatoargentate-III [29, 30], can act as strong oxidizing agents to degrade such PADs in the aqueous form. The transition metals of such ligands are capable of forming stable complexes. The properties of DPC (III) were found by studying the kinetics and mechanisms behind the alkaline oxidation of the iodide ion [31]. In aqueous micellar media, alkaline Copper (III) periodate complex synthesis and an analysis of its redox properties have been studied [32]. The geometry of DPC (III) is square planar, and it exhibits a diamagnetic nature and dsp^2 hybridization [32, 33]. Cu (III) performs as an active intermediate species between Cu (III)/Cu (II) couple of several electron transfer reactions [34, 35]. Researchers have studied Cobalt (III) complexes as antiviral and antibacterial agents [36].

We evaluated the degradation of oxacillin in water by anodic oxidation with Ti/IrO2 anodes [37]. Ionizing radiation was used to eliminate oxacillin from water, its antibacterial activity, and its toxicity [37]; polyaniline, gold nanourchins, and graphene oxide were molecularly imprinted on screen-printed electrodes to detect oxacillin by voltammetry [38] and heavy metals, their transport, and fate in water, sediment, and some biota were assessed [39]. Likewise, photo-Fenton, electrochemical, and TiO2-

Edelweiss Applied Science and Technology
ISSN: 2576-8484
Vol. 8, No. 3: 102-124, 2024
DOI: 10.55214/25768484.v8i3.1095

photocatalysis have been compared for treating oxacillin in water to remove antibiotic activity [40]. Loading penicillin and oxacillin on PEGylated graphene oxide increases the antibiotics' ability to combat methicillin-resistant staphylococcus aureus [41]. Permanganate ion oxidative degradation of some antibiotics in alkaline medium: kinetics and mechanistic [41, 42] and adsorption on water treatment remnants for removing amoxicillin, a member of PADs, from water [43] are discussed.

1.1. Significance of the Research

The diperiodatocupratic (III) oxidation method, which uses this degradation technique, gives the present research significant importance. Hence, the proposed study aims to disclose a novel application in the context of the degradation of non-biodegradable PADs or antibiotics in the aqueous alkaline medium, which may be fruitful in the direction of selecting the best and most rapid ways to reduce pollution and illness problems along with the proper diagnosis of bacterial microorganisms and deactivate their growing potential in the future for the coming generation.

1.2. Objectives of the Research

The purpose of this research is to create a degradation method followed by a UV/Visible spectrophotometry technology and to investigate a plausible mechanism that accounts for activation, thermodynamic characteristics, various rate constants, and the order of the oxidation reaction by examining the kinetics for oxidation of oxacillin by DPC (III) through LC-MS, FT-IR, melting point, and other spot tests through the proper structural and spectral analysis of these complexes and stable products.

2. Materials and Methods

2.1. Materials

Potassium hydroxide (KOH), sodium thiosulphate ($Na_2S_2O_3$), potassium persulphate ($K_2S_2O_8$), and potassium iodide (KI) were procured from EMPLURA^R (Merck Life Science, Pvt. Ltd., India). Similarly, potassium nitrate and copper (II) sulphate were procured from LOBA CHEMIE Pvt. Ltd., India, while oxacillin, potassium periodates, and cobalt (III) chloride (hexa-hydrated) were managed by Sigma Aldrich (New Zealand). We used only triple-distilled water throughout the entire research process.

2.2. Instruments

ELICO LI613 pH meter (India) was available for pH measurement. Absorbance readings were noted from the Microprocessor, UV-VIS spectrophotometer with double beam (Model No. 290, Serial No. 1713-2014-03-162, Labtronics, India) with a range of 200-1000 nm. Thermo Nicolet's Avatar 370 FT-IR spectrometer, SHIMADZU Corporation, United States of America, which operates as a KBr disc and has an m/z range of 4000-400 cm^{-1}, was used to record the FT-IR spectra of the complexes and their products. LC-MS of the complex and products was captured within the 0–1000 m/z range by using UPLC-TQD Mass Spectrometer (India) in the positive mode.

2.3. Synthesis of the Reagent (Oxidant)

DPC (III) was synthesized by mixing 3.54 g of $CuSO_4$, 6.8 g of KIO_4, 2.20 g of $K_2S_2O_8$, and 9.0 g of KOH in a 250 ml round-bottomed (RB) flask [44, 45]. After shaking the mixture frequently, a metal stirrer was used to heat it for nearly 2 hours until the mixture turned intense red followed by possibly removal of extra potassium persulphate. After cooling the dark reddish-brown solution, we used a sintered glass crucible G-4 to filter it and dilute it to 250 ml. DPC (III) was standardized using the thiocyanate method [46] and its concentration was determined. The emergence of an absorption band with its maximum peak at 415 nm confirmed the existence of DPC (III). Possible figures of Diperiodatocuprate or DPC (III), and Monoperiodatocuperate or MPC (III), are depicted in Figure 2.

Edelweiss Applied Science and Technology
ISSN: 2576-8484
Vol. 8, No. 3: 102-124, 2024
DOI: 10.55214/25768484.v8i3.1095

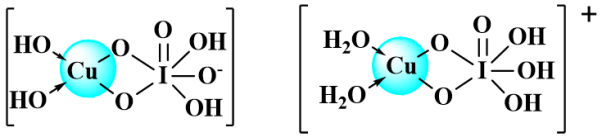

$[Cu(H_2IO_6)(OH)_2]$
Monoperiodatocuprate
MPC (III)

$[Cu(H_3IO_6)(H_2O)_2]$
Monoperiodatocuprate
MPC (III)

Figure 2.
Displays the possible MPC (III) structures.

2.4. Synthesis of the Oxacillin- MPC (III) Complex

The research work was initiated in the UV/Visible spectrophotometer with a double-beam facility. A 100 ml RB flask was filled with 10 ml of standard oxacillin solution (0.132 mol dm^{-3}) to conduct the experiment. To this end, standard solutions of 1.0 ml of each KIO_4, KNO_3, and 2.0 ml of KOH were added in a 1:4 stoichiometric ratio and stirred for 24 hours on a hot plate before continuing to stir during refluxing with condensation. After cooling naturally for three days, we filtered the mixture through Whatman No. 1. While this was going on, $CuSO_4$, the first product added, didn't exhibit any significant interference. Finally, we mixed acrylonitrile in the reaction mixture in the inert atmosphere; the absence of precipitate upon dilution with ethyl alcohol confirmed the absence of any free interfering radical.

2.5. Kinetic Proceedings

After 20 minutes of warming up for calibration, the standardized DPC (III) solution was mixed into a quartz cuvette inside the double-beam UV/Visible Spectrophotometer to start the reaction. It was then poured into a fixed volume of oxacillin, which had predetermined standard solutions of KIO_4, KOH, and KNO_3 to complete the reaction. A UV-Visible spectrophotometer was used to collect data at a wavelength of 415 nm while maintaining a pH of 9.0–9.2 and following the pseudo-first-order suppression order of absorbance at (293.15, 298.15, 303.15, and 308.15) ± 0.2 K, unless otherwise specified. The regression coefficient (r) and standard deviation (s) of the experimental data were calculated using Origin 9.6 (2017) software. Uncatalyzed rate constants (k_u) were calculated from slopes after log (abs) versus time plots showed a straight line. Finally, assuming the quantity present in DPC (III) and adding additional amounts allowed us to determine the total concentration of KIO_4 and KOH. The reaction composition Table (Table 1) presented herewith shows the effect of changing [DPC (III)], [OXC], [KIO_4], and [KOH] to oxidize oxacillin by DPC (III) in the alkaline medium at a temperature of 298 K and 0.10 mol dm^{-3} ionic strength.

Table 1.
Displays the reaction composition table.

(Effect of changing [KIO_4], [DPC (III)]*, [KOH] and [OXC] to oxidize oxacillin)					
[DPC]x 10^5 M	[OXC]x 10^4 M	[KOH]x10^2 M	[KIO_4]x10^5 M	k_ux10^{-4}(s^{-1})	Order
1.0	5.0	0.12	1.0	2.41	~1
3.0	5.0	0.12	1.0	2.41	
5.0	5.0	0.12	1.0	2.23	
8.0	5.0	0.12	1.0	2.21	
10.0	5.0	0.12	1.0	2.35	
5.0	1.0	0.12	1.0	0.81	0.706
5.0	3.0	0.12	1.0	1.14	
5.0	5.0	0.12	1.0	2.23	
5.0	8.0	0.12	1.0	3.48	
5.0	10.0	0.12	1.0	4.15	
5.0	5.0	0.04	1.0	1.02	0.562
5.0	5.0	0.08	1.0	1.35	
5.0	5.0	0.12	1.0	2.01	

Edelweiss Applied Science and Technology
ISSN: 2576-8484
Vol. 8, No. 3: 102-124, 2024
DOI: 10.55214/25768484.v8i3.1095

(Effect of changing [KIO_4], [DPC (III)]*, [KOH] and [OXC] to oxidize oxacillin)					
[DPC]x 10^5 M	[OXC]x 10^4 M	[KOH]x10^2 M	[KIO_4]x10^5 M	k_u x10^{-4} (s^{-1})	Order
5.0	5.0	0.16	1.0	2.23	
5.0	5.0	0.20	1.0	2.35	
5.0	5.0	0.12	1.0	2.23	
5.0	5.0	0.12	3.0	1.84	-0.265
5.0	5.0	0.12	5.0	1.58	
5.0	5.0	0.12	8.0	1.42	
5.0	5.0	0.12	10.0	1.29	

Note: *Concentration (Mol dm^{-3}) in the bold figure indicates its variation mode.

Scheme 1 illustrates the reaction of oxacillin and diperiodatocuprate (III) in an alkaline medium as follows:

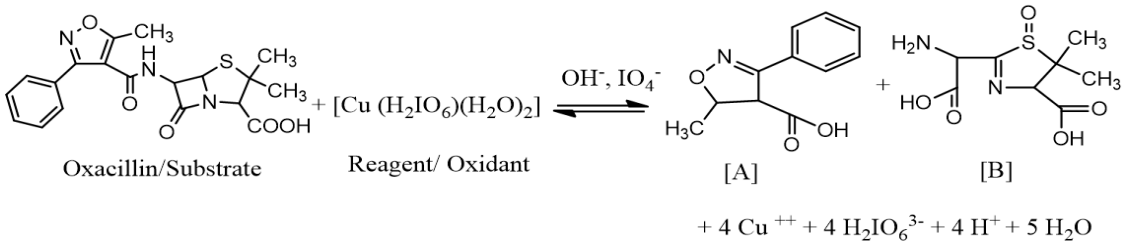

Scheme 1.
'A' represents 5-methly-3-phenyl-4,5-dihydroisoxazole-4-carboxyclic acid and 'B' represents 2- (Amino (Carbo) methyl-(5,5)-dimethyl-(4,5)-dihydrothiazole-4-carboxylic acid-1-oxide.

3. Results and Discussion

3.1. Verification of Beer-Lambert's Law

The complex was cleaned up and re-crystallized in ethanol until only crystals remained after the complete evaporation of the solvent. We observed the maximum absorption peak of the oxidant DPC (III) at 415 nm. Table 2 and Figure 3 represent the absorbance plot against [DPC (III)] to confirm Beer-Lambert's law verification. Similarly, the results from Table 3 indicate a decreasing order of absorbance data collected from the UV/visible spectrophotometer.

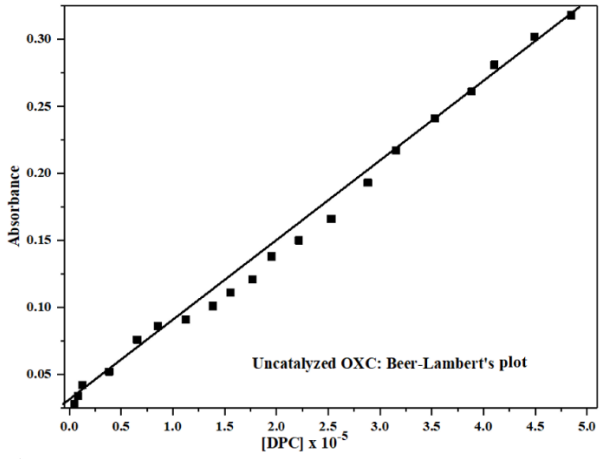

Figure 3.
Displays values for the absorbance vs. [DPC (III)] plot.

Edelweiss Applied Science and Technology
ISSN: 2576-8484
Vol. 8, No. 3: 102-124, 2024
DOI: 10.55214/25768484.v8i3.1095

Table 2.
Displays data for the plot of [DPC (III)] vs. absorbance from UV/Visible spectrophotometer.

Time in min	Absorbance at 415 nm	[DPC] x 10^{-5} M
0.0	0.318	4.845
0.2	0.302	4.491
0.4	0.281	4.104
0.6	0.261	3.885
0.8	0.241	3.527
1.0	0.217	3.154
1.2	0.193	2.883
1.4	0.166	2.528
1.6	0.15	2.215
1.8	0.138	1.952
2.0	0.121	1.768
2.2	0.111	1.556
2.4	0.101	1.385
2.6	0.091	1.125
2.8	0.086	0.856
3.0	0.076	0.654
3.2	0.052	0.385
3.4	0.042	0.125
3.6	0.034	0.085
3.8	0.028	0.049

3.2. Reaction Order

Fresh DPC (III) was diluted between (1.0 x 10^{-5} - 1.0 x 10^{-4}) mol dm^{-3}. A plot of time in minutes against log (Absorbance) was linear and nearly parallel, indicating a unit order reaction in DPC (III). Figure 4 and Table 3 confirmed a pseudo-first-order reaction in DPC (III).

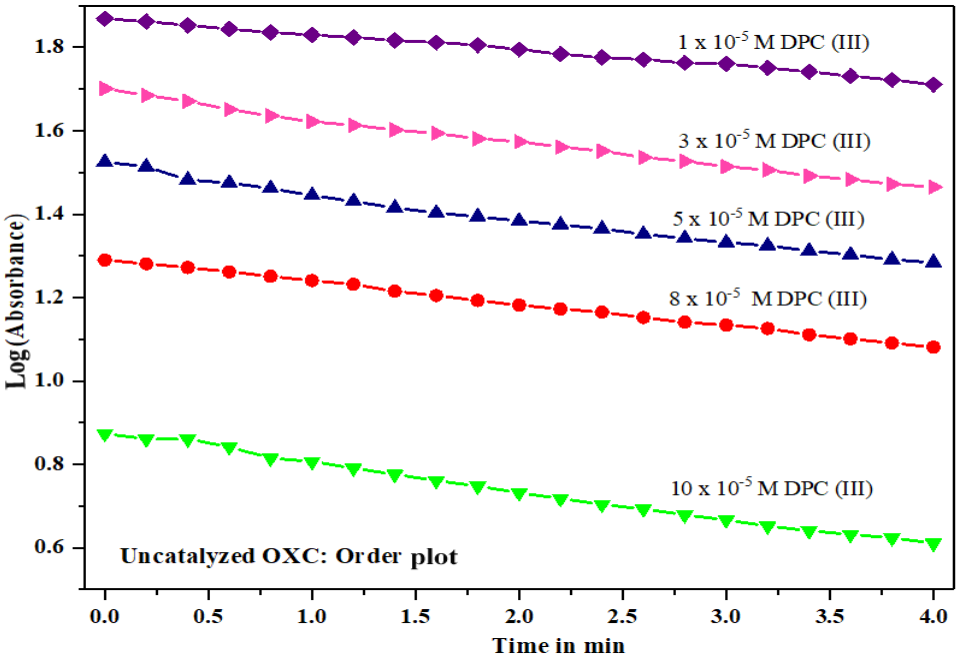

Figure 4.
Displays data for the log (Absorbance) vs. time plot.
Note: Green, red, blue, pink, and purple lines indicate corresponding concentrations of DPC (III) respectively.

Edelweiss Applied Science and Technology
ISSN: 2576-8484
Vol. 8, No. 3: 102-124, 2024
DOI: 10.55214/25768484.v8i3.1095

Table 3.
Displays data for order plot for oxidation of PADs (oxacillin) by DPC (III).

Abs→ Time↓Min	For 1 x 10^{-5} M DPC (III)	For 3 x10^{-5} M DPC (III)	For 5 x 10^{-5} M DPC (III)	For 8 x 10^{-5} M DPC (III)	For 10x 10^{-5} M DPC (III)
0	0.874	1.29	1.525	1.701	1.869
0.2	0.861	1.281	1.514	1.685	1.862
0.4	0.861	1.272	1.482	1.671	1.853
0.6	0.842	1.262	1.475	1.651	1.844
0.8	0.815	1.251	1.462	1.636	1.836
1	0.807	1.241	1.445	1.622	1.83
1.2	0.791	1.232	1.431	1.613	1.824
1.4	0.776	1.215	1.415	1.602	1.817
1.6	0.761	1.205	1.403	1.594	1.812
1.8	0.748	1.193	1.394	1.581	1.806
2	0.732	1.182	1.384	1.574	1.795
2.2	0.718	1.173	1.375	1.561	1.784
2.4	0.704	1.165	1.365	1.552	1.776
2.6	0.693	1.152	1.352	1.536	1.771
2.8	0.679	1.141	1.342	1.527	1.763
3	0.667	1.134	1.332	1.514	1.761
3.2	0.652	1.126	1.325	1.506	1.751
3.4	0.641	1.111	1.312	1.492	1.742
3.6	0.632	1.101	1.303	1.483	1.731
3.8	0.624	1.091	1.291	1.472	1.722
4	0.611	1.081	1.284	1.465	1.711

3.3. Stoichiometric and Spectral Analysis

The accurate stoichiometry was confirmed to be 1:4 for OXC: DPC (III) by Job's method [47] after 2.5 hours of storing various batches of reaction mixtures with different DPC (III) to oxacillin ratios in the presence of consistent molarities of KOH and KNO_3 in a sealed vessel within N_2 atmosphere.

FT-IR and LC-MS spectra are represented in the Appendix as A1 and A2 respectively. Figure A1 declares an absorption peak at 3413.5 cm^{-1} (caused by the carboxylic OH group) [39] and 1276.7 cm^{-1} (caused by the carboxylic C=O group) as well as a peak at 3380.7 cm^{-1} (caused by the N-H stretching) [41] 1464.4 cm^{-1} and 1386.6 cm^{-1} (caused by the geminal CH_3 as well as due to stretching mode of (C-N) vibration band [48]1641.2 cm^{-1} (caused by the carboxylic/ketonic C=O group) [48, 49]. Similarly, the complex ($C_{19}H_{25}CuIN_3O_{13}S$) and products were both identified using LC-MS, represented in Figure A2, which produced the first product, $C_{11}H_{11}NO_3$, with a m/z of 204 (m+1) while the second product, $C_8H_{12}N_2O_5S$, showed m/z value at 246 (m+2) respectively.

3.4. Effect and Orders of Influencing Factors

Varying concentrations of DPC (III), OXC, and KIO_4 appear as the primary influencing factors, along with their significant effects in the confirmation of the order of reaction. Table 3 and Figure 4 indicate a pseudo-unimolecular reaction with an almost uniformly ordered reaction with respect to DPC (III), which was confirmed by the linearity and parallelism plots of log (absorbance) against time (in minutes). Similarly, the order of oxacillin was declared to be **0.687** ($r \geq 0.999$, $s \leq 0.000014$) after examining within the concentration of (0.0001-0.001) mol dm^{-3}; uncatalyzed rate constants (k_u) rose up with a rise in the active mass of DPC (III), as illustrated in Figure 5. After investigating the impact of alkali within a molarity range of (0.04 -0.2) mol dm^{-3}, the rate constant increased by raising the active mass of alkali (KOH), and the reaction order was ascertained to be **0.562** ($r \geq 0.994$, $s \leq 0.00115$), as confirmed by Figure 6. Meanwhile, the order of reaction for potassium periodate (KIO_4) was studied within its active mass between (0.00001- 0.0001) mol dm^{-3} which showed a reaction order of **-0.250** ($r \geq 0.998$, $s \leq 0.00012$) as presented in Figure 7.

Edelweiss Applied Science and Technology
ISSN: 2576-8484
Vol. 8, No. 3: 102-124, 2024
DOI: 10.55214/25768484.v8i3.1095

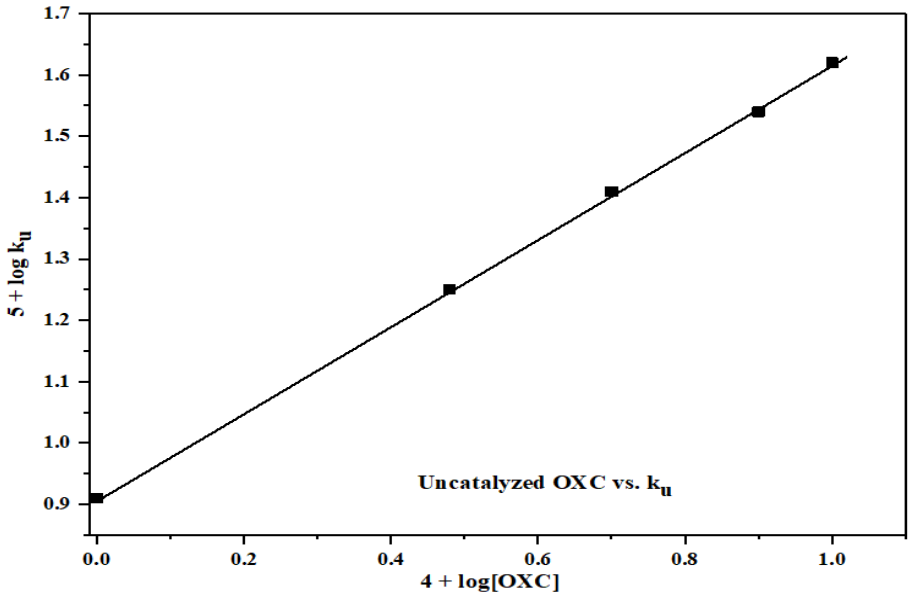

Figure 5.
Displays the plot of 4 + log [OXC] vs. (5+ log k_u).

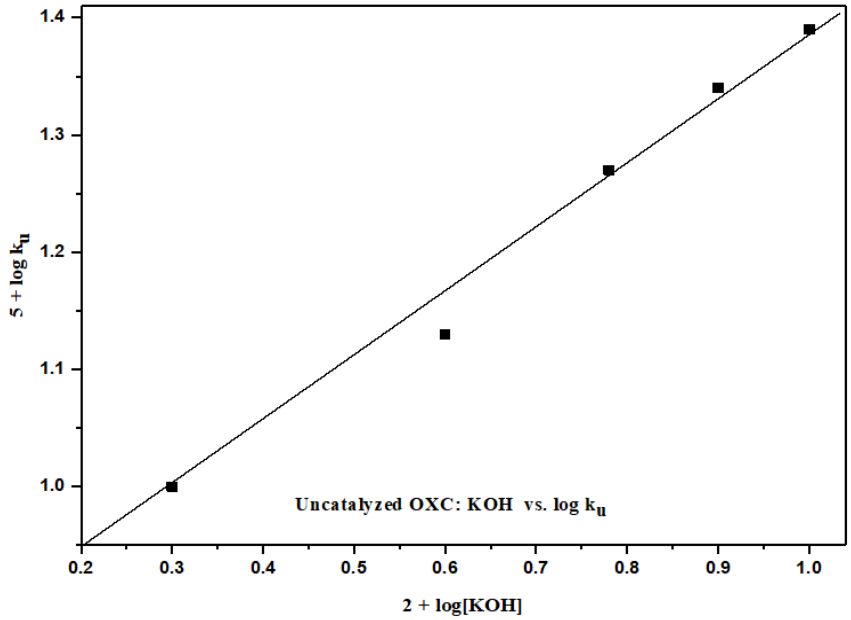

Figure 6.
Displays the plot of (5 + log k_u) vs. 2 + log [KOH].

Edelweiss Applied Science and Technology
ISSN: 2576-8484
Vol. 8, No. 3: 102-124, 2024
DOI: 10.55214/25768484.v8i3.1095

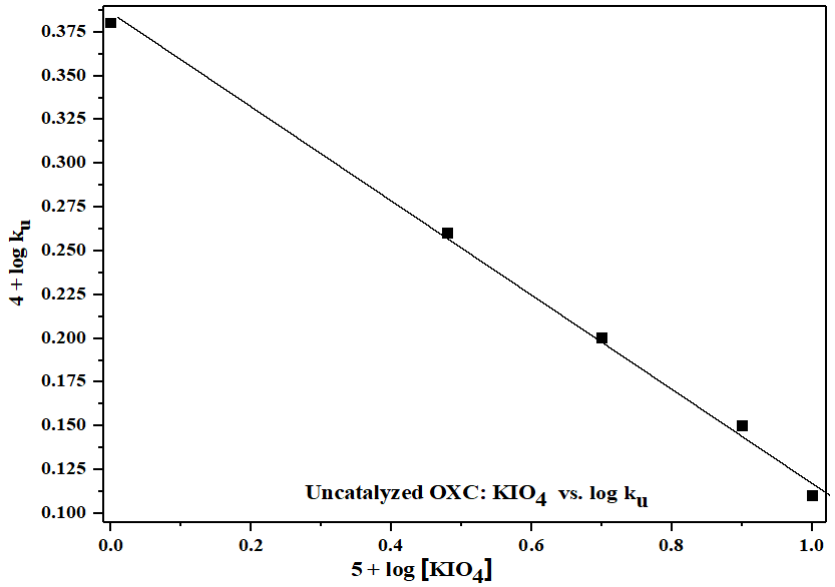

Figure 7.
Displays the plot of 5 + log [KIO_4] versus (4 + log k_u).

3.5. Effect of Temperature

Temperature exhibited a significant effect on the order of reaction. While keeping the concentrations of OXC, KIO_4, KOH, and DPC (III) constant and varying the other conditions, the effect of temperature on the rate of the oxidation reaction was examined at four different temperatures. The rise in temperature resulted in higher uncatalyzed rate constants in the case of the substrate (oxacillin), oxidizing reagent (DPC-III), and alkali. Only periodate exhibited the retarding effect. With the aid of the Origin 9.6 program, the activation energy and the least square method were used to calculate additional activation parameters. Conducting kinetics in a nitrogen gas atmosphere to examine the impact of periodates, ionic strength, dissolved oxygen, etc. did not reveal any appreciable changes. A plot of (log k_u vs. 1/T) is supported to compute activational parameters due to the uncatalyzed rate constant, represented in Figure 8 and Table 4. Similarly, another plot of the slow step rate constant (k) vs. reciprocal to temperature helped to determine these activation parameters, represented in Figure 9 and Table 5.

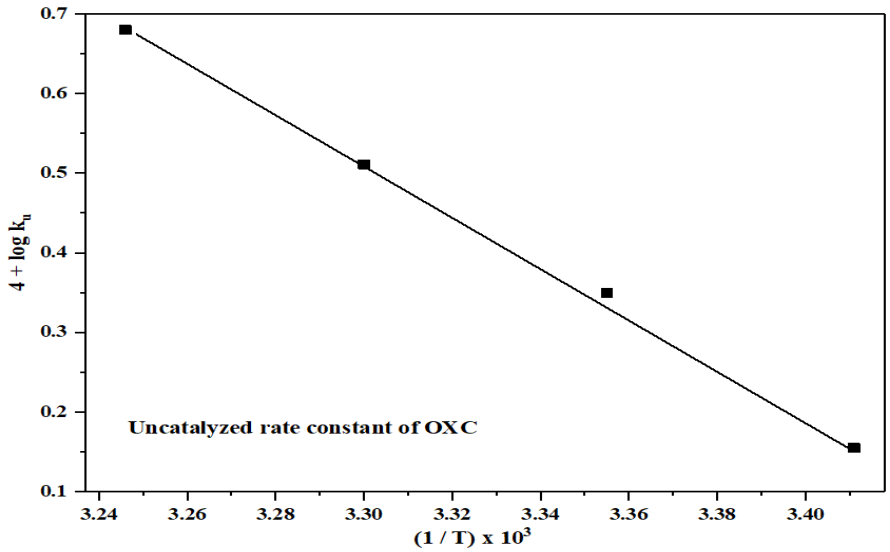

Figure 8.

Edelweiss Applied Science and Technology
ISSN: 2576-8484
Vol. 8, No. 3: 102-124, 2024
DOI: 10.55214/25768484.v8i3.1095

Displays the plot of (1 / T) x 10^3 vs. (4 + log k_u).

Table 4.
Displays activation parameters concerning the uncatalyzed rate constant (k_u).

Activation parameters	Values
Ea	60.44 (kJ mol^{-1})
$\Delta H^{\neq}$	57 ± 2 (kJ mol^{-1})
$\Delta S^{\neq}$	-101 ± 1 (JK^{-1} mol^{-1})
$\Delta G^{\neq}$	8 8 ± 2 (kJ mol^{-1})
Log A	6.9 ± 0.2

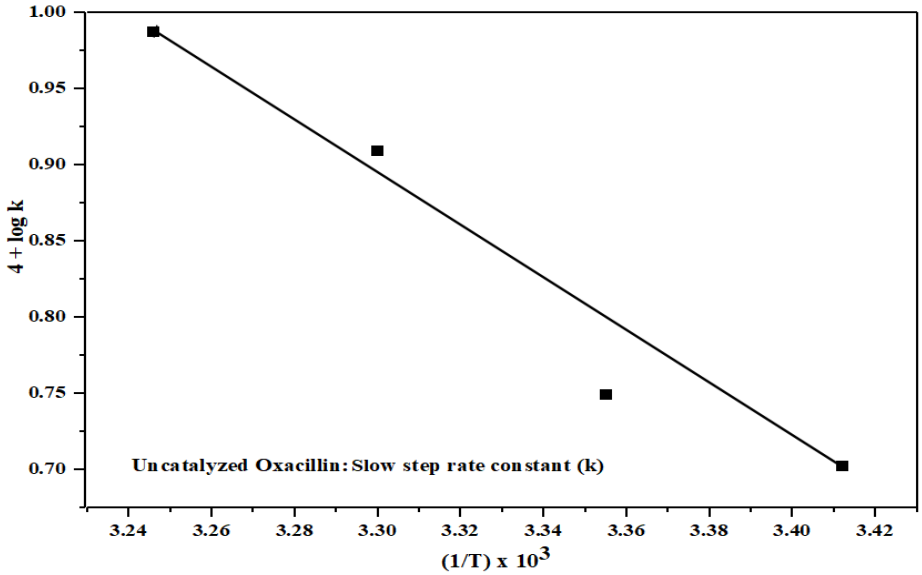

Figure 9.
Displays the plot of (1 / T) x10^3 versus (4 + log k).

Table 5.
Displays activation parameters in relation to the slow step rate constant (k).

Activation parameters	Values
Ea	35.09 (kJ mol^{-1})
$\Delta H^{\neq}$	32.6 ± 1 (kJ mol^{-1})
$\Delta S^{\neq}$	-213 ± 2 (JK^{-1} mol^{-1})
$\Delta G^{\neq}$	98.6 ± 2 (kJ mol^{-1})
Log A	2.4 ± 0.2

4. Plausible Mechanism

Different β-lactam antibiotics, or PADs, have been subjected to oxidation in the basic medium because DPC (III) functions as both a chelating and an oxidizing agent. Higher alkali concentrations cause the equilibrium forms of periodic acid (H_5IO_6) to change into dimerizing $H_4IO_6^{-1}$, $H_3IO_6^{-2}$, and $H_2IO_6^{-3}$ periodate ions. This experimental evidence suggests an appropriate reaction mechanism and the appropriate participation of all reacting species. During the initial phase of the reaction, DPC (III) interacts with the hydroxide ion, producing the deprotonated form of DPC (III). Then, this type of DPC (III) combines with water to produce MPC (III) and free periodate. A new MPC mole (III) and the complex combine to form the intermediate (A). A new mole of MPC (III) and the complex combine to form the intermediate (A). A new mole of MPC (III) and an active intermediate (A) are combined in the following step to produce an intermediate (B), which combines with two more moles of MPC (III) to

Edelweiss Applied Science and Technology
ISSN: 2576-8484
Vol. 8, No. 3: 102-124, 2024
DOI: 10.55214/25768484.v8i3.1095

create phenyl-5-methyl-4, 5-dihydroisoxazole-4-carboxylic acid, and 3-(2-(amino (carboxy) methyl)-5, 5-dimethyl-4, 5-dihydrothiazole-4-carboxylic acid-1-oxide, respectively, as mentioned by Scheme 2.

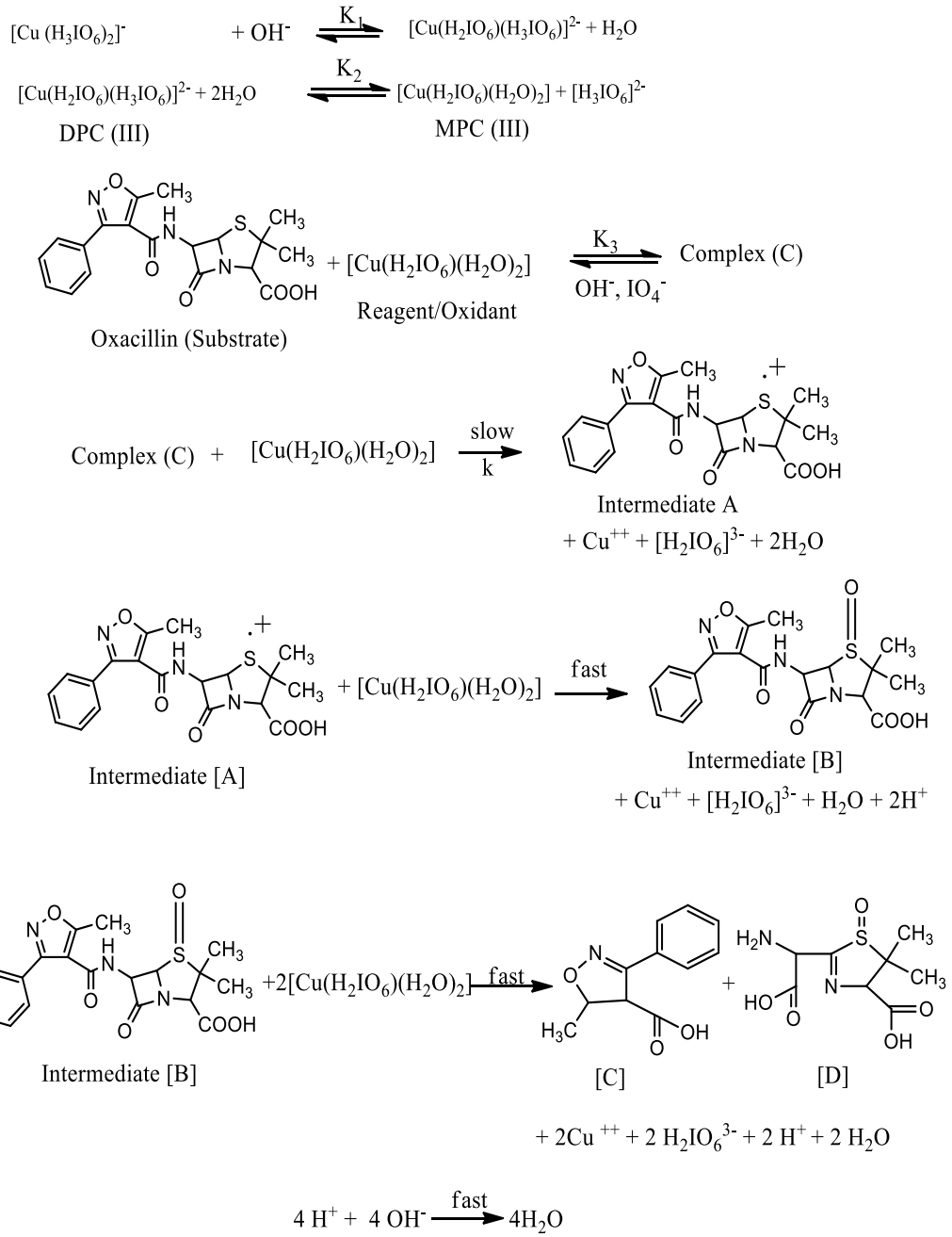

Scheme 2.
An elaborate scheme for DPC (III) to oxidize oxacillin.

Figure 10 represents a possible structure for Complex C.

Edelweiss Applied Science and Technology
ISSN: 2576-8484
Vol. 8, No. 3: 102-124, 2024
DOI: 10.55214/25768484.v8i3.1095

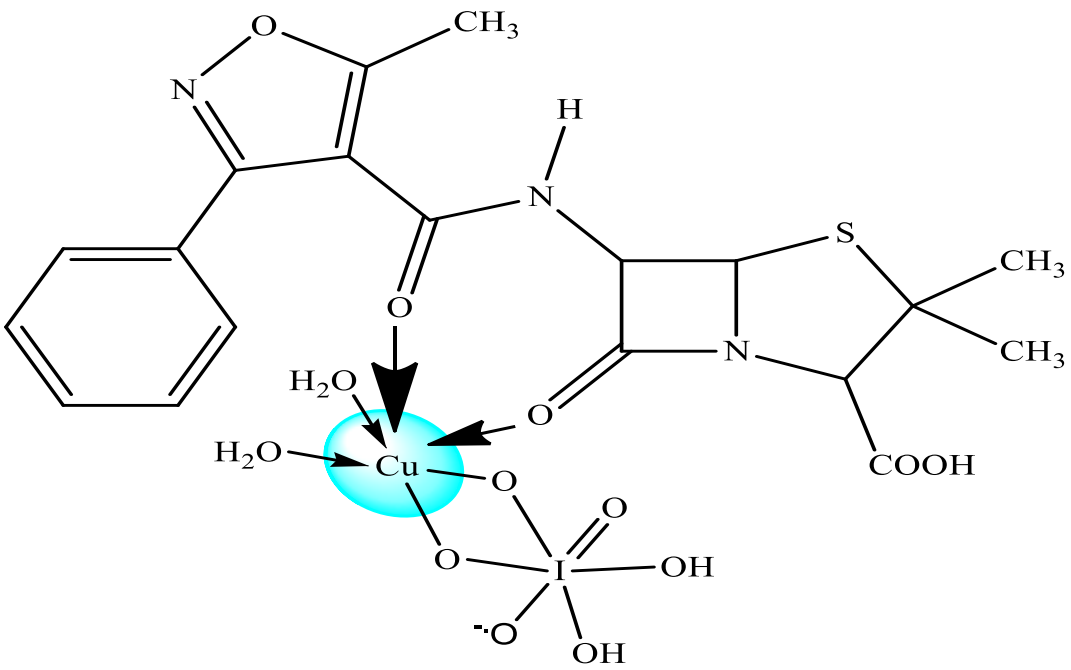

Figure 10.
Displays the plausible structure of the complex (C).

The rate law Equation 2 is obtained by Scheme 2 as -

$$\text{Rate} = -\frac{d[DPC]}{dt} = k[C] \qquad [1]$$

$$k_{obs} = \frac{kK_1K_2K_3[DPC][OXC][OH^-]}{[H_3IO_6{}^{2-}]+ K_1[OH^-][H_3IO_6{}^{2-}]+ K_1K_2[OH^-]+K_1K_2K_3[OH^-][OXC]} \qquad [2]$$

All of the observed kinetic orders for various species are described by Equation 2.
Equation 3, suitable for verification, can be created by rearrangement of the rate law Equation 2.

$$\frac{1}{k_{obs}} = \frac{[H_3IO_6{}^{2-}]}{kK_1K_2K_3[OXC][OH^-]} + \frac{[H_3IO_6{}^{2-}]}{kK_2K_3[OXC]} + \frac{1}{kK_3[OXC]} + \frac{1}{k} \qquad [3]$$

The basic equations 5.1 and 5.2 provide the fundamental formula for calculating the activation parameters and the entire rate law derivation, respectively. Finally, verification graphs were reproduced by placing the reciprocal of the uncatalyzed rate constant against the reciprocal of substrate and alkali, while the linearity of periodate was also verified by plotting the reciprocal of the uncatalyzed rate constant against monoperiodatic active masses $[H_2IO_6]^{-3}$. A decrease in the rate of reaction or fractional retarding negative values for periodate may be due to the accumulation of periodate ions, both from DPC (III) as well as from potassium periodate (KIO_4) mixed externally in the reaction mixture, which may conduct as common ions. The values of active masses of DPC (III), KIO_4, KOH, oxacillin, and slow step rate constants at different temperatures, as well as slopes and intercepts obtained, were utilized to determine equilibrium constants (K_1, K_2, and K_3). The verification or validation plots are displayed in (Figures 11-13) for diperiodatocupratic oxidation of oxacillin. According to Equation 7 the plots of $(1/k_u)$ vs. $1/[OXC]$ ($r \geq 0.999$, $\leq s\ 0.0042$) (Figure 11), $(1/k_u)$ vs.$1/[KOH]$ ($r \geq 0.999$, $\leq s\ 0.0028$) (Figure 12), and $(1/k_u)$ vs. $[H_2IO_6]^{3-}$ ($r \geq 0.999$, $\leq s\ 0.003$) (Figure 13) are found to be linear. Other plots of equilibrium constants were reproduced by plotting K_1, K_2 and K_3 against reciprocal temperature (Figures 14-16) respectively.

Edelweiss Applied Science and Technology
ISSN: 2576-8484
Vol. 8, No. 3: 102-124, 2024
DOI: 10.55214/25768484.v8i3.1095

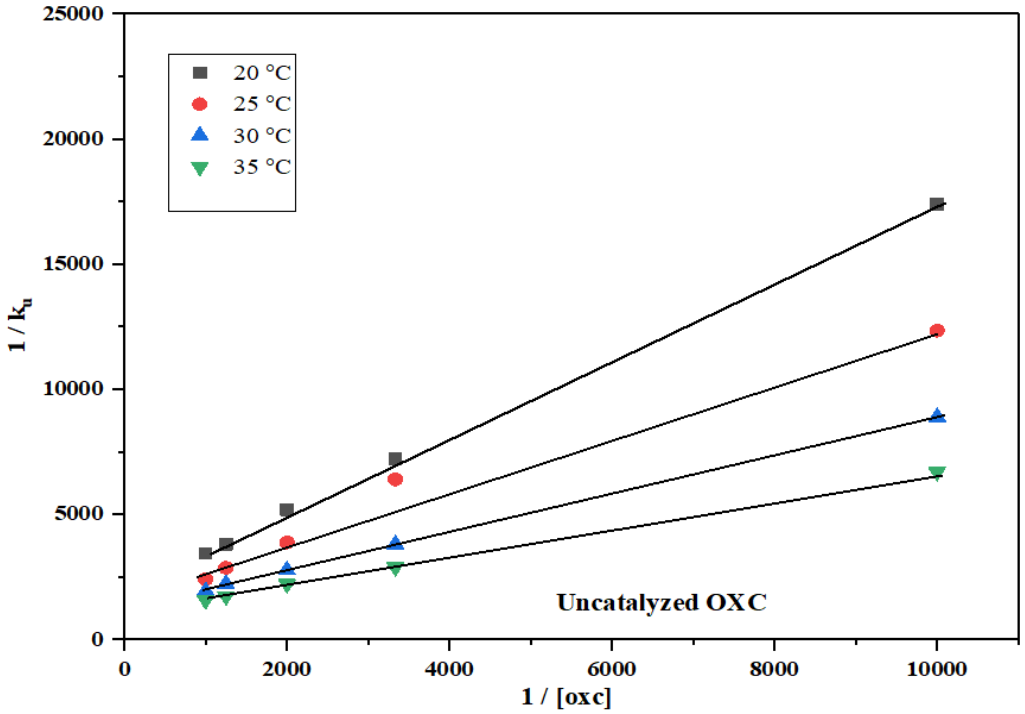

Figure 11.
Displays the first verification plot of (1/OXC) vs. $1/k_u$.

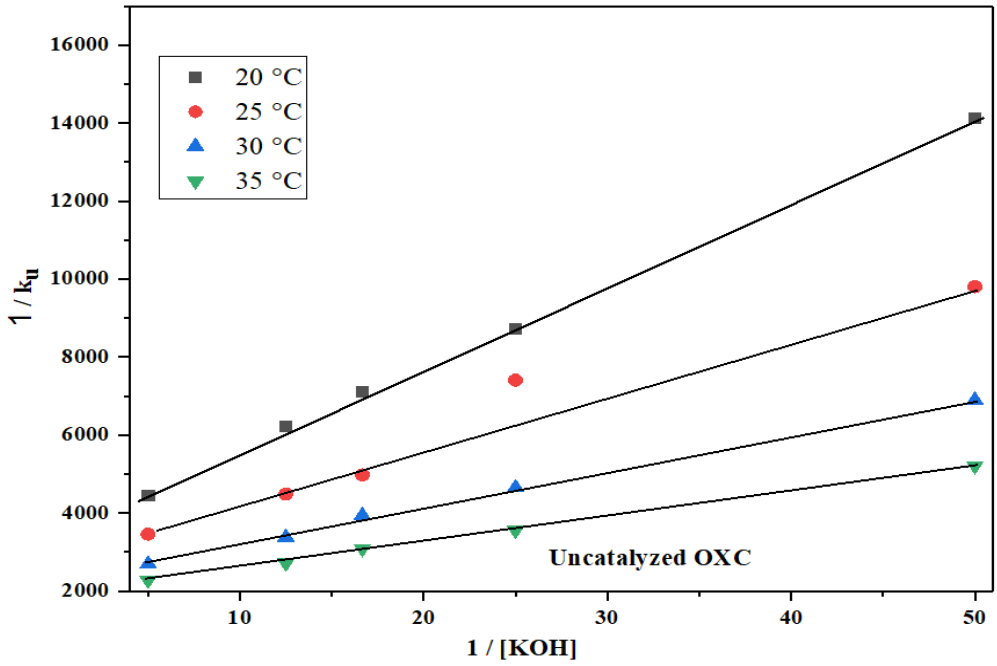

Figure 12.
Displays the second verification plot of $1/[KOH]$ vs. $(1/k_u)$.

Edelweiss Applied Science and Technology
ISSN: 2576-8484
Vol. 8, No. 3: 102-124, 2024
DOI: 10.55214/25768484.v8i3.1095

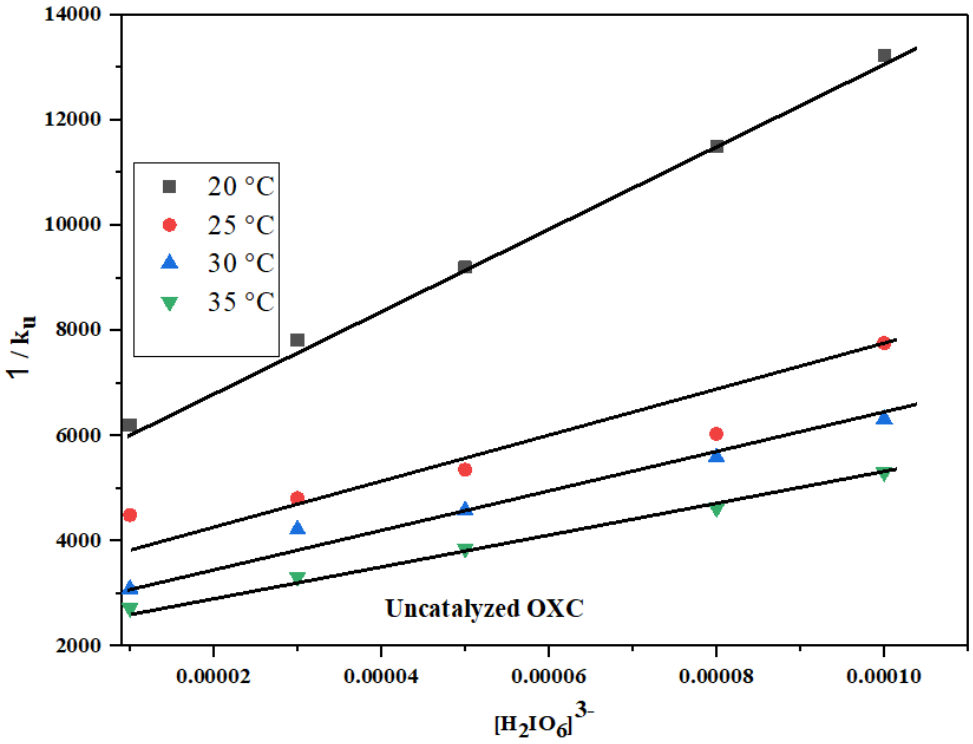

Figure 13.
Displays the third verification plot of $(1/k_u)$ vs. $[H_2IO_6]^{3-}$.

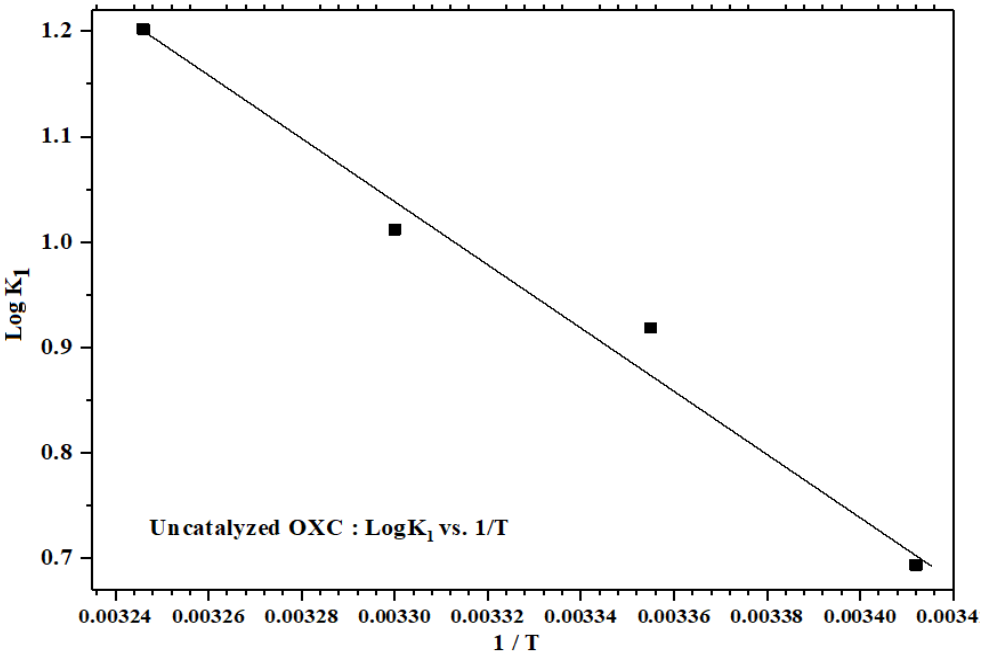

Figure 14.
Displays the first equilibrium constant plot of $\log K_1$ vs. $(1/T)$.

Edelweiss Applied Science and Technology
ISSN: 2576-8484
Vol. 8, No. 3: 102-124, 2024
DOI: 10.55214/25768484.v8i3.1095

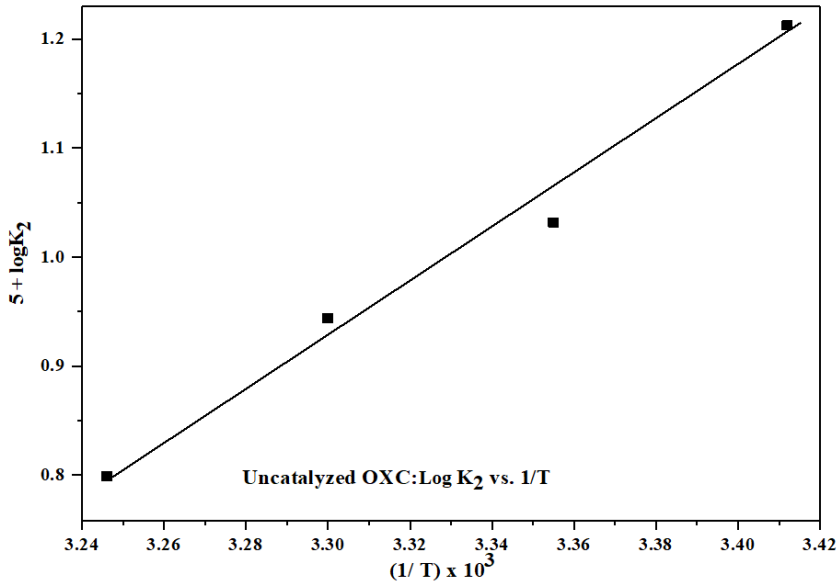

Figure 15.
Displays the second equilibrium constant plot of $(5 + \log K_2)$ vs. $(1/T) \times 10^3$.

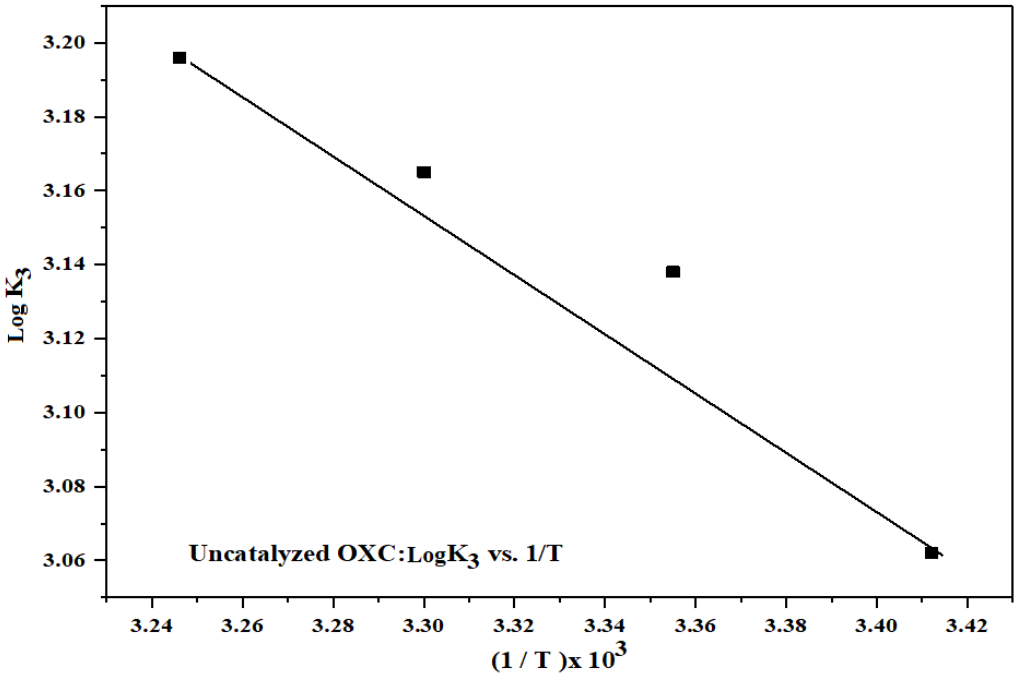

Figure 16.
Displays the third equilibrium constant plot of $\log K_3$ vs. $(1/T) \times 10^3$.

Slow step rate constants, equilibrium constants, and various thermodynamic parameters at 298 K are presented in Tables 6 & 7 respectively.

Edelweiss Applied Science and Technology
ISSN: 2576-8484
Vol. 8, No. 3: 102-124, 2024
DOI: 10.55214/25768484.v8i3.1095

Table 6.
Displays various equilibrium constants and the slow step rate constant.

Equilibrium constants ↓	**Values at variable temperatures**			
Temperature →	20 ℃	25 ℃	30℃	35 ℃
k (Slow step rate constant) x 10^{-4}	5.045	5.622	8.112	9.710
K_1	4.936	8.290	10.280	15.922
K_2 x 10^{-4}	1.631	1.091	0.879	0.629
K_3	1153.453	1374.041	1462.177	1570.362

Table 7.
Displays thermodynamic parameters from various equilibrium constants at 298 K.

Thermodynamic parameters	**Values (From K_1)**	**Values (From K_2)**	**Values (From K_3)**
ΔH°_{298} (K J mol^{-1})	56.068	-11.005	-3.560
ΔS°_{298} (J K^{-1} mol^{-1})	204.924	-32.066	26.219
ΔG°_{298} (K J mol^{-1})	- 4.900	9.540	- 7.817

5. Basic Equations

5.1. Inter-Conversion of Absorbance into Rate Constant

The rate constant was calculated from the rate law equation for a first-order reaction as follow:

$$ln(Abs)_t = -k_u t + ln(Abs)_0$$
$$2.303\ log\ (Abs)_t = -k_u t + 2.303\ log\ (Abs)_0$$
$$\text{Or, } k_u\ t = 2.303\ log\ (Abs)_0 - 2.303\ log\ (Abs)_t$$
$$\text{Hence, } k_u = \frac{2.303}{t}\ [log\ (Abs)_0 - log\ (Abs)_t]$$
$$\text{Or, } k_u = \frac{2.303}{t}\ [log\ \frac{(Abs)0}{(Abs)_t}]$$

Here, k_u denotes the uncatalyzed rate constant, $(Abs)_0$ indicates initial absorbance at time '0' sec or just before mixing, and $(Abs)_t$ stands for absorbance at any time sec after mixing all species in the solution phase.

5.2. Equations for Calculating Activational Parameters

The activation energy was calculated by,

$$\text{Ea} = -2.303\ \text{R slope}$$

The Arrhenius factor 'A' was calculated by,

$$\text{logA} = \text{log}k_u + \frac{\text{Ea}}{2.303\ \text{RT}}$$

The entropy of activation was determined by,

$$\frac{\Delta S^{\#}}{4.576} = \text{log}k_u - 10.753 - \text{log}T + \frac{E_a}{4.576T}$$

The enthalpy of activation was determined by,

$$\Delta H^{\#} = E_a - RT$$

The free energy of activation was determined by,

$$\Delta G^{\#} = \Delta H^{\#} - T\Delta S^{\#}$$

In the above equations, T denotes the temperature in Kelvin, Ea denotes the activation energy expressed in calories, R denotes the universal gas constant, # denotes the activation parameter, and k_u/k_{obs} denotes the uncatalyzed rate constant expressed in seconds.

Edelweiss Applied Science and Technology
ISSN: 2576-8484
Vol. 8, No. 3: 102-124, 2024
DOI: 10.55214/25768484.v8i3.1095

5.3. Derivation of the Rate Law Equation

From Scheme 2

$$\text{Rate} = -\frac{d[DPC]}{dt} = k[\text{Complex}] = k[C] \qquad [A\text{-}1]$$

The third equilibrium constant can be calculated using the law of mass action and is given by

$$K_3 = \frac{[C]}{[Cu(H_2IO_6)(H_2O)_2[OXC]}$$

Upon rearrangement,

$$[C] = K_3[Cu(H_2IO_6)(H_2O)_2][OXC] \qquad [A\text{-}2]$$

Replacing the value of C from eqn. [**A-2**]

$$\text{Rate} = -\frac{d[DPC]}{dt} = K_1K_3[Cu(H_2IO_6)(H_2O)_2[OXC] \qquad [A\text{-}3]$$

In the above equation, OXC represents oxacillin.

The second equilibrium constant can be calculated by

$$K_2 = \frac{[Cu(H_2IO_6)(H_2O)_2[H_3IO_6{}^{2-}]}{[Cu(H_2IO_6)(H_3IO_6]^{2-}}$$

This can be rearranged into: -

$$[Cu(H_2IO_6)(H_2O)_2] = \frac{K_2\,[Cu(H_2IO_6)(H_3IO_6]^{2-}}{[H_3IO_6]^{2-}} \qquad [A\text{-}4]$$

The first equilibrium constant can be represented by

$$K_1 = \frac{[Cu(H_2IO_6)(H_3IO_6]^{2-}}{[Cu(H_3IO_6)_2]^{-}[OH^{-}]}$$

This can be rearranged into

$$[Cu(H_2IO_6)(H_3IO_6]^{2-} = K_1\,[Cu(H_3IO_6)_2]^{-}[OH^{-} \qquad [A\text{-}5]$$

Substituting eqn. [**A-4**] to [**A-5**] in eqn. [**A-3**], we get

$$\text{Rate} = -\frac{d[DPC]}{dt} = \frac{kK_1K_2K_3[OXC]_f[DPC]_f[OH^{-}]_f}{[H_3IO_6)_2]^{-}} \qquad [A\text{-}6]$$

The total concentration of [DPC] can be given as

$$[DPC]_T = [DPC]_f + [Cu(H_2IO_6)(H_3IO_6]^{2-} + [Cu(H_2IO_6)(H_2O)_2] + [C] \qquad [A\text{-}7]$$

Where T and f denote total and free concentrations

$$= [DPC]_f + K_1[Cu(H_2IO_6)_2]^{-}[OH^{-}] + \frac{K_1K_2[Cu(H_2IO_6)_2]^{-}[OH^{-}]}{[H_3IO_6{}^{2-}]} + \frac{K_1K_2K_3[Cu(H_3IO_6)_2]^{-}[OH^{-}][OXC]}{[H_3IO_6]^{2-}}$$

$$[DPC]_T = [DPC]_f + K_1[DPC]_f[OH^{-}] + \frac{K_1K_2[DPC]_f[OH^{-}]}{[H_3IO_6{}^{2-}]} + \frac{K_1K_2K_3[DPC]_f[OH^{-}][OXC]}{[H_3IO_6{}^{2-}]}$$

$$[DPC]_f = \frac{[DPC]_T[H_3IO_6{}^{2-}]}{[H_3IO_6{}^{2-}] + K_1[OH^{-}][H_3IO_6{}^{2-}] + K_1K_2[OH^{-}] + K_1K_2K_3[OH^{-}][OXC]} \qquad [A\text{-}8]$$

The total concentration of [OH-] can be given by

Edelweiss Applied Science and Technology
ISSN: 2576-8484
Vol. 8, No. 3: 102-124, 2024
DOI: 10.55214/25768484.v8i3.1095

$$[OH^-]_T = [OH^-]_f + [Cu(H_2IO_6)(H_3IO_6]^{2-} + [Cu(H_2IO_6)(H_2O)_2] + [C]$$

$$[OH^-]_T = [OH^-]_f + K_1[DPC][OH^-]_f + \frac{K_1K_2[DPC][OH^-]_f}{[H_3IO_6]^{2-}} + \frac{K_1K_2K_3[DPC][OH^-]_f[OXC]}{[H_3IO_6]^{2-}}$$

$$[OH^-]_T = [OH^-]_f \{1 + K_1[DPC] + \frac{K_1K_2[DPC]}{[H_3IO_6]^{2-}} + \frac{K_1K_2K_3[DPC][OXC]}{[H_3IO_6]^{2-}})$$

Because DPC (III) and $H_3IO_6^{-2}$ were used in such small amounts, these terms can be neglected.

$$[OH^-]_T = [OH^-]_f \qquad [A\text{-}9]$$

Similarly, in the case of low concentrations of DPC (III) and $H_3IO_6^{2-}$ used

$$[OXC]_T = [OXC]_f \qquad [A\text{-}10]$$

Substituting the value of [DPC]$_f$ from eq^n. [**A-8**], [OH$^-$]$_f$ from eq^n. [**A-9**] and [OXC]$_f$ from eq^n. [**A-10**] in eq^n. [**A-6**] After omitting subscripts T and f, we get,

$$\text{Rate} = -\frac{d[DPC]}{dt} = \frac{kK_1K_2K_3[OXC][DPC][OH^-]}{[H_3IO_6{}^{2-}] + K_1[OH^-][H_3IO_6{}^{2-}] + K_1K_2[OH^-] + K_1K_2K_3[OH^-][OXC]}$$

$$\text{Or, } \frac{1}{k_{obs}} = \frac{[H_3IO_6{}^{2-}]}{kK_1K_2K_3[OXC][OH^-]} + \frac{[H_3IO_6{}^{2-}]}{k\,K_2K_3[OXC]} + \frac{1}{kK_3[OXC]} + \frac{1}{k} \qquad [A\text{-}11]$$

6. Conclusion

MPC (III) is regarded as the main active species, as [Cu (H_2IO_6)(H_2O)$_2$], for the current research work to oxidize oxacillin in an alkaline medium. The mechanism clearly demonstrates the involvement of neutral species because of the constant ionic strength and dielectric constant. The moderate activation entropy and enthalpy values are beneficial for electron transfer reactions, as they are within the range of electron coupling and uncoupling processes, resulting in the loss of a degree of freedom and a rigid transition state. According to the intermediate complex, it is likely to be more highly ordered than the reacting species, according to the intermediate complex's higher negative value of entropy of activation. The aforementioned findings, supporting evidence, and smaller rate constant for slow steps suggest that an inner-sphere mechanism is most likely responsible for oxidation. Lack of a catalyst most likely causes the substrate's reducing ability, while raising the activation energy lengthens the uncatalyzed reaction's pathway. At various temperatures, activation and thermodynamic parameters are calculated and computed concerning equilibrium constants (K_1, K_2, and K_3), uncatalyzed rate constant (ku), and the slow step rate constant (k). The overall sequences presented herein are supported by all available experimental data, including product, spectral, mechanistic, and kinetic studies that establish the pseudo-unimolecular nature of oxacillin oxidation in the alkaline medium.

Funding:

This study received no specific financial support.

Institutional Review Board Statement:

Not applicable.

Transparency:

The authors confirm that the manuscript is an honest, accurate, and transparent account of the study; that no vital features of the study have been omitted; and that any discrepancies from the study as planned have been explained. This study followed all ethical practices during writing.

Edelweiss Applied Science and Technology
ISSN: 2576-8484
Vol. 8, No. 3: 102-124, 2024
DOI: 10.55214/25768484.v8i3.1095

Competing Interests:
The authors declare that they have no competing interests.

Authors' Contributions:
All authors contributed equally to the conception and design of the study. All authors have read and agreed to the published version of the manuscript.

References
[1] J. Wang, S. Xu, K. Zhao, G. Song, S. Zhao, and R. Liu, "Risk control of antibiotics, antibiotic resistance genes (ARGs) and antibiotic resistant bacteria (ARB) during sewage sludge treatment and disposal: A review," *Science of The Total Environment*, vol. 877, p. 162772, 2023. https://doi.org/10.1016/j.scitotenv.2023.162772

[2] X. Guo, C. Feng, E. Gu, C. Tian, and Z. Shen, "Spatial distribution, source apportionment and risk assessment of antibiotics in the surface water and sediments of the Yangtze Estuary," *Science of the Total Environment*, vol. 671, pp. 548-557, 2019. https://doi.org/10.1016/j.scitotenv.2019.03.393.

[3] S. R. Hughes, P. Kay, and L. E. Brown, "Global synthesis and critical evaluation of pharmaceutical data sets collected from river systems," *Environmental Science & Technology*, vol. 47, no. 2, pp. 661-677, 2013. https://doi.org/10.1021/es3030148

[4] B. I. Escher, R. Baumgartner, M. Koller, K. Treyer, J. Lienert, and C. S. McArdell, "Environmental toxicology and risk assessment of pharmaceuticals from hospital wastewater," *Water Research*, vol. 45, no. 1, pp. 75-92, 2011. https://doi.org/10.1016/j.watres.2010.08.019.

[5] Y. Guan and Z. Wang, "Analysis of bacterial community characteristics, abundance of antibiotics and antibiotic resistance genes along a pollution gradient of Ba River in Xi'an, China," *Frontiers in Microbiology*, vol. 9, p. 415188, 2018. https://doi.org/10.3389/fmicb.2018.03191.

[6] I. C. Vasilachi, D. M. Asiminicesei, D. I. Fertu, and M. Gavrilescu, "Occurrence and fate of emerging pollutants in water environment and options for their removal," *Water*, vol. 13, no. 2, p. 181, 2021. https://doi.org/10.3390/w13020181

[7] C. J. Vörösmarty *et al.*, "Global threats to human water security and river biodiversity," *Nature*, vol. 467, no. 7315, pp. 555-561, 2010. https://doi.org/10.1038/nature09440

[8] J. L. Martínez, T. M. Coque, and F. Baquero, "What is a resistance gene? Ranking risk in resistomes," *Nature Reviews Microbiology*, vol. 13, no. 2, pp. 116-123, 2015. https://doi.org/10.1038/nrmicro3399

[9] P. K. Pandis *et al.*, "Key points of advanced oxidation processes (AOPs) for wastewater, organic pollutants and pharmaceutical waste treatment: A mini review," *Chem Engineering*, vol. 6, no. 1, p. 8, 2022. https://doi.org/10.3390/chemengineering6010008

[10] J. L. Reberski, J. Terzić, L. D. Maurice, and D. J. Lapworth, "Emerging organic contaminants in karst groundwater: A global level assessment," *Journal of Hydrology*, vol. 604, p. 127242, 2022. https://doi.org/10.1016/j.jhydrol.2021.127242

[11] S. Xiang *et al.*, "Response of microbial communities of karst river water to antibiotics and microbial source tracking for antibiotics," *Science of the Total Environment*, vol. 706, p. 135730, 2020. https://doi.org/10.1016/j.scitotenv.2019.135730

[12] T. Z. Addis, J. T. Adu, M. Kumarasamy, and M. Demlie, "Occurrence of trace-level antibiotics in the Msunduzi River: An investigation into South African environmental pollution," *Antibiotics*, vol. 13, no. 2, p. 174, 2024. https://doi.org/10.3390/antibiotics13020174

[13] J.-L. Liu and M.-H. Wong, "Pharmaceuticals and personal care products (PPCPs): A review on environmental contamination in China," *Environment International*, vol. 59, pp. 208-224, 2013. https://doi.org/10.1016/j.envint.2013.06.012

[14] M. Zhuang *et al.*, "Distribution of antibiotic resistance genes in the environment," *Environmental Pollution*, vol. 285, p. 117402, 2021. https://doi.org/10.1016/j.envpol.2021.117402

[15] M. S. De Ilurdoz, J. J. Sadhwani, and J. V. Reboso, "Antibiotic removal processes from water & wastewater for the protection of the aquatic environment-a review," *Journal of Water Process Engineering*, vol. 45, p. 102474, 2022. https://doi.org/10.1016/j.jwpe.2021.102474.

[16] M. Hassan *et al.*, "Removal of antibiotics from wastewater and its problematic effects on microbial communities by bioelectrochemical Technology: Current knowledge and future perspectives," *Environmental Engineering Research*, vol. 26, no. 1, 2021. https://doi.org/10.4491/eer.2019.405

[17] Y. Zhang, Y.-G. Zhao, F. Maqbool, and Y. Hu, "Removal of antibiotics pollutants in wastewater by UV-based advanced oxidation processes: Influence of water matrix components, processes optimization and application: A review," *Journal of Water Process Engineering*, vol. 45, p. 102496, 2022. https://doi.org/10.1016/j.jwpe.2021.102496.

[18] S. Gajdoš *et al.*, "Synergistic removal of pharmaceuticals and antibiotic resistance from ultrafiltered WWTP effluent: Free-floating ARGs exceptionally susceptible to degradation," *Journal of Environmental Management*, vol. 340, p. 117861, 2023. https://doi.org/10.1016/j.jenvman.2023.117861

[19] T. Spit, J. P. van der Hoek, C. de Jong, D. van Halem, M. de Kreuk, and B. B. Perez, "Removal of antibiotic resistance from municipal secondary effluents by ozone-activated carbon filtration," *Frontiers in Environmental Science*, vol. 10, p. 834577, 2022. https://doi.org/10.3389/fenvs.2022.834577

[20] I. Velo-Gala, M. J. Farré, J. Radjenovic, and W. Gernjak, "Influence of water matrix components on the UV/chlorine process and its reactions mechanism," *Environmental Research*, vol. 218, p. 114945, 2023. https://doi.org/10.1016/j.envres.2022.114945

[21] Y. R. Sahu, R. K. Dev, N. K. Chaudhary, and A. Bhattarai, "Kinetics of catalytic oxidation of carbenicillin: A degradation approach for penicillanic acid derivatives (PADs)," *Journal of Nepal Chemical Society*, vol. 43, no. 2, pp. 159-170, 2023.

[22] P. Krupa, J. Bystroń, M. Podkowik, J. Empel, A. Mroczkowska, and J. Bania, "Population structure and oxacillin resistance of Staphylococcus aureus from pigs and pork meat in South-West of Poland," *BioMed Research International*, vol. 2015, pp. 1-10, 2015. https://dx.doi.org/10.1155/2015/141475

[23] J.-h. Shan, Y. Li, S.-y. Huo, and C.-h. Yin, "The oxidation of 2-(2-methoxyethoxy) ethanol and 2-(2-ethoxyethoxy) ethanol by ditelluratocuprate (III): A kinetic and mechanistic study," *Journal of Chemistry*, vol. 2013, pp. 1-6, 2013. https://doi.org/10.1155/2013/627324

[24] J. Shan, Y. Liu, and J. Zhang, "Kinetics and mechanism of oxidation of 1-methoxy-2-propanol and 1-ethoxy-2-propanol by ditelluratocuprate (III) in alkaline medium," *Chinese Journal of Chemistry*, vol. 29, no. 4, pp. 639-642, 2011. https://doi.org/10.1002/cjoc.201190134

[25] I. A. Amer, "Kinetics and mechanism of the oxidation of 2-methylindole by alkaline potassium hexacyanoferrate (III)," *Egyptian Journal of Chemistry*, vol. 64, no. 3, pp. 1441-1446, 2021. https://doi.org/10.21608/ejchem.2020.22459.2338

[26] M. Thriveni, I. Mallikarjuna, S. Bellappa, and T. Shivalingaswamy, "Oxidation of caffeine by Diperiodatocuprate (III) with and without Ruthenium (III) in alkaline medium," *Russian Journal of Physical Chemistry A*, vol. 95, no. Suppl 1, pp. S44-S55, 2021. https://doi.org/10.1134/S0036024421140235

[27] M. D. Meti, S. T. Nandibewoor, and S. A. Chimatadar, "Oxidation of procainamide by diperiodatocuprate (III) complex in aqueous alkaline medium: A comparative kinetic study," *Inorganic and Nano-Metal Chemistry*, vol. 50, no. 4, pp. 195-204, 2020. https://doi.org/10.1080/24701556.2019.1662041

[28] C. Kathari, P. Pol, and S. T. Nandibewoor, "The kinetics and mechanism of oxidation of vanillin by diperiodatonickelate (IV) in aqueous alkaline medium," *Turkish Journal of Chemistry*, vol. 26, no. 2, pp. 229-236, 2002.

[29] Y. Zhao, M. Qi, R. Hao, J. Jiang, and B. Yuan, "A novel catalytic oxidation process for removing elemental mercury by using diperiodatoargentate (III) in the catalysis of trace ruthenium (III)," *Journal of Hazardous Materials*, vol. 381, p. 120964, 2020. https://doi.org/10.1016/j.jhazmat.2019.120964

[30] R. R. Hosamani, N. P. Shetti, and S. T. Nandibewoor, "Mechanistic investigation on the oxidation of ampicillin drug by diperiodatoargentate (III) in aqueous alkaline medium," *Journal of Physical Organic Chemistry*, vol. 22, no. 3, pp. 234-240, 2009. https://doi.org/10.1002/poc.1460

[31] S. Nadimpalli, J. Padmavathy, and K. K. Yusuff, "Determination of the nature of the diperiodatocuprate (III) species in aqueous alkaline medium through a kinetic and mechanistic study on the oxidation of iodide ion," *Transition Metal Chemistry*, vol. 26, pp. 315-321, 2001. https://doi.org/10.1023/A:1007116932047

[32] B. Chowdhury, M. H. Mondal, M. K. Barman, and B. Saha, "A study on the synthesis of alkaline copper (III)-periodate (DPC) complex with an overview of its redox behavior in aqueous micellar media," *Research on Chemical Intermediates*, vol. 45, pp. 789-800, 2019. https://doi.org/10.1007/S11164-018-3643-2

[33] W. Levason and M. D. Spicer, "The chemistry of copper and silver in their higher oxidation states," *Coordination Chemistry Reviews*, vol. 76, pp. 45-120, 1987. https://doi.org/10.1016/0010-8545(87)85002-6

[34] H.-Y. Xie, Z.-R. Wang, and Z.-F. Fu, "Highly sensitive trivalent copper chelate–luminol chemiluminescence system for capillary electrophoresis chiral separation and determination of ofloxacin enantiomers in urine samples," *Journal of Pharmaceutical Analysis*, vol. 4, no. 6, pp. 412-416, 2014. https://doi.org/10.1016/j.jpha.2014.05.004

[35] B. Sethuram, *Some aspects of electron transfer reaction involving organic molecules*. New Delhi: Allied Publishers Pvt. Ltd, 2003.

[36] L. Eberson, "Electron-transfer reactions in organic chemistry," *Advances in Physical Organic Chemistry*, vol. 18, pp. 79-185, 1982. https://doi.org/10.1016/S0065-3160(08)60139

[37] A. L. Giraldo, E. D. Erazo-Erazo, O. A. Flórez-Acosta, E. A. Serna-Galvis, and R. A. Torres-Palma, "Degradation of the antibiotic oxacillin in water by anodic oxidation with Ti/IrO2 anodes: Evaluation of degradation routes, organic by-products and effects of water matrix components," *Chemical Engineering Journal*, vol. 279, pp. 103-114, 2015. https://doi.org/10.1016/j.cej.2015.04.140

[38] E. Takács *et al.*, "Elimination of oxacillin, its toxicity and antibacterial activity by using ionizing radiation," *Chemosphere*, vol. 286, p. 131467, 2022. https://doi.org/10.1016/j.chemosphere.2021.131467

Edelweiss Applied Science and Technology
ISSN: 2576-8484
Vol. 8, No. 3: 102-124, 2024
DOI: 10.55214/25768484.v8i3.1095

[39] R. M. Moghadam, L. Salehi, S. Jafari, N. Nasirizadeh, and J. Ghasemi, "Voltammetric sensing of oxacillin by using a screen-printed electrode modified with molecularly imprinted polyaniline, gold nanourchins and graphene oxide," *Microchimica Acta*, vol. 186, pp. 1-7, 2019. https://doi.org/10.1007/s00604-019-3981-9

[40] A. F. Kaizal, J. M. Salman, and P. Kot, "Evaluation of some heavy metals, their fate and transportation in water, sediment, and some biota within Al-Musayyib River, Babylon Governorate, Iraq," *Baghdad Science Journal*, vol. 20, no. 2, pp. 0436-0436, 2023. http://dx.doi.org/10.21123/bsj.2022.7599

[41] M. Mohammadi Tabar, M. Khaleghi, E. Bidram, A. Zarepour, and A. Zarrabi, "Penicillin and oxacillin loaded on pegylated-graphene oxide to enhance the activity of the antibiotics against methicillin-resistant staphylococcus aureus," *Pharmaceutics*, vol. 14, p. 2049, 2022. https://doi.org/10.3390/pharmaceutics14102049

[42] S. M. Ibrahim, N. Saad, M. M. Ahmed, and M. Abd El–Aal, "Novel synthesis of antibacterial pyrone derivatives using kinetics and mechanism of oxidation of azithromycin by alkaline permanganate," *Bioorganic Chemistry*, vol. 119, p. 105553, 2022. https://doi.org/10.1016/j.bioorg.2021.105553

[43] M. M. Barbooti and S. H. Zahraw, "Removal of amoxicillin from water by adsorption on water treatment residues," *Baghdad Science Journal*, vol. 17, no. 3 (Suppl.), pp. 1071-1071, 2020. http://dx.doi.org/10.21123/bsj.2020.17.3(Suppl.).1071

[44] P. Jaiswal and K. Yadava, "Determination of sugars and organic acids with periodato complex of Cu (III)," *Chemischer Informationsdienst*, vol. 4, no. 51, pp. 837-838, 1973.

[45] G. H. Jeffery, J. Basset, R. C. Mendham, and R. C. Denney, *Vogel's textbook of qualitative chemical analysis*, 5th ed. Essex U. K: ELBS, Longman, 1996.

[46] G. Panigrahi and A. Pathy, "Kinetics and mechanism of oxidation of S 2 O 3 2− by potassium bis (tellurato) cuprate (III)," *Journal of Chemical Sciences*, vol. 96, pp. 301-308, 1986. https://doi.org/10.1007/bf02895725

[47] J. S. Renny, L. L. Tomasevich, E. H. Tallmadge, and D. B. Collum, "Method of continuous variations: Applications of job plots to the study of molecular associations in organometallic chemistry," *Angewandte Chemie International Edition*, vol. 52, no. 46, pp. 11998-12013, 2013. https://doi.org/10.1002/anie.201304157

[48] E. Coşkun, E. Duman, N. Acar, and E. Biçer, "Electrochemical, spectroscopic and computational studies on complexation of oxacillin with Cu (II) and Co (II) ions. Synthesis and ligand hydrolysis," *International Journal of Electrochemical Science*, vol. 12, no. 10, pp. 9364-9377, 2017. https://doi.org/10.20964/2017.10.43

[49] S. Ramotowska, M. Wysocka, J. Brzeski, A. Chylewska, and M. Makowski, "A comprehensive approach to the analysis of antibiotic-metal complexes," *TrAC Trends in Analytical Chemistry*, vol. 123, p. 115771, 2020. https://doi.org/10.1016/j.trac.2019.115771

Edelweiss Applied Science and Technology
ISSN: 2576-8484
Vol. 8, No. 3: 102-124, 2024
DOI: 10.55214/25768484.v8i3.1095

Appendix

FT-IR and LC-MS spectral evidence have been represented herein as Figures A1 and A2.

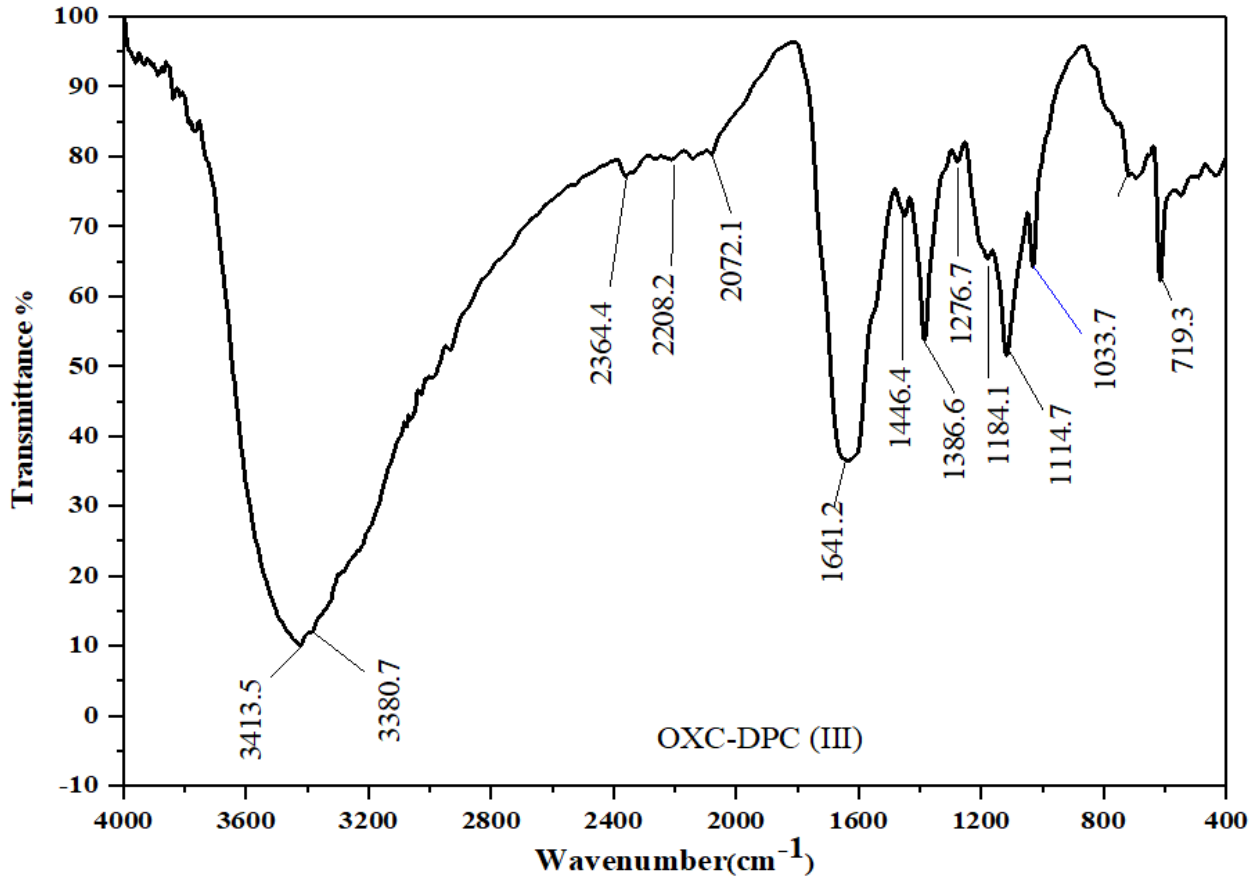

Figure A1.
Displays the oxacillin oxidation by DPC (III): FT-IR spectrum.

Edelweiss Applied Science and Technology
ISSN: 2576-8484
Vol. 8, No. 3: 102-124, 2024
DOI: 10.55214/25768484.v8i3.1095

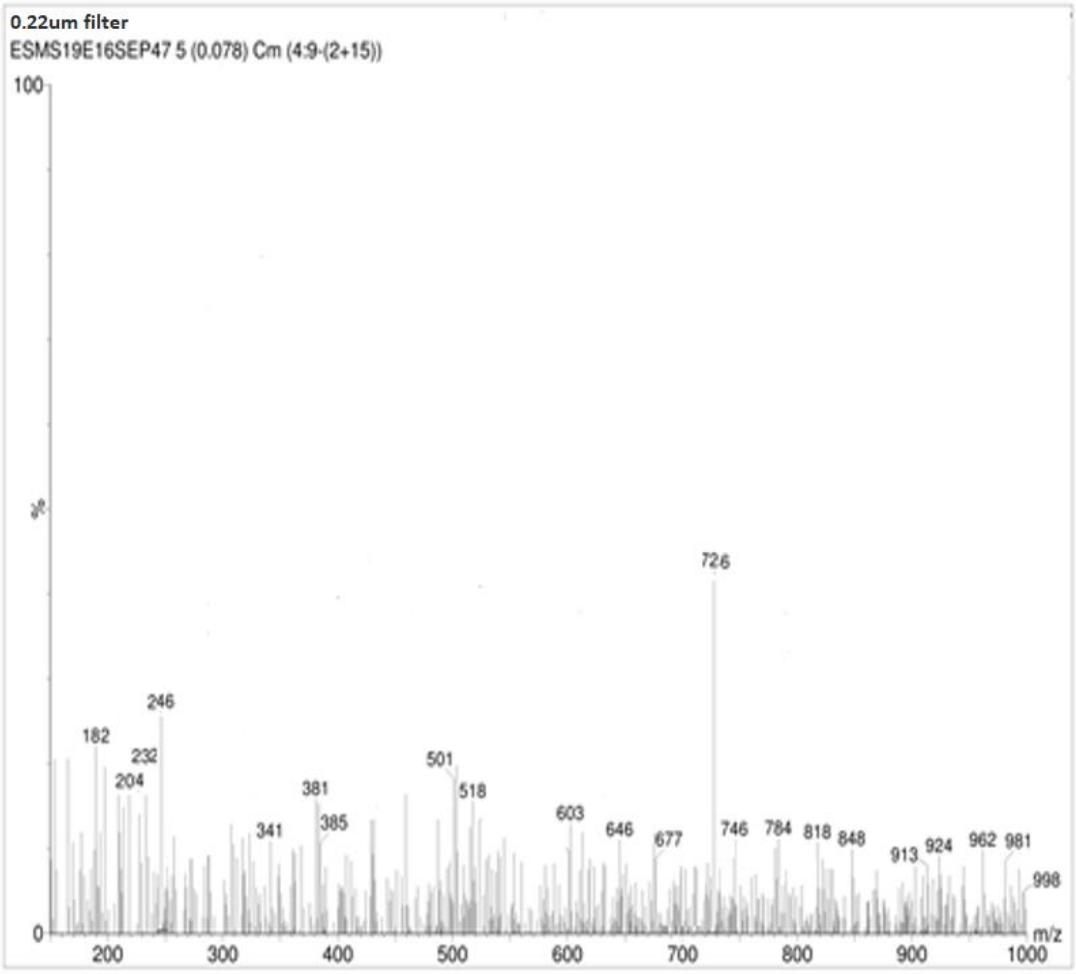

Figure A2.
Displays the LC-MS spectrum of the OXC-MPC (III) complex and its products.

Edelweiss Applied Science and Technology
ISSN: 2576-8484
Vol. 8, No. 3: 102-124, 2024
DOI: 10.55214/25768484.v8i3.1095

JNCS
Journal of Nepal Chemical Society
March/April 2023, Vol. 43, No. 2, 159-170
ISSN: 2091-0304 (print)
DOI: https://doi.org/10.3126/jncs.v43i2.53814
RESEARCH ARTICLE

Kinetics of Catalytic Oxidation of Carbenicillin: A Degradation Approach for Penicillanic Acid Derivatives (PADs)

Yuv Raj Sahu, Rohit Kumar Dev, Narendra Kumar Chaudhary, and Ajay Bhattarai*

Department of Chemistry, Mahendra Morang Adarsh Multiple Campus, Biratnagar, Tribhuvan University, Nepal

*Corresponding Author: **bkajaya@yahoo.com**

Submitted: 15 Oct 2022, Revised 5 Feb 2023, accepted 7 Feb 2023

Abstract

Diperiodatocuprate [DPC (III)] was selected to predict the kinetic studies for carbenicillin (CRBC) oxidation in the basic media. The investigation was completed in the presence of $CoCl_3$ as catalyst by using a UV/Visible spectrophotometer at 298K temperature and 0.01 mol-dm^{-3} ionic strength which confirmed a 1:4 stoichiometry between CRBC and DPC (III). Both spectral and elemental analysis was used to identify the final products. Monoperiodatocuperate [MPC (III)] was found to be the primary active species of DPC (III). Pseudo-first order reaction was declared for DPC (III), while fractional order reactions were noticed in case of CRBC (substrate), Co (III) catalyst as well as KOH (alkali). However, for periodate, the reaction was determined to be in negative fractional order. Spectral evidence, determination of various rate constants, and both activation as well as thermodynamic parameters were used to predict plausible mechanism.

Keywords: *Diperiodatocuprate, rate constant, carbenicillin, mechanism, oxidation*

Introduction

One of the commonly consumed classes of antibacterial agents is the so-called β-lactam antibiotics or penicillanic acid derivatives (PADs), which contain a nucleus including a 2-azatidinone (3-lactam) ring that is either connected to a thiazolidine or a dihydro-1, 3-thiazine ring. Compounds whose nuclei contain a thiazolidine ring are noted generically as penicillins, whereas those with a nucleus containing a dihydrothiazine ring are referred to as cephalosporins. Benzylpenicillin (penicillin G), phenoxymethylpenicillin (penicillin V), ampiciliin, oxacillin, amoxicillin, dicloxacillin, and carbenicillin, etc. are some common samples of PADs. Antibiotics or PADs, antimicrobial medications' "silver bullets" are hailed as one of modern medicine's greatest discoveries of the 20th century [1]. However, despite the worldwide consumption of PADs as essential chemotherapeutic agents, they still suffer from some style of shortcomings; therefore, certain members don't respond to certain microorganisms. These PADs are widely consumed in cosmetics, drugs, personal care products (PCPs), hospitals, and sewage for the improvement of our daily life [2-4]. Approximately 30% of these antibiotics or PADs get consumed inside the host body and the remaining non-degraded PADs get discharged into natural water sources in several ways which pollute the entire ecosystem. It has been previously described [5] how antibiotic resistance genes are distributed in the environment. Such contamination in water, air, and soil starts converting them into unfit/unhealthy for drinking purposes by enhancing antibacterial resistance [6-7]. For the deterioration of these emerging contaminants, a number of advanced oxidation processes (AOPs) have been used [8–10]. Hence the degradation of carbenicillin, through catalytic oxidation, will prove an appreciative research work for chemists and drug industries.

Copper, osmium, ruthenium, cobalt, and manganese are common transition metals which catalyze chemical reactions either alone or as binary mixtures. The development of reactive intermediates or highly unstable complexes, substrate oxidation, or free radicals appearance are just a few examples of the redox processes that are involved in Co (III) catalysis, which has garnered a lot of interest [11]. Transition metals can typically be stabilized by chelating with polydentate ligands, such as diperiodatoargentate (III) [12], diperiodatocuprate (III) [13, 14], and diperiodatonickelate (IV) [15] which are utilized as strong oxidants in analytical chemistry and chemical research. The Cu (III): Cu (II) couple plays a significant role in many reactions since both Cobalt (III) and Cu (III) are active intermediate species in multi-electron transfer reactions [16]. DPC (III) synthesis, stability, analytical uses, structural analysis, and analytical applications have all been covered in several research, which were initially created more than 50 years ago [17, 18]. Carbenicillin, a 4th generation antibiotic, is a semi-synthetic analogue of benzyl-penicillin with carboxyl and benzyl groups. The molar mass and formula of carbenicillin are 378.401 g mol^{-1} and $C_{17}H_{18}N_2O_6S$ respectively. FIGURE 1 depicts its structure.

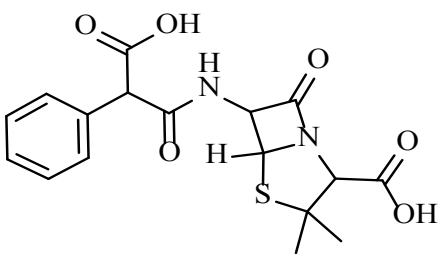

Figure 1. *Structure of Carbenicillin*

Charles B. Smith et al. have described the activity of carbenicillin in vitro and absorption and excretion in normal young men [19]. Kenneth Butler et al. have explained the chemistry of carbenicillin and the mode of its action [20]. Arthur R. English et al. have explained the carbenicillin indanyl sodium, an orally active derivative of carbenicillin [21].

The effects of carbenicillin, cefotaxime, and vancomycin on tobacco and chrysanthemum TCL morphogenesis and Agrobacterium growth have been discussed by Jaime Teixeira da Silva et al. [22]. Kolek Marta et al. have explained the hydrolysis of penicillin G and carbenicillin in pure water through HPLC/ESI-MS reports [23]. T. C. Eickhoff has reported the effect of polymyxin B or gentamycin in combination with carbenicillin in vitro against Pseudomonas aeruginosa [24]. Melvin I. Marks et al. have reported pharmacologic studies of carbenicillin and gentamycin in patients with cystic fibrosis and pseudomonas pulmonary infections [25]. The interactions between carbenicillin or ticarcillin and aminoglycoside antibiotics have been described by H. A. Holt [26]. Pharmaceutical features of the administration of ticarcillin and carbenicillin have been reported by B. Lynn [27]. Rosdahl N. and Thomsen V. F. [28] have already discussed the carbenicillin activity against gram-negative rods in comparison to that of penicillin, cephalosporins, and ampicillin.

The kinetics of uncatalyzed oxidation of Carbenicillin by DPC (III) has been investigated experimentally [29]. As a result, the primary goal is to investigate the kinetics of carbenicillin oxidation and to anticipate a likely process while also determining activation and thermodynamic parameters. Similar to this, accurate calculations have been made for different rate constants, equilibrium constants, and catalytic constants at various four temperatures.

Materials and Methods

Materials and instruments

Throughout the research process, analytically graded chemicals and distilled water were applied. Separate solutions of potassium periodate (Sigma Aldrich) and 0.01 mol dm^{-3} CRBC (Sigma Aldrich, New Zealand) were made. Molarity of KIO_4 solution was obtained using an iodometric technique [30]. An ELICO LI 613 pH meter was used to measure the pH of the solutions. A Varian CARY 5000 UV-VIS spectrophotometer was accustomed to recording electronic absorption spectra in the region of 200-1000 nm. Similarly, FT-IR spectra were recorded by Thermo Nicolet, Avatar 370 FT-IR spectrometer within a region of 4000-400 cm^{-1} with the help of KBr disc. The products' LC-MS

spectra were captured on the positive mode of UPLC-TQD Mass spectrometer between 0 and 1000 m/z.

Synthesis of DPC (III) and CRBC- Co (III) Complex

The oxidizing agent as well as the reagent copper (III) diperiodate [DPC (III)] was prepared [31] and a sintered glass crucible G-4 was applied to filter; a red-brown coloured solution was obtained as filtrate, and 250 ml solution was made after dilution. The iodometric titration ($Na_2S_2O_3$, starch, KI, and KH_2PO_4) was applied to standardize the DPC (III) solution by using the thiocyanate method [32] that helped to determine its concentration. Chemicals like sodium thiosulphate, potassium iodide, potassium persulphate, monopotasium phosphate, and KOH were managed from EMPLURA^R (Merck Life Science Pvt. Ltd. India). Similarly, KNO_3, and $CuSO_4$ were brought from LOBA CHEMIE Pvt. Ltd. India, and the catalyst ($CoCl_3$) was managed from Sigma Aldrich (New Zealand). A UV-visible spectrophotometer verified the existence of DPC (III) which showed absorption bands at 265 nm, 385 nm, as well as the maximum peak at 415 nm. 10 ml CRBC solution of 0.132 mol dm^{-3} and 10 ml DPC (III) solution of 0.528 mol dm^{-3} were mixed along with KOH solution (2.0 ml) of fixed molarity, 1.0 ml of each KNO_3, $CoCl_3$, and KIO_4 solution, stirred for twenty-four hours before re-fluxing and condensation. After cooling for three days, the mixture was filtered; and the purified products were then crystallized again in ethanol until the ethanol evaporated, leaving behind crystals of a greyish tint. Synthesis of the complex was verified by the emergence of peaks in the UV-Visible spectrophotometer. Figure 2 depicts the potential structure of the CRBC- Co (III) complex.

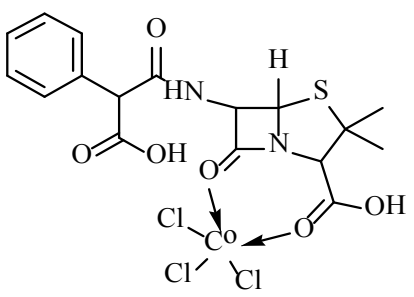

Figure 2. *CRBC- Co (III) Complex*

Kinetic Study Procedure

With the help of a micro-pipette, the DPC (III) solution was retained in an extremely dried cuvette which already had pre-fixed concentrated solutions of Co (III), KIO_4 along with KNO_3, and KOH in which CRBC solution of variable concentration was blended gently and carefully. With the aid of a UV-Visible spectrophotometer, absorbance measurements were made quickly and individually while the reaction progressed at 20°C, 25°C, 30°C, and 35°C ± 0.5°C separately within pH range of (9.2-10) and a wavelength of 415 nm. The UV-Visible spectrophotometer was monitored to collect data for DPC (III) at a molar extinction coefficient (€) of 6242.50 dm^3 mol^{-1} cm^{-1}, in decreasing order of absorbance. Using the software Origin 9.6 (2017), values for the parametric statistics regression coefficient (r) and standard deviation or variance (s) were collected. For every concentration of DPC (III), log (Absorbance) against time plots, Figure 5, produced a straight line, allowing rate constants (k_c) to be derived from the slopes.

Results and Discussion

Stoichiometry and Product Analysis

The precise stoichiometry of CRBC: DPC (III) was confirmed by Job's method [33]; it was declared to be 1:4 for CRBC: DPC (III). Various sets of reaction mixtures containing a variable ratio of DPC (III) and CRBC along with an invariable ratio of $CoCl_3$, KOH, and KNO_3 (III) after keeping the reaction mixture for three hours within a closed vessel filled with nitrogen gas atmosphere. Phenyl-malonic acid ($C_9H_8O_4$) and 2-(amino (carboxy) methyl)-5, 5-dimethyl-4, 5-dihydrothiazole-4-carboxylic acid-1-oxide were confirmed as the primary products when CRBC reacted with DPC (III) and Co (III) catalyst in the aqueous alkaline medium which were recovered from ethanol and separated using column chromatography with an eluent of 80% benzene and 20% chloroform over neutral alumina.

The catalyzed reaction between CRBC and DPC (III) in an aqueous alkaline medium [29] can be presented by:

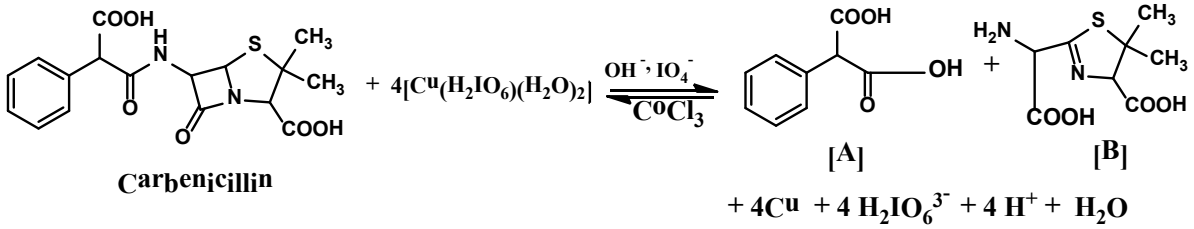

Carbenicillin

Where A = 2-phenylmalonic acid ($C_9H_8O_4$) and B = 2-(amino (carboxy) methyl)-5, 5-dimethyl-4, 5-didydrothiazole-4-carboxylic acid-1-oxide ($C_8H_{12}N_2O_4S$)

Table 1: *Elemental analysis*

Complex/Product	C%	H%	N%	Co%	Cl%	S%	O%
$C_{17}H_{18}Cl_3CoN_2O_6S$	36.85 (37.55)	3.30 (3.34)	5.31 (5.15)	11.02 (10.84)	19.28 (19.56)	5.08 (5.40)	19.15 (18.15)
(A) $C_9H_8O_4$	60.11 (60.00)	4.55 (4.48)	-	-	-	-	35.33 (35.51)
(B) $C_8H_{12}N_2O_4S$	41.53 (41.37)	5.37 (5.21)	12.16 (12.06)	-	-	13.88 (13.81)	27.05 (27.54)

Characterization

Elemental analysis

The Co (III)- CRBC complex ($C_{17}H_{18}Cl_3CoN_2O_6S$), as well as two products A ($C_9H_8O_4$), and B ($C_8H_{12}N_2O_4S$) showed the following % elemental analysis as presented in Table 1.

Spectral analysis

Figure 3 and Figure 4 represent the FT-IR and LC-MS spectra respectively [29].

In FT-IR spectrum, carboxylic OH group shows a peak at 3413.5 cm^{-1}, N-H stretching group at 3380.7 cm^{-1}, methyl stretching group at 1464.4 cm^{-1} & 1386.6 cm^{-1}, carboxylic C=O stretching at 1276.7 cm^{-1} while another peak at 1641.2 cm^{-1} is noticed due to ketonic or carboxylic group. Figure 4 shows the m/z values for the complex and its products. The complex ($C_{17}H_{18}Cl_3CoN_2O_6S$) showed an m/z value at 544 while (m/z) value for 2-phenylmalonic acid was at 182 (m + 2), and that of 2-(amino (carboxy) methyl)-5, 5-dimethyl-4, 5-dihydrothiazole-4-carboxylic acid-1-oxide was at 232 (m+1).

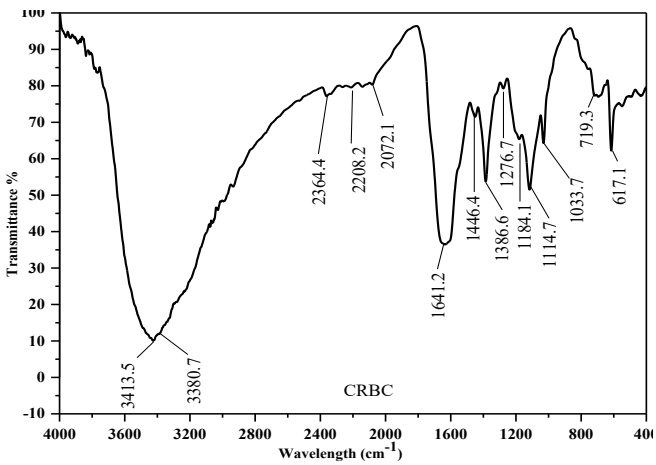

Figure 3: *FT-IR Spectrum for the catalyzed oxidation of CRBC*

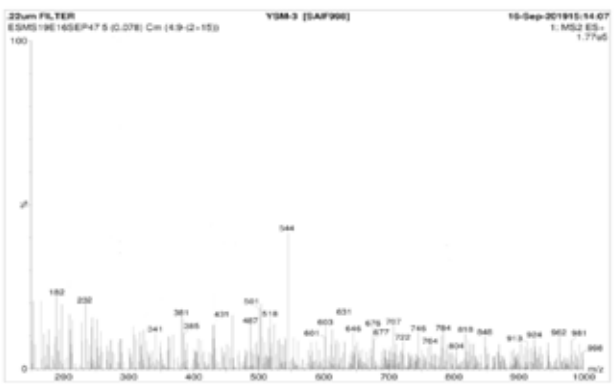

Figure 4: *LC-MS Spectrum for the catalyzed oxidation of CRBC*

Reaction Orders

With variable concentration of CRBC, $CoCl_3$, KIO_4, KOH, and constant concentration of DPC (III), reaction orders were obtained from the slopes of log (absorbance) vs. time, independently for each concentration of DPC (III) [29]. The plots are shown in Figure 5 and Table 2.

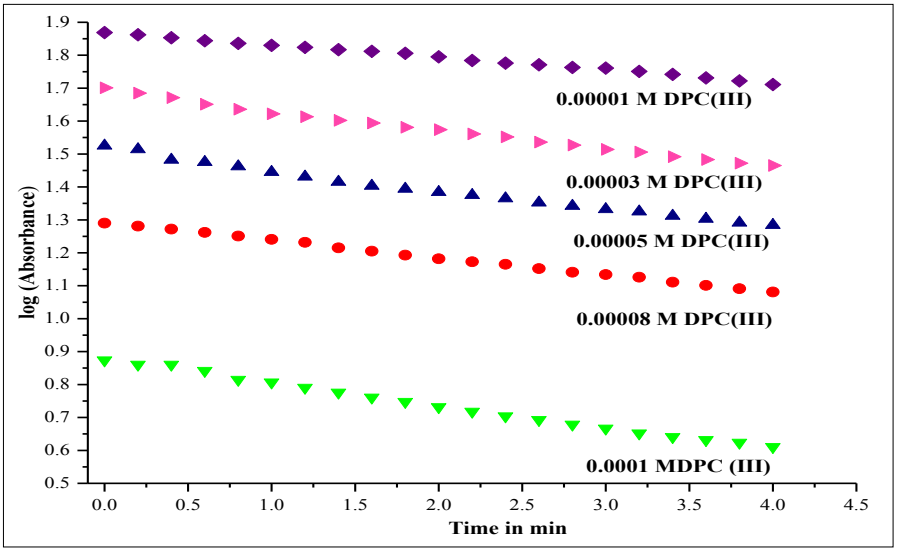

Figure 5: *Order Plot of log (Absorbance) vs. time [for each concentration of DPC (III)]*

Effects of [DPC (III)], [CRBC], and [KOH]

The pseudo-first-order process involving DPC (III) was confirmed by the linearity and nearly parallel

Table 2: *Co (III) catalyzed oxidation of carbenicillin by DPC (III) in an aqueous alkaline medium at 298 K and I = 0.10 / mol dm^{-3}: effect of variation of [DPC]*, [CRBC], $CoCl_3$, KIO_4, and [KOH]*

[DPC] x 10^5 M	[CRBC]x 10^4 M	[OH^-] x10^2 M	[IO_4^-] x10^5 M	[$CoCl_3$] x10^7 M	k_Ux10^4 (s^{-1})	k_Tx 10^3 (s^{-1})	k_Cx 10^3 (s^{-1})
1.0	5.0	0.8	1.0	5.0	1.20	1.47	1.35
3.0	5.0	0.8	1.0	5.0	1.30	1.49	1.36
5.0	5.0	0.8	1.0	5.0	**1.20**	**1.49**	**1.37**
8.0	5.0	0.8	1.0	5.0	1.30	1.48	1.35
10.0	5.0	0.8	1.0	5.0	1.10	1.45	1.35
5.0	**1.0**	0.8	1.0	5.0	0.40	0.50	0.46
5.0	**3.0**	0.8	1.0	5.0	0.80	1.03	0.95
5.0	**5.0**	0.8	1.0	5.0	**1.20**	**1.49**	**1.37**
5.0	**8.0**	0.8	1.0	5.0	1.80	2.01	1.83
5.0	**10.0**	0.8	1.0	5.0	2.30	2.61	2.38
5.0	5.0	**0.2**	1.0	5.0	0.60	0.72	0.66
5.0	5.0	**0.4**	1.0	5.0	0.80	0.98	0.90
5.0	5.0	**0.6**	1.0	5.0	1.00	1.19	1.09
5.0	5.0	**0.8**	1.0	5.0	**1.20**	**1.49**	**1.37**
5.0	5.0	**1.0**	1.0	5.0	1.60	1.85	1.69
5.0	5.0	0.8	**1.0**	5.0	**1.20**	**1.49**	**1.37**
5.0	5.0	0.8	**3.0**	5.0	1.0	1.39	1.29
5.0	5.0	0.8	**5.0**	5.0	0.90	1.05	0.96
5.0	5.0	0.8	**8.0**	5.0	0.70	0.82	0.75
5.0	5.0	0.8	**10.0**	5.0	0.60	0.71	0.65
5.0	5.0	0.8	1.0	**1.0**	1.20	0.46	0.34
5.0	5.0	0.8	1.0	**3.0**	1.20	1.03	0.91
5.0	5.0	0.8	1.0	**5.0**	**1.20**	**1.49**	**1.37**
5.0	5.0	0.8	1.0	**8.0**	1.20	2.07	1.95
5.0	5.0	0.8	1.0	**10.0**	1.20	2.61	2.49

* All solutions were prepared in mole dm^{-3}.

plots of log (Absorbance) vs. time which are in good agreement with Table 2 and Figure 5. Figure 6 represents the plot of (4+ log [CRBC]) vs. (4+ log k_c) vs. and declared that the catalyzed rate constants (k_c) increased as [CRBC] increased, and that the order of CRBC was 0.596 ($r \geq 0.9977$, $s \leq 0.00103$). Similarly, Figure 7 represents the plot of (4 + log k_c) vs. (2 + log [KOH]), and showed an increase in the values of catalyzed rate constants (k_c) as [KOH] increased , and thus the order of reaction with KOH was found to be 0.595 ($r \geq 0.9816$, $s \leq 0.004$).

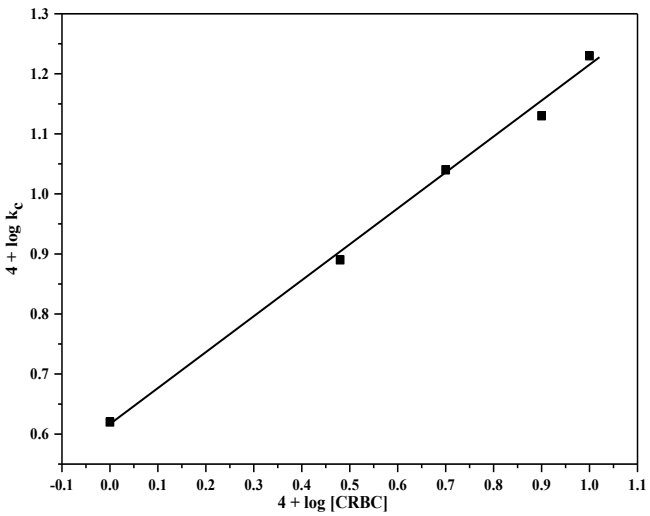

Figure 6: *Plot of 4 + log [CRBC] vs. 4 + log k_c*

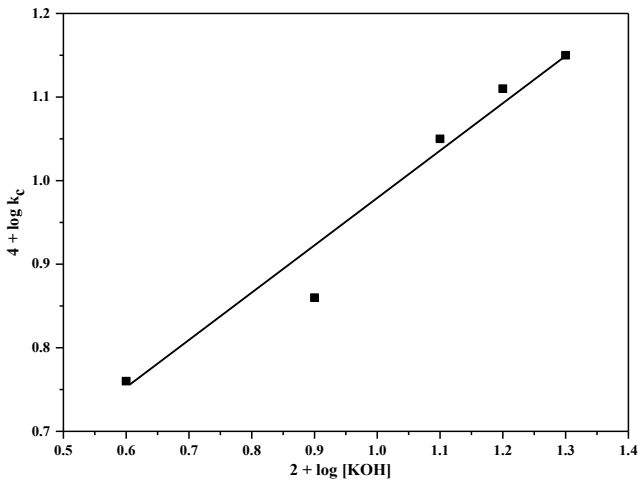

Figure 7: *Plot of 2 + log [KOH] vs.4 + log k_c*

Effects of [Periodate], dielectric constant (D), and ionic strength (I)

The rate constant decreased with a rise in [KIO_4] having an order of -0.488 ($r \geq 0.997$, $s \leq 0.0006$) which is represented in Figure 8 as a plot of 5 + log [KOI_4] vs. (4 + log k_c). The rate of reaction was not significantly impacted by an increase in ionic strength while the rate of the catalyzed reaction was unaffected by the dielectric constant.

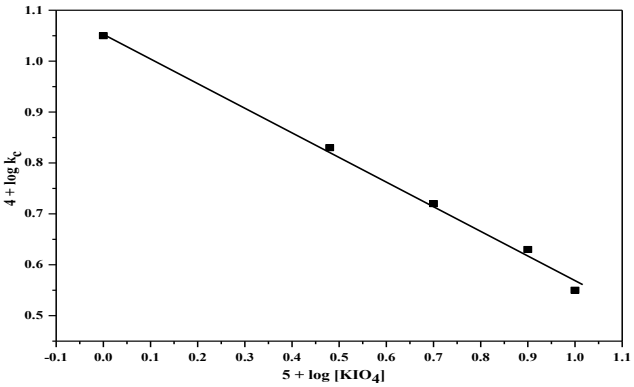

Figure 8: *Plot of 5 + log [KIO_4] vs. (4 + log k_c)*

Effect of Temperature

The temperature effect on carbenicillin oxidation rate was studied at variable temperatures and it was concluded that rate constants increased with a temperature rise. The smallest amount least square method supported to determine activation parameters from i) plots of catalyzed rate constants (Figure 9 and Table 3), ii) catalytic constants (Figure 10 and Table 4), and slow step rate constants (Figure 11 and Table 5). Finally, equilibrium constants were determined from verification plots whose slopes and intercepts supported in the determination of both activation in addition as thermodynamic parameters (Figures 12, 13, 14, and Tables 6, and 7 respectively).

Activation parameters concerning catalyzed rate constant (k_c) for CRBC

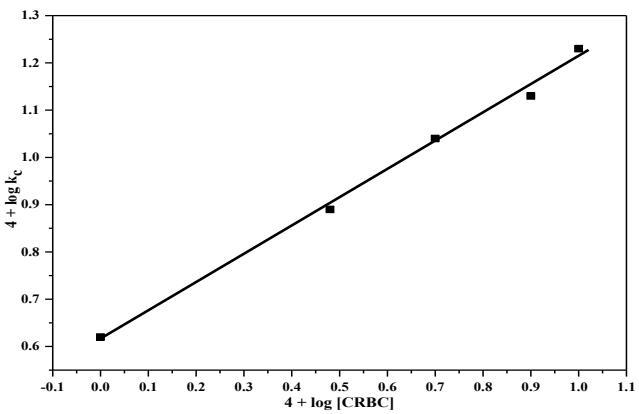

Figure 9: *Plot of 4 + log [CRBC] vs. 4 + log k_c]*

Table 3: *Activation parameters from k_c*

Activation Quantities	Values
Activation Energy	40.84 (k J/mol)
Enthalpy Change	38 ± 1 (k J/mol)
Entropy Change	-169 ± 3 (J/K/mol)
Free Energy Change	87 ± 2 (k J/mol)
Log A	4.3 ± 0.3

Activation parameters concerning catalytic constant (K_c) for CRBC

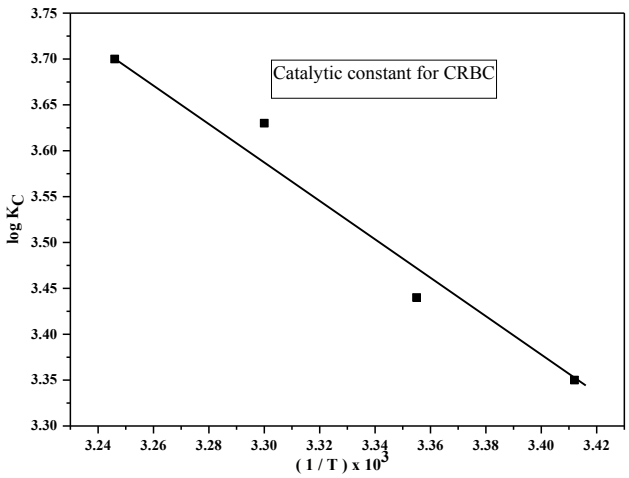

Figure 10: *Plot of (1 /T) x 10^3 vs. log* $\mathbf{K_c}$

Table 4: *Activation parameters from Kc*

Activation Quantities	Values
Activation Energy	43.095 (k J/mol)
Enthalpy Change	40 ± 1 (k J/mol)
Entropy Change	-163 ± 1 (J/K/mol)
Free Energy Change	89 ± $2^{\neq}$ (k J/ mol)
Log A	10.6 ± 0.2

Activation parameters concerning slow step rate constant (k) for CRBC

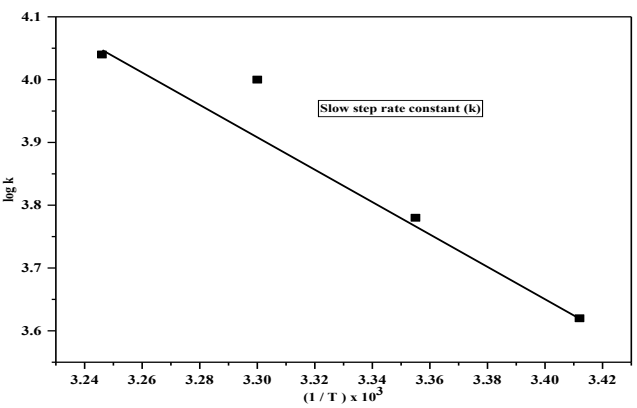

Figure 11: *Plot of (1 / T) x 10^3 vs. log k for CRBC*

Table 5: *Activation parameters from k*

Activation Quantities	Values
Activation Energy	51.53 (k J/mol)
Enthalpy Change	49 ± 2 (k J/mol)
Entropy Change	-8.6 ± 0.8 (J/K/mol)
Free Energy Change	49 ± 2 (k J/mol)
Log A	12.4 ± 0.4

DPC (III) functions both as a robust oxidant as well as a chelating agent at the same time. DPC (III) exists as $[Cu\ (H_3IO_6)_2]^-$ and $[Cu\ (H_2IO_6)\ (H_3IO_6)_2]^{2-}$ as equilibrium state in water due to its solubility where as MPC (III) can exist in the sort of $[Cu\ (H_2IO_6)\ (H_2O)_2]$ as the foremost active species for the current study as confirmed by mechanism.

Probable Mechanism of Catalyzed Oxidation of CRBC

An appropriate mechanism (Scheme 1) was proposed with engagement of all reacting species based on experimental evidence. First, DPC (III) combines with the hydroxide ions to produce its divalent anionic form that combines with water to produce MPC (III) and free periodate. The complex formation between the Co (III) catalyst and CRBC is thought to be the cause of the fractional order seen in relation to CRBC. Intermediate (A) is formed when an MPC (III) interacts with that complex by releasing the catalyst which further reacts with fresh MPC (III) to produce a new active intermediate (B) in the second step which finally reacts with another fresh MPC (III) resulting in the production of stable products (C) as 2-phenylmalonic acid ($C_9H_8O_4$), as well (D) as 2-(amino (carboxy) methyl)-5, 5-dimethyl-4, 5-dihydrothiazole-4-carboxylic acid-1-oxide ($(C_8H_{12}N_2O_4S)$).

The below mechanism (**Scheme 1**) supports the derivation of the rate law equation [34] for the catalytic oxidation of carbenicillin as-

$$\text{From Scheme 1, rate} = -\mathrm{d}\frac{[\mathrm{CRBC}]}{\mathrm{dt}} = \mathrm{k(Complex)}$$

$$= \mathrm{k\,K_1K_2K_3}\frac{[\mathrm{CRBC}][\mathrm{OH^-}][\mathrm{Co(III)}][\mathrm{DPC}]}{[\mathrm{H_3IO_6}]^{2-}} \qquad \ldots(1)$$

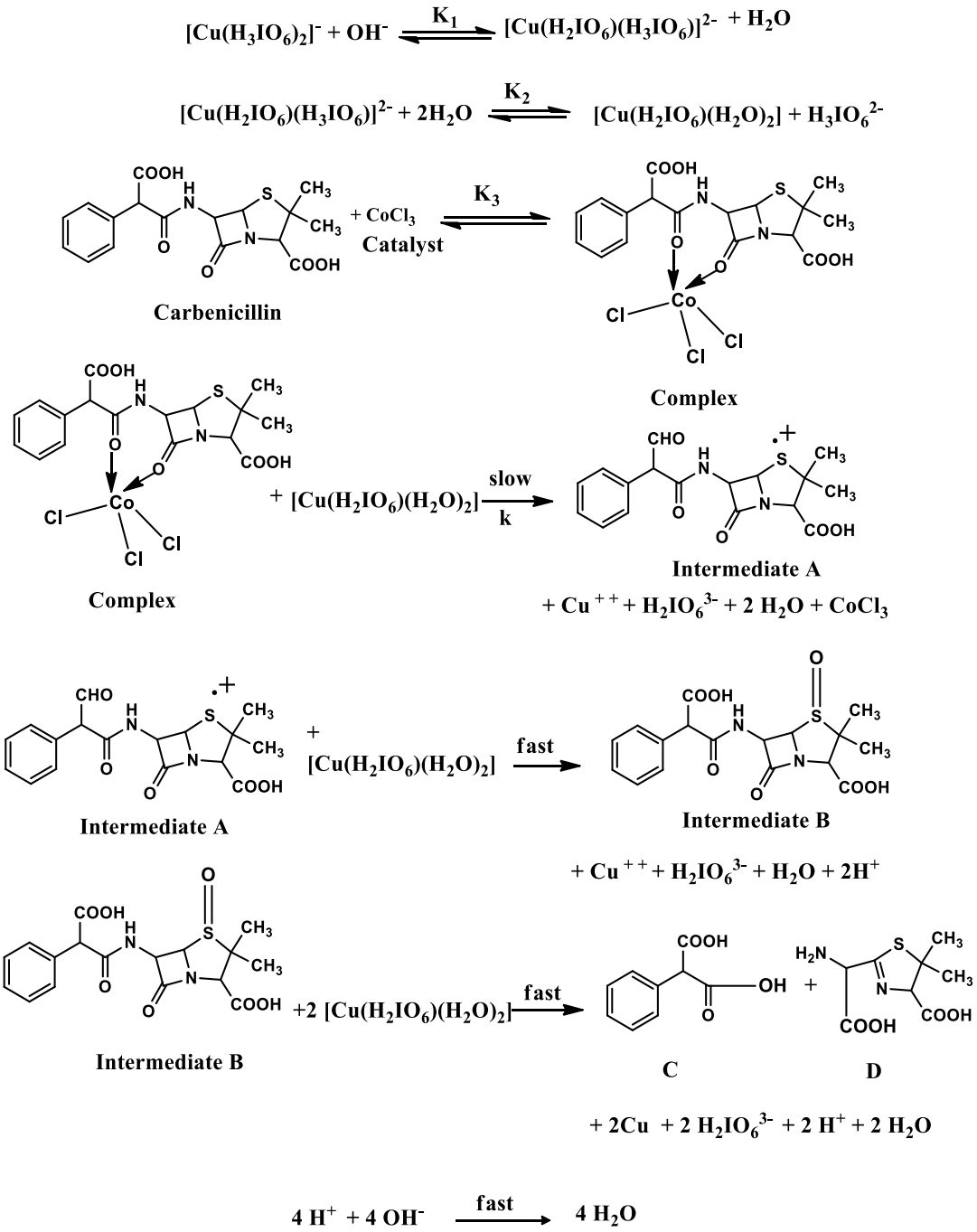

Scheme 1: *Carbenicillin oxidation by DPC (III) and Co (III)*

The total concentration of DPC can be given as

$$[DPC]_T = [DPC]_f + [Cu(H_2IO_6)(H_3IO_6)]^{2-} + [Cu(H_3IO_6)_2(H_2O)_2]^{2-}$$

$$[DPC]_f \left[\frac{K_1K_2[OH^-] + [H_3IO_6]^{2-} + K_1[OH^-][H_3IO_6]^{2-}}{[H_3IO_6]^{2-}}\right]$$

$$[DPC]_f = \left[\frac{[DPC]_T[H_3IO_6]^{2-}}{K_1K_2[OH]^- + [H_3IO_6]^{2-} + K_1[OH^-][H_3IO_6]^{2-}}\right] \quad \ldots(2)$$

Similarly, $[CRBC]_T = [CRBC]_f + [C]$

$= [CRBC]_f + K_3[CRBC]_f[Co(III)] = [CRBC]_f[1 + K_3[Co(III)]$

Here, **'T'** stands for total molarity and **'f'** stands for free molarity of related species.

Owing to quite lower molarities of AMP and $CoCl_3$

$[CRBC]_T = [CRBC]_f$, $[OH^-]_T = [OH^-]_f$ … (3)

$$\text{And } [H_3IO_6^{2-}]_T = [H_3IO_6^{2-}]_f \quad \ldots (4)$$

$$[Co(III)_T] = [[Co(III)_f] + [C]$$

$$= [Co]_f + K_3[CRBC][Co(III)_f]$$

$$[Co(III)]_f = \left[\frac{[Co(III)_T]}{1 + K_3[CRBC]}\right] \quad \ldots. (5)$$

Substituting values of eqⁿ (2), (3), (4), and (5) in eqⁿ (1), we get

$$\text{rate} = -\frac{d[DPC]}{dt}$$

$$= \frac{kK_1K_2K_3\,[CRBC][Co(III)][DPC][OH]}{K_1K_2[OH]^- + [H_3IO_6]^{2-} + K_1[OH]^-[H_3IO_6]^{2-} + K_1K_2K_3[CRBC][OH]^-} \quad \ldots. (6)$$

After rearrangement, we get

$$\frac{1}{k_{obs}} = \frac{[H_3IO_6]^{2-}}{kK_1K_2K_3[OH]^-[CRBC]} + \frac{[H_3IO_6]^{2-}}{kK_2K_3[CRBC]} + \frac{1}{kK_3[CRBC]} + \frac{1}{k} \quad \ldots (7)$$

Verification plots

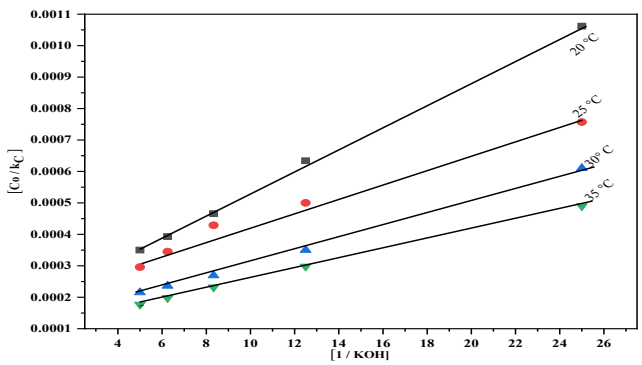

Figure 12: *Plot of 1/[KOH] vs. [Co/k_c]*

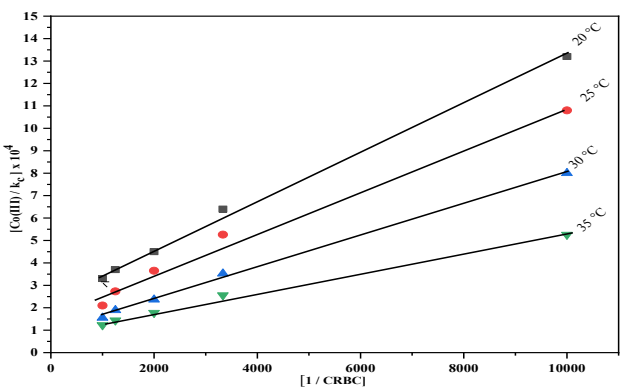

Figure 13: *Plot of 1/[CRBC] vs. [Co/k_c]*

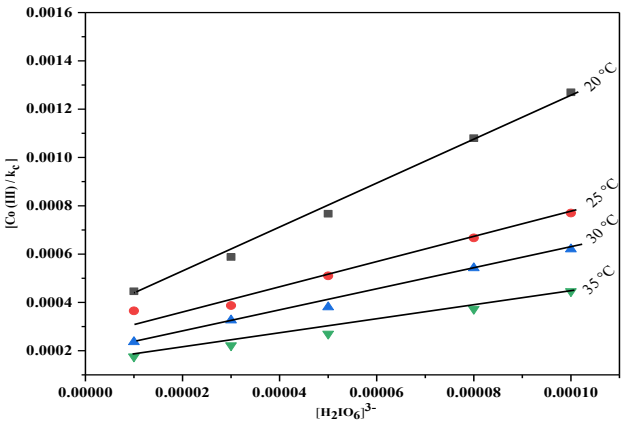

Figure 14: *Plot of $[H_2IO_6]^{3-}$ vs. [Co/k_c]*

The verification plots are shown above in Figures (12, 13, and 14). In accordance with equation (7), the plots of [Co (III)/k_c] vs.1/[KOH] ($r \geq 0.9996, \leq s\ 0.0012$), [Co (III)/$k_c$] vs. 1/[CRBC] ($r \geq 0.998, \leq s\ 0.0085$), and [Co (III)/$k_c$] vs. $[H_2IO_6]^{3-}$ ($r \geq 0.997, s \leq 0.0002$), and are found linearly as shown in Figures 12, 13, and 14 respectively.

Table 6: *Slow step rate constant (k) and equilibrium constants for Co (III) catalyzed oxidation of CRBC*

Equilibrium Constants ↓	**Absolute Temperatures**			
Temperature →	20 °C	25 °C	30 °C	35 °C
k x 10^4	4.1928	6.1349	10.214	11.033
K_1	1.35	2.168	2.638	3.365
K_2 x 10^{-4}	0.905	1.243	1.39	2.20
K_3 x 10^4	5.470	2.734	2.160	1.934

Table 7: *Thermodynamic Parameters for Co (III) catalyzed Oxidation of CRBC*

Thermodynamic Quantities	**Values from K_1**	**Values from K_2**	**Values from K_3**
ΔH°_{298} (k J mol^{-1})	44.41	41.9	-50.91
ΔS°_{298} (J K^{-1} mol^{-1})	154.59	161.24	-103.17
ΔG°_{298} (k J mol^{-1})	-1.66	-6.15	-20.16

Conclusions

Experimental research was completed in an alkaline media on the carbenicillin by DPC (III) that was accelerated by Co (III). For the title study, MPC (III) was confirmed as the primary active species in the form of [Cu (H_2IO_6) (H_2O) $_2$]. Different activation parameters were calculated by using the software Origin 9.6 (2017). Similar to that,

equilibrium constants were determined at various four temperatures and thermodynamic characteristics pertaining to equilibrium constants were also calculated. A comparison between the uncatalyzed and catalyzed oxidation of Carbenicillin showed an overall increment in the rate of Carbenicillin oxidation, in addition to a major increment in numerous rate constants as well as equilibrium constants ($\mathbf{K_1}$, and $\mathbf{K_2}$) while the third equilibrium constant ($\mathbf{K_3}$) showed a slight decrement. Values of thermodynamic parameters increased overall. The values obtained for activation parameters for both the uncatalyzed as well as catalyzed oxidation of Carbenicillin were slightly increased. All experimental evidence, including the results of products, spectral and elemental analysis, mechanism, reaction order plot, and kinetic studies, support and confirm the certainty of overall sequences presented here.

Acknowledgments

The first author (YRS) would like to acknowledge Purwanchal Campus, Dharan for providing financial support, Surface Chemistry Laboratory of MMAM Campus, Biratnagar for providing double beam UV-Visible spectrophotometer, STIC (Cochin), CDRI-CSIR (Lucknow), SAIF (Mumbai), India for providing LC-MS and FT-IR spectral data as well as National Research Foundation (NRF), Birgunj for providing melting point data.

REFERENCES

[1] G. D. Wright, The antibiotic resistome: the nexus of chemical and genetic diversity, *Nat. Rev. Microbiol.,* 2007, 5, 175-186. (DOI: 10.1038/nrmicro1614)

[2] M. Golchin, M. Khani, M. Sadani, M. Sadeghi, & M. Jahangiri-rad,Occurrence and Fate of Amoxicillin and Penicillin G Antibiotics in Hospital Wastewater Treatment Plants: A Case Study -Gonbad Kavous, Iran, *South African Journal of Chemistry*, 2021, 75, 98-105. (https://doi.org/10.17159/0379-4350/2021/v75a11)

[3] Z. Wang, Xi-Hui Zhang, Y. Huang, & H. Wang, Comprehensive evaluation of pharmaceuticals and personal care products (PPCPs) in typical highly urbanized regions across China, *Environmental Pollution*, 2015, 204, 223-232, ISSN 0269-7491, (DOI: 10.1016/j.envpol.2015.04.021)

[4] D. Fatta-Kasiiinsons, S. Meric, and A. Nikolaun, Pharmaceutical residues in environmental waters and wastewater: current state of knowledge and future research. *Anal Biocanal. Chem*, 2011, 399, 251-275. (DOI: 10.1017/s00216-010-4300-9)

[5] M. Zhuang, Y. Achmon, Y. Cao, X. Liang, L. Chen, H. Wang, B. A. Siame, & K. Y. Leung, Distribution of antibiotic resistance genes in the environment, *Environmental Pollution,* 2021, 285,117402. (DOI: 10.1016/j.envpol.2021.117402)

[6] M. Haenni, C. Dagot, O. Chesneau, D. Bibbal, J. Labanowski, M. Vialette, D. Bouchard, F. Martin-Laurent, L. Calsat, S. Nazaret, F. Petit, A. M. Pourcher, A. Togola, M. Bachelot, E. Topp, & D. Hocquet, Environmental contamination in a high-income country (France) by antibiotics, antibiotic-resistant bacteria, and antibiotic resistance genes: Status and possible causes. *Environ Int*., 2022. (DOI: 10.1016/j.envint.2021.107047)

[7] A. Booth, D. S. Aga, & A. L. Wester, Retrospective analysis of the global antibiotic residues that exceed the predicted no effect concentration for antimicrobial resistance in various environmental matrices, *Environ Int*., 2020. (DOI: 10.1016/j.envint.2020.105796)

[8] A. R. Bracamontes-Ruelas, L. A. Ordaz-Díaz. A. M. Bailón-Salas, J. C. Ríos-Saucedo, Y. Reyes-Vidal, & L. Reynoso-Cuevas, Emerging Pollutants in Wastewater, Advanced Oxidation Processes as an Alternative Treatment and Perspectives, *Processes*, 2022, 10, 1041. (DOI: 10.3390/pr10051041)

[9] R. Andreozzi, R. Marotta, & N. Paxeus, Antibiotic Removal from Wastewaters: The Ozonation of Amoxicillin, *Journal of hazardous materials*, 2005, 122, 243-250. (DOI: 10.1016/j.jhazmat.2005.03.00)

[10] P. P. Marcinowski, J. P. Bogacki, and J. H. Naumczyk, Cosmetic wastewater treatment using the Fenton, Photo-Fenton and H_2O_2/UV processes, *Journal of Environmental Science and Health, Part A*, 2014,49(13):1531–1541. (DOI: 10.1080/10934529.2014.938530)

[11] E. L. Chang, C. Simmers, & D. A. Knight, Cobalt Complexes as Antiviral and Antibacterial Agents. *Pharmaceuticals*, 2010, 3 (6), 1711–1728. (DOI: 10.3390/ph3061711)

[12] C. V. Hiremath, S. D. Kulkarni, and S. T. Nandibewoor, Oxidation of-Leucine by Alkaline Diperiodatoargentate (III) Deamination and Decarboxylation: A Kinetic and Mechanistic Study, *Industrial & Engineering Chemistry Research,* 2006, 45 (24), 8029–8035. (DOI: 10.1021/ie060612d)

[13] A. M. Angadi, & S. Tuwar, Oxidation of Fursemide by Diperiodatocuprate (III) in Aqueous Alkaline Medium—a Kinetic Study, *Journal of Solution Chemistry*, 2010, 39, 165-177. (DOI: 10.1007/s10953-009-9492-2)

[14] A] J. I. Gowda, R. M. Hansabaratti, Nandini A. Paattanash, & S. T. Nandibewoor, Oxidation of glycine by Diperiodatocuprate (III) in aqueous alkaline medium, *Indian Journal of Chemistry*, 2013, 52, 200-206.

[14] B] Z. Ahmad, M. Asghar, S. Ali, N. Munawar, A. Nabi, & M. Yaqoob, Flow Injection Determination of Asparagine and Histidine Using Diperiodatocuperate Based on Spectrophotometric Inhibition Detection in Amino Acid Supplements, *Indo Am. J. P. Sci*., 2017; 4(11). ISSN: 2349-7750. (DOI: 10.5281/zenodo.1048813)

[15] S. A. Chimatadar, T. Basavaraj, and S. T. Nandibewoor, A study of the kinetics and mechanism of oxidation of L-tryptophan by diperiodatonickelate (IV) in aqueous alkaline medium, *Russ. J. Phys. Chem*, 2007, 81, 1046–1053. (DOI: 10.1134/S0036024407070072)

[16] M. W. Lister. The stability of some complexes of trivalent copper*, Canadian Journal of Chemistry*, 1953; 31(7):638-652. (DOI: 10.1139/v53-087)

[17] S. Nadimpalli, J. Padmavathy, & K. K. M. Yusuff, Determination of the nature of the diperiodatocuprate (III) species I aqueous alkaline medium through a kinetic and mechanistic study on the oxidation of iodide ions*, Transition Metal Chemistry*, 2001, 26 (3): 315-321. (DOI: 10.1023/A:1007116932047)

[18] B. Chowdhury, M. H. Mondal, M. K. Barman, and B. Saha, A study on the synthesis of alkaline Copper (III) periodate (DPC) complex with an overview of its redox behavior in aqueous micellar media, *Research on Chemical Intermediates (Springer*), 2018. (DOI: 10.1007/S11164-018-3643-2)

[19] C. B. Smith, & M. Finland, Carbenicillin: Activity in vitro and absorption and excretion in normal young men, *Applied Microbiology*, 1968, 16, 1753-1760, American Society for Microbiology.

[20] K. Butler, A. R. English, V. A. Ray, & A. E. Timereck, Carbenicillin: Chemistry and mode of action*, The Journal of Infectious Diseases,* 1970, *122, (issue supplement 1), S1-S8.* (DOI: 10.1093/infdis/122.Supplement_1.S1)

[21] A. R. English, J. A. Retsema, V. A. Ray, & J. E. Lynch, Carbenicillin Indanyl Sodium, An Orally Active Derivative Of Carbenicillin, *Antimicrobial Agents And Chemotherapy*, 1972, 1(3), 185-191. American Society for Microbiology.

[22] J. T. da Silva, & S. Fukai, The impact of carbenicillin, cefotaxime, and vancomycin on chrysanthemum and tobacco TCL morphogenesis and Agrobacterium growth, *J. Appl. Hort*., 2001, 3. (DOI: 10.37855/jah.2001.v03i01.01)

[23] K. Marta, F. Rafal, & F. Magdalena, Hydrolysis of Penicillin G and Carbenicillin in Pure Water - As Studied by HPLC/ESI-MS, *Mass Spectrometry Letters*, 201910, 4, 108-111. (DOI: 10.5478/MSL.2019.10.4.108)

[24] T. C. Eickhoff, In vitro effects of carbenicillin combined with gentamycin or polymyxin B against Pseudomonas aeruginosa, *Appl Microbiol*, 1969, 18 (3), 469-473. PMID: 4313764; PMCID: PMC378006

[25] M. I. Marks, R. Prentice, R. Swarson, E. K. Cotton, & T. C. Eickhoff, Carbenicillin and gentamicin: Pharmacologic studies in patients with cystic fibrosis and pseudomonas pulmonary infections, *The Journal of Paediatrics,* 1971, 79, 5, 822-828, 1971. (DOI: 10.1016/S0022-3476(71)80401-8)

[26] H. A. Holt, J. M. Broughall, M. McCarthy, and D. S. Reeves, Interactions between Aminoglycoside Antibiotics and Carbenicillin or Ticarcillin, *Infection*, 1976, 4 (2), 107–109. (DOI: 10.1007/BF01638726)

[27] B. Lynn, Administration of carbenicillin and ticarcillin-pharmaceutical aspects, *European Journal of Cancer* (1965), 1973, 9 (6), 425-433. (DOI: 10.1016/0014-2964 (73)90107-2)

[28] N. Rosdahl, & V. F. Thomsen, Activity of carbenicillin against gram negative rods compared with that of penicillin, ampicillin, and cephalosporins, *Chemotherapy*, 1970, 15, 137-147. (DOI: 10.1159/000220677)

[29] Y. R. Sahu, & P. Mishra, Kinetics and Mechanism of Oxidation of Carbenicillin by Copper (III) Periodate Complex in Aqueous Alkaline Medium, *Journal of Chemistry (Hindawi*), 2020, Article ID 4060984, 13 pages. (DOI: 10.1155 2020 4060984)

[30] G. P. Panigrahi & P. K. Misro, Kinetics and mechanism of oxidation of osmium (VIII) catalyzed oxidation of unsaturated acids by sodium periodates, *Indian Journal of Chemistry*, 1977, 15A,1066–1069.

[31] P. K. Jaiswal, & K. L. Yadava, Determination of sugars and organic acids with periodato complex of Cu (III), *Indian Journal of Chemistry*, 1973, 11, 837-838.

[32] G. P. Panigrahi, & A. C. Pathy, Kinetics and mechanism of oxidation of potassium thiocyanate by the Potassium Bis(tellurato)cuprate (III), *Indian Journal of Chemistry*, 1986, 25A, 354-357.

[33] K. C. Ingham, On the application of Job's method of continuous variation to the stoichiometry of protein-ligand complexes, *Analytical Biochemistry*, 1975, 68 (2), 660–663. (DOI: 10.1016/0003-2697 (75)90666-1)

[34] A] L. Michaelis, & M. Menten, Die kinetik der invertinwirkung, *Biochemistry Zeitung,* 1913, 79, 333-369.

[34] B] B. Srinivasan, A Guide to the Michaelis-Menten equation: Steady state and beyond, *The FEBS Journal*. 289, 20, 6086–6098. (DOI: 10.1111/febs.16124)

Hindawi
Journal of Chemistry
Volume 2020, Article ID 4060984, 13 pages
https://doi.org/10.1155/2020/4060984

Research Article

Kinetics and Mechanism of Oxidation of Carbenicillin by Copper (III) Periodate Complex in Aqueous Alkaline Medium

Yuv Raj Sahu and Parashuram Mishra

Bio-Inorganic and Materials Chemistry Research Laboratory, Department of Chemistry, Mahendra Morang Adarsha Multiple Campus, Biratnagar, Tribhuwan University, Nepal

Correspondence should be addressed to Parashuram Mishra; prmmishra@rediffmail.com

Received 4 May 2020; Accepted 14 May 2020; Published 6 June 2020

Academic Editor: Leonardo Palmisano

Kinetics and mechanism of oxidation of carbenicillin by diperiodatocuprate [DPC-III] in aqueous alkaline medium were studied spectrophotometrically at 298 K and an ionic strength of 0.10 mol·dm^{-3}. The reaction between DPC (III) and carbenicillin in the alkaline medium showed (CRBC : DPC-III) 1 : 4 stoichiometry. The reaction products were identified by the CHNS test, FT-IR, and LC-MS spectral reports. The reaction was of pseudo-first order with respect to DPC (III) and fractional order with respect to carbenicillin as well as alkali but retarding effect with respect to periodate. Monoperiodatocuprate (MPC-III) was found to be the main active species in the alkaline medium in the form of [Cu (H_2IO_6) (H_2O)$_2$]. Activation and thermodynamic parameters with respect to uncatalyzed rate constants (k_u) and slow step rate constant (k) as well as equilibrium constants were determined. The plausible mechanism consistent with experimental results was proposed and discussed in detail.

1. Introduction

Penicillanic acid derivatives (PADs) are composed of beta lactam ring and thiazolidine ring as the integral part which have growing demands in daily life, medicines, health tonics, etc. [1]. Carbenicillin, one of the PADs, is the 4th generations' semisynthetic [2] analogue of naturally occurring benzyl-penicillin with carboxyl and benzyl group penicillin which is synthesized from the 6-aminopenicillanic acid nucleus, discovered at Beecham as "Pyopen." It is active against *Pseudomonas aeruginosa* in vitro [3] and hence used successfully in the treatment of pseudomonal infections [4–6] due to sensitivities of many strains of *P. aeruginosa* to carbenicillin within a reasonably narrow range of concentrations which can be safely obtained in vivo [7]. It is an acid liable antibiotic that inhibits bacterial cell wall synthesis and is commonly used in place of ampicillin to reduce the production of satellite colonies. It is more stable than ampicillin at low pH, which usually arises during bacterial fermentation.

It is soluble in water (solubility 451 mg/L). Its molecular formula, molar mass, and IUPAC name are $C_{17}H_{18}N_2O_6S$, 378.401 g mol^{-1}, and (2S, 5R, 6R)-6-{[carboxy (phenyl) acetyl] amino}-3,3-dimethyl-7-oxo-thia-1-azabicyclo [3.2.0] heptanes-2-carboxylic acid or 6-(a-carboxy-phenyl acetamido) penicillanic acid), respectively. Its structure is given in Figure 1.

Ampicillin, amoxicillin, dicloxacillin, carbenicillin, tetracycline, etc. belong to PADs family that are widely applied in hospitals, households, sewages [8], veterinary drugs, cosmetics [9], and fragrances or nutraceutical products [10] against different diseases to improve quality of personal health for the whole ecosystem. Characteristics, distribution, and source analysis of the main persistent toxic substances in karst groundwater have been reported [11]. These PADs do not degrade and mix into aquatic environment directly/indirectly, accumulate in natural water reservoirs, and contaminate drinking water, discharge or wastes, surface water, and ground water as well as air and soil. These effects enhance bacterial or viral resistance [12, 13] against different

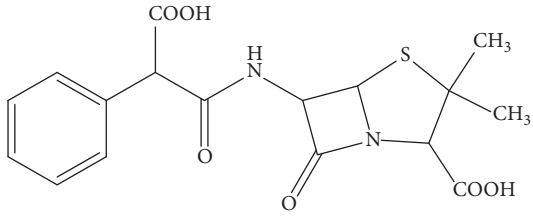

Figure 1: Carbenicillin.

PADs, and hence, it is a great challenge before researchers and drug manufacturers [14] to modify their composition along with updated specific function with a view to get fast relief from the illness. Personal care products (PCPs) [15–17] and antibiotic resistance represent a serious health problem, and different advanced oxidation processes (AOPs) have to be applied to degrade such emergent chemical pollutants [18–20] because most of the intermediates, formed transiently, can be definitely mineralized into CO_2, water, and mineral species due to possible oxidation-degradation reactions. The proposed work will disclose a novel application in the field of pharmaceuticals as well as kinetics for degradation of drugs and will be adequately applied in wastewater treatment at the sites polluted by PADs antibacterial agents.

Transition metals can form stable complexes with polydentate ligands such as diperiodatocuprate (DPC-III) [21, 22], diperiodatoargentate (DPA-III) [23], diperiodatonickelate (DPN-IV) [24], ditelluratocuprate (DTC-II) [25, 26], and hexacyanoferrate (HCF-III) [27]. At first, Malatesta had synthesized DPC (III) more than a half century ago, and Panigrahi and Pathy [28] followed that method. Determination of the nature of the diperiodatocuprate (III) species in the aqueous alkaline medium through a kinetic and mechanistic study on the oxidation of iodide ion has been reported in the previous literature [29]. DPC (III) has a square planar geometry with dsp^2 hybridization and diamagnetic nature. Cu (III) appears as an active intermediate species in many electron transfer reactions [30] and supports to know the role of Cu (III)/Cu (II) couple, as described in earlier literature [31]. Review of literature regarding carbenicillin is quite scanty. Only limited previous literature studies could have been included herewith. Some studies are voltammetric oxidation of carbenicillin and its electroanalytical applications at gold electrode [32], in vitro effects of carbenicillin combined with Gentamicin or polymyxin B against Pseudomonas aeruginosa [33], interactions of carbenicillin and Ticarcillin with gentamicin [34], interaction between aminoglycoside antibiotics and carbenicillin or ticarcillin [35], effect of time and concentration upon interaction between gentamicin, tobramicin, netilmicin, or amikacin and carbenicillin or ticarcillin [36], in vivo inactivation of gentamicin by carbenicillin and ticarcillin [37], administration of carbenicillin and ticarcillin-pharmaceutical aspects [38], Carbenicillin and ticarcillin [39], synergy between Ticarcillin and Tobramycin against *Pseudomonas aeruginosa* and enterobacteriaceae in vitro and in vivo [40], Carbenicillin administration in patients with severe renal failure [41], etc.

The present research work aimed to investigate the kinetics and mechanism of oxidation of carbenicillin without any catalyst and thence to arrive at plausible mechanism including determination of order of reaction, activation, and thermodynamic properties with respect to uncatalyzed rate constant (k_u), slow step rate constant (k), and equilibrium constants (K_1, K_2, and K_3) at different temperatures.

2. Materials and Methods

2.1. Reagents and Chemicals. Chemicals used were of Analytical Reagent (AR) grade and double distilled water was used throughout the work. The stock solution of carbenicillin (Sigma Aldrich (0.01 mol·dm^{-3})) was prepared by dissolving 0.378 g of recrystallized carbenicillin in 100 ml double distilled water. Potassium periodate solution was prepared by dissolving 0.023 g (0.01 mol·dm^{-3}) of KIO_4 (Sigma Aldrich) in 100 ml double distilled hot water and the solution was used only after 24 hours. The concentration of the potassium periodate solution was determined by the iodometric method [42].

2.2. Instrumentation. The pH of the solution was measured by ELICO LI 613 pH meter. The electronic absorption spectra were recorded on Varian CARY 5000 UV-VIS spectrophotometer in the range of 200–1000 nm. The infrared spectra of the complexes were recorded on Thermo Nicolet, Avatar 370 FT-IR spectrometer, in the range of 4000–400 cm^{-1} that was run as KBr disc. The mass spectrum of the products was recorded on the UPLC-TQD mass spectrometer in the positive mode in the range of 0–1000 m/z.

2.3. Synthesis of Reagents. (DPC-III) was prepared [43, 44] by mixing copper sulphate (3.54 g), potassium periodate (6.80 g), potassium persulphate (2.20 g), and potassium hydroxide (9.0 g) in a 250 ml double distilled water in a RB flask. After collecting all chemicals, the whole mixture was frequently shaken thoroughly and heated on a hot plate for about 2 hours. As the mixture turned to intense red, the flask was heated again further for 20 minutes to remove potassium persulphate completely from the mixture by decomposing persulphate. After completion of the reaction, the mixture was cooled and filtered through sintered glass crucible G-4 and the dark red-brown solution was diluted to 250 ml by adding double distilled water. The aqueous solution of DPC (III) was standardized by iodometric titration ($Na_2S_2O_3$, starch, KI, and KH_2PO_4) by the thiocyanate method, and its exact concentration was ascertained. The existence of DPC (III) was verified by using a UV-visible spectrophotometer that showed an absorption band with a maximum peak at 415 nm. However, the accurate concentration of DPC was calculated by using a UV-visible spectrophotometer. Similarly, KOH (BDH) and the other required solutions were prepared and stored safely. A study on the synthesis of alkaline copper (III) periodate (DPC) complex with an overview of its

redox behavior in aqueous micellar media including stability and redox nature of Cu (III) periodate complex in a microheterogeneous environment has been reported in the recent literature [45].

2.4. Synthesis of Complex. 10 ml of carbenicillin solution (0.132 mol·dm^{-3}) was taken in a 100 ml RB flask. To this, 10 ml DPC (III) (0.528 mol·dm^{-3}) was mixed in 1 : 4 stoichiometric ratio along with 1.0 ml of KNO_3 (HiMedia) and KIO_4 (Sigma Aldrich) and 2.0 ml of KOH (HiMedia) solution of fixed molarities and stirred on a hot plate followed by restirring during refluxing with condensation for 24 hours. Then, the mixture was cooled naturally for 3 days and filtered by using a Whatman No. 1 filter paper. The products were purified and recrystallized in ethanol till the whole solvent evaporated, leaving behind crystals only. The appearance of peaks in UV-visible spectrophotometer showed the formation of the complex. The possible structures of DPC (III) and MPC (III) are given in Figure 2.

2.5. Kinetic Measurements. Since the reaction is very fast, its absorbance was taken quite rapidly along with the progress of the reaction by following pseudo-first-order state when the active mass of CRBC was greater than that of DPC (III) at 20°C, 25°C, 30°C, and 35°C ± 0.1°C unless specified. The reaction was initiated by mixing required quantities of previously thermostated solutions of CRBC into DPC (III) that already contained a definite concentration of KIO_4 along with KNO_3 and KOH. Data were obtained from a UV-visible spectrophotometer at pH (9.0–9.2) and 415 nm wavelength due to DPC (III) by monitoring the decrease in absorbance at the molar extinction coefficient (€) of 6144 ± 50 dm^3·mol^{-1}·cm^{-1}. The UV-visible spectrophotometer was run up to 85% reaction wherein initially added products and dielectric constant did not exhibit any interference in the reaction. There was no effect of ubiquitous contamination of initially added carbonate in the reaction. Fresh solutions were nevertheless used to carry out each kinetic run. Regression analysis of experimental data to obtain regression coefficient (r) and standard deviation(s) of points from the regression line was completed with the help of Origin 9.6 (2017) software. Plots of log (abs) versus time gave a straight line and hence uncatalyzed rate constants (k_u) were calculated from slopes. The k_u values agreed within ±5% error and were the average of at least three independent kinetic runs. A constant concentration of periodate was mixed into reaction mixture all the time. Finally, the total concentrations of KIO_4 and KOH were determined by assuming the amount present in DPC (III) and added additionally. No significant changes could be observed by conducting kinetics into nitrogen gas atmosphere with a view to check the effect of periodate, ionic strength, dissolved oxygen, added carbonate, etc. The application of Beer–Lambert's law was verified from plot of absorbance vs. [DPC-III], presented in Figure 3 ($r \geq 0.999$, $s \leq 0.0003$), and it was found that negligible interference was entertained in the

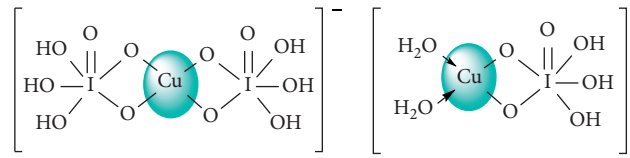

$[Cu(H_3IO_6)_2]^-$
Diperiodatocuprate (DPC)
(a)

$[Cu(H_3IO_6)(H_2O)_2]$
Monoperiodatocuprate (MPC)
(b)

Figure 2: Structure of (a) DPC (III) and (b) MPC (III).

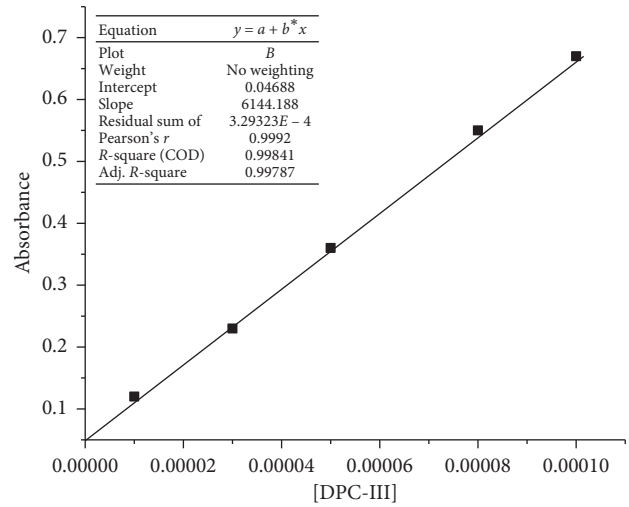

Figure 3: Plot of absorbance vs. [DPC] at 25°C.

reaction. The maximum wavelength of DPC (III) was noticed at 415 nm.

3. Results and Discussion

3.1. Stoichiometry and Product Analysis. Several sets of reaction mixtures with varying ratio of DPC (III) to CRBC in presence of constant amounts of KOH and KNO_3 were kept for 2.5 hours in a closed vessel under N_2 atmosphere and the remaining concentration of DPC (III) was analyzed to confirm the accurate stoichiometry by Job's method which was confirmed to be 1 : 4 for CRBC : DPC. When CRBC reacts with DPC (III) in alkaline medium, 2-phenylmalonic acid ($C_9H_8O_4$) and 2-(amino (carboxy) methyl)-5, 5-dimethyl-4, 5-dihydrothiazole-4-carboxylic acid-1-oxide ($C_8H_{12}N_2O_4S$) were formed as the main products which were recrystallized from ethanol, separated by Column Chromatography over neutral alumina by using 80% benzene and 20% chloroform as eluent. Side product CO_2 was qualitatively detected by bubbling N_2 gas through the acidified reaction mixture and passing the gas liberated through the tube filled with lime water.

The reaction between carbenicillin and diperiodatocuprate (III) in alkaline medium is given as

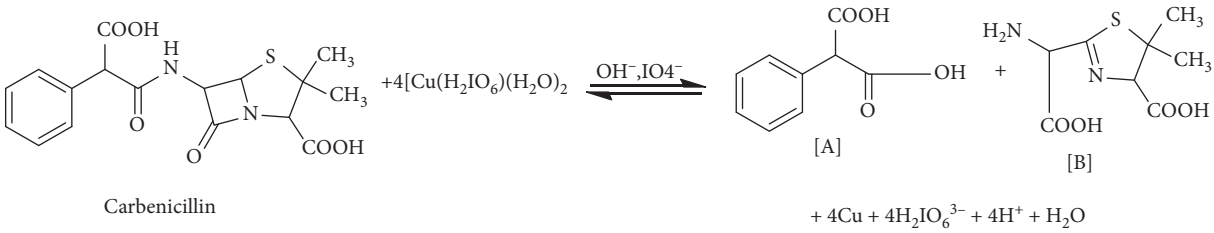

Carbenicillin

Here, *A* is 2-phenylmalonic acid ($C_9H_8O_4$) and *B* is 2-(amino (carboxy) methyl)-5, 5-dimethyl-4, 5-dihydrothiazole-4-carboxylic acid-1-oxide ($C_8H_{12}N_2O_4S$).

Scheme 1. Reaction showing the formation of complex.

The FT-IR and LC-MS are presented in Figures 4 and 5, respectively.

Both complex and products were characterized by LC-MS, which gave m/z at 703 for complex ($C_{17}H_{24}CuIN_2O_6S$): the first product (2-phenylmalonic acid) gave m/z at 182 (m + 2) and the second product (2-(amino (carboxy) methyl)-5, 5-dimethyl-4, 5-dihydrothiazole-4-carboxylic acid-1-oxide) at 232 (m + 1), respectively. A sharp absorption peak was at 1641.2 cm^{-1} (due to ketonic/carboxylic C=O stretch), 1464.4 and 1386.6 cm^{-1} (due to CH_3 stretch), 3413.5 cm^{-1} (due to carboxylic OH group), and 1276.7 cm^{-1} (due to carboxylic C=O stretch) and a broad peak was at 3380.7 cm^{-1} (due to N-H stretching). The MPC (III)-CRBC complex ($C_{17}H_{24CuI}N_2O_{14}S$) showed % elemental analysis as C-29.05 (28.78), H-3.44 (3.39), Cu-9.04 (9.14), I-18.05 (18.16), N-3.99 (4.08), and S-4.54 (4.28) besides oxygen. The first product, 2-phenylmalonic acid ($C_9H_8O_4$), showed C-60.00 (60.11) and H-4.48 (4.55) besides oxygen. The second product, 2-(amino (carboxy) methyl)-5, 5-dimethyl-4, 5-dihydrothiazole-4-carboxylic acid-1-oxide ($C_8H_{12}N_2O_4S$), showed C- 41.37 (41.53), H-5.21 (5.37), N-12.06 (12.16), and S-13.81 (13.88) besides oxygen.

3.2. Reaction Orders. The orders of reaction were determined from the slope of log k_{abs} versus log (concentration) from different time plots as given in Figure 6 and Table 1 by varying concentrations of carbenicillin, KIO_4, and KOH while keeping the other parameters constant except the concentration of DPC (III).

3.3. Effect of [DPC (III)]. The DPC concentrate was varied in the range of 1.0×10^{-5} to 1.0×10^{-4} mol·dm^{-3}. The linearity and almost parallelism plots of log absorbance versus time up to 85% completion of the reaction by keeping other concentrations remaining constant indicated a reaction order of unity in DPC (III). Table 1 and Figure 6 are in the support of pseudo-first-order reaction with respect to DPC (III).

3.4. Effect of [CRBC]. The effect of [CRBC] was studied within a range of 1×10^{-4} to 1×10^{-3} mol·dm^{-3}. The rate constants (k_u) increased with increase in [CRBC] and order with respect to carbenicillin was found to be 0.718 ($r \geq 0.997$, $s \leq 0.0014$) which was also confirmed from the plot of (5 + log k_u) vs. 4 + log [CRBC], as shown in Figure 7 and Table 1.

3.5. Effect of Alkali. The effect of alkali was studied by varying [OH^-] in the range of 0.04 to 0.2 mol·dm^{-3} DPC (III) and CRBC, as well as ionic strength. Rate constant (k_u) increased with increase in [alkali] and order of reaction with respect to alkali was found to be 0.50 ($r \geq 0.999$, $s \leq 0.0005$), confirmed by the linear plot of (5 + log k_u) vs. 2 + log [KOH]), as shown in Figure 8 and Table 1.

3.6. Effect of Periodate. The effect of [KIO_4] was observed by varying the concentration range from 1.0×10^{-5} to 1.0×10^{-4} mol·dm^{-3}, while the other remaining active masses and conditions were constant. It was observed that rate constants decreased with an increase in [IO_4^-] and the order of reaction was −0.265 ($r \geq 0.997$, $s \leq 0.0002$) as presented in Figure 9 and Table 1.

3.7. Effect of Ionic Strength (I) and Dielectric Constant (D). Ionic strength is applied to know the participation of specific species in the reaction like ion-dipole, ion-ion, and dipole-dipole with the same or opposite charge, etc. The effect of ionic strength was studied by varying the concentration of KNO_3 in the range of 0.1–0.2 M by keeping the concentration of DPC, CRBC, and KOH constant and we found that increasing ionic strength did not have any significant effect on the rate of reaction. The dielectric constant of the medium (*D*) can be studied by varying t-butyl alcohol at a constant concentration of DPC, CRBC, KOH, and KNO_3 by using equation $D = D_1V_1 + D_2V_2$, where D_1 and D_2 are the dielectric constants of water and t-butyl alcohol and V_1 and V_2 are volume fractions of those, respectively. There was no effect of dielectric constant on the rate of the catalyzed reaction.

3.8. Effect of Initially Added Products. Initially added product ($CuSO_4$ (II)) did not show any significant effect on the rate of reaction.

3.9. Polymerization Study. A known quantity of acrylonitrile [46] monomer was initially added to the reaction mixture

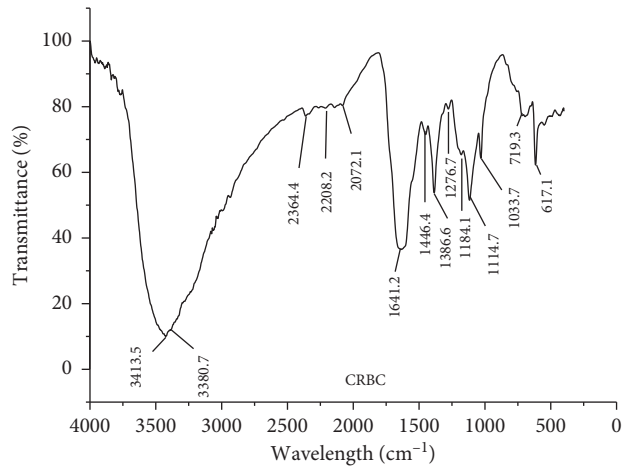

Figure 4: FT-IR spectrum for oxidation of CRBC by DPC (III) in alkaline medium.

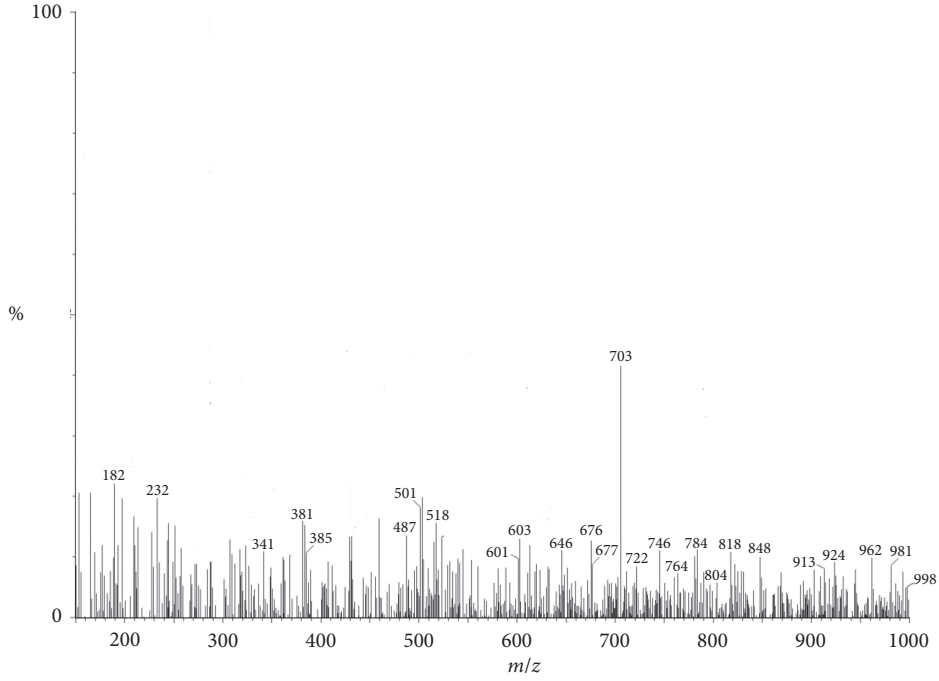

Figure 5: LC-MS spectrum of complex and products.

and allowed to remain in the inert atmosphere for 3.0 hours. The mixture gave no precipitate on dilution with methanol indicating the absence of free radicals.

3.10. Effect of Temperature. The effect of temperature on the rate of oxidation reaction was studied at four different temperatures under the constant concentration of CRBC, KOH, and DPC (III) keeping other conditions constant. Rate constants increased with the rise in temperature. The energy of activation and other activation parameters were calculated by the least square method from the plot of log k_u versus $1/T$ and thence computed in Table 2 and Figure 10.

The energy of activation and other activation parameters were calculated by using least square method from the plot of $(4 + \log k)$ versus $1/T$ and thence computed in Table 3 and Figure 11.

Since DPC (III) is chelating as well as the oxidizing agent, oxidation of different β-lactam antibiotics has been carried out in an alkaline medium. The activity of DPC is a function of pH and is capable of subtle control.

DPC (III) is water-soluble oxidizing reagent that exists as $[Cu(HIO_6)_2(OH)_2]^{7-}$ as well as $[HIO_6]^{4-}$ under higher pH condition. It has been evident that it can also exist as $[Cu(H_3IO_6)_2]^{-}$ or $[Cu(H_2IO_6)(OH)_2]^{2-}$ or $[Cu(H_2IO_6)(H_2O)_2]$ or $[Cu(H_3IO_6)(H_2O)_2]$ in aqueous alkaline medium. Periodic acid exists as H_5IO_6 in acid medium. The main species most active for the title work is $[Cu(H_2IO_6)(H_2O)_2]$ as reported in earlier literature. At higher alkali concentration, periodate ion tends to dimerize.

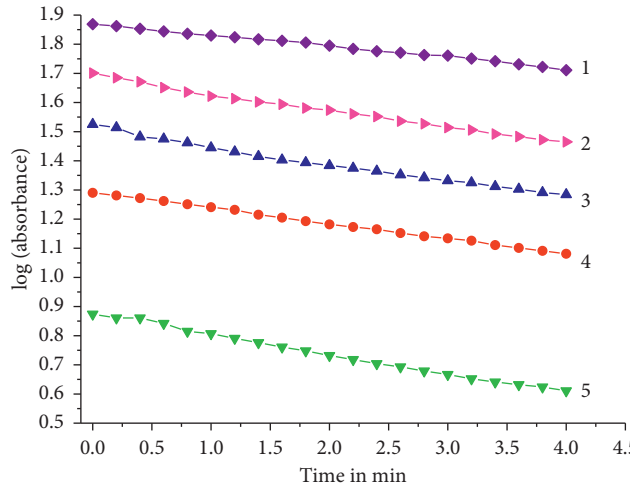

Figure 6: Order plot of log (abs) vs. time for the oxidation of CRBC by DPC (III).

Table 1: Effect of variation of [DPC]*, [CRBC], and [KOH] on the oxidation of carbenicillin by diperiodatocuprate (III) in aqueous alkaline medium at 298 K and $I = 0.10/\text{mol dm}^{-3}$.

$[DPC] \times 10^5$	$[CRBC] \times 10^4$	$[OH^-] \times 10^2$	$[IO_4^-] \times 10^5$	$k_u \times 10^{-4}$ (s^{-1})	Order
1.0	5.0	0.8	1.0	1.22	
3.0	5.0	0.8	1.0	1.24	
5.0	5.0	0.8	1.0	**1.25**	
8.0	5.0	0.8	1.0	1.21	
10.0	5.0	0.8	1.0	1.22	
5.0	**1.0**	0.8	1.0	0.41	
5.0	**3.0**	0.8	1.0	0.81	
5.0	**5.0**	0.8	1.0	**1.25**	**0.718**
5.0	**8.0**	0.8	1.0	1.80	
5.0	**10.0**	0.8	1.0	2.34	
5.0	5.0	**0.2**	1.0	0.62	
5.0	5.0	**0.4**	1.0	0.82	
5.0	5.0	**0.6**	1.0	1.01	**0.50**
5.0	5.0	**0.8**	1.0	**1.25**	
5.0	5.0	**1.0**	1.0	1.61	
5.0	5.0	0.8	**1.0**	**1.25**	
5.0	5.0	0.8	**3.0**	1.05	
5.0	5.0	0.8	**5.0**	0.85	**−0.265**
5.0	5.0	0.8	**8.0**	0.72	
5.0	5.0	0.8	**10.0**	0.68	

*Concentrations are expressed in mol dm^{-3}. Bold values in $[DPC] \times 105$, $[CRBC] \times 104$, $[OH^-] \times 102$, and $[IO4^-] \times 105$ signify the variable concentration of each solution for each kinetic run, whereas other values signify constant concentration of solutions used in experiments. Bold values in ku × 10−4 (s−1) signify the average rate constant calculated after conducting the experiment for the corresponding bold value (concentration) of that solution only. Bold values in order signify the exact order of reaction as obtained from the plot.

$$H_5IO_6 \rightleftharpoons H_4IO_6^- + H^+, K_1 = 5.1 \times 10^{-4}$$
$$H_4IO_6^- \rightleftharpoons H_3IO_6^{2-} + H^+, K_2 = 4.9 \times 10^{-9}$$
$$H_3IO_6^{2-} \rightleftharpoons H_2IO_6^{3-} + H^+, K_3 = 2.5 \times 10^{-12}$$

3.11. Probable Mechanism of Reaction. The oxidation reaction between MPC (III) and carbenicillin showed 1 : 2 stoichiometry and exhibited pseudo-first-order reaction with respect to DPC (III), fractional order with respect to carbenicillin and alkali, but negative fractional-order periodate. Based on this experimental evidence, a suitable mechanism is proposed along with the proper involvement of all species. In the first step, DPC (III) reacts with the hydroxide ion to form a deprotonated form of DPC (III) which in presence of water yields MPC (III) along with free periodates species. Hence fractional order with respect to carbenicillin presumably results due to the formation of the complex by the interaction between carbenicillin and MPC (III) species. This complex interacts with one mole of MPC (III) in a slow step to give intermediate A along with regeneration of free periodate ion and Cu^{++} ion. In the next step, intermediate A reacts with fresh mole of MPC (III) to

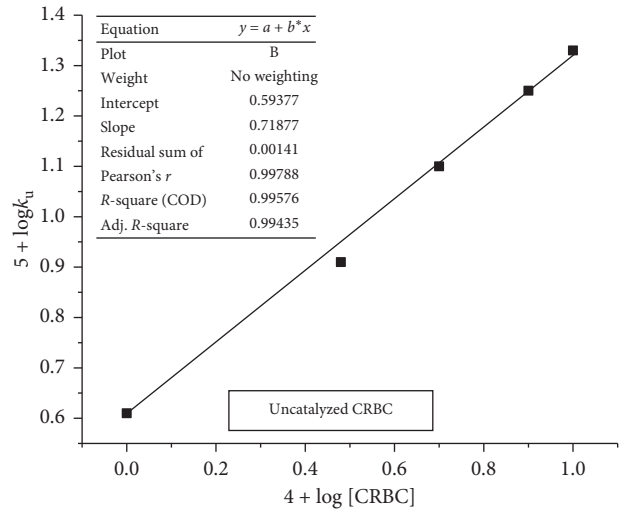

Figure 7: Plot of $(5 + \log k_u)$ vs. $4 + \log$ [CRBC].

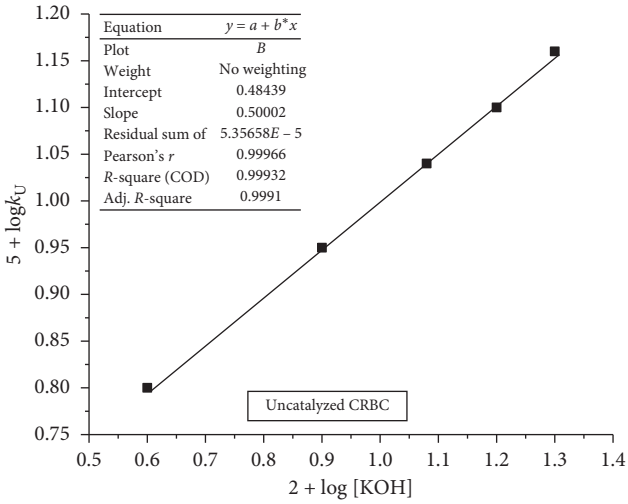

Figure 8: Plot of $(4 + \log k_u)$ vs. $2 + \log$ [KOH].

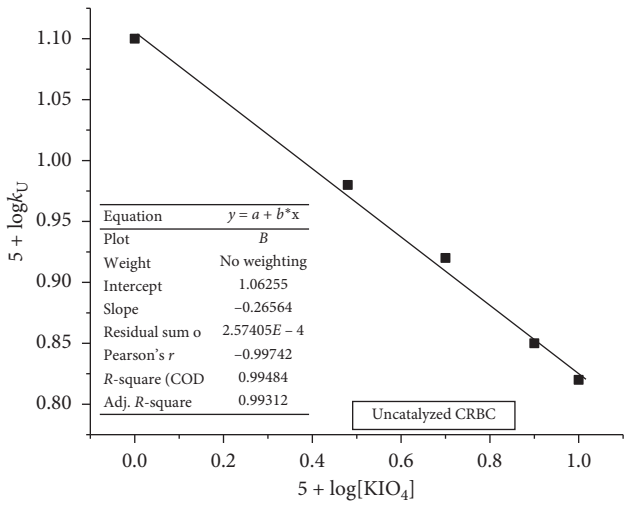

Figure 9: Plot of $(5 + \log k_u)$ vs. $5 + \log$ [KIO_4].

Table 2: Activation parameters with respect to uncatalyzed rate constant (k_u).

Parameters	Values
Ea (K J mol^{-1})	30.94
$\Delta H^{\neq}$ (K J mol^{-1})	28 ± 1
$\Delta S^{\neq}$ (J K^{-1} mol^{-})	-205 ± 3
$\Delta G^{\neq}$ (k $Jmol^{-1}$)	89 ± 2
LogA	2.5 ± 0.6

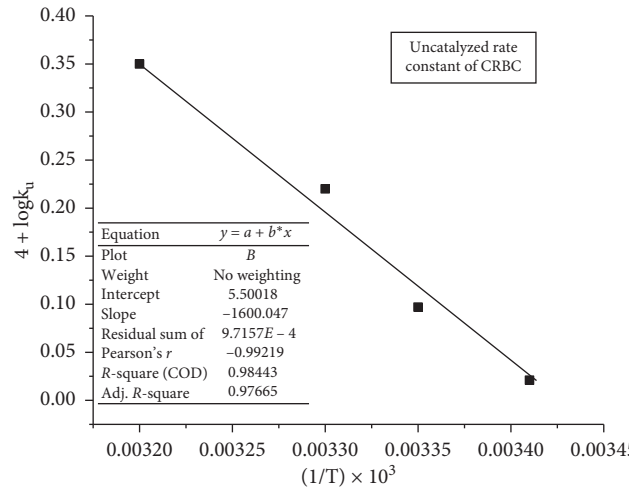

Figure 10: Plot of $(4 + \log k_u)$ vs. $(1/T) \times 10^3$.

Table 3: Activation parameters with respect to slow step rate constants (k).

Parameters	Values
Ea (K J mol^{-1})	50.45
$\Delta H^{\neq}$ (K J mol^{-1})	48 ± 1
$\Delta S^{\neq}$ (J K^{-1} mol^{-})	-150 ± 2
$\Delta G^{\neq}$ (k $Jmol^{-1}$)	92 ± 2
LogA	5.3 ± 0.2

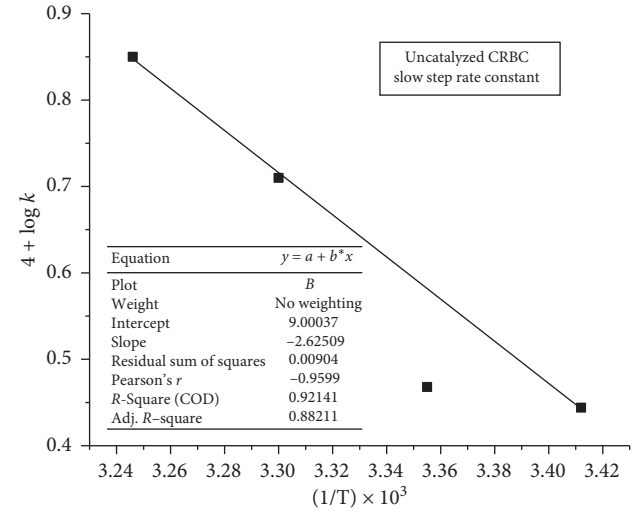

Figure 11: Plot of $(4 + \log k)$ vs. $(1/T) \times 10^3$.

form intermediate B which undergoes hydrolysis to yield the other final products, i.e., 2-phenylmalonic acid gave m/z at 182 (m + 2) and the second product 2-(amino (carboxy) methyl)-5, 5-dimethyl-4, 5-dihydrothiazole-4-carboxylic acid-1-oxide) as explained in Scheme 1.

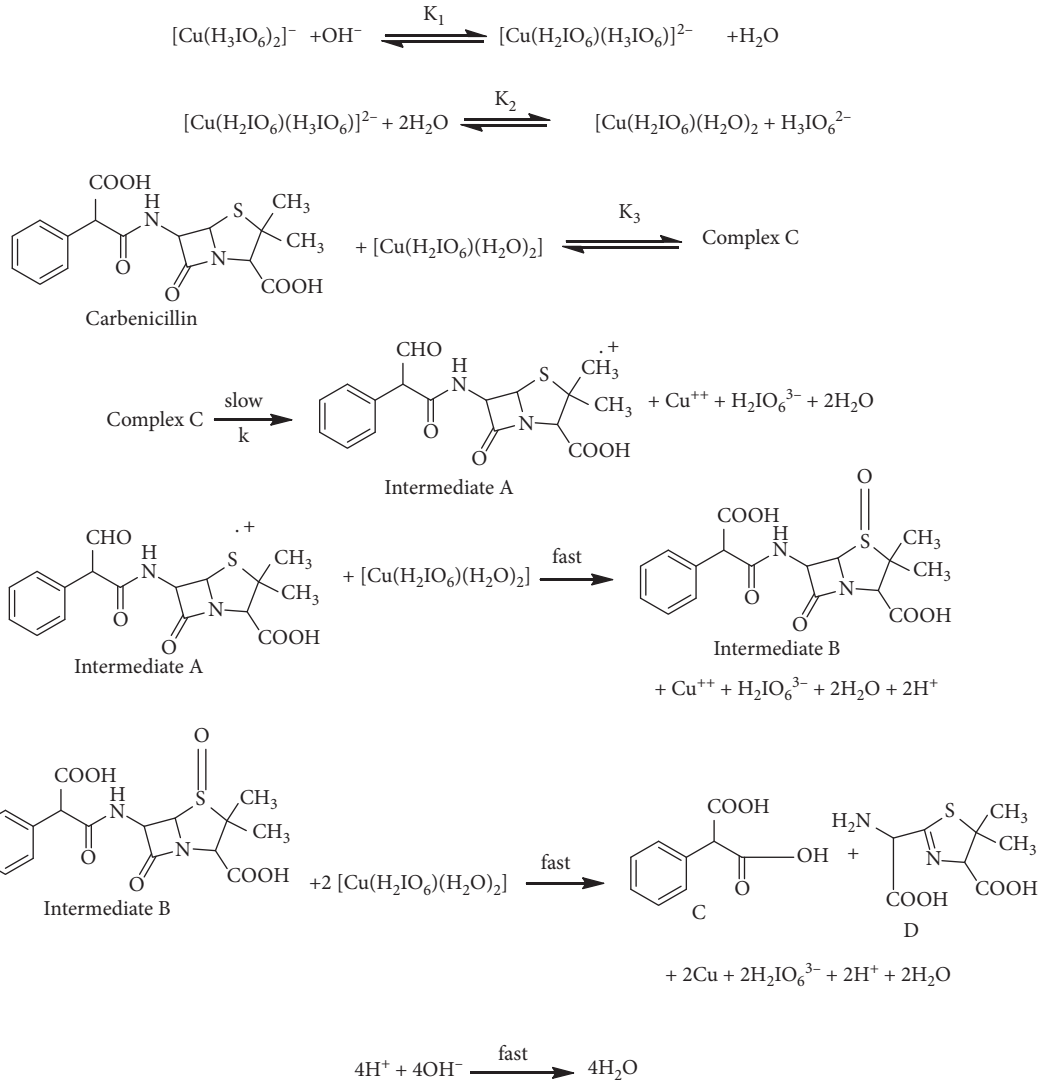

.

The probable structure of complex C is given as follows:

Spectroscopic evidence for the complex formation between reagent DPC (III) and substrate (CRBC) was obtained from UV-visible spectra by resisting CRBC (5.0×10^{-4} M), KOH (0.12 M), and a mixture of all. A bathochromic shift was obtained. The Michaelis–Menten plot is in great support for complex formation, Figure 9.

schemee 1 leads to rate law equation (2) as

$$\text{rate} = -\frac{d[\text{DPC}]}{dt} = k[\text{C}] \tag{1}$$

$$k_{obs} = \frac{kK_1K_2K_3[\text{DPC}][\text{CRBC}][\text{OH}^-]}{[\text{H}_3\text{IO}_6{}^{2-}] + K_1[\text{OH}^-][\text{H}_3\text{IO}_6{}^{2-}] + K_1K_2[\text{OH}^-] + K_1K_2K_3[\text{OH}^-][\text{CRBC}]} \tag{2}$$

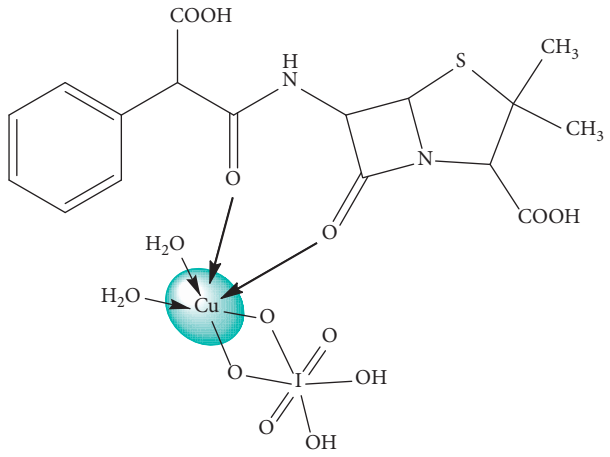

Scheme 1: Detailed scheme for uncatalyzed oxidation of CRBC by DPC (III).

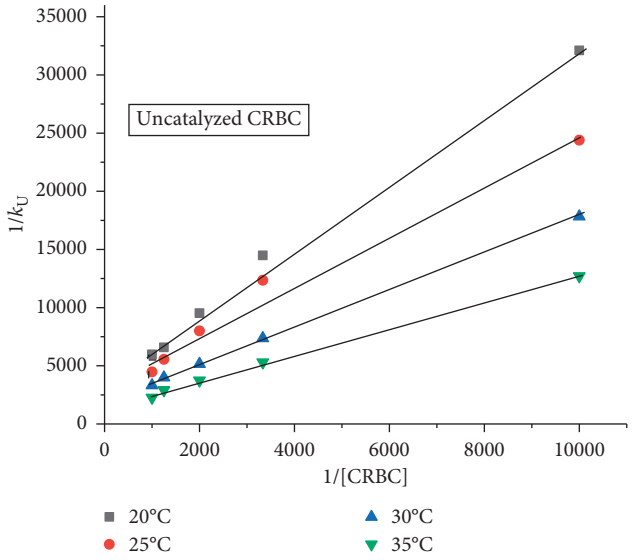

Figure 12: Plot of $[1/k_u$ vs.1/[CRBC].

Equation (2) describes all kinetic orders observed for different species. The rate law equation (2) can be rearranged into equation (3) that suits for verification:

$$\frac{1}{k_{obs}} = \frac{[H_3IO_6{}^{2-}]}{kK_1K_2K_3[CRBC][OH^-]} + \frac{[H_3IO_6{}^{2-}]}{kK_2K_3[CRBC]} + \frac{1}{kK_3[CRBC]} + \frac{1}{k} \quad (3)$$

The basic rule to calculate the activation energy and other activation parameters and the complete rate law derivation are given in Appendices A and B, respectively.

Figures 12–14 represent verification plots for oxidation of CRBC by DPC (III) in alkaline medium. According to equation (3), other remaining conditions being constant, the plots of $[1/k_u$ vs.1/[KOH] ($r \geq 0.999$, $\leq s\ 0.003$), $[1/k_u$ vs. 1/[CRBC] ($r \geq 0.997$, $\leq s\ 0.004$), and $[1/k_u$ vs. $[H_2IO_6]^{3-}$ ($r \geq 0.999$, $\leq s\ 0.003$) should be linear and are found to be so as in Figures 12–14.

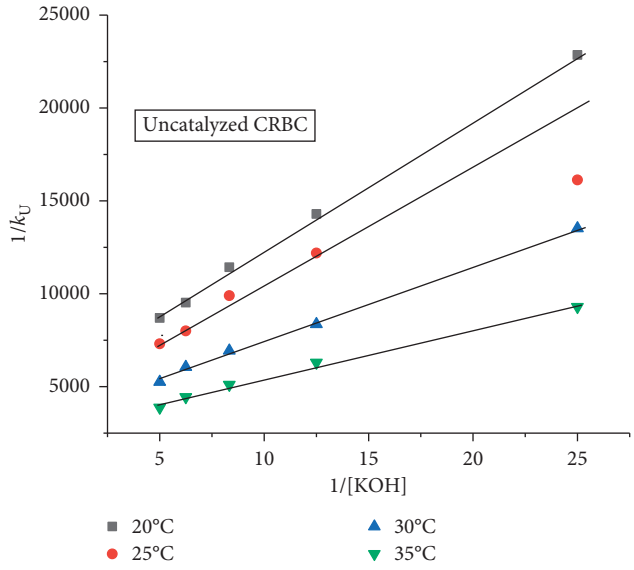

Figure 13: Plot of $[1/k_u$ vs.1/[KOH].

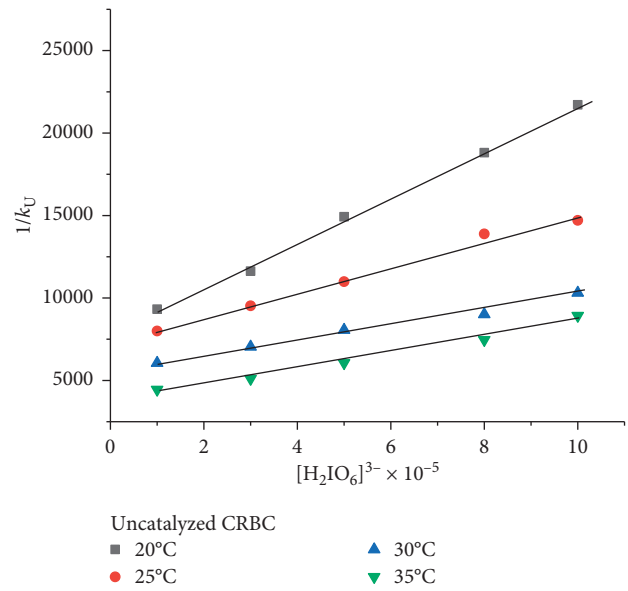

Figure 14: Plot of $[1/k_u$ vs.$[H_2IO_6]^{3-}$.

Overall slow step rate constants and equilibrium constants are presented in Tables 4 and 5 including thermodynamic parameters at 298 K.

schemee 1 clarifies the participation of neutral species in the reaction due to invariable ionic strength and dielectric constant. The modest values of both enthalpy and entropy of activation, within the range of electron pairing and unpairing process for the loss of degree of freedom and rigid transition state, are favourable for electron transfer reactions. The higher negative value of $\Delta S^{\ddagger}$ suggests that the intermediate complex is probably highly ordered compared to the reacting species. The above results, evidences,

Table 4: Equilibrium constants and slow step rate constant for CRBC.

Equilibrium constants	Absolute temperatures			
	20°C	25°C	30°C	35°C
k (slow step rate constant) $\times 10^{-4}$	2.78	2.94	5.18	7.2
K_1	1.18	1.23	1.417	1.64
$K_2 \times 10^{-4}$	2.09	2.27	3.146	4.2
K_3	1719.76	1478.0	1283.91	1036.42

Table 5: Thermodynamic parameters from equilibrium constants for CRBC.

Thermodynamic quantities	Values from K_1	Values from K_2	Values from K_3
ΔH°_{298} (k·J·mol^{-1})	16.98	36.74	−25.03
ΔS°_{298} (J·K^{-1}·mol^{-1})	59.06	131.027	−23.12
ΔG°_{298} (k·J·mol^{-1})	−0.59	−2.30	−18.14

and lower rate constant for slow steps indicate that the oxidation presumably occurs via an inner-sphere mechanism. The reducing property of the substrate is, probably, reduced in the absence of catalyst and the path of the uncatalyzed reaction is extended by increasing the activation energy.

4. Conclusions

The oxidation of carbenicillin by DPC (III) was studied experimentally in aqueous alkaline medium. (MPC-III) [Cu (H_2IO_6) $(H_2O)_2$] was considered to be the active species for the present work. Activation and thermodynamic parameters with respect to uncatalyzed rate constant (k_u), slow step rate constant (k), and equilibrium constants at different temperatures were calculated and computed. Overall sequences described here are inconsistent with all experimental evidences including product, spectral analysis, and mechanistic and kinetics studies.

Appendix

(A). Calculation of Activation Parameters

The energy of activation for the present reaction was calculated by

$$E_a = -2.303\, R \text{ slope}. \tag{A.1}$$

The Arrhenius factor "A" was calculated by

$$\log A = \log k_u + \frac{E_a}{2.303\,\mathrm{RT}}. \tag{A.2}$$

The entropy of activation was calculated by

$$\frac{\Delta S^{\#}}{4.576} = \log k_u - 10.753 - \log T + \frac{E_a}{4.576\mathrm{T}}. \tag{A.3}$$

The enthalpy of activation was calculated by

$$\Delta H^{\#} = E_a - RT. \tag{A.4}$$

The free energy of activation was calculated by

$$\Delta G^{\#} = \Delta H^{\#} - T\Delta S^{\#}, \tag{A.5}$$

where k_u/k_{obs} is uncatalyzed rate constant in sec^{-1}, T is temperature in Kelvin, E_a is energy of activation in calories, R is universal gas constant, and # is activation parameter.

(B). Derivation of Rate Law

From schemee 1,

$$\text{rate} = -\frac{\mathrm{d}[\mathrm{DPC}]}{\mathrm{dt}} = \mathrm{k}[\text{complex}] = \mathrm{k}[\mathrm{C}]. \tag{B.1}$$

From the law of mass action, the third equilibrium constant can be given by

$$\mathrm{K}_3 = \frac{[\mathrm{C}]}{\left[\mathrm{Cu}\left(\mathrm{H_2IO_6}\right)\left(\mathrm{H_2O}\right)_2[\mathrm{CRBC}\right]} \tag{B.2}$$

After rearrangement, we get

$$[\mathrm{C}] = \mathrm{K}_3\left[\mathrm{Cu}\left(\mathrm{H_2IO_6}\right)\left(\mathrm{H_2O}\right)_2[\mathrm{CRBC}\right] \tag{B.3}$$

Substituting the value of C from equation (B.3), we get

$$\text{rate} = -\frac{\mathrm{d}[\mathrm{DPC}]}{\mathrm{dt}} = \mathrm{K}_1\mathrm{K}_3\left[\mathrm{Cu}\left(\mathrm{H_2IO_6}\right)\left(\mathrm{H_2O}\right)_2[\mathrm{CRBC}\right] \tag{B.4}$$

The second equilibrium constant can be given by

$$\mathrm{K}_2 = \frac{\left[\mathrm{Cu}\left(\mathrm{H_2IO_6}\right)\left(\mathrm{H_2O}\right)_2\left[\mathrm{H_3IO_6^{2-}}\right]\right]}{\left[\mathrm{Cu}\left(\mathrm{H_2IO_6}\right)\left(\mathrm{H_3IO_6}\right]^{2-}} \tag{B.5}$$

This can be rearranged into

$$\left[\mathrm{Cu}\left(\mathrm{H_2IO_6}\right)\left(\mathrm{H_2O}\right)_2\right] = \frac{\mathrm{K}_2\left[\mathrm{Cu}\left(\mathrm{H_2IO_6}\right)\left(\mathrm{H_3IO_6}\right]^{2-}}{\left[\mathrm{H_3IO_6}\right]^{2-}} \tag{B.6}$$

The first equilibrium constant can be given by

$$\mathrm{K}_1 = \frac{\left[\mathrm{Cu}\left(\mathrm{H_2IO_6}\right)\left(\mathrm{H_3IO_6}\right]^{2-}}{\left[\mathrm{Cu}\left(\mathrm{H_3IO_6}\right)_2\right]^{-}[\mathrm{OH}^-]} \tag{B.7}$$

This can be rearranged into

$$\left[Cu\left(H_2IO_6\right)\left(H_3IO_6\right)\right]^{2-} = K_1\left[Cu\left(H_3IO_6\right)_2\right]^{-}[OH^{-} \tag{B.8}$$

Substituting equation (B.6) into (B.8) in equation (B.4), we get

$$\text{Rate} = -\frac{d[DPC]}{dt} = \frac{kK_1K_2K_3[CRBC]_f[DPC]_f[OH^-]_f}{\left[H_3IO_6\right)_2]^-} \tag{B.9}$$

The total concentration of [DPC] can be given as

$$[DPC]_T = [DPC]_f + \left[Cu\left(H_2IO_6\right)\left(H_3IO_6\right]^{2-} + \left[Cu\left(H_2IO_6\right)\left(H_2O\right)_2\right] + [C] \tag{B.10}$$

where T and f denote total and free concentrations:

$$= [DPC]_f + K_1\left[Cu\left(H_2IO_6\right)_2\right]^{-}[OH^-] + \frac{K_1K_2\left[Cu\left(H_2IO_6\right)_2\right]^{-}[OH^-]}{\left[H_3IO_6^{2-}\right]} + \frac{K_1K_2K_3\left[Cu\left(H_3IO_6\right)_2\right]^{-}[OH^-][CRBC]}{\left[H_3IO_6\right]^{2-}}$$

$$[DPC]_T = [DPC]_f + K_1[DPC]_f[OH^-] + \frac{K_1K_2[DPC]_f[OH^-]}{\left[H_3IO_6^{2-}\right]} + \frac{K_1K_2K_3[DPC]_f[OH^-][CRBC]}{\left[H_3IO_6^{2-}\right]}$$

$$[DPC]_f = \frac{[DPC]_T\left[H_3IO_6^{2-}\right]}{\left[H_3IO_6^{2-}\right] + K_1[OH^-]\left[H_3IO_6^{2-}\right] + K_1K_2[OH^-] + K_1K_2K_3[OH^-][CRBC]} \tag{B.11}$$

The total concentration of [OH^-] can be given by

$$[OH^-]_T = [OH^-]_f + \left[Cu\left(H_2IO_6\right)\left(H_3IO_6\right]^{2-} + \left[Cu\left(H_2IO_6\right)\left(H_2O\right)_2\right] + [C]$$

$$[OH^-]_T = [OH^-]_f + K_1[DPC][OH^-]_f + \frac{K_1K_2[DPC][OH^-]_f}{\left[H_3IO_6\right]^{2-}} + \frac{K_1K_2K_3[DPC][OH^-]_f[CRBC]}{\left[H_3IO_6\right]^{2-}} \tag{B.12}$$

$$[OH^-]_T = [OH^-]_f\left\{1 + K_1[DPC] + \frac{K_1K_2[DPC]}{\left[H_3IO_6\right]^{2-}} + \frac{K_1K_2K_3[DPC][CRBC]}{\left[H_3IO_6\right]^{2-}}\right\}$$

In view of low concentrations of DPC and $H_3IO_6^{2-}$ used, the last three terms inside brackets can be neglected in comparison with unity:

$$[OH^-]_T = [OH^-]_f \tag{B.13}$$

Similarly, in case of low concentrations of DPC and $H_3IO_6^{2-}$ used,

$$[CRBC]_T = [CRBC]_f \tag{B.14}$$

Putting these values of $[DPC]_f$ from equation (B.11), $[OH^-]_f$ from equation (B.13), and $[CRBC]_f$ from equation (B.14) in equation (B.9) after omitting subscripts T and f, we get

$$\text{Rate} = \frac{d[DPC]}{dt} = \frac{kK_1K_2K_3[CRBC][DPC][OH^-]}{\left[H_3IO_6^{2-}\right] + K_1[OH^-]\left[H_3IO_6^{2-}\right] + K_1K_2[OH^-] + K_1K_2K_3[OH^-][CRBC]}$$

$$\text{or, } \frac{1}{k_{obs}} = \frac{\left[H_3IO_6^{2-}\right]}{kK_1K_2K_3[CRBC][OH^-]} + \frac{\left[H_3IO_6^{2-}\right]}{kK_2K_3[CRBC]} + \frac{1}{kK_3[CRBC]} + \frac{1}{k} \tag{B.15}$$

Data Availability

The data used to support the findings of this study are available from the corresponding author upon request.

Conflicts of Interest

The authors declare that there are no conflicts of interest regarding the publication of this paper.

Acknowledgments

The first author (YRS) strongly acknowledges Diamond Jubilee and Lifetime Prof. Dr. Sharnappa. T. Nandibewoor, and Prof. Dr. Shivamurti A. Chimatadar, Karnatak University, Dharwad, India, for invaluable cooperation as well as STIC (Cochin), SAIF (Mumbai), and CDRI-CSIR (Lucknow), India, for providing spectral evidence. The first author (Yuv Raj Sahu) also acknowledges Purwanchal Campus, Dharan, Institute of Engineering (IOE), T.U., Nepal, for financial support.

References

[1] J. B. Ellis, "Pharmaceutical and personal care products (PPCPs) in urban receiving waters," *Environmental Pollution*, vol. 144, no. 1, pp. 184–189, 2006.

[2] K. E. Price, "Structure-activity relationships of semisynthetic penicillins," *Advances in Applied Microbiology*, vol. 11, pp. 17–75, 1970.

[3] M. J. Basker, K. R. Comber, R. Sutherland, and G. H. Valler, "Carfecillin: antibacterial activity in vitro and in vivo," *Chemotherapy*, vol. 23, no. 6, pp. 424–435, 1977.

[4] P. Acred, D. M. Brown, E. T. Knudsen, G. N. Rolinson, and R. Sutherland, "New semi-synthetic penicillin active against Pseudomonas pyocyanea," *Nature*, vol. 215, no. 5096, pp. 25–30, 1967.

[5] B. Moyá, A. Beceiro, G. Cabot et al., "Pan-β-Lactam resistance development in *Pseudomonas aeruginosa* clinical strains: molecular mechanisms, penicillin-binding protein profiles, and binding affinities," *Antimicrobial Agents and Chemotherapy*, vol. 56, no. 9, pp. 4771–4778, 2012.

[6] I. Saikawa, S. Minami, and Y. Watanabe, "Development of β-lactams with antipseudomonal activity," *Journal of Infection and Chemotherapy*, vol. 2, no. 2, pp. 53–64, 1996.

[7] W. Brumfitt, A. Percival, and D. A. Leigh, "CLINICAL and laboratory studies with carbenicillin a new penicillin active against Pseudomonas pyocyanea," *The Lancet*, vol. 289, no. 7503, pp. 1289–1293, 1967.

[8] T. Rodríguez-Castillo, J. Barquín, M. Álvarez-Cabria, F. J. Peñas, and C. Álvarez, "Effects of sewage effluents and seasonal changes on the metabolism of three Atlantic rivers," *Science of The Total Environment*, vol. 599-600, pp. 1108–1118, 2017.

[9] P. P. Marcinowski, J. P. Bogacki, and J. H. Naumczyk, "Cosmetic wastewater treatment using the Fenton, Photo-Fenton and H2O2/UV processes," *Journal of Environmental Science and Health, Part A*, vol. 49, no. 13, pp. 1531–1541, 2014.

[10] M. M. de Oliveira e Sa′, M. S. Miranda, and J. C. G. Esteves da Silva, "Occurrence of personal care products and transformation processes in chlorinated waters," *The Handbook of Environmental Chemistry*, Springer, Berlin, Germany, pp. 123–136, 2014.

[11] H. Shang, X. Qi, M. Zhang, H. Li, G. Li, and L. Yang, "Characteristics, distribution, and source analysis of the main persistent toxic substances in karst groundwater at jinan in north China," *Journal of Chemistry*, vol. 2020, Article ID 4217294, 18 pages, 2020.

[12] E. S. Elmolla and M. Chaudhuri, "Degradation of the antibiotics amoxicillin, ampicillin and cloxacillin in aqueous solution by the photo-Fenton process," *Journal of Hazardous Materials*, vol. 172, no. 2-3, pp. 1476–1481, 2009.

[13] K. Kemmerer, "Antibiotics in the aquatic environment-A Review-part I," *Chemosphere*, vol. 75, no. 4, pp. 417–431, 2009.

[14] S. K. Khetan and T. J. Collins, "Human pharmaceuticals in the aquatic environment: a challenge to green chemistry," *Chemical Reviews*, vol. 107, no. 6, pp. 2319–2364, 2007.

[15] B. R. Ramaswamy, "Environmental risk assessment of personal care products," *Personal Care Products in the Aquatic Environment*, Springer, Berlin, Germany, pp. 139–163, 2014.

[16] A. G. Asimakopoulos, I. N. Pasias, K. Kannan, and N. S. Thomaidis, "Human exposure to chemicals in personal care products and health implications," *The Handbook of Environmental Chemistry*, Springer, Berlin, Germany, pp. 165–187, 2014.

[17] K. Demeestere, P. Gago-Ferrero, H. Van Langenhove, M. S. Díaz-Cruz, and D. Barceló, "Ozonation as an advanced treatment technique for the degradation of personal care products in water," *The Handbook of Environmental Chemistry*, Springer, Berlin, Germany, pp. 375–397, 2014.

[18] K. Ikehata, M. Gamal El-Din, and S. A. Snyder, "Ozonation and advanced oxidation treatment of emerging organic pollutants in water and wastewater," *Ozone: Science & Engineering*, vol. 30, no. 1, pp. 21–26, 2008.

[19] M. Klavarioti, D. Mantzavinos, and D. Kassinos, "Removal of residual pharmaceuticals from aqueous systems by advanced oxidation processes," *Environment International*, vol. 35, no. 2, pp. 402–417, 2009.

[20] A. Pessina, P. Lüthi, P. L. Luisi, J. Prenosil, and Y.-S. Zhang, "Amide-bond syntheses catalyzed by penicillin acylase," *Helvetica Chimica Acta*, vol. 71, no. 3, pp. 631–641, 1988.

[21] D. C. Hiremath, T. S. Kiran, and S. T. Nandibewoor, "Oxidation of vanillin by diperiodatocuprate(III) in aqueous alkaline medium: a kinetic and mechanistic study by stopped flow technique," *International Journal of Chemical Kinetics*, vol. 39, no. 4, pp. 236–244, 2007.

[22] D. S. Munavalli, P. N. Naik, G. G. Ariga, S. T. Nandibewoor, and S. A. Chimatadar, "Kinetics and mechanistic studies of oxidation of fluoroquionoline antibacterial agent norfloxacin by diperiodatocuprate(III) in aqueous alkaline medium," *Cogent Chemistry*, vol. 1, no. 1, 2015.

[23] R. R. Hosamani, N. P. Shetti, and S. T. Nandibewoor, "Mechanistic investigation on the oxidation of ampicillin drug by diperiodatoargentate (III) in aqueous alkaline medium," *Journal of Physical Organic Chemistry*, vol. 22, no. 3, pp. 234–240, 2008.

[24] R. S. Shettar, N. P. Shetti, and S. T. Nandibewoor, "Mechanistic study on the oxidation of 4-hydroxycoumarin by diperiodatonickelate(IV) in aqueous alkaline medium," *E-Journal of Chemistry*, vol. 6, no. 3, pp. 601–610, 2009.

[25] K. B. Reddy, C. P. Murthy, B. Sethuram, and T. N. Rao, "Kinetics & mechanism of Os (VIII) catalysed & uncatalysed oxidation of cyclopentanol , cyclohexanol & Cycloheptanol by Ditelluratocuprate (III) in Alkaline Medium," *Indian Journal of Chemistry*, vol. 20A, pp. 272–275, 1981.

[26] A. Balikungeri, M. Pelletier, and D. Monnier, "Contribution to the study of the complexes bis(dihydrogen tellurato) cuprate(III) and argentate(III), bis(hydrogen periodato) cuprate(III) and argentate(III)," *Inorganica Chimica Acta*, vol. 22, pp. 7–14, 1977.

[27] M. D. Meti, K. S. Byadagi, S. T. Nandibewoor, and S. A. Chimatadar, "Mechanistic studies of uncatalyzed and ruthenium(III)-catalyzed oxidation of the antibiotic drug chloramphenicol by hexacyanoferrate(III) in aqueous alkaline medium: a comparative kinetic study," *Monatshefte für*

Chemie-Chemical Monthly, vol. 145, no. 10, pp. 1561–1573, 2014.

[28] G. P. Panigrahi and A. C. Pathy, "Kinetics and mechanism of oxidation of S2O 3 2–by potassiumbis(tellurato) cuprate(III)," *Journal of Chemical Sciences*, vol. 96, no. 5, pp. 301–308, 1986.

[29] S. Nadimpali, J. Padmvasthy, and K. K. M. Yusuff, "Determination of the nature of the diperiodatocuprate (III) species in aqueous alkaline medium through a kinetic and mechanistic study on the oxidation of iodide ion," *Transition Metal Chemistry*, vol. 26, pp. 315–321, 2001.

[30] B. Sethuram, *Some Aspects of Electron Transfer Reaction Involving Organic Molecules*, pp. 71–78, Allied Publishers Pvt Ltd, New Delhi, India, 2003.

[31] H.-Y. Xie, Z.-R. Wang, and Z.-F. Fu, "Highly sensitive trivalent copper chelate-luminol chemiluminescence system for capillary electrophoresis chiral separation and determination of ofloxacin enantiomers in urine samples," *Journal of Pharmaceutical Analysis*, vol. 4, no. 6, pp. 412–416, 2014.

[32] M. D. Meti, J. C. Abbar, S. T. Nandibewoor, and S. A. Chimatadar, "Voltammetric oxidation of carbenicillin and its electro analytical applications at gold electrode," *Cogent Chemistry*, vol. 2, no. 1, 2016.

[33] T. C. Eickhoff, "In vitro effects of carbenicillin combined with gentamicin or polymyxin B against *Pseudomonas aeruginosa*1," *Applied Microbiology*, vol. 18, no. 3, pp. 469–473, 1969.

[34] M. Davies, J. R. Morgan, and C. Anand, "Interactions of carbenicillin and ticarcillin with gentamicin," *Antimicrobial Agents and Chemotherapy*, vol. 7, no. 4, pp. 431–434, 1975.

[35] H. A. Holt, J. M. Broughall, M. McCarthy, and D. S. Reeves, "Interactions between aminoglycoside antibiotics and carbenicillin or ticarcillin," *Infection*, vol. 4, no. 2, pp. 107–109, 1976.

[36] L. K. Pickering and P. Gearhart, "Effect of time and concentration upon interaction between gentamicin, Tobramycin, netilmicin, or amikacin and carbenicillin or ticarcillin," *Antimicrobial Agents and Chemotherapy*, vol. 15, no. 4, pp. 592–596, 1979.

[37] W. A. Kradjan and R. Burger, "In vivo inactivation of gentamicin by carbenicillin and ticarcillin," *Archives of Internal Medicine*, vol. 140, no. 12, pp. 1668–1670, 1980.

[38] B. Lynn, "Administration of carbenicillin and ticarcillin—pharmaceutical aspects," *European Journal Of Cancer*, vol. 9, no. 6, pp. 425–433, 1965.

[39] H. C. Neu, "Carbenicillin and ticarcillin," *Medical Clinics of North America*, vol. 66, no. 1, pp. 61–77, 1982.

[40] K. R. Comber, M. J. Basker, C. D. Osborne, and R. Sutherland, "Synergy between ticarcillin and Tobramycin against *Pseudomonas aeruginosa* and Enterobacteriaceae in vitro and in vivo," *Antimicrobial Agents and Chemotherapy*, vol. 11, no. 6, pp. 956–964, 1977.

[41] J. B. Eastwood and J. R. Curtis, "Carbenicillin administration in patients with severe renal failure," *BMJ*, vol. 1, no. 5590, pp. 486-487, 1968.

[42] G. P. Panigrahi and P. K. Misro, "Kinetics and mechanism of oxidation of osmium (VIII) catalyzed oxidation of unsaturated acids by sodium periodate," *Indian Journal of Chemistry*, vol. 15A, pp. 1066–1069, 1977.

[43] P. K. Jaiswal and K. L. Yadava, "Determination of sugars and organic acids with periodato complex of Cu (III)," *Indian Journal of Chemistry*, vol. 11, pp. 837-838, 1973.

[44] G. H. Jeffery, J. Basset, R. C. Mendham, and R. C. Denney, *Vogel's Textbook of Qualitative Chemical Analysis*, Vol. 455, ELBS, London, UK, 5th edition, 1996.

[45] B. Chowdhury, M. H. Mondal, M. K. Barman, and B. Saha, "A study on the synthesis of alkaline Copper (III)-periodate (DPC) complex with an overview of its redox behavior in aqueous micellar media," *Research on Chemical Intermediates*, Springer, Berlin, Germany, 2018.

[46] R. V. Jagadeesh and J. Puttaswamya, "Ru(III), Os(VIII), Pd(II) and Pt(IV) catalysed oxidation of glycyl-glycine by sodiumN-chloro-p-toluenesulfonamide: comparative mechanistic aspects and kinetic modelling," *Journal of Physical Organic Chemistry*, vol. 21, no. 10, pp. 844–858, 2008.

Research Article

Kinetics and Mechanism of Oxidation of Amoxicillin by Copper (III) Periodate Complex in Alkaline Medium

Yuv Raj Sahu[1], Narendra K. Chaudhary[1], Parashuram Mishra[*]

[1]Bio-inorganic and Materials Chemistry Research Laboratory, Department of Chemistry, Mahendra Morang Adarsha Multiple Campus, Biratnagar, (Tribhuwan University), Nepal.

***Corresponding author's E-mail:** prmmishra@rediffmail.com

Received: 10-11-2019; **Revised:** 23-12-2019; **Accepted:** 02-01-2020.

ABSTRACT

Oxidation of amoxicillin was investigated by copper (III) periodate complex by UV-Visible spectrophotometer to study its kinetics and mechanism in alkaline medium at ionic strength of 0.1 mol dm-3 and 298 K. The oxidation of amoxicillin and DPC (III) was of 1:2 stoichiometry (AMX: DPC-III) in alkaline medium. Spot test, FT-IR and LC-MS spectral studies supported to identify the reaction products. It was of pseudo-first order reaction with respect to diperiodatocuprate (III) and fractional order with respect to amoxicillin as well as alkali. A negative fractional order was observed by periodate. The main active species for the proposed oxidation reaction was monoperiodatocuprate (MPC-III) as [Cu (H2IO6) (H2O)2]. Determination of activation parameters from different rate constants, spectral evidences and proposal of a plausible mechanism consistent with experimental results supported the reaction properly.

Keywords: Amoxicillin, Kinetics, Mechanism, Diperiodatocuprate, Rate constant.

INTRODUCTION

For the continuation of our ongoing research in modifications in structural design and in vitro antibiotic study of amoxicillin derived complexes[1], the current study is an attempt to familiarize kinetic and mechanistic aspects of degradation of this antibiotic by Cu(III) periodate complex in alkaline medium. The antibiotics are commonly employed in the prevention and treatment of various kinds of diseases in animals and plants. Recently, antibiotic resistance has broken the clinical rules of its applications in the disease treatment process. Unwise and misconduct use of antibiotics is the major cause of antibiotic resistance. Clinically administered antibiotics do not show 100 % activity; rather they come out from livings as unused residue and even release in the environment from the drug manufacturing industries and promote pollution. The industrial effluents coming out from the drug manufacturing industries accumulate in wastewater treatment plants and if release untreated, can pollute natural water reservoirs. This contamination of antibiotics in natural water can lead to the development of antibacterial resistance in indirect way. Hence antibiotic resistance represents a serious health problem and different advanced oxidation processes (AOPs) have to be applied in the degradation of such emergent chemical pollutants[2-5].

It is a semi-synthetic broad-spectrum β-lactam antibiotic that belongs to the class penicillin [6-9]. Amoxicillin is highly effective in the treatment of various infections or diseases caused by gram-positive and gram-negative bacteria and hence widely used due to its better absorption capacity, low toxicity, and low minimum inhibitory concentration (MIC) value against bacteria[10].It consists of a β-lactam heterocyclic ring fused to thiazolidine ring containing one sulphur atom.

Recent studies on the highest oxidation state transition metals have attracted many researchers in the field of kinetic chemistry to put the plausible mechanism of oxidation reactions. Transition metals can form stable complexes with polydentate ligands like diperiodatocuprate (DPC-III)[11], Diperiodatoargentate (DPA-III)[12], diperiodatonickelate (DPN-IV)[13]. These oxidants are used for the analysis of different organic oxidation reactions including amino acids[14]. Copper (III) complexes have occupied a major role in the oxidation chemistry due to their relative abundance and relevance in biological chemistry[15]. Diperiodatocuprate (III) was first synthesized by Malatesta [16] more than a half-century ago and thence followed by G. P. Panigrahi and A. C. Pathy[17].Many research works have been reported on the determination of the nature of this complex [18]. Synthesis, Stability and redox nature of Cu (III) periodate complex in a micro heterogeneous environment like the surfactant-micelle medium has been reported in recent literature[19].Diperiodatocuprate (III) has a flexible one electron-donating nature and biochemistry, stability as well as sensitivity of trivalent copper are already described in literatures [20]. It acts as an analytical reagent and hence used in many biological and analytical electron transfer reactions [21]. Since Cu (III) is generally involved as an active intermediate species appearing in many electron transfer reactions [22], it becomes quite essential to know the role of Cu (III) / Cu (II) couple, as described in earlier literature [23]. While copper (III) periodate involves multiple equilibrium between different copper (III) species and it would be fascinating to identify the most active species participated in the present reaction.

Several oxidation methods of amoxicillin in acid as well as in alkaline medium have been described in earlier literature like oxidation of amoxicillin by chloramine-T in acid medium [24], oxidative degradation of amoxicillin by thermally activated persulphate [25], oxidation of amoxicillin by hexacyanoferrate (III) in aqueous alkaline medium[26], Co (III) catalyzed oxidation of amoxicillin by DPC (III) in alkaline medium [27]. Now, this is our new attempt to study the kinetics of amoxicillin by DPC (III) without any catalyst to have a comparative study in terms of kinetics of amoxicillin. So, we have undertaken the present research work to investigate the kinetics and mechanism of oxidation of amoxicillin in the alkaline medium in the absence of catalyst and hence to arrive at plausible mechanisms including determination of activation properties.

MATERIALS AND METHODS

Reagents and Chemicals

All the chemicals used were of Analytical Reagent (AR) grade and double distilled water was used throughout the work. Melting point 196 °C (literature m. pt. 194.2 °C) was measured to check the purity of amoxicillin (Sigma Aldrich). The stock solution of amoxicillin (0.01 mol dm^{-3}) was prepared by dissolving 0.3654 g of recrystallized amoxicillin in 100 ml double distilled water. Potassium periodate solution was prepared by dissolving 0.023 g (0.01mol dm^{-3}) of KIO_4 (Sigma Aldrich) in 100 ml double distilled hot water and the solution was used only after 24 hours. The concentration of the potassium periodate solution was determined by the iodometric method at neutral pH maintained by using phosphate buffer[28].

Instrumentation

The pH of the solution was measured by ELICO LI 613 pH meter. The electronic absorption spectra were recorded on Varian CARY 5000 UV-VIS spectrophotometer in the range of 200-1000 nm. The infra-red spectra of the complexes were recorded on Thermo Nicolet, Avatar 370 FT-IR spectrometer in the range of 4000-400 cm^{-1} that was run as KBr disc. The mass spectrum of the products was recorded on the UPLC-TQD Mass spectrometer in positive mode in the range of 0 – 1000 m/z.

Synthesis of Reagent

The Copper (III) diperiodate (DPC-III) was prepared [29-30] by mixing copper sulphate (3.54 g), potassium periodate (6.80 g), potassium persulphate (2.20 g) and potassium hydroxide (9.0 g) in a 250 ml double distilled water in a round bottomed flask. The whole mixture was frequently shaken thoroughly and heated on a hot plate for about 2 hours. During this period, the mixture turned to intense red and the flask was heated further for 20 minutes to remove potassium persulphate completely from the mixture by decomposing persulphate. After completion of the reaction, the mixture was cooled and filtered through sintered glass crucible G-4 and the dark red-brown solution was diluted to 250 ml by adding double-distilled water. The aqueous solution of DPC (III) was standardized by iodometric titration ($Na_2S_2O_3$, starch, KI and KH_2PO_4) by thiocyanate method and its exact concentration was ascertained. The existence of DPC (III) was verified by UV-visible spectrophotometer that showed an absorption band with a maximum peak at 415 nm. However, the accurate concentration of DPC (III) was calculated by UV-visible spectrophotometer. DPC (III) has a square planar geometry with dsp^2 hybridization and diamagnetic nature. Similarly, KOH (BDH) and the other required solutions were prepared and stored safely.

Synthesis of Complex

10 ml of amoxicillin solution (0.132 mol dm^{-3}) was taken in a 100 ml RB flask. To this 10 ml DPC (III) (0.528 mol dm^{-3}) was mixed in 1:2 stoichiometric ratio along with 1.0 ml of each KNO_3 (Himedia), KIO_4 and 2.0 ml of KOH solution of fixed molarities and stirred on metal hot plate for 24 hours followed by re-stirring during re-fluxing with condensation for 24 hours. The products were purified and recrystallized in ethanol till the whole solvent evaporated leaving behind crystals only. The appearance of peaks in UV-Visible spectrophotometer showed the formation of the complex. The possible structures of DPC and MPC are given below.

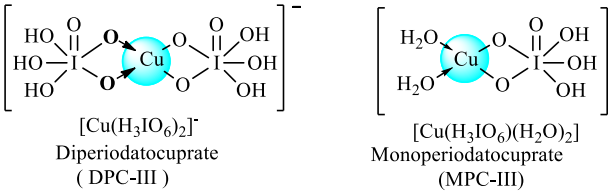

$[Cu(H_3IO_6)_2]^-$
Diperiodatocuprate
(DPC-III)

$[Cu(H_3IO_6)(H_2O)_2]$
Monoperiodatocuprate
(MPC-III)

DPC (III) and MPC (III)

Kinetic Measurements

Since the reaction is very fast, its absorbance was taken quite rapidly along with the progress of the reaction by following pseudo-first-order state when the active mass of AMX was greater than that of DPC at 20°C, 25°C, 30°C and 35°C ± 0.1°C unless specified. The reaction was initiated by mixing required quantities of previously thermo stated solutions of amoxicillin into DPC (III) which already contained a fixed concentration of KIO_4 along with KNO_3 and KOH. Data were obtained from UV-Visible spectrophotometer at pH (9.2-10) and 415 nm wavelength due to DPC by monitoring the decrease in absorbance at the molar extinction coefficient (€) of **6242 ± 50** dm^3 $mol^{-1}cm^{-1}$. The UV visible spectrophotometer was run up to 85% reaction wherein initially added products and dielectric constant didn't exhibit any interference in the reaction.

There was no effect of ubiquitous contamination of initially added carbonate in the reaction. Fresh solutions were nevertheless used to carry out each kinetic run. Regression analysis of experimental data to obtain regression coefficient (r) and standard deviation (s) of points from the regression line was completed with the help of Origin 9.6 (2017) software. Plots of log(abs) versus time gave a straight line and hence rate constants (k_{obs}) were calculated from slopes. The k_{obs} values agreed within ± 5%

error and were the average of at least three independent kinetic runs. A constant concentration of periodate was mixed into reaction mixture all the time. Finally, the total concentration of KIO_4 and KOH were determined by assuming the amount present in DPC and added additionally. To check the effect of periodate, ionic strength, dissolved oxygen, etc, kinetics was also conducted into the N_2 atmosphere wherein no significant changes were observed. Added carbonate and periodate dielectric constant etc., didn't show any effect.

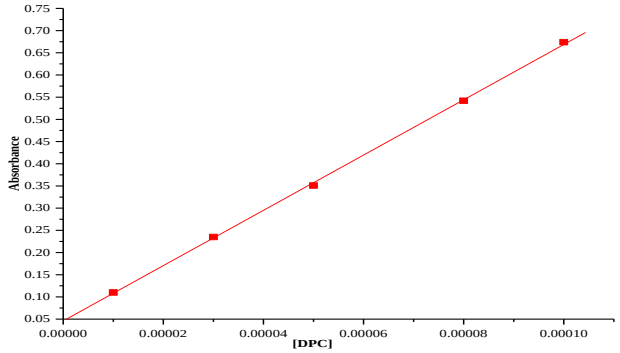

Figure 1: Plot of absorbance vs. [DPC] at 25 °C

The application of Beer-Lambert's law was verified from Figure 1 and found that negligible interference was entertained in the reaction. The maximum wavelength of DPC (III) was noticed at 415 nm.

RESULTS AND DISCUSSION

Stoichiometry and Product Analysis

Several sets of reaction mixtures with varying ratio of DPC to amoxicillin in presence of constant amounts of KOH and KNO_3 were kept for 2.5 hrs in a closed vessel under N_2 atmosphere and the remaining concentration of DPC was analyzed to confirm the accurate stoichiometry by Job's method which was confirmed to be 1:2 for AMX: DPC (III). When amoxicillin reacts with DPC in alkaline medium, 4-hydroxybenzonitrile, 2-amino-2-formylacetic acid and 1-amino-2-methylpropane-2-thiol were formed as the main product which was recrystallized from ethanol, separated by Column Chromatography over neutral alumina by using 80% benzene and 20% chloroform as eluent. Side product CO_2 was qualitatively detected by bubbling N_2 gas through the acidified reaction mixture and passing the gas liberated through the tube filled with lime water. The reaction between Amoxicillin and Diperiodatocuprate (III) in alkaline medium is given as Scheme 1.

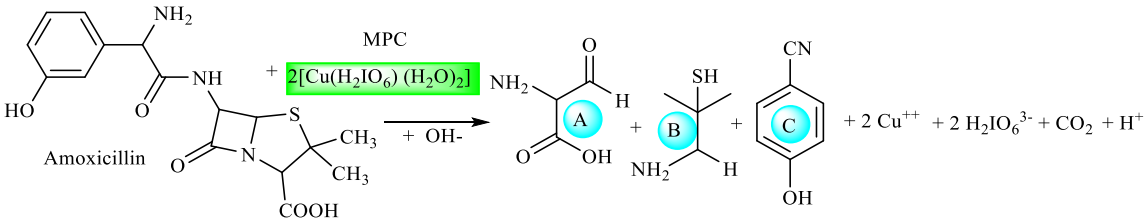

Where, A = 2-amino-2-formylacetic acid; B = 1-amino-2-methylpropane-2-thiol; C = 4-hydroxybenzonitrile

Scheme 1: Reaction showing the formation of complex

Similar oxidation products were already isolated in the uncatalyzed oxidation of amoxicillin by hexacyanoferrate (III) in the alkaline medium as reported earlier [8]. The complex showed a molecular ion peak at 686 m/z. The oxidation product 4-hydroxybenzonitrile was identified by the FT-IR spectrum that showed an absorption peak at 2048.13 cm^{-1} due to CN stretch, because of the presence of the hydroxyl group which was evident through the broad peak at 3440.55 cm^{-1}. The products 4-hydroxybenzonitrile, 2-amino-2-formylacetic acid, and 1-amino-2methylpropane-2-thiol showed a molecular ion peak at 119,102 and 106 m/z in LC-MS. Both LC-MS and FT-IR spectrum are presented in Figure **S 1 and S 2**.

Reaction Orders

The orders of reaction were determined from the slope of log k_{abs} versus log (concentration) from different time plots as given in Figure 6 and Table-1 by varying concentrations of amoxicillin, KIO_4, and KOH while keeping the other parameters constant except the concentration of DPC (III).

Effect of [DPC (III)]

The DPC concentrate was varied in the range of 1.0 x 10^{-5} to 1.0 x 10^{-4} mol dm^{-3}. The linearity and almost parallelism plots of log absorbance versus time up to 85% completion of the reaction by keeping other concentrations remaining constant indicated a reaction order of unity in DPC (III). Table 1 and Figure **2** are in the support of pseudo first-order reaction with respect to DPC (III).

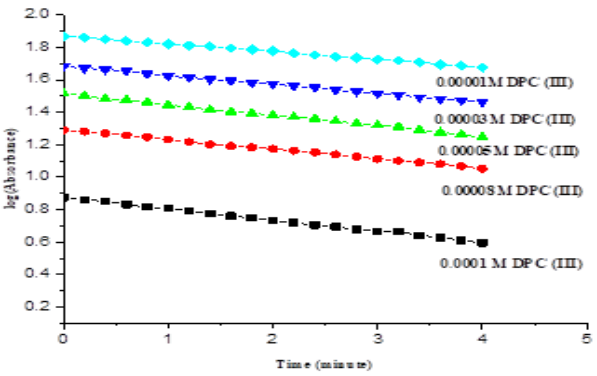

Figure 2: Order Plot of log(abs) vs. time for the oxidation of AMX by DPC (III)

Effect of [AMX]

The effect of [AMX] was studied within a range of 1 x 10^{-4} to 1 x 10^{-3}mol dm^{-3}. The rate constants (k_{obs}), increased with increase in [AMX] and order with respect to amoxicillin was found to be 0.69 (r ≥0.9894, s ≤ 0.0071) which was also confirmed from the plot of (4+ log k_{obs}) vs 5+ log [AMX], **Figure S 3 and Table 1.**

Effect of [Alkali]

The effect of alkali was studied by varying [OH^-] in the range of 0.04 to 0.2 mol dm^{-3} DPC, AMX, as well as ionic strength. Rate constant (k_{obs}) increased with increase in [alkali] and order of reaction with respect to alkali was found to be 0.53 (r ≥0.987, s ≤ 0.00217), confirmed by the linear plot of (4 + log k_{obs}) vs. 4 + log [KOH]), Figure **S 4** and Table 1.

Effect of [Periodate]

The effect of [KIO_4] was observed by varying the concentration range from 1.0 x 10^{-5} to 1.0 x 10^{-4} mol dm^{-3} remaining other active masses and conditions were constant. It was observed that rate constants decreased with an increase in [IO_4^-] and the order of reaction was -0.732 as computed in Table 1.

Table 1: Effect of variation of [DPC]*, [AMX] and [KOH] on the oxidation of Amoxicillin by Diperiodatocuprate (III) in aqueous alkaline medium at 298 K and I = 0.10 / mol dm^{-3}

[DPC] x 10^5	[AMX]x 10^4	[OH^-] x10^1	[IO_4^-] x10^5	K_{obs} x10^4 (s^{-1})	Order
1.0	5.0	0.8	1.0	3.95	
3.0	5.0	0.8	1.0	3.99	
5.0	5.0	0.8	1.0	**3.87**	**1.0**
8.0	5.0	0.8	1.0	3.82	
10.0	5.0	0.8	1.0	3.84	
5.0	**1.0**	0.8	1.0	1.5	
5.0	**3.0**	0.8	1.0	2.12	
5.0	5.0	**0.2**	1.0	1.87	
5.0	**5.0**	0.8	1.0	**3.87**	**0.69**
5.0	**8.0**	0.8	1.0	5.43	
5.0	**10.0**	0.8	1.0	7.56	
5.0	5.0	**0.4**	1.0	2.66	
5.0	5.0	**0.6**	1.0	2.99	
5.0	5.0	**0.8**	1.0	**3.87**	**0.53**
5.0	5.0	**1.0**	1.0	4.52	
5.0	5.0	0.8	**1.0**	**3.87**	**- 0.73**
5.0	5.0	0.8	**3.0**	2.99	
5.0	5.0	0.8	**5.0**	1.98	
5.0	5.0	0.8	**8.0**	1.00	
5.0	5.0	0.8	**10.0**	0.69	

*Concentrations are expressed in mol dm^{-3}.

Effect of Ionic Strength (I) and Dielectric Constant (D)

Ionic strength is applied to know the participation of specific species in the reaction like ion-dipole, ion-ion, dipole-dipole with the same or opposite charge, etc. The effect of ionic strength was studied by varying the concentration of KNO_3 in the range of (0.1 - 0.2 M by keeping the concentration of DPC (III), AMX and KOH constant and we found that increasing ionic strength did not have any significant effect on the rate of reaction. The dielectric constant of the medium (D) can be studied by varying t-butyl alcohol at a constant concentration of DPC (III), AMX, KOH and KNO_3 by using the equation $D = D_1V_1 + D_2V_2$ where D_1 and D_2 are the dielectric constant of water and t-butyl alcohol and V_1 and V_2 are volume fractions of those respectively. There was no effect of dielectric constant on the rate of the catalyzed reaction.

Effect of Initially Added Products

Initially added product ($CuSO_4$ (II)) didn't show any significant effect on the rate of reaction.

Polymerization Study

A known quantity of acrylonitrile[31] monomer was initially added to the reaction mixture and allowed to remain in the inert atmosphere for 3.0 hours. The mixture gave no precipitate on dilution with methanol indicating the absence of free radicals.

Effect of Temperature

The effect of temperature on the rate of oxidation reaction was studied at four different temperatures under the constant concentration of AMX, KOH, and DPC (III) keeping other conditions constant. The rate constants increased with the rise in temperature. Slope obtained from the plot of (log k_{obs} vs. 1/T) helped to calculate the activation

parameter and energy of activation and thence computed in Table 2 and Figure **S 5**.

Table 2: Effect of temperature and activation parameters by rate constants (k_{obs})

Temp (K)	(1/T) 10^3	K_{obs} x 10^4	4 + log k_{obs}
293	3.41	1.86	0.27
298	3.35	3.87	0.59
303	3.30	4.10	0.61
308	3.24	5.76	0.76

Activation Parameters	Values
Ea (K j mol^{-1})	51.43
$\Delta H^{\neq}$ (K j mol^{-1})	49 ± 2
$\Delta S^{\neq}$ (J K^{-1} mol^{-})	-149± 2
$\Delta G^{\neq}$ (k $Jmol^{-1}$)	94 ± 2
LogA	5 ± 0.3

Since DPC (III) is chelating as well as the oxidizing agent, oxidation of different β-lactam antibiotics has been carried out in an alkaline medium. The activity of DPC is a function of pH and is capable of subtle control.DPC (III) is water-soluble oxidizing reagent that exists as $[Cu(HIO_6)_2(OH)_2]^{7-}$ as well as $[HIO_6]^{4-}$ under higher pH condition. It has been evident that it can also exist as $[Cu(H_3IO_6)_2]^{-}$ or $[Cu(H_2IO_6)(OH)_2]^{2-}$ or $[Cu(H_2IO_6)(H_2O)_2]$ or $[Cu(H_3IO_6)(H_2O)_2]$ in aqueous alkaline medium. Periodic acid exists as H_5IO_6 in acid medium. The main species most active for the title work is $[Cu(H_2IO_6)(H_2O)_2]$ as reported in earlier literature. At higher alkali concentration, periodate ion tends to dimerize.

$$H_5IO_6 \rightleftharpoons H_4IO_6^{-} + H^{+}, \quad K_1 = 5.1 \times 10^{-4}$$

$$H_4IO_6^{-} \rightleftharpoons H_3IO_6^{2-} + H^{+}, \quad K_2 = 4.9 \times 10^{-9}$$

$$H_3IO_6^{2-} \rightleftharpoons H_2IO_6^{3-} + H^{+}, \quad K_3 = 2.5 \times 10^{-12}$$

Probable Mechanism of Reaction

The oxidation reaction between MPC and amoxicillin showed 1:2 stoichiometry and exhibited pseudo-first order reaction with respect to DPC(III), fractional order with respect to amoxicillin and alkali but negative fractional-order periodate. Based on this experimental evidence, a suitable mechanism is proposed along with the proper involvement of all species. In the first step, DPC(III) reacts with the hydroxide ion to form a deprotonated form of DPC which in presence of water yields MPC(III) along with free periodate species. Hence fractional with respect to amoxicillin presumably results due to the formation of the complex by the interaction between amoxicillin and MPC species. This complex interacts with one mole of MPC in a slow step to give 4-hydroxybenzonitrile, an intermediate I along with regeneration of free periodate ion and Cu^{++} ion. In the next step, the intermediate I reacts with one mole of MPC to form intermediate II which undergoes hydrolysis to yield the other final products ie; 2-amino-2-formylacetic acid and 1-amino-2-methylpropane-2-thiol as explained in Scheme 2.

Spectroscopic evidence for the complex formation between reagent DPC(III) and substrate (AMX) was obtained from UV –visible spectra by resisting (5.0×10^{-4} M) AMX, (0.12 M) KOH and a mixture of all. A bathochromic shift was obtained. The Michaelis – Menten plot is in great support for complex formation, Figure **S 5**.

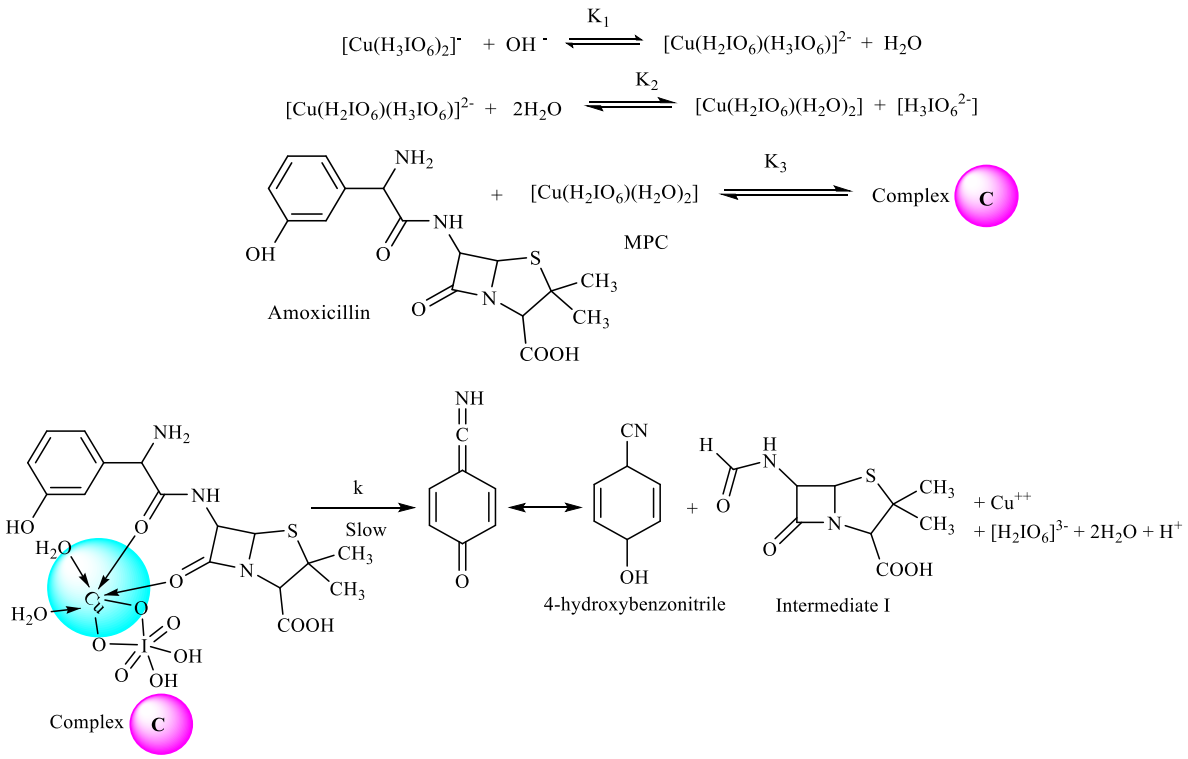

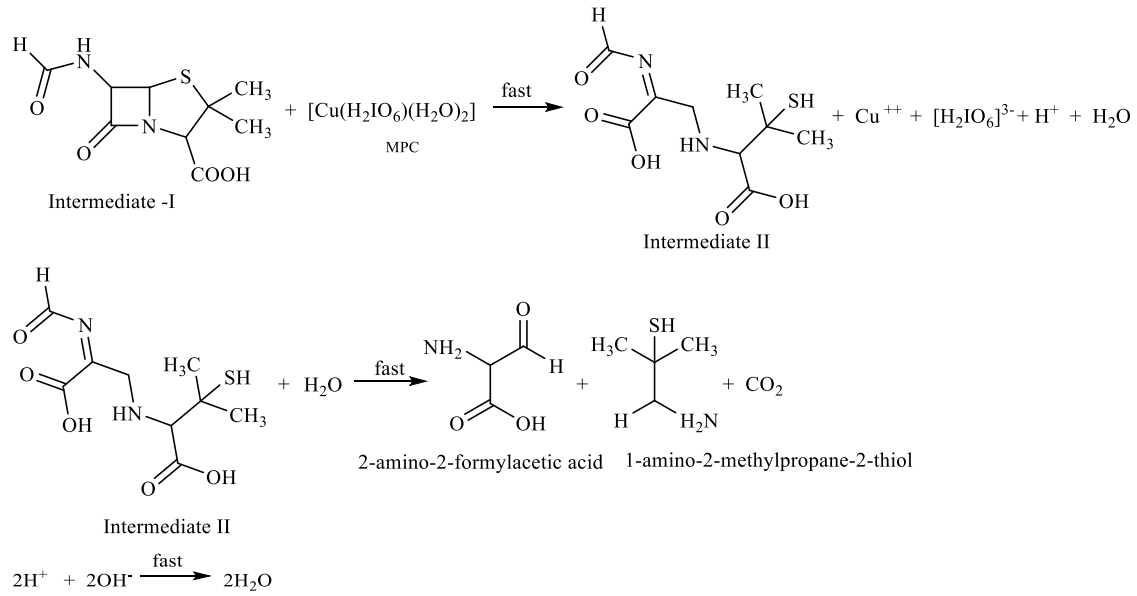

Scheme 2: Detailed Scheme for uncatalyzed oxidation of AMX by DPC(III)

Scheme 2 leads to the rate law equation (6) as -

$$\text{rate} = -\frac{d[DPC]}{dt} = k[C] \qquad [5]$$

$$k_{obs} = \frac{kK_1K_2K_3[DPC][AMX][OH^-]}{[H_3IO_6{}^{2-}] + K_1[OH^-][H_3IO_6{}^{2-}] + K_1K_2[OH^-] + K_1K_2K_3[OH^-][AMX]} \qquad [6]$$

This equation (6) describes all kinetic orders observed for different species. The rate law equation (6) can be rearranged into equation (7) that suits for verification.

$$\frac{1}{k_{obs}} = \frac{[H_3IO_6{}^{2-}]}{kK_1K_2K_3[AMX][OH^-]} + \frac{[H_3IO_6{}^{2-}]}{kK_2K_3[AMX]} + \frac{1}{kK_3[AMX]} + \frac{1}{k} \qquad [7]$$

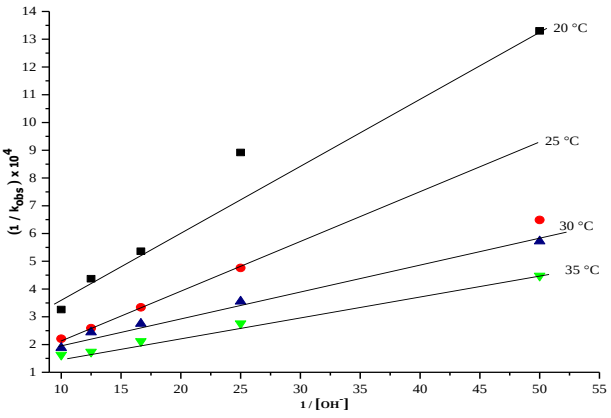

Figure 3: Plot of [1/ k_{obs} vs.1/[KOH]

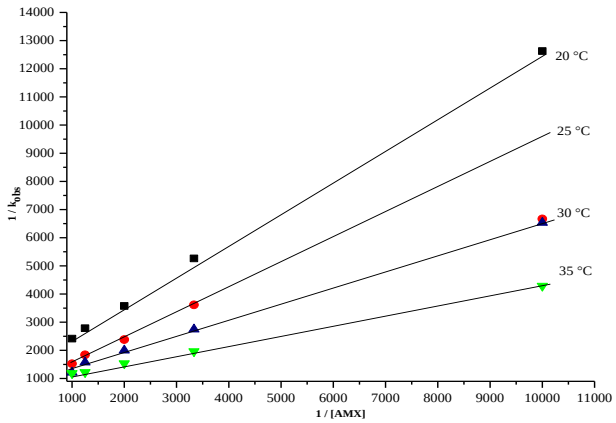

Figure 4: Plot of [1/k_{obs} vs.1/[AMX]

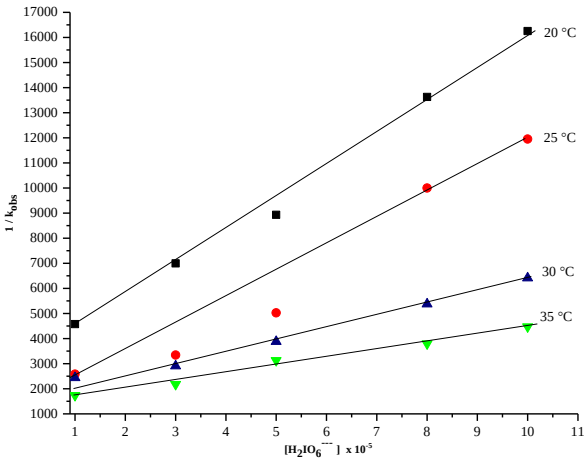

Figure 5: Plot of [1/k_{obs} vs.$[H_2IO_6]^{3-}$

Figure (3-5) represent verification plots for oxidation of AMX by DPC(III) in alkaline medium. According to equation (7), remaining other conditions being constant, the plots of [1 / k_{obs} vs.1 / [KOH] ($r \geq 0.995, \leq s\ 0.00356$), [1 / k_{obs} vs. 1/[AMX] ($r \geq 0.9791, \leq s\ 0.0045$) and [1/ k_{obs} vs. $[H_2IO_6]^{3-}$ (presented in Figure **3, 4** and **5**) should be linear and are found to be so as in Figure 3, 4 and 5. Similarly, activation parameters and thermodynamic parameters for un-catalyzed oxidation of AMX by DPC (III) in aqueous alkaline medium with respect to **slow step** rate constant (k) of Scheme I is presented in Table 3 and Figure **S 6**.

Table 3

Temp (K)	(1/T) 10^3	k x 10^4	4 + log k
293	3.41	7.35	0.87
298	3.35	8.63	0.94
303	3.30	9.75	0.96
308	3.24	12.2	1.09
Activation Parameters		**Values**	
Ea (k J mol^{-1})		24.12	
$\Delta H^{\neq}$ (k J mol^{-1})		21.63 ± 2	
$\Delta S^{\neq}$ (J K^{-1} mol^{-})		-137 ±1	
$\Delta G^{\neq}$ (k J mol^{-1})		62 ± 2	
LogA		1.14 ± 0.4	

Scheme 1 clarifies the participation of neutral species in the reaction due to invariable ionic strength and dielectric constant. The modest values of both enthalpy and entropy of activation, within the range of electron pairing and unpairing process for the loss of degree of freedom and rigid transition state, are favourable for electron transfer reaction. The higher negative value of $\Delta S^{\neq}$ suggests that the intermediate complex is probably highly ordered than the reacting species. The above results, evidences and lower rate constant for slow steps indicate that the oxidation presumably occurs via an inner-sphere mechanism. The reducing property of the substrate is, probably, reduced in the absence of catalyst and the path of the uncatalyzed reaction is extended by increasing the activation energy.

CONCLUSION

The oxidation of Amoxicillin by DPC (III) was studied experimentally in an alkaline medium. (MPC-III) [Cu (H_2IO_6) $(H_2O)_2$] was considered to be the active species for the present work. Activation parameters with respect to rate constant (k_{obs}) at different temperatures were computed. Overall sequences described here are inconsistent with all experimental evidences including product, spectral analysis, mechanistic and kinetics studies.

Supplementary Information: Some of essential Figures and spectrum are arranged into SI file, being attached along with this Manuscript **(SI).**

Acknowledgements: The first author (Y. R. Sahu) is highly acknowledged to Purwanchal Campus, Dharan, Institute of Engineering (IOE), T.U., Nepal for financial support, Prof. Dr. S. T. Nandibewoor and Prof. Dr. S.A. Chimatadar, Karnatak University, Dharwad , India for invaluable guidelines and suggestions and SAIF –IIT, Bombay, STIC-SAIF, Cochin and CDRI-CSIR, Lucknow, India for technical support in providing spectrum results.

REFERENCES

1. Chaudhary NK and Mishra P., Spectral investigation and in vitro antibacterial evaluation of Ni^{II} and Cu^{II} complexes of Schiff base derived from Amoxicillin and α-formalthiophene (αft), Journal of Chemistry, Vol. 2015. Doi.10.1155/2015/136285.
2. Fernando S S, Vanessa V d S, Catiusa K R, Hainzenreder L, Arenzon A & Liliana Al F , Comparison of different advanced oxidation processes for the removal of amoxicillin in aqueous solution, Environmental Technology, Taylor & Francis, Vol. 39, no. 5, 2018, pp.549-557. Doi: 10.1080/09593330.2017.1306116 PMID: 28287908
3. Elmolla E S and Chaudhuri M, Degradation of the antibiotics amoxicillin, ampicillin and cloxacillin in aqueous solution by the photo-Fenton process, Journal of Hazardous Materials, Vol. 172, no. (2-3), 2009, 1476-1481. PMID: 19717236, Doi: 10.1016/j.jhazmat.2009.08.015
4. Filiz Ay, and Fikret Kargi, "Advanced oxidation of amoxicillin by Fenton's reagent treatment," Journal of Hazardous Materials, Vol. 179, no.(1-3), 2010, 622-627. Doi: 10.1016/j.jhazmat.2010.03.048
5. Singh R and Mishra P, Synthesis, spectroscopic, XRPD and computational study of transition metal-organic framework (TMOFs) derived from (6 R)-6-(alpha-phenyl-D-glycylamino) penicillanic acid, Russian Journal of Inorganic Chemistry, Vol. 54, 2009, 1301-1309. Doi: 10.1134/S0036023609080208
6. Kaur S P, Rao R and Nanda S, Amoxicillin, a broad spectrum antibiotic, International Journal of Pharmacy and Pharmaceutical Sciences, Vol. 3, 3, 2011 (ISSN- 0975-1491).
7. Mukherjee G and Ghosh T, Metal ion interaction with penicillin part-vii: mixed ligands complexes formation of Co, Ni, Cu and Zn with ampicillin and nucleus bases, Journal of Inorganic and Biochemistry, Vol. 59, 1995, 827.
8. Alekseev V G, and Samuilova I S, Co-Gly beta lactam antibiotics complex formation in system, Russian Journal of Inorganic Chemistry, Vol. 53, 2008, 327.
9. Sutherland R, Croydon E A and Rolinson G N, Amoxycillin: new semi-synthetic penicillin. Br Med J., 3, 1972, 13 – 6.

   http://www.ncbi.nlm.nih.gov/pubmed/4402672.
10. Antibacterial and Common Infections: Stewardship, Effectiveness, Safety and Clinical Pearls, October 2016. Link: RxFiles.Ca©Oct 2016.
11. Hiremath D C, Kiran T S and Nandibewoor S T, Oxidation of vanillin by diperiodatocuprate (III) in aqueous alkaline medium: A kinetic and mechanistic study by stopped flow technique, International Journal of Chemical Kinetics, Vol. 39, 2007, no. 4. Doi.org/10.1002/kin.20233
12. Hosmani R R and Nandibewoor S T, Mechanistic study of Ruthenium (III) catalyzed oxidation of L-Lysine by Diperiodatoargentate (III) in aqueous alkaline medium, Journal of chemical sciences, 2009, 121, 275-281. www.ias.ac.in/article/fulltext/jcsc/121/03/0275-0281.
13. Shettar R S and Nandibewoor S T, Kinetic, mechanistic and spectral investigations of Ruthenium (III)-catalyzed oxidation of 4-hydroxycoumarin by alkaline diperiodatonickelate (IV) (stopped flow technique), Journal of Molecular Catalysis A: Chemical, Vol. 234, no. 1-2, 2005, pp. 137-143,. Doi.org/10.1016/j.molcata.2005.02.026
14. Reddy K B, Sethuram B and Rao T N , Kinetics of oxidative determination and decarboxylation of some amino acids by diperiodatocuprate (III) in alkaline medium, Indian Journal of Chemistry, Vol. 20A, 1981, pp. 395.
15. Solomon E I, Chen P, Metz M, Lee S K and Palmer A E, Oxygen binding, activation and reduction to water by copper proteins, Angew Chemistry, International Edition, Vol. 40, 2001, no.24, , pp. 4570 -4590. Doi.org/10.1002/1521-3773 (20011217)

16. Malatesta L , Salts of Trivalent Copper and Silver (II), Gazz. Chimica Ital. Vol. 71, 1941, pp. 580-584.

17. Panigrahi G, P. and A. C. Pathy A. C., Kinetics and mechanism of oxidation of potassium thiocyanate by potassium bis(tellurate) cuprate(III), Indian Journal of Chemistry, Vol.25A, 1986, pp. 354-357.

18. Nadimpali S, Padmvasthy J and Yusuff K K M, Determination of the nature of the diperiodatocuprate (III) species in aqueous alkaline medium through a kinetic and mechanistic study on the oxidation of iodide ion, Transition Metal Chemistry, Vol. 26, no. 3 , 2001, pp. 315-321,. Doi.org/10.1023/A:1007116932047

19. Chowdhury B, Mondal M H, Barman M K and Saha B, A study on the synthesis of alkaline Copper (III)-periodate (DPC) complex with an overview of its redox behavior in aqueous micellar media, Research on Chemical Intermediates (Springer), 2018. Doi.org/10.1007/S11164-018-3643-2.

20. Xie H Y, Wang Z R, and Fu Z F, Highly sensitive trivalent copper chelate-luminol chemiluminescence system for capillary electrophoresis chiral separation and determination of ofloxacin enantiomers in urine samples, Journal of pharmaceutical analysis, Science Direct, 4(6), 2014, 412-416. doi.org/10.1016/j.jpha.2014.05.004.

21. Byadagi K S, Nandibewoor S T and Chimatadar S A, Catalytic activity of ruthenium (III) on the oxidation of an Anticholinergic drug-atropine sulphate monohydrate by copper (III) periodate complex in aqueous alkaline medium-Decarboxylation and free radical mechanism, Acta Chimica Slovenica, 60(3), 2013, 617- 627.

22. Sethuram B, Some aspects of electron transfer reaction involving organic molecules, Allied Publishers Pvt. Ltd, New Delhi, 2003, 71-78.

23. Lister M W, The stability of some complexes of trivalent copper, Canadian Journal of Chemistry, Vol. 31, no. 7, 1953, 638-652. doi.org/10.1139/v53-087.

24. Veena M S , Prashanth M K, Kumar K Y, Muralidhara H B and Nayaka Y A, Kinetics and mechanistic study of oxidation of amoxicillin by Chloramine-T in acid medium, Journal of the Chilean Chemical Society, 60(3), 2015. Doi.org/10.4067/S0717-97072015000300019.

25. Zhao J, Sun Y, Wu F, Shi M and Liu X, Oxidative degradation of amoxicillin in aqueous solution by thermally activated persulphate, Journal of Chemistry, Article ID 2505823, Vol. 2019. Doi: org/10.1155/2019/2505823.

26. Durgannavar A K, Patgar M B and Chimatadar S A, Oxidation of amoxicillin by hexacyanoferrate (III) in aqueous alkaline medium- a kinetic and mechanistic Approach, Indian Journal of Chemistry, Vol. 54A, 2015, pp. 1085-1091.

27. Sahu Y R, Mishra P, Chimatadar S A and Nandibewoor S T, A kinetic and mechanistic approach for Co (III) catalyzed oxidation of amoxicillin by copper (III) periodate complexes in alkaline medium, World Journal of Pharmacy and Pharmaceutical Sciences. Vol. 8, no. 9, 2019, pp.1034-1051. Doi: 10.20959/wjpps20199-14676.

28. Jeffery G H, Basset J., Mendham R C and Denney R C, Vogel's Textbook of Qualitative Chemical Analysis, 5th Edition, ELBS, Longman, Essex U.K.455, 1996.

29. Panigrahi G P and Misro P K, Kinetics and mechanism of oxidation of osmium (VIII) catalyzed oxidation of unsaturated acids by sodium periodate, Indian Journal of Chemistry, 15A, 1977, 1066 -1069.

30. Jaiswal P K and Yadava K L, Determination of sugars and organic acids with periodato complex of Cu (III), Indian Journal of Chemistry, Vol. 11, 1973, pp. 837-838.

31. Jagadeesh R V and Puttaswamy J, Chemical transformation in synthetic organic chemistry, Journal of Physical and Organic Chemistry, Vol. 21, no. 10, 2008, pp. 844-858.

Source of Support: Nil, **Conflict of Interest:** None.

APPENDIX

(C) Derivation of rate law

From Scheme 1 $\text{Rate} = -\frac{d[DPC]}{dt} = k[\text{Complex}] = k[C]$ **[A-1]**

From the law of mass action, the third equilibrium constant can be given by $K_3 = \frac{[C]}{[Cu(H_2IO_6)(H_2O)_2[AMX]}$

After rearrangement, we get, $[C] = K_3[Cu(H_2IO_6)(H_2O)_2[AMX]$ **[A-2]**

Substituting the value of C from eq. [A-2], we get, $\text{Rate} = -\frac{d[DPC]}{dt} = K_1K_3[Cu(H_2IO_6)(H_2O)_2[AMX]$ **[A-3]**

The second equilibrium constant can be given by $K_2 = \frac{[Cu(H_2IO_6)(H_2O)_2[H_3IO_6{}^{2-}]}{[Cu(H_2IO_6)(H_3IO_6]^{2-}}$

This can be rearranged into $[Cu(H_2IO_6)(H_2O)_2] = \frac{K_2\,[Cu(H_2IO_6)(H_3IO_6]^{2-}}{[H_3IO_6]^{2-}}$ **[A-4]**

The first equilibrium constant can be given by $K_1 = \frac{[Cu(H_2IO_6)(H_3IO_6]^{2-}}{[Cu(H_3IO_6)_2]^{-}[OH^-]}$

This can be rearranged into $[Cu(H_2IO_6)(H_3IO_6]^{2-} = K_1\,[Cu(H_3IO_6)_2]^{-}[OH^-$ **[A-5]**

Substituting eq. [A-4] to [A-5] in eq. [A-3], we get

$$\text{Rate} = -\frac{d[DPC]}{dt} = \frac{kK_1K_2K_3[AMX]_f[DPC]_f[OH^-]_f}{[H_3IO_6)_2]^-} \quad \textbf{[A-6]}$$

The total concentration of [DPC] can be given as

$$[DPC]_T = [DPC]_f + [Cu(H_2IO_6)(H_3IO_6]^{2-} + [Cu(H_2IO_6)(H_2O)_2] + [C] \quad \textbf{[A-7]}$$

Where T and f denote total and free concentrations $= [DPC]_f + K_1[Cu(H_2IO_6)_2]^-[OH^-] + \frac{K_1K_2[Cu(H_2IO_6)_2]^-[OH^-]}{[H_3IO_6{}^{2-}]} + \frac{K_1K_2K_3[Cu(H_3IO_6)_2]^-[OH^-][AMX]}{[H_3IO_6]^{2-}}$

$$[DPC]_T = [DPC]_f + K_1[DPC]_f[OH^-] + \frac{K_1K_2[DPC]_f[OH^-]}{[H_3IO_6{}^{2-}]} + \frac{K_1K_2K_3[DPC]_f[OH^-][AMX]}{[H_3IO_6{}^{2-}]}$$

$$[DPC]_f = \frac{[DPC]_T[H_3IO_6{}^{2-}]}{[H_3IO_6{}^{2-}] + K_1[OH^-][H_3IO_6{}^{2-}] + K_1K_2[OH^-] + K_1K_2K_3[OH^-][AMX]} \quad \textbf{[A-8]}$$

The total concentration of [OH^-] can be given by

$$[OH^-]_T = [OH^-]_f + [Cu(H_2IO_6)(H_3IO_6]^{2-} + [Cu(H_2IO_6)(H_2O)_2] + [C]$$

$$[OH^-]_T = [OH^-]_f + K_1[DPC][OH^-]_f + \frac{K_1K_2[DPC][OH^-]_f}{[H_3IO_6]^{2-}} + \frac{K_1K_2K_3[DPC][OH^-]_f[AMX]}{[H_3IO_6]^{2-}} \qquad [OH^-]_T = [OH^-]_f\{1 + K_1[DPC] + \frac{K_1K_2[DPC]}{[H_3IO_6]^{2-}} + \frac{K_1K_2K_3[DPC][AMX]}{[H_3IO_6]^{2-}}\}$$

In view of low concentrations of DPC and $H_3IO_6^{2-}$ used, last three terms inside bracket can be neglected in comparison with unity.

$$[OH^-]_T = [OH^-]_f \quad \textbf{[A-9]}$$

Similarly, in case of low concentrations of DPC and $H_3IO_6^{2-}$ used $[AMX]_T = [AMX]_f$ **[A-10]**

Putting these values of $[DPC]_f$ from eq^n. [A-8], $[OH^-]_f$ from eq^n. [A-9] and $[AMX]_f$ from eq^n. [A-10] in eq^n. [A-6] after omitting subscripts T and f ,we get, Rate = $-\frac{d[DPC]}{dt} = \frac{kK_1K_2K_3[AMX][DPC][OH^-]}{[H_3IO_6{}^{2-}] + K_1[OH^-][H_3IO_6{}^{2-}] + K_1K_2[OH^-] + K_1K_2K_3[OH^-][AMX]}$

Or, $$\frac{1}{k_{obs}} = \frac{[H_3IO_6{}^{2-}]}{kK_1K_2K_3[AMX][OH^-]} + \frac{[H_3IO_6{}^{2-}}{k\,K_2K_3[AMX]} + \frac{1}{kK_3[AMX]} + \frac{1}{k} \quad \textbf{[A-11]}$$

Journal of Chemical Science and Engineering
JCSE, 3(2): 163-178
www.scitcentral.com

ISSN: 2642-0406

Original Research: Open Access

Kinetics and Mechanism of Oxidation of Dicloxacillin by Copper (III) Diperiodate Complex in Aqueous Alkaline Medium

Sahu YR, Mishra P* and Chaudhary NK

*Department of Chemistry, Tribhuwan University, Mahendra Morang Adarsha Multiple Campus, Biratnagar, Nepal.

Received April 13, 2020; Accepted June 03, 2020; Published July 10, 2020

ABSTRACT

The kinetics and mechanism of oxidation of Dicloxacillin by diperiodatocuprate [DPC (III)] in aqueous alkaline medium was studied spectrophotometrically at 298 K and ionic strength of 0.10 mol dm^{-3}. The reaction between DPC (III) and Dicloxacillin (DCLX) in alkaline medium showed (DCLX: DPC-III) 1:4 stoichiometry. The reaction products were identified by spot test, elemental analysis, FT-IR and LC-MS spectral studies. The reaction was of pseudo-first order with respect to DPC (III) and fractional order with respect to Dicloxacillin as well as alkali but periodate showed retarding fractional order. Monoperiodatocuprate (MPC-III) was found to be the main active species in the aqueous alkaline medium in the form of [Cu (H_2IO_6) $(H_2O)_2$]. Activation and thermodynamic parameters with respect to uncatalyzed rate constant (k_U), slow step rate constant (k) and equilibrium constants were determined. The plausible mechanism consistent with experimental results was proposed and discussed in detail.

Keywords: Kinetics, Diperiodatocuprate (III), Oxidation, Dicloxacillin, Mechanism

INTRODUCTION

Penicillanic Acid Derivatives (PADs) are composed of beta lactam ring fused with a thiazolidine ring. Among various PADs, beta-lactam antibiotics are widely applied by human and animals against different diseases due to narrow/broad spectrum anti-bacterial potency with a huge demand in hospitals, households, sewages and veterinary applications [1]. PADs, after application, do not degrade and get emitted into the aquatic environment and contaminate drinking water, regional discharge or waste samples, surface water, ground water, rivers, lakes and coastal waters [2,3]. For the degradation of PADs in aqueous solution, modern oxidation processes are to be developed as most of intermediates, hence formed, can be definitely mineralized into CO_2, water and mineral species. Effluents from the drug manufacturing industries [4]. Accumulate in wastewater and cosmetic wastewater treatment [5]. Plants and can pollute natural water reservoirs and such contamination can induce bacterial resistance even at environmental concentrations. Hence personal care products (PCPs) and antibiotic resistance represents a serious health problem and different advanced oxidation processes (AOPs) have to be developed for the degradation of such emergent chemical pollutants [6-11].

Dicloxacillin, discovered in 1961 and introduced in 1968, is one of the chlorinated PADs with narrow spectrum potency which is widely effective against gram positive bacteria or beta lactamases [6] producing organisms like ***Staphylococcus aureus***. It acts by inhibiting the synthesis of bacterial cell wall or cross linkage between linear peptidoglycon polymer chains which is quite essential component of cell wall of gram-positive bacteria [12,13]. Isoxazolyl group, present on the side chain of penicillin nucleus, supports the action of beta lactamases resistant as these are intolerant of side chain steric hindrance. Hence it binds penicillin-binding proteins and inhibits peptidoglycon cross-linkage[d]. Its molecular formula, molar mass and IUPAC name are $C_{19}H_{17}Cl_2N_3O_5S$, 470.327g mol^{-1} and (2S,5R,6R)-6-{[3-(2,6-dichlorophenyl)-5-methyl-oxazole-4-carbonyl]amino}-3,3-dimethy-7-oxo-4-thia-l-azabicyclo[3.2.0]heptanes-2-carboxylic acid respectively. Its structure is given in **Figure 1**.

Corresponding author: Parashuram Mishra, Bio-inorganic and Materials Chemistry Research Laboratory, Department of chemistry, Tribhuwan University, M.M.A.M. Campus, Biratnagar, Nepal Tel: +977-9742129647, E-mail: prmmishra@rediffmail.com

Citation: Sahu YR, Mishra P & Chaudhary NK. (2020) Kinetics and Mechanism of Oxidation of Dicloxacillin by Copper (III) Diperiodate Complex in Aqueous Alkaline Medium. J Chem Sci Eng, 3(2): 163-178.

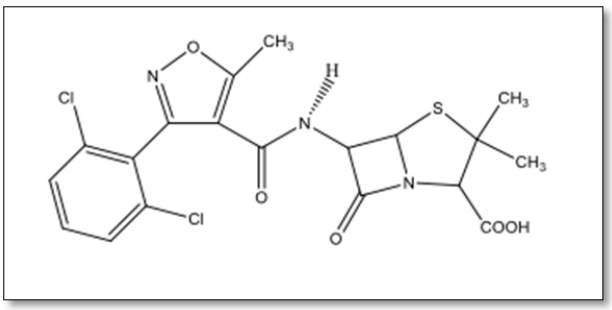

Figure 1. Structure of dicloxacillin.

Diperiodatocuprate (DPC-III) [14], Diperiodatoargentate (DPA-III) [15], Diperiodatonickelate (DPN-IV) [16], etc. are common polydentate ligands as well as oxidizing agents which can form stable complexes with transition metals. Malatesta [17,18] had initially synthesized diperiodatocuprate (III) more than a half-century ago. Many research works have been reported on the synthesis, structural determination stability, nature and analytical applications of this complex [19,20]. Diperiodatocuprate (III) has a flexible one electron-donating nature [21] and DPC (III) has a square planar geometry with dsp^2 hybridization and diamagnetic nature. It acts as an analytical reagent and hence used in many biological and analytical electron transfer reactions [22,23].

Literature regarding to dicloxacillin is scanty and hence a limited report on oxidation of dicloxacillin in acid as well as in alkaline medium could have been encountered in earlier literatures. Abdelrahman MM et al. (2018) [24] have described the oxidation of dicloxacillin by Chromatographic methods for quantitative determination of ampicillin, dicloxacillin and their impurity 6-aminopenicillanic acid. Kumar et al. (2015) [25] have reported the kinetics and mechanism of oxidation of dicloxacillin sodium [DXS] by chloramine-T [CAT] in [HCl] medium. Similarly, Bhinge and Malipatil (2015) [26] have reported the development and validation of a stability indicating method for the simultaneous estimation of cefixime and dicloxacillin using the RP-HPLC method**.** Stage et al. (2018) [27] have described that dicloxacillin induces CYP2C- and CYP3A-mediated drug metabolism - *in vivo* and *in vitro*. Guzman et al. (2015) [28] have explained the evaluation of water matrix effects, experimental parameters, and the degradation pathway during the TiO_2 photo catalytical treatment of the antibiotic dicloxacillin. Acharya et al. (2013) [29] have reported the development and validation of RP-HPLC method simultaneous estimation of amoxicillin and dicloxacillin in bulk drug and capsule.

We have already investigated the oxidation of different PADs like ampicillin, amoxicillin, catalyzed dicloxacillin and carbenicillin along with publications in different reputed journals [30]. Now, the present research work is aimed to investigate the kinetics and mechanism of oxidation of dicloxacillin in the absence of catalyst and hence to arrive at plausible mechanisms including determination of both activation and thermodynamic properties as well as calculation of uncatalyzed rate constant (k_U), slow step rate constant (k) and equilibrium constants at different temperatures.

EXPERIMENTAL PART

Reagents and chemicals

All chemicals of Analytical Reagent (AR) grade and double distilled water were used throughout the work. The stock solution of dicloxacillin (0.01 mol dm^{-3}) was prepared by dissolving 0.470 g of recrystallized dicloxacillin in 100 ml double distilled water. Potassium periodate solution was prepared by dissolving 0.023 g (0.01mol dm^{-3}) of KIO_4 (Sigma Aldrich) in 100 ml double distilled hot water and the solution was used only after 24 h. Iodometric method was used to determine the concentration of potassium periodate solution [31].

Instrumentation

ELICO LI 613 pH meter was used to measure the pH of the solution. The electronic absorption spectra were recorded on Varian CARY 5000 UV-VIS spectrophotometer in the range of 200-1000 nm. The infra-red spectra of the complexes were recorded on Thermo Nicolet, Avatar 370 FT-IR spectrometer in the range of 4000-400 cm^{-1} that was run as KBr disc. The mass spectrum of the products was recorded on the UPLC-TQD Mass spectrometer in positive mode in the range of 0 – 1000 m/z.

Synthesis of reagent

Copper (III) diperiodate complex was prepared [32,33]. by mixing copper sulphate (3.54 g), potassium periodate (6.80 g), potassium persulphate (2.20 g) and potassium hydroxide (9.0 g) in a 250 ml double distilled water in a round bottomed flask, shaken frequently thoroughly and heated on a hot plate for about 2 h. During this period, the mixture turned to intense red and the flask was heated further for 20 min to ensure the removal of excess potassium persulphate completely from the mixture upon degradation of persulphate. After completion of the reaction, the mixture was cooled and filtered through sintered glass crucible G-4 and the dark red-brown solution (filtrate) was diluted to 250 ml by adding double-distilled water. The aqueous solution of DPC (III) was standardized by iodometric titration ($Na_2S_2O_3$, starch, KI and KH_2PO_4) by thiocyanate method and its exact concentration was ascertained. The existence of DPC (III) was verified by UV-visible spectrophotometer that showed an absorption band with a maximum peak at 415 nm. Finally, the accurate concentration of DPC (III) was calculated by UV-visible spectrophotometer.

Synthesis of complex

10 ml of dicloxacillin solution (0.132 mol dm^{-3}) was taken in a 100 ml RB flask. To this 10 ml DPC(III) (0.528 mol

dm^{-3}) was mixed in 1:4 stoichiometric ratio along with 1.0 ml of each KNO_3 (Himedia), KIO_4 and 2.0 ml of KOH solution of fixed molarities and stirred on metal hot plate for 24 hours followed by re-stirring during re-fluxing with condensation for 24 hours. Then the mixture was cooled naturally for 3 days and filtered by Whatsman no.1. The products were purified and recrystallized in ethanol till the whole solvent evaporated leaving behind crystals only. The formation of DPC (III) complex was confirmed by the appearance of peaks in UV-Visible spectrophotometer. The possible structures of DPC (III) and MPC (III) are given in **Figure 2**.

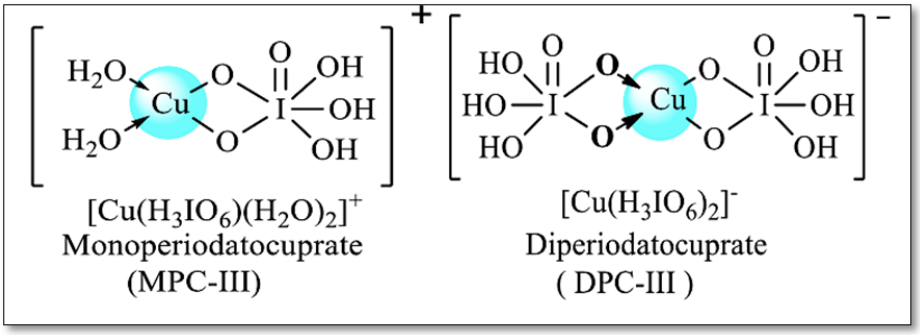

Figure 2. Possible structures of MPC (III) & DPC (III).

KINETIC MEASUREMENTS

The reaction is very fast in nature, its absorbance was taken rapidly along with the progress of the reaction when the active mass of dicloxacillin was greater than that of DPC (III) at 20□, 25□, 30□ and 35□ ± 0.5□ unless specified. The reaction was conducted by mixing required quantities of previously thermo-stated solutions of dicloxacillin into DPC (III) which already contained a fixed concentration of KIO_4 along with KNO_3 and KOH. Data were recorded from UV-Visible spectrophotometer at pH (9.2-10) and 415 nm wavelength by monitoring the decrease in absorbance at the molar extinction coefficient (**€**) of 6242 ± 50 $dm^3\ mol^{-1}cm^{-1}$. The UV visible spectrophotometer was run up to 87 % reaction.

Regression analysis of experimental data to obtain regression coefficient (r) and standard deviation (s) of points from the regression line was completed with the help of Origin 9.6 (2017) software. Plots of log (abs) versus time gave a straight line and hence rate constants (k_U) were calculated from slopes. Those k_U values agreed within ± 5% error and were the average of at least three independent kinetic runs. A constant concentration of periodate and nitrate were mixed into reaction mixture frequently in each time. Finally, the total concentration of KIO_4 and KOH were determined by assuming the amount present in DPC (III) and added additionally. To check the effect of periodate, ionic strength, dissolved oxygen, etc, kinetics were also conducted into the N_2 atmosphere wherein no significant changes were observed. Added carbonate and periodate dielectric constant etc didn't show any effect. The application of Beer-Lambert's law was verified from **Figure 3** and found that negligible interference was entertained in the reaction. The maximum wavelength of DPC (III) was noticed at 415 nm.

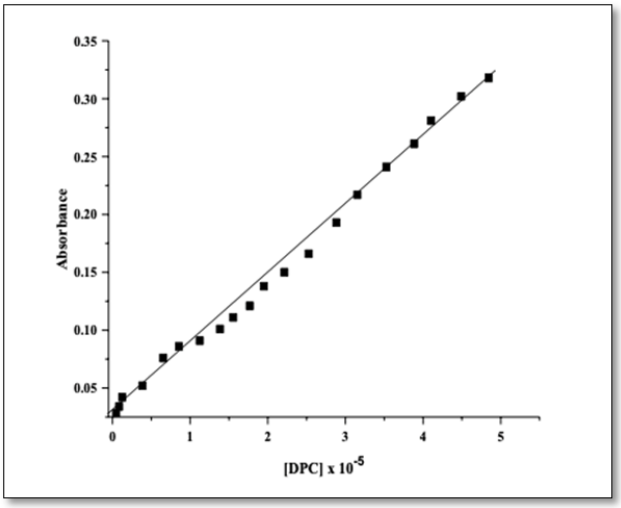

Figure 3. Plot of absorbance vs. [DPC] at 25°C.

RESULTS AND DISCUSSION

Stoichiometry and product analysis

Different sets of reaction mixtures with varying ratio of DPC (III) to dicloxacillin in presence of constant amounts of KOH and KNO_3 were kept for 3 h in a closed vessel under N_2 atmosphere and the remaining concentration of DPC (III) was analyzed to confirm the accurate stoichiometry by ***Job's method*** which was confirmed to be ***1:4*** for DCLX: DPC (III). When dicloxacillin reacts with DPC (III) in aqueous alkaline medium, 2, 6-dichlorophenyl)-5-methyl-4, 5-dihydroisoxazole-4-carboxylic acid ($C_{11}H_9Cl_2NO_3$) and 3-(2-(amino (carboxy) methyl)-5, 5-dimethyl-4, 5-dihydrothiazole-4-carboxylic acid-1-oxide were formed as the main product which was recrystallized from ethanol, separated by Column Chromatography over neutral alumina by using 80% benzene and 20% chloroform as eluent. Side product CO_2 was qualitatively detected by bubbling N_2 gas through the acidified reaction mixture and passing the gas liberated through the tube filled with lime water.

The reaction between dicloxacillin and Diperiodatocuprate (III) in alkaline medium is given as:

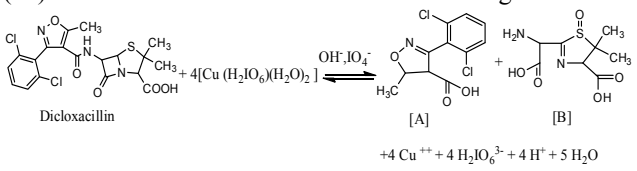

$$+4\,Cu^{++} + 4\,H_2IO_6^{3-} + 4\,H^+ + 5\,H_2O$$

where A = (2,6)-dichlorophenyl-5methyl-4-dihydroisoxazole-4-carboxylic acid & B = 3-(2-(amino (carboxyl) methyl-(5, 5)-dimethyl-(4,5)-dihydrothiazole-4-carboxylic acid-1-oxide

(Scheme 1: Reaction between uncatalyzed dicloxacillin and Copper (III) diperiodate)

Both DCLX- DPC (III) complex and products were characterized by LC-MS, which gave m/z at 792 (m-2) for complex ($C_{19}H_{23}Cl_2N_3CuIO_{13}S$), the first product (2, 6-dichlorophenyl)-5-methyl-4, 5-dihydroisoxazole-4-carboxylic acid) gave m/z at 248 and the second product (3-(2-(amino (carboxy) methyl)-5, 5-dimethyl-4, 5-dihydrothiazole-4-carboxylic acid-1-oxide) at 273 (m+1) respectively. A sharp absorption peak at 1633.4cm^{-1} (due to ketonic / carboxylic C=O stretch) ,1388.5 & 1118.5 cm^{-1} (due to CH_3 stretch) and 3448.2 cm^{-1} (due to N-H stretching) and a broad peak at 2917.9 cm^{-1} (due to carboxylic OH group). The first product, 2, 6-dichlorophenyl)-5-methyl-4, 5-dihydroisoxazole-4-carboxylic acid ($C_{11}H_9Cl_2NO_3$) showed C- 48.20(48.35), H-3.31(3.25), Cl-25.87(25.72), N-5.11(5.04) besides oxygen. The second product 3-(2-(amino (carboxy) methyl)-5, 5-dimethyl-4, 5-dihydrothiazole-4-carboxylic acid-1-oxide ($C_8H_{12}N_2O_5S$) showed C- 41.37(41.43), H-5.21(5.34) N-12.06(11.83) and S –13.81(13.95) besides oxygen. Both LC-MS and FT-IR spectrum are presented in **Figure 3** and **Figure 4** respectively.

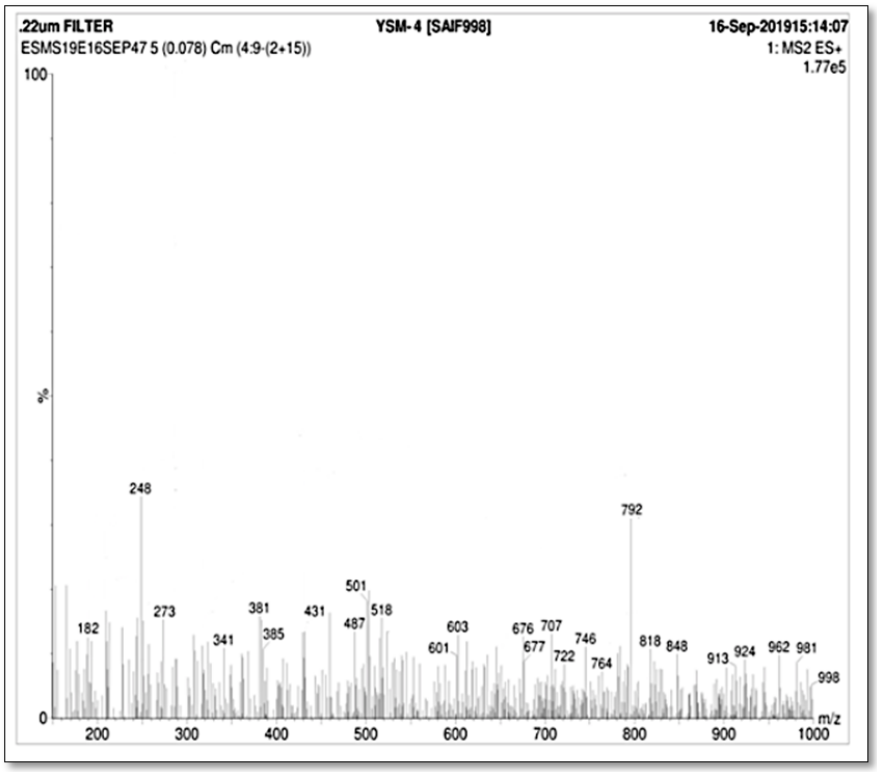

Figure 3. LC-MS of Complex & product formation for Oxidation of DCLX by DPC (III).

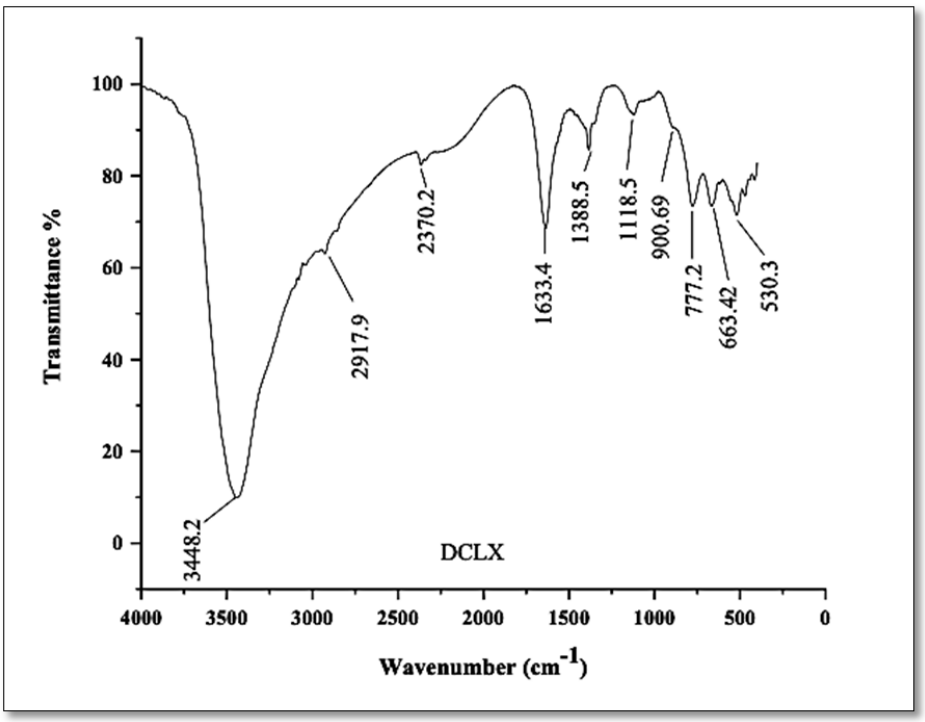

Figure 4. FT-IR of products formation for Oxidation of DCLX by DPC (III).

Reaction orders

Reaction orders were determined from the slope of log (absorbance) versus time plots as given in **Figure 5** and **Table 1** by varying concentrations of dicloxacillin, KIO_4 and KOH remaining other parameters constant except the concentration of DPC (III).

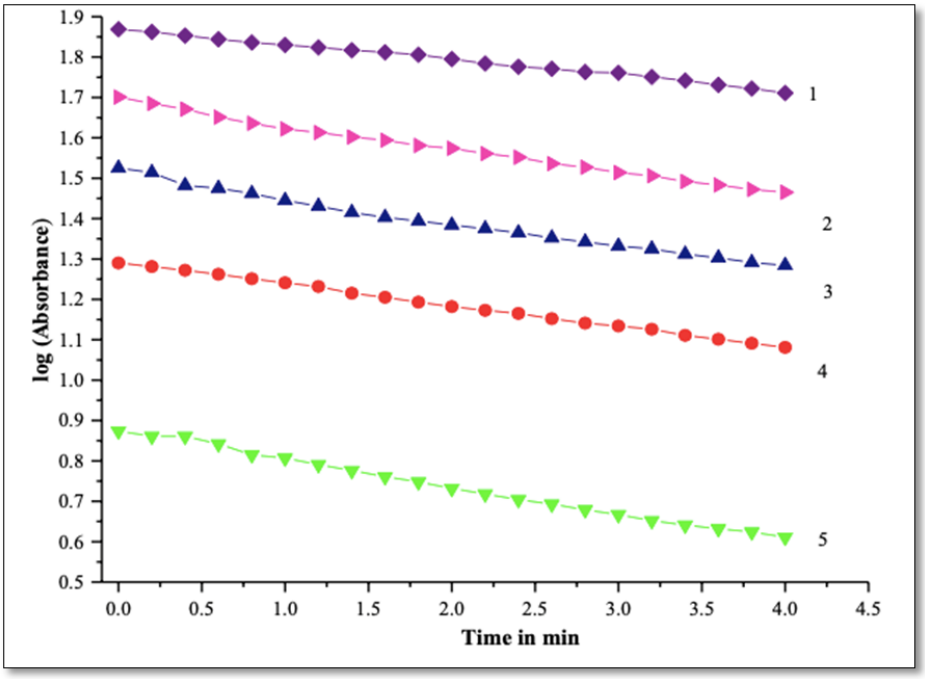

Figure 5. Order Plot of log (absorbance) vs. time for the oxidation of DCLX by DPC (III).

Table 1. Effect of variation of [DPC], DCLX], [KIO_4] and [KOH] on the oxidation of dicloxacillin by Diperiodatocuprate (III) in aqueous alkaline medium at 298 K and I = 0.10 / mol dm^{-3}.

*[DPC] x 10^5	*[DCLX] x 10^4	*[OH^-] x 10^2	*[IO_4^-] x 10^5	**k_U x 10^{-4} (s^{-1})	Order
1.0	5.0	0.8	1.0	1.80	
3.0	5.0	0.8	1.0	1.85	
5.0	5.0	0.8	1.0	**1.86**	
8.0	5.0	0.8	1.0	1.82	
10.0	5.0	0.8	1.0	1.88	
5.0	**1.0**	0.8	1.0	0.68	
5.0	**3.0**	0.8	1.0	1.35	
5.0	**5.0**	0.8	1.0	**1.86**	**0.75**
5.0	**8.0**	0.8	1.0	2.55	
5.0	**10.0**	0.8	1.0	3.24	
5.0	5.0	**0.2**	1.0	0.75	
5.0	5.0	**0.4**	1.0	1.12	
5.0	5.0	**0.6**	1.0	1.57	
5.0	5.0	**0.8**	1.0	**1.86**	**0.531**
5.0	5.0	**1.0**	1.0	2.31	
5.0	5.0	0.8	**1.0**	**1.86**	**-0.203**
5.0	5.0	0.8	**3.0**	1.55	
5.0	5.0	0.8	**5.0**	1.31	
5.0	5.0	0.8	**8.0**	0.86	
5.0	5.0	0.8	**10.0**	0.53	

**Concentrations are expressed in mol dm^{-3}. ** k_U denotes uncatalyzed rate constant*

Effect of [DPC (III)]

DPC (III) concentration was varied within the range of 1.0 x 10^{-5} to 1.0 x 10^{-4} mol dm^{-3}.The linearity and almost parallelism plots of log absorbance versus time up to 87% completion of the reaction by keeping other concentrations remaining constant indicated first order reaction in DPC (III). **Table 1** and **Figure 2** are in good support of pseudo first-order reaction with respect to DPC (III).

Effect of [DCLX]

The effect of [DCLX] was studied by varying [DCLX] within a range of 1 x 10^{-4} to 1 x 10^{-3}mol dm^{-3}. Rate constants (k_U) increased with increase in [DCLX] and order with respect to dicloxacillin was found to be 0.75 ($r \geq 0.994$, $s \leq 0.004$), as confirmed from linear plot of (5 + log k_U) vs 4 + log [DCLX], **(Figure 6** and **Table 1)**.

Effect of [Alkali]

The effect of alkali was studied by varying [OH^-] within the range of 0.02 to 0.1 mol dm^{-3}. Rate constants (k_U) increased with increase in [alkali] and order of reaction with respect to alkali was found to be 0.531 ($r \geq 0.997$, $s \leq 0.0003$), as confirmed by the linear plot of (5 + log k_c) vs. 4 + log [KOH]), **(Figure 7** and **Table 1)**.

Effect of [Periodate]

The effect of [KIO_4] in case of DCLX was observed by varying the [KIO_4] within the range of 1.0 x 10^{-5} to 1.0 x 10^{-4} mol dm^{-3}

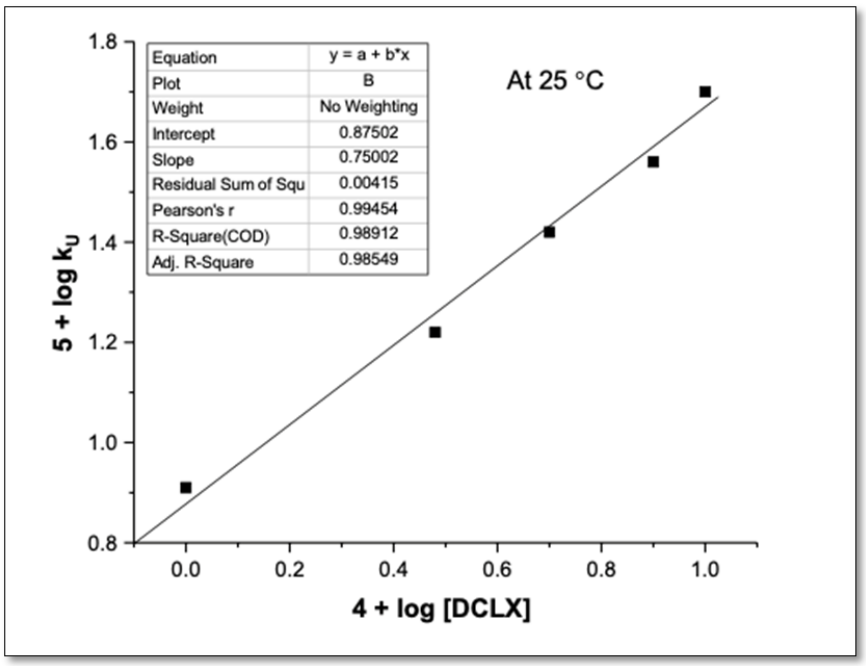

Figure 6. Plot of (5 + log k_U) vs. 4 + log [DCLX].

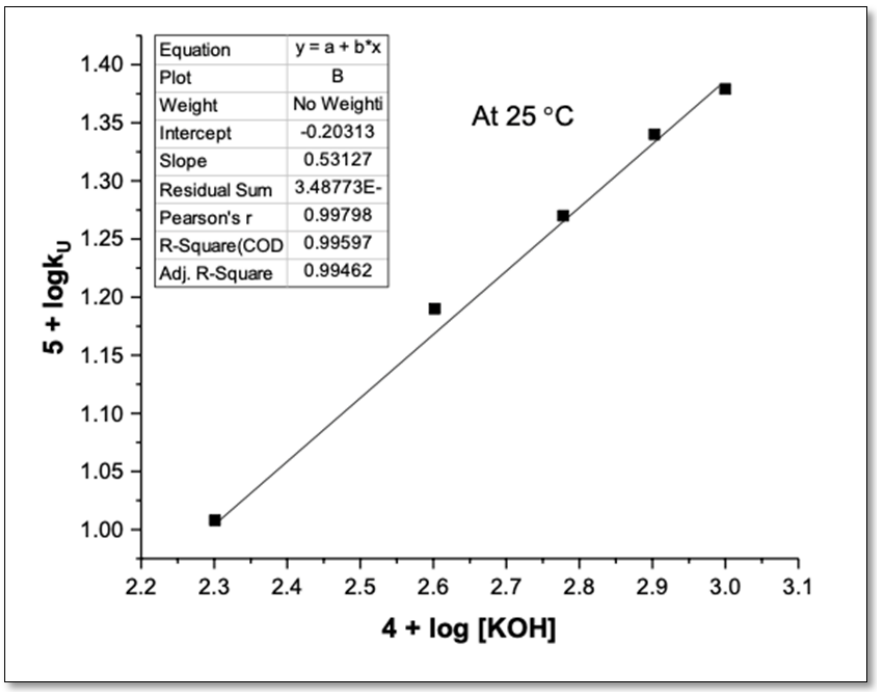

Figure 7. Plot of (5 + log k_U) vs. 4 + log[KOH].

remaining other active masses and constant. Rate constants decreased with an increase in [IO_4^-] and the order of reaction was - 0.203 ($r \geq 0.998$, $s \leq 0.009$), as confirmed by the linear plot of (4 + log k_U) vs. 5 + log [KOI_4]), as computed in **Figure 8** and **Table 1**.

Effect of ionic strength (I) and dielectric constant (D)

Increase in ionic strength did not have any significant effect on the rate of reaction. There was no effect of dielectric constant on the rate of the catalyzed reaction.

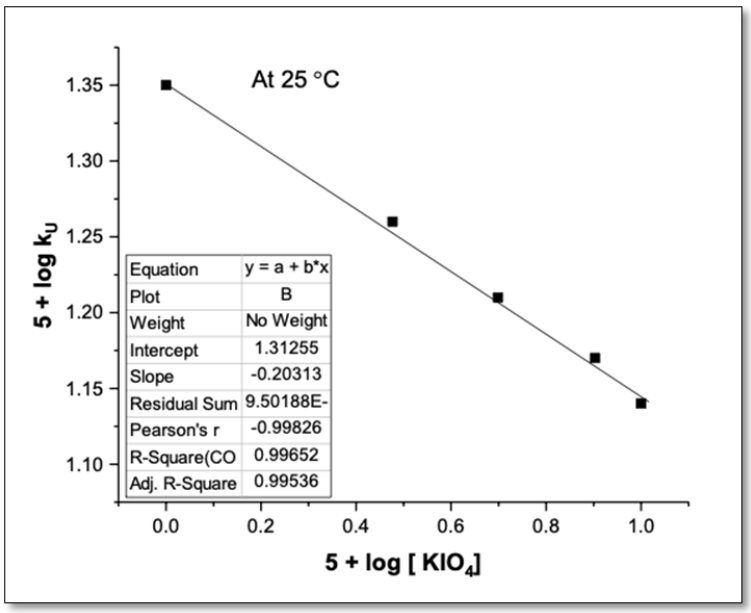

Figure 8. Plot of 5 + log [KIO_4] vs. 4 + log k_U.

Effect of initially added products and polymerization study

Initially added product ($CuSO_4$ -II)) did not exhibit any significant effect on the rate of reaction. A known quantity of acrylonitrile [34] monomer was initially added to the reaction mixture and allowed to remain in the inert atmosphere for 3.0 h. No precipitate was obtained from the mixture on dilution with methanol indicating the absence of free radicals.

Effect of temperature

Effect of temperature on the rate of oxidation reaction was studied at four different temperatures under the constant concentration of DCLX, KOH, and DPC (III) keeping other conditions constant. The rate constants increased with the rise in temperature. Slopes obtained from the plot of uncatalyzed rate constant ($\mathbf{k_U}$) and slow step rate constant (**k**) helped to calculate activation as well as thermodynamic parameters and thence computed in **(Table 2** and **3**) and **(Figure 9a** and **9b)**. Similarly, slopes and intercepts obtained from the plot of equilibrium constant versus reciprocal of temperature helped to calculate activation as well as thermodynamic parameters and thence computed in **Figure 10a, 10b** and **10c** and **Table 4a** and **4b.**

Table 2. Activation parameters from uncatalyzed rate constant ($\mathbf{k_U}$) for DCLX.

Parameters	**Values**
Ea (k $Jmol^{-1}$)	50.0
$\Delta H^{\neq}$ (k $Jmol^{-1}$)	47.0 ± 2
$\Delta S^{\neq}$ ($JK^{-1}mol^{-1}$)	-152.0 ± 3
$\Delta G^{\neq}$ (kJ mol^{-1})	92.0 ± 4
LogA	4.92 ± 0.04

Table 3. Activation parameters from slow step rate constant (**k**) for DCLX.

Parameters	**Values**
Ea (k $Jmol^{-1}$)	68.85
$\Delta H^{\neq}$ (k $Jmol^{-1}$)	66 ±2
$\Delta S^{\neq}$ ($JK^{-1}mol^{-1}$)	-88 ± 4
$\Delta G^{\neq}$ (k J mol^{-1})	94 ± 3
LogA	8 ± 1.0

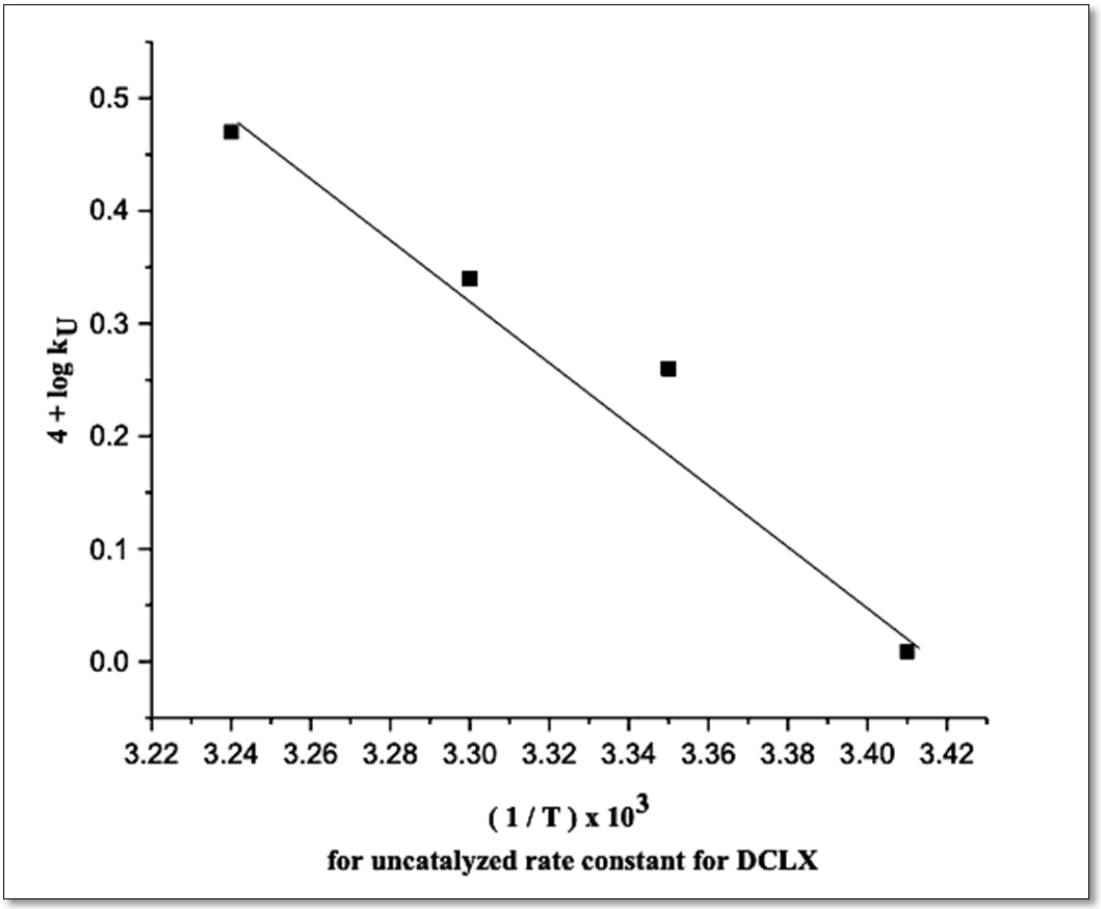

Figure 9a. Plot of 4 + log k_U vs. 1/ T.

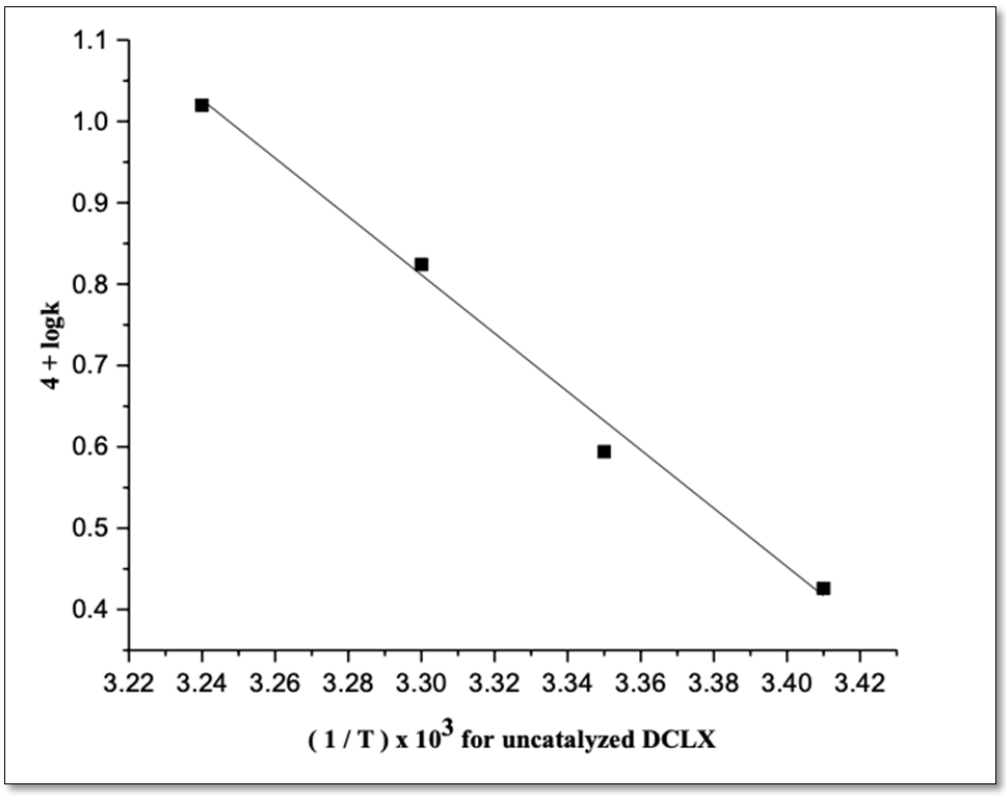

Figure 9b. Plot of (4 + log k) vs 1/T.

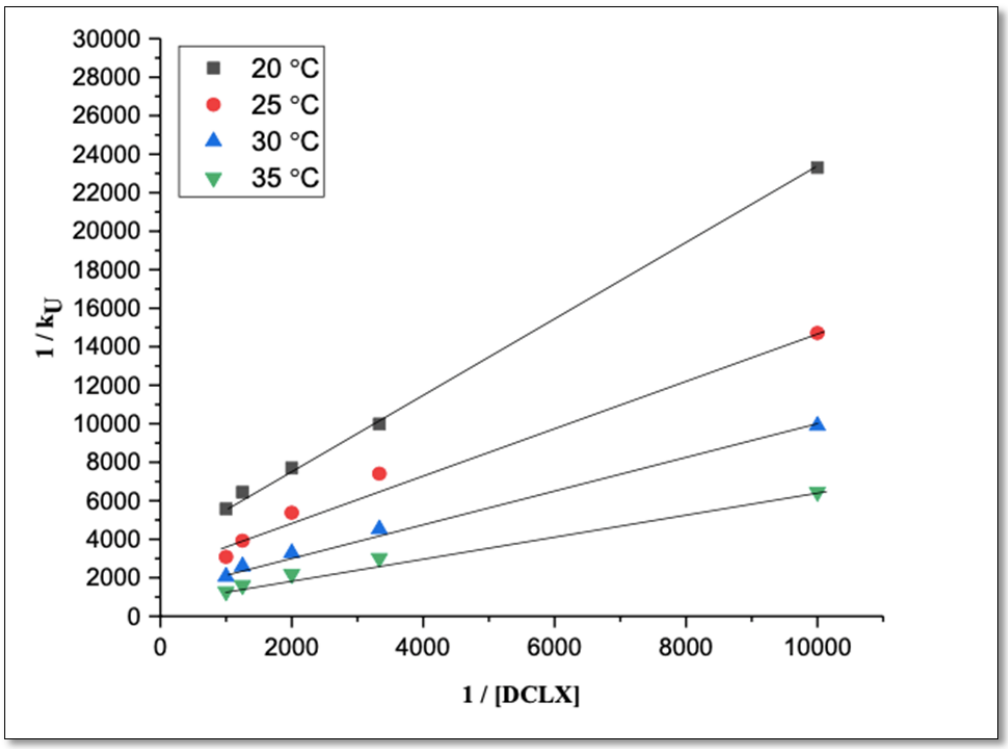

Figure 10a. Plot of { (1 / [DCLX] vs [1 / k_U]}.

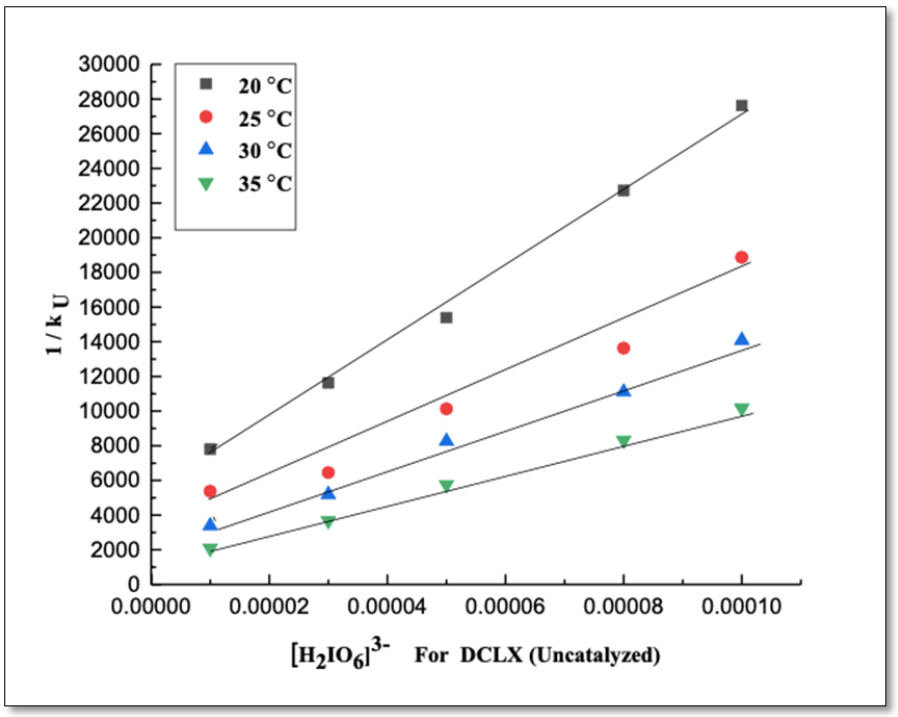

Figure 10b. Plot of { $[H_2IO_6]^{3-}$ vs $[1 / k_U]$} for DCLX.

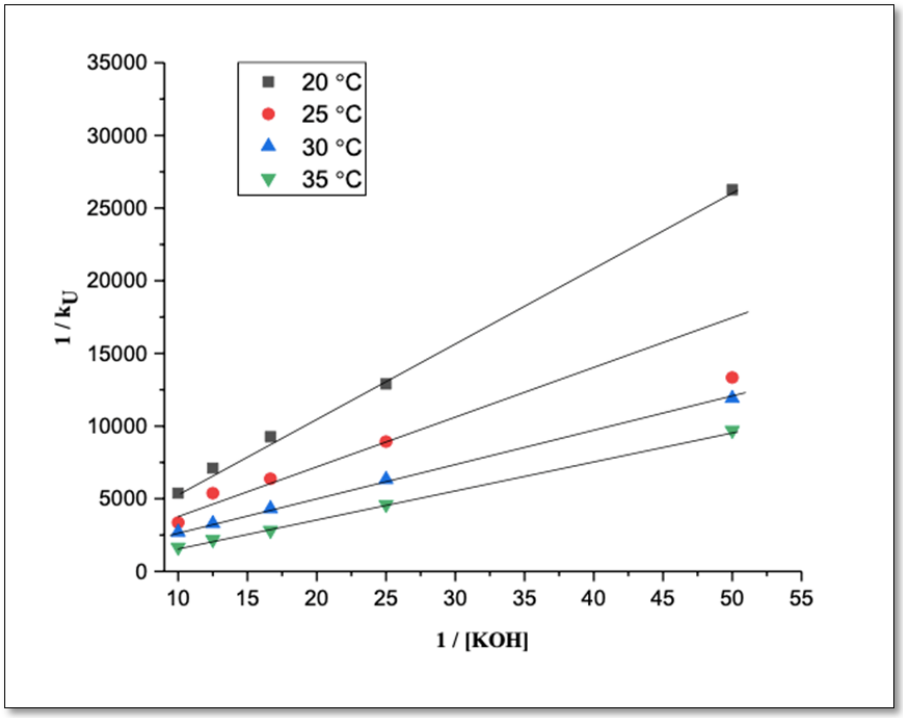

Figure 10c. Plot of {(1 / [KOH] vs $[1 / k_U]$} for DCLX.

Figure 10a, 10b and **10c** represent verification plots for uncatalyzed oxidation of DCLX by DPC (III) in alkaline medium. According to equation (7), remaining other conditions being constant, the plots of $[1 / k_U$ vs. 1/[DCLX] ($r \geq 0.999, \leq s\ 0.009$) , $[1 / k_U$ vs. $[H_2IO_6]^{3-}$ ($r \geq 0.998, \leq s$ 0.0001) and $[1 / k_U$ vs. 1 / [KOH] ($r \geq 0.999, \leq s\ 0.008$) should be linear and are found to be so as in **Figure 10a, 10b** and **10c**.

Table 4a. Equilibrium constants and slow step rate constant for DCLX.

Equilibrium Constants ↓	**Absolute Temperatures**			
Temperature →	20 □	25 □	30□	35 □
k (Slow step rate constant) x 10^{-4}	2.67	3.93	6.68	10.49
K_1	1.22	1.84	2.36	2.95
K_2 x 10^{-5}	5.61	7.8	8.21	12.53
K_3	10609.37	7661.47	5818.38	1848.65

Table 4b. Thermodynamic parameters from equilibrium constants for DCLX.

Thermodynamic Quantities	**Values from K_1**	**Values from K_2**	**Values from K_3**
ΔH°_{298} (k J mol^{-1})	44.96	36.89	-82.64
ΔS°_{298} (J K^{-1} mol^{-1})	155.33	140.21	-203.03
ΔG°_{298} (k J mol^{-1})	-1.33	-4.89	-22.14

Since DPC (III) is a strong oxidant as well as chelating agent, oxidation of different β-lactam antibiotics has been carried out in an alkaline medium. The activity of DPC (III) is a function of pH and is capable of subtle control. DPC (III) is water-soluble oxidizing reagent that exists as $[Cu(HIO_6)_2(OH)_2]^{7-}$ as well as $[HIO_6]^{4-}$ under higher pH condition. It has been evident that it can also exist as $[Cu(H_3IO_6)_2]^{-}$ or $[Cu(H_2IO_6)(OH)_2]^{2-}$ or $[Cu(H_2IO_6)(H_2O)_2]$ or $[Cu(H_3IO_6)(H_2O)_2]^{+}$ in aqueous alkaline medium. Periodic acid exists as H_5IO_6 in acid medium. The main species most active for the title work is $[Cu(H_2IO_6)(H_2O)_2]$ as reported in earlier literature. At higher alkali concentration, periodate ion tends to dimerize.

$$H_5IO_6 \rightleftharpoons H_4IO_6^- + H^+, \quad K_1 = 5.1 \times 10^{-4}$$

$$H_4IO_6^- \rightleftharpoons H_3IO_6^{2-} + H^+, \quad K_2 = 4.9 \times 10^{-9}$$

$$H_3IO_6^{2-} \rightleftharpoons H_2IO_6^{3-} + H^+, \quad K_3 = 2.5 \times 10^{-12}$$

Probable mechanism of reaction

Reaction between DPC (III) and dicloxacillin exhibits 1:4 stoichiometry and confirms pseudo-first order reaction with respect to DPC (III) while fractional orders with respect to DCLX, alkali and periodate. Based on these experimental evidences, a suitable mechanism is proposed along with proper involvement of all species. In the first step, DPC (III) reacts with hydroxide ion to form the de-protonated form of DPC (III) which yields MPC (III) and free periodate in the presence of water. Occurrence of fractional order with respect to DCLX presumably results due to formation of complex by reaction between DCLX and DPC (III). This complex interacts with fresh one mole of MPC (III) to yield an intermediate (A) along with regeneration of oxidant (DPC-III). In the second step, the active intermediate (A) reacts with fresh mole of MPC (III) to form another intermediate B that interacts with another two moles of MPC (III) to yield the final products as 2, 6-dichlorophenyl)-5-methyl-4, 5-dihydroisoxazole-4-carboxylic acid and 3-(2-(amino (carboxy) methyl)-5, 5-dimethyl-4, 5-dihydrothiazole-4-carboxylic acid-1-oxide, as represented in the mechanism correspondingly below by scheme 1 **(Figure 12)**. The complete probable structure of **Complex C** is presented in **Figure 13**.

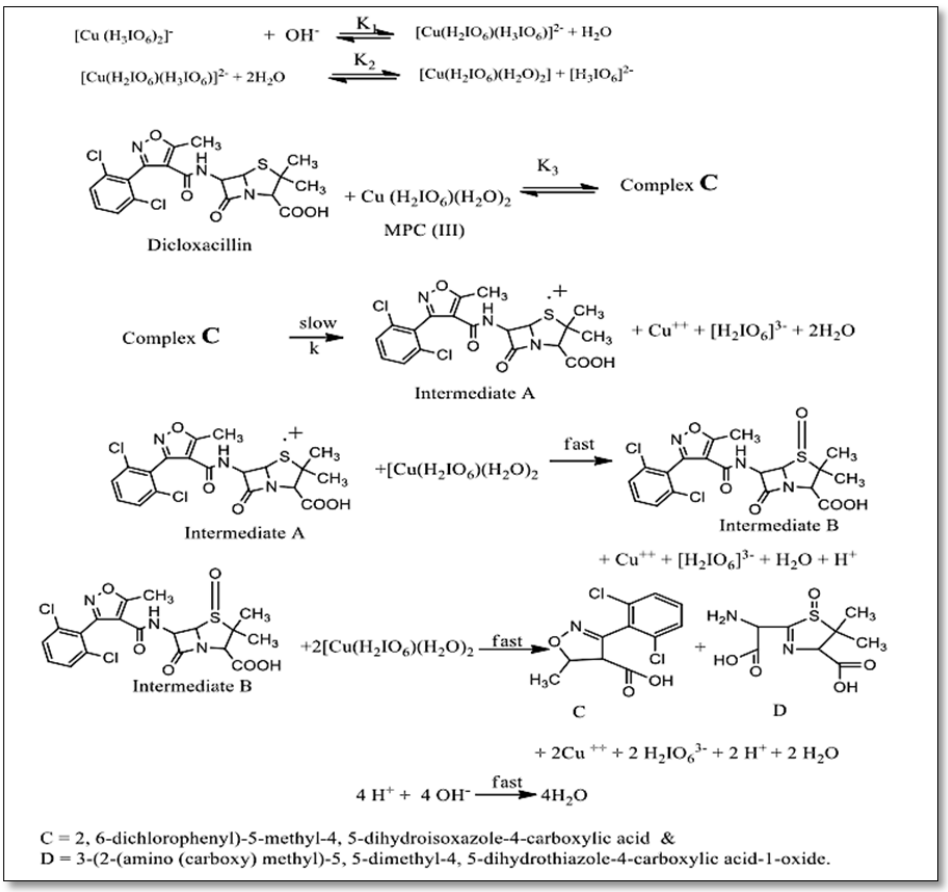

Figure 12. Scheme 1: Detailed Scheme for catalyzed oxidation of DCLX by DPC (III).

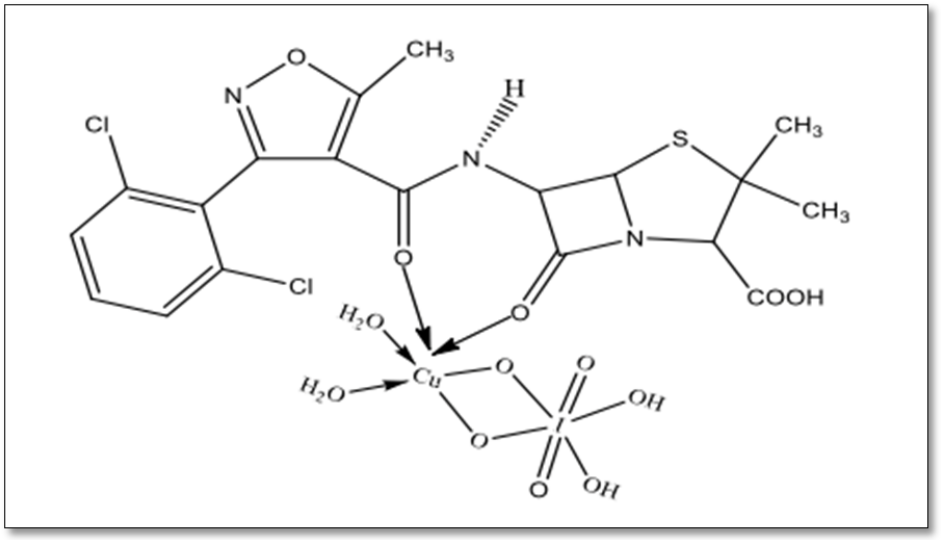

Figure 13. Probable structure of **Complex C.**

Spectroscopic evidence for the complex formation between reagent DPC (III) and substrate (DCLX) was obtained from UV –visible spectra by resisting (5.0 x 10^{-4} M) AMX, (0.12 M) KOH and a mixture of all. A bathochromic shift was obtained. The Michaelis – Menten plot is in great support for complex formation, **(Figure 5)**.

Scheme 1 leads to the rate law equation (6) as -

$$\text{rate} = -\frac{d[DPC]}{dt} = k[C] \quad [5]$$

$$k_{obs} = \frac{kK_1K_2K_3[DPC][DCLX][OH^-]}{[H_3IO_6^{2-}] + K_1[OH^-][H_3IO_6^{2-}] + K_1K_2[OH^-] + K_1K_2K_3[OH^-][DCLX]} \quad [6]$$

This equation (6) describes all kinetic orders observed for different species. The rate law equation (6) can be rearranged into equation (7) that suits for verification.

$$\frac{1}{k_{obs}} = \frac{[H_3IO_6^{2-}]}{kK_1K_2K_3[DCLX][OH^-]} + \frac{[H_3IO_6^{2-}]}{kK_2K_3[DCLX]} + \frac{1}{kK_3[DCLX]} + \frac{1}{k} \quad [7]$$

(k_{obs} is equivalent to k_U and stands for uncatalyzed rate constant.)

DERIVATION OF RATE LAW

From Scheme 1,

$$\text{Rate} = -\frac{d[DPC]}{dt} = k[\text{Complex}] = k[C] \quad \textbf{[A-1]}$$

From the law of mass action, the third equilibrium constant can be given by,

$$K_3 = \frac{[C]}{[Cu(H_2IO_6)(H_2O)_2[DCLX]}$$

After rearrangement, we get,

$$[C] = K_3[Cu(H_2IO_6)(H_2O)_2[DCLX] \quad \textbf{[A-2]}$$

Substituting the value of C from eq. [A-2], we get,

$$\text{Rate} = -\frac{d[DPC]}{dt} = K_1K_3[Cu(H_2IO_6)(H_2O)_2[DCLX] \quad \textbf{[A-3]}$$

The second equilibrium constant can be given by

$$K_2 = \frac{[Cu(H_2IO_6)(H_2O)_2[H_3IO_6^{2-}]}{[Cu(H_2IO_6)(H_3IO_6]^{2-}}$$

This can be rearranged into

$$[Cu(H_2IO_6)(H_2O)_2] = \frac{K_2\,[Cu(H_2IO_6)(H_3IO_6]^{2-}}{[H_3IO_6]^{2-}} \quad \textbf{[A-4]}$$

The first equilibrium constant can be given by:

$$K_1 = \frac{[Cu(H_2IO_6)(H_3IO_6]^{2-}}{[Cu(H_3IO_6)_2]^-[OH^-]}$$

This can be rearranged into

$$[Cu(H_2IO_6)(H_3IO_6]^{2-} = K_1\,[Cu(H_3IO_6)_2]^-[OH^- \quad \textbf{[A-5]}$$

Substituting eq. [A-4] to [A-5] in eq. [A-3], we get,

$$\text{Rate} = -\frac{d[DPC]}{dt} = \frac{kK_1K_2K_3[DCLX]_f[DPC]_f[OH^-]_f}{[H_3IO_6)_2]^-} \quad \textbf{[A-6]}$$

The total concentration of [DPC] can be given as

$$[DPC]_T = [DPC]_f + [Cu(H_2IO_6)(H_3IO_6]^{2-} + [Cu(H_2IO_6)(H_2O)_2] + [C] \quad \textbf{[A-7]}$$

where T and f denote total and free concentrations

$$= [DPC]_f + K_1[Cu(H_2IO_6)_2]^-[OH^-] + \frac{K_1K_2[Cu(H_2IO_6)_2]^-[OH^-]}{[H_3IO_6^{2-}]} + \frac{K_1K_2K_3[Cu(H_3IO_6)_2]^-[OH^-][DCLX]}{[H_3IO_6]^{2-}}$$

$$[DPC]_T = [DPC]_f + K_1[DPC]_f[OH^-] + \frac{K_1K_2[DPC]_f[OH^-]}{[H_3IO_6^{2-}]} + \frac{K_1K_2K_3[DPC]_f[OH^-][DCLX]}{[H_3IO_6^{2-}]}$$

$$[DPC]_f = \frac{[DPC]_T[H_3IO_6^{2-}]}{[H_3IO_6^{2-}] + K_1[OH^-][H_3IO_6^{2-}] + K_1K_2[OH^-] + K_1K_2K_3[OH^-][DCLX]} \quad \textbf{[A-8]}$$

The total concentration of $[OH^-]$ can be given by

$$[OH^-]_T = [OH^-]_f + [Cu(H_2IO_6)(H_3IO_6]^{2-} + [Cu(H_2IO_6)(H_2O)_2] + [C]$$

$$[OH^-]_T = [OH^-]_f + K_1[DPC][OH^-]_f + \frac{K_1K_2[DPC][OH^-]_f}{[H_3IO_6]^{2-}} + \frac{K_1K_2K_3[DPC][OH^-]_f[DCLX]}{[H_3IO_6]^{2-}} \quad [OH^-]_T = [OH^-]_f\{1 + K_1\,[DPC] + \frac{K_1K_2[DPC]}{[H_3IO_6]^{2-}} + \frac{K_1K_2K_3[DPC][DCLX]}{[H_3IO_6]^{2-}}\}$$

In view of low concentrations of DPC and $H_3IO_6^{2-}$ used, last three terms inside bracket can be neglected in comparison with unity.

$$[OH^-]_T = [OH^-]_f \quad \textbf{[A-9]}$$

Similarly, in case of low concentrations of DPC and $H_3IO_6^{2-}$ used

$$[DCLX]_T = [DCLX]_f \quad \textbf{[A-10]}$$

Putting these values of $[DPC]_f$ from eq^n. [A-8], $[OH^-]_f$ from eq^n. [A-9] and $[DCLX]_f$

from eq^n. [A-10] in eq^n. [A-6] after omitting subscripts T and f, we get,

$$\text{Rate} = -\frac{d[DPC]}{dt} = \frac{kK_1K_2K_3[DCLX][DPC][OH^-]}{[H_3IO_6^{2-}] + K_1[OH^-][H_3IO_6^{2-}] + K_1K_2[OH^-] + K_1K_2K_3[OH^-][DCLX]}$$

Or, $$\frac{1}{k_{obs}} = \frac{[H_3IO_6^{2-}]}{kK_1K_2K_3[DCLX][OH^-]} + \frac{[H_3IO_6^{2-}}{k\,K_2K_3[DCLX]} + \frac{1}{kK_3[DCLX]} + \frac{1}{k} \quad \textbf{[A-11]}$$

Scheme 1 clarifies the participation of neutral species in the reaction due to invariable ionic strength and dielectric constant. The modest values of both enthalpy and entropy of activation, within the range of electron pairing and unpairing process for the loss of degree of freedom and rigid transition state, are favourable for electron transfer reaction.

The higher negative value of $\Delta S^{\neq}$ suggests that the intermediate complex is probably highly ordered than the reacting species. The above results, evidences and lower rate constant for slow steps indicate that the oxidation presumably occurs via an inner-sphere mechanism. The reducing property of the substrate is, probably, reduced in the absence of catalyst and the path of the uncatalyzed oxidation is extended by increasing the activation energy.

CONCLUSION

Oxidation of dicloxacillin by DPC (III) was studied experimentally in aqueous alkaline medium. (MPC-III) [Cu (H_2IO_6) $(H_2O)_2$] was considered to be the main active species for the present work. Activation and thermodynamic parameters with respect to uncatalyzed rate constant **(k_U)**, slow step rate constant (**k**) as well as equilibrium constants **(K_1, K_2** and **K_3)** at different temperatures were determined. Overall sequences described here are inconsistent with all experimental evidences including products, spectral analysis, mechanistic and kinetics studies in the favour of pseudo-first order reaction.

ACKNOWLEDGEMENT

The first author (Y. R. Sahu) is highly acknowledged to Purwanchal Campus, Dharan, Institute of Engineering (IOE), T.U., Nepal for financial support, Prof. Dr. S. T. Nandibewoor and Prof. Dr. S.A. Chimatadar, Karnatak University, Dharwad, India for invaluable guidelines and suggestions and SAIF–IIT, Bombay, STIC-SAIF, Cochin and CDRI-CSIR, Lucknow, India for technical support in providing spectrum results.

REFERENCES

1. Miranda-Novales G, Leaños-Miranda BE, Vilchis-Pérez M, Solórzano-Santos F (2006) *In vitro* activity effects of combinations of cephalothin, dicloxacillin, imipenem, vancomycin and amikacin against methicillin-resistant Staphylococcus spp. strains. Ann Clin Microbiol Antimicrob 5: 25.
2. Kümmerer K (2009) Antibiotics in the aquatic environment-A Review-Part I. Chemosphere 75: 417-434.
3. Hirsch R, Ternes T, Haberer K, Kratz KL (1999) Occurrence of antibiotics in the aquatic environment. The science of the total environment 225 :109-118.
4. Larsson DGJ, Pedro CD, Paxeus N (2007) Effluent from drug manufactures contains extremely high levels of pharmaceuticals. J Hazard Mater 148: 751-755.
5. Marcinowski PP, Bogacki JP, Naumczyk JH (2014) Cosmetic wastewater treatment using the Fenton, Photo-Fenton and H2O2/UV processes. J Environ Sci Health, Part A 49: 1531-1541.
6. Homem V, Santos L (2011) Degradation and removal methods of antibiotics from aqueous matrices - A review. J Environ Manag 92: 2304-2347.
7. Ellis JB (2006) Pharmaceutical and personal care products (PPCPs) in urban receiving waters. Environ Pollut 144: 184-1899.
8. Ikehata K, Gamal El-Din M, Snyder SA (2008) Ozonation and advanced oxidation treatment of emerging organic pollutants in water and Wastewater. Ozone: Science & Engineering 30: 21-26.
9. Klavarioti M, Mantzavinos D, Kassinos D (2009) Removal of residual pharmaceuticals from aqueous systems by advanced oxidation processes. Environ Int 35: 402-417.
10. Huang X, Zhu N, Mao F, Ding Y, Zhang S, et al. (2019) Enhanced heterogeneous photo-fenton catalytic degradation of tetracycline over yceo2/fh composites: performance, degradation pathways, fe2+ regeneration and mechanism. Chem Eng J 123636.
11. Deng Y, Zhao R (2015) Advanced oxidation processes (aops) in wastewater treatment. Curr Pollut Rep 1: 167-176.
12. Bush K, Bradford PA (2019) Interplay between β-lactamases and new β-lactamase inhibitors. Nat Rev Microbiol 17: 295-306.
13. Sutcliffe IC (2010) A phylum level perspective on bacterial cell envelope architecture. Trends Microbiol 18: 464-470.
14. Lamani SD, Veeresh TM, Nandibewoor ST (2011) Mechanism of uncatalyzed and Osmium (VIII) Catalyzed Oxidation of L-alanine by Copper (III) Periodate complex in aqueous alkaline medium. Synthesis and Reactivity in Inorganic, Metal-Organic, and Nano-Metal Chemistry 41: 394-404.
15. Malode SJ, Abbar JC, Nandibewoor ST (2010) Mechanistic aspects of uncatalyzed and ruthenium (III) catalyzed oxidation of dl-ornithine monohydrochloride by silver (III) periodate complex in aqueous alkaline medium. Inorganica Chimica Acta 363: 2430-2442.
16. Shettar RS, Nandibewoor ST (2005) Kinetic, mechanistic and spectral investigations of ruthenium (III)-catalysed oxidation of 4-hydroxycoumarin by alkaline diperiodatonickelate (IV) (stopped flow technique). J Mol Catal A: Chem 234: 137-143.
17. Malatesta L (1941) Salts of Trivalent Copper and Silver (II). Gazz Chimica Ital 71: 580-584.
18. Panigrahi GP, Pathy AC (1986) Kinetics and mechanism of oxidation of potassium thiocyanate by potassium bis (tellurate) cuprate (III). Ind J Chem 25A: 354-357.

19. Nadimpali S, Padmvasthy J, Yusuff KKM (2001) Determination of the nature of the diperiodatocuprate (III) species in aqueous alkaline medium through a kinetic and mechanistic study on the oxidation of iodide ion. Transit Met Chem 26: 315-321.

20. Chowdhury B, Mondal MH, Barman MK, Saha B (2018) A study on the synthesis of alkaline copper (III)-periodate (DPC) complex with an overview of its redox behaviour in aqueous micellar media. Research on Chemical Intermediates.

21. Xie HY, Wang ZR, Fu ZF (2014) Highly sensitive trivalent copper chelate–luminol chemiluminescence system for capillary electrophoresis chiral separation and determination of ofloxacin enantiomers in urine samples. J Pharm Anal 4: 412-441.

22. Sethuram B (2003) Some aspects of electron transfer reaction involving organic molecules. Allied Publishers Pvt. Ltd, New Delhi, pp: 71-78.

23. Lister MW (1953) The stability of some complexes of trivalent copper. Canad J Chem 31: 638-665.

24. Abdelrahman MM, Naguib IA, Elsayed MA, Zaazaa HA (2017) Chromatographic Methods for Quantitative Determination of Ampicillin, Dicloxacillin and Their Impurity 6-Aminopenicillanic Acid. J Chromatogr Sci 56: 209-215.

25. Naveen Kumar T, Venkatesh TV, Malini S, Rangaraju PR (2014) Kinetics and mechanism of oxidation of Dicloxacillin Sodium [DXS] by Chloramine-t [cat] in [HCL] medium. World J Pharm Pharm Sci 4: 673-684.

26. Bhinge SD, Malipatil SM (2016) Development and validation of a stability-indicating method for the simultaneous estimation of cefixime and dicloxacillin using the RP-HPLC method. J Taibah Univ Sci 10: 734-744.

27. Stage TB, Graff M, Wong S, Rasmussen LL, Nielsen F, et al. (2018) Dicloxacillin induces CYP2C19, CYP2C9 and CYP3A4 in vivo and *in vitro*. Brit J Clin Pharmacol 84: 510-519.

28. Villegas-Guzman P, Silva-Agredo J, González-Gómez D, Giraldo-Aguirre AL, Flórez-Acosta O, et al. (2014) Evaluation of water matrix effects, experimental parameters, and the degradation pathway during the TiO2photocatalytical treatment of the antibiotic dicloxacillin. J Environ Sci Health, Part A 50: 40-48.

29. Acharya DR, Patel DB (2013) Development and validation of RP-HPLC Method for simultaneous estimation of Cefpodoxime Proxetil and Dicloxacillin Sodium in tablets. Ind J Pharm Sci 75: 31-35.

30. Sahu YR, Chaudhary NK, Mishra P (2020) Kinetics and mechanism of oxidation of Amoxicillin by Copper (III) Periodate Complex in Alkaline Medium. Int J Pharm Sci Rev Res 60: 138-146.

31. Panigrahi GP, Misro PK (1977) Kinetics & Mechanism of Os (VIII)-catalysed Oxidation of Aromatic Aldehydes by Sodium Periodate. Ind J Chem 15A: 1066-1069.

32. Jeffery GH, Basset J, Mendham RC, Denney RC (1996) Vogel's textbook of qualitative chemical analysis, 5th Edition, ELBS, Longman, Essex U.K. 455.

33. Jaiswal PK, Yadava KL (1973) Determination of sugars and organic acids with periodato complex of copper (III). Ind J Chem 11: 837- 838.

34. Jagadeesh RV, Puttaswamya (2008) Ru (III), Os (VIII), Pd (II) and Pt (IV) catalysed oxidation of glycyl-glycine by sodium N-chloro-p-toluenesulfonamide: Comparative mechanistic aspects and kinetic modelling. J Phys Org Chem 21: 844-858.

Government of Nepal

Ministry of Youth and Sports

National Youth Council

Sanothimi, Bhaktapur

राष्ट्रिय युवा परिषद्-नेपाल
२०७२

This **certificate** is awarded to

YUV RAJ SAHU

in recognition of your valuable contribution

as a **Poster Presenter** in ***Provincial Youth Symposium on Science & Technology 2019***

Province-1, Biratnagar, Nepal

March 1-2, 2019

Suresh Bhattarai
Co-ordinator
Organizing Committee

Madhab P. Dhungel
Executive Vice-Chairperson
National Youth Council

Hon.Sherdhan Rai
Chief Minister
Province-1, Nepal
Chief Guest

This is to Certify that

MR. YUV RAJ SAHU

has Successfully Completed

Workshop on Research Writing and Publishing

March 29 – 30, 2019

Organized by

Nepal Physical Society
Eastern Chapter, Biratnagar

Co-organized by

Mahendra Morang Adarsh Multiple Campus, Tribhuvan University, Biratnagar
&
HISSAN, Morang

Mr. Kul Prasad Limbu	Dr. Shashit Kumar Yadav	Prof. Dr. Devendra Adhikari	Prof. Dr. Shiva Kumar Rai
Facilitator	*Secretary / Facilitator* Nepal Physical Society Eastern Chapter	*President / Facilitator* Nepal Physical Society Eastern Chapter	*Facilitator*

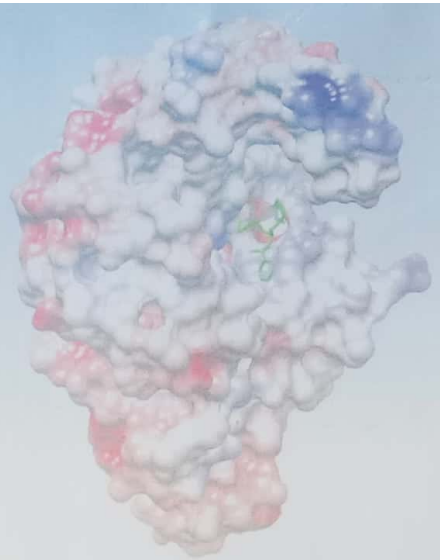

Current Trends in Drug Discovery Research
7th CTDDR

7th International Symposium on

CURRENT TRENDS IN DRUG DISCOVERY RESEARCH

February 20-23, 2019

Certificate

The Organising Committee certifies and appreciates that

Yuv Raj Sahu, Bio-inorganic & materials lab, T.U, Nepal.

has participated and delivered a Flash Talk in the Symposium held in CSIR-CDRI during February, 20-23, 2019

(Prof. Tapas K Kundu)
Chairperson

(Dr. Sanjay Batra)
Organizing Secratary

CSIR-Central Drug Research Institute

Sector 10, Jankipuram Extension, Sitapur Road, Lucknow-226031, UP, India

23RD INTERNATIONAL CONFERENCE OF INTERNATIONAL ACADEMY OF PHYSICAL SCIENCES

(CONIAPS XXIII)

On

Advances in Physical Sciences to Achieve Sustainable Development Goals

November 18, 2018

Organized by

NEPAL ACADEMY OF SCIENCE AND TECHNOLOGY, KATHMANDU, NEPAL

Certificate

This is to certify that Prof. /Dr./ Mr./Ms. Y. R. Sahu

Department of Purwanchal Engineering campus, Dharan Nepal has participated in the **23rd International Conference of International Academy of Physical Sciences** on **Advances in Physical Sciences to Achieve Sustainable Development Goals** held at **Nepal Academy of Science and Technology** during November 16-18, 2018 and delivered Invited Lecture/Chaired a Session/ Presented a paper /Presented a paper in Young Scientist Award Category.

Title of the Invited Lecture/Paper Kinetics and Mechanism of oxidation of Ampicillen by diperiodatocuprate and Cobalt (iii)

Prof. P. N. Pandey
General Secretary
IAPS

Dr. Buddhi Ratna Khadge
Convenor
CONIAPS XXIII

Ms. Ramila Raut
Organizing Secretary
CONIAPS XXIII

CERTIFICATE OF PARTICIPATION

SOPHISTICATED TEST AND INSTRUMENTATION CENTRE

COCHIN UNIVERSITY CAMPUS, KOCHI – 682 022

This is to certify that

~~Dr~~./Mr./~~Ms~~ Yuv Raj Sahu, Research Scholar

of Institute of Engineering, Tribhuvan University, Nepal

successfully participated in the three-day workshop on

Diffraction Techniques: X-Ray and Electron Diffraction

Organized jointly by

Sophisticated Test and Instrumentation Centre (STIC)

and

Kerala State Council for Science Technology and Environment (KSCSTE)

during 7th to 9th February 2018

09 FEBRUARY 2018
KOCHI — 682 022

SOPHISTICATED TEST & INSTRUMENTATION CENTRE ★ COCHIN- 22

DR. J. JAGANNATH BHAT
Director I/c.

ICC-2018

International Chemical Congress

- Chemistry for Sustainable Development-

Organized by

Nepal Chemical Society

In co-operation with

Department of Chemistry

Birendra M. Campus, Bharatpur, Tribhuvan University

Chitwan, Nepal

Certificate of Participation

This is to certify that

Mr. Yuv Raj Sahu

participated as Plenary/Keynote/Invited/Oral Lecture/Poster /Delegate in the International Chemical Congress Chemistry for Sustainable Development

March 8-10, 2018, Sauraha, Chitwan, Nepal

Dr. Surya Kant Kalauni
General Secretary
Nepal Chemical Society

Govind Sapkota
Co-patron ICC-2018
Campus Chief, Birendra M. Campus

Chief Guest

Prof. Dr. Amar Prasad Yadav
Convener ICC-2018
President Nepal Chemical Society

International Seminar on "Frontiers in Chemistry 2018"

ENLIGHTENMENT TO PERFECTION

UNIVERSITY OF NORTH BENGAL

Accredited by NAAC with Grade A

Organized by

DEPARTMENT OF CHEMISTRY, UNIVERSITY OF NORTH BENGAL & CRSI North Bengal Local Chapter

CERTIFICATE

This is to certify that

Prof./Dr./Mr./Ms. Jyoti Raj Sahu

of Tribhuban University, Nepal

has delivered an invited lecture/ presented a poster/participated in the

International Seminar on "Frontiers in Chemistry 2018"

held at the Department of Chemistry, University of North Bengal on August 27th, 2018.

Prof. (Dr.) A. Misra
Convenor
Department of Chemistry, N. B. U

Dr. S. Das
Secretary, Organizing Committee
Department of Chemistry, N. B. U

CERTIFICATE

International Conference
on
Emerging Trends in Science and Technology

March 22-23, 2014
Biratnagar

Organized by

Research Council of Science and Technology (RCOST)
Biratnagar, Nepal

This is to Certify that

Prof. / Dr. / Mr. / Ms Yub Raj Sahu

has participated/presented a scientific paper in the

International Conference on Emerging Trends in Science and Technology.

We wish the participant all success.

Prof. Dr. Pradeep Raj Pradhan	Prof. Dr. Sujeet Kumar Chatterjee	Prof. Dr. Devendra Adhikari
Chairman	Chairman	Convener
(RCOST)	(Organizing Committee)	(Organizing Committee)

(नेपाल सरकारबाट स्वीकृत)

नेपाल केमिकल सोसाइटी
Nepal Chemical Society

Regd. No. 8/042/043 Ref. No.: Date: 2075-12-21

Workshop on Tools &Techniques in Chemistry

Organized by

Nepal Chemical Society in co-operation with Central Department of Chemistry, TU, Kirtipur

Certificate

This is to certify that

Prof./Dr./Mr./Ms. YUV RAJ SAHU

From Biratnagar, Nepal Participated as resource person/participant in 3 days workshop held from April 2-4, 2019 (Chaitra 19-21, 2075) at Central Department of Chemistry, TU, Kirtipur.

Prof. Dr. Amar Prasad Yadav
President
Nepal Chemical Society

Dr. Surya Kant Kalauni
General Secretary
Nepal Chemical Society

Prof. Dr. Ram Chandra Basnyat
Head
Central Dept. of Chemistry

Contact Point:
Central Department of Chemistry, Tribhuvan University, Kirtipur, Kathmandu, Nepal
P. O. Box: 6145, Kathmandu, Nepal, Mobile: +977-9840166321, Email: info@ncs.org.np, Website: www.ncs.org.np

WORKSHOP ON

Carbon Dots (CDs): An amazing multi functional nano particle

2 August, 2022

Certificate Of Participation

Awarded to

Mr. Yuv Raj Sahu

For contributing as a participant in Carbon Dots (CDs): An amazing multi functional nano particle one-day workshop organized by Department of Chemistry, Mahendra Morang Adarsh Multiple Campus, Tribhuvan University and Nepal Chemical Society, Biratnagar, Province 1, Nepal.

Ghanshyam Shrivastav	Prof. Dr. Ajaya Bhattarai	Dr. Surendra Kumar Gautam	Prof. Dr. Roger M. Leblanc
Chairman	President	President	Fulbright Specialist
Department of Chemistry, M.M.A.M.C., T.U. Biratnagar-12	Nepal Chemical Society, Province 1	Nepal Chemical Society, Kathmandu	Department of Chemistry University of Miami, FL, USA

REGIONAL CONFERENCE
ON
SCIENCE AND TECH

Certificate of Participation

It is to certify that

Yub Raj Sahu

Mahendra Morang Adarsha Multiple Campus, TU, Biratnagar

presented a research paper in the RCST2024, held on May 7-8, 2024 Organized by the Central Campus of Technology (CCT), Institute of Science and Technology (IOST), Tribhuvan University (TU), Dharan, Nepal.

2024

Dr. Lalit K. Rai	**Dr. Dil K. Limbu**	**Prof. Dr. Binil Aryal**
Coordinator	Campus Chief	Dean
RCST2024	CCT, Dharan	IOST, TU

18th International Congress on Thermal Analysis and Calorimetry (ICTAC 2024)
&
14th National Conference of the Indian Thermodynamics Society

This is to certify that

Yuv Raj Sahu
of
Tribhuvan University, Nepal

has participated and delivered an oral presentation entitled "**Kinetics and Mechanism for Catalyzed Oxidation of Oxacillin**" in the 18th International Congress on Thermal Analysis and Calorimetry (ICTAC 2024) & the 14th National Conference of the Indian Thermodynamics Society, organized at IIT Madras, India, during September 02-07, 2024.

Prof. Ranjit K. Verma
Chairman, National Organizing Committee

Prof. Ramesh L. Gardas
Convener, ICTAC 2024